THE CARBON SEQUESTRATION AND SOIL RESPIRATION
AFTER LAND USE CONVERSION IN BIOFUEL CROPPING ECOSYSTEMS

By

Yahn-Jauh Su

A DISSERTATION

Submitted to
Michigan State University
in partial fulfillment of the requirements
for the degree of

Geography—Doctor of Philosophy

2017

ABSTRACT

THE CARBON SEQUESTRATION AND SOIL RESPIRATION AFTER LAND USE CONVERSION IN BIOFUEL CROPPING ECOSYSTEMS

By

Yahn-Jauh Su

Global climate change alters Earth's carbon, hydrological and energy cycles from local to global scales, changing our climate patterns and impacting our lifestyles and prosperity. The development of bioenergy may partially mitigate the release of carbon dioxide during the combustion of fossil fuel. However, the carbon emissions from the bioenergy-induced land use change have long been debated and it is not certain whether they really represent a reduction of carbon emission. In this study, I monitored the components of the net ecosystem exchange (NEE) of CO_2, including gross primary production (GPP), ecosystem respiration (R_{eco}), total soil respiration (R_s), autotrophic soil respiration (R_a) and heterotrophic soil respiration (R_h), to understand their responses to climate variability and in particular a severe drought event. I studied three major bioenergy crops (continuous corn, switchgrass and restored multicultural prairie) on fields with two different land use histories (conventional corn-soybean rotation and Conservation Reserve Program brome grass fields). I found that the amplitude, the duration and the seasonality of microclimatic variables (temperature and precipitation) were important for the carbon dynamics in the bioenergy cropping systems. The soil water content affected the annual NEE, GPP and R_{eco} although it did not have strong correlations with these components of carbon fluxes at short-term scale. The short-term (1-2 week) normal summer water deficit may affect annual NEE while long-term (spring-summer) drought may change the community structure and affect the carbon cycling processes in the following years. The temperature sensitivities of soil respiration were shifted within and between years. In addition, crop types and land use histories

affect the responses of ecosystem to climate events. The different phenology between annual and perennial crops and the establishment of dense root systems in perennial crops can change the ratio of the components of NEE and change the direction and the amounts of net ecosystem carbon flux. Annual and perennial crops have different strategies responding to different climate scenarios and their combinations. The monitoring of climate patterns at intra-annual scale is required to understand how the ecosystem respond to climate change.

Dedicated to my parents and my wife,
who have been always supportive and encouraging

ACKNOWLEDGEMENTS

I would like to thank my advisor, Dr. Jiquan Chen, for his support and guidance throughout the past five year. He gave me a chance to start my PhD study in environmental sciences and ecosystem ecology with the wide exploration of geography, biogeochemistry and mathematic modeling, as well as pushing me for academic journal writing. I learned independent learning, problem solving in field, and developing new methods to resolve present knowledge gaps. I also deeply thank my committees. Dr. G. Philip Robertson for teaching me to look at academic questions from a big picture and encouraging me to think about fundamental questions and how research findings can be implemented in our society. Dr. Stephen K. Hamilton stimulates my thinking from details of study results and encourage me to try any new ideas. He and Suzanne Sippel give me the warmest help when I faced big challenges during my PhD life. Dr. Jeffrey A. Andresen assisted me for the basic knowledge of agricultural meteorology and gave me support in Geography.

I like to thank all members in LEES lab, Robertson lab and Hamilton lab and professors, researchers and students in the W.K. Kellogg Biological Station (KBS). I cannot finish the heavy field work, data analysis, method development and dissertation writing without their support. I also thank Michael Abraha, who worked with me closely in the field and in the lab. The discussions with him, both regarding research and life, always helped me mitigate my stress. I am grateful to Ilya Gelfand, Stecey VanderWulp, Kevin Kahmark, Sven Bohm, Changliang Shao, Housen Chu, Zutao Ouyang, Sarah Roley, Gabriela Shirkey, Ranjeet John, Terenzio Zenone, Wei Shan, Yi Fan, and Cheyenne Lei. I also thank the support from the Department of Geography, Environment, and Spatial Sciences. Dr. Ashton Shortridge and Ms. Sharon Ruggles

gives me help when I have any question in Geography and assist me when I need department's support. I specially thank my wife, Hsun-Yi Hsieh, and my parents. Your support at any time is the most important in enhancing my progress.

TABLE OF CONTENTS

LIST OF TABLES

LIST OF FIGURES

KEY TO ABBREVIATIONS

9d-T_a Nine day moving average of daily mean air temperature

AIC   Akaike Information Criterion

AGR   Corn-Soybean Rotational Conventional Agricultural Field

β_{R_a} The temperature sensitivity of logarithm autotrophic soil respiration

β_{R_h} The temperature sensitivity of logarithm heterotrophic soil respiration

β_{R_s} The temperature sensitivity of logarithm total soil respiration

C   Corn

CO2e   Carbon dioxide equivalent, a standard unit for measuring carbon footprints

CROP   Crop types

CRP   Conservation Reserve Program

DLUC   Direct land use change

EC   Eddy-covariance

ECE   Extreme climatic event

ET   Evapotranspiration

EVI   Enhanced Vegetation Index

eWUE   Ecosystem water-use efficiency, calculated by GPP/ET

F:B ratio   Fungi to bacteria ratio

GHG   Greenhouse gas

GPP   Gross primary production

GWI   Global warming impact

GWP   Global warming potential

ILUC	Indirect land use change
LR_{20}	Log_{10} soil respiration rate at 20 °C
$LR_{20_{R_a}}$	The logarithm autotrophic soil respiration rate at 20°C
$LR_{20_{R_h}}$	The logarithm heterotrophic soil respiration rate at 20°C
$LR_{20_{R_s}}$	The logarithm total soil respiration rate at 20°C
LUC	Land use conversion/change
LUH	Land use history
MODIS	Moderate Resolution Imaging Spectroradiometer
NDVI	Normalized Difference Vegetation Index
NEE	Net ecosystem exchange
nir	Near infrared red
PAR	Photosynthetically active radiation
P_N	Photosynthesis
R	Respiration, including different types of respiration. i.e., R_s and R_a in Ch.1 and 2 and R_a, R_{eco}, R_h, and R_s in Ch. 3.
R_a	Autotrophic soil respiration
RC	Root contribution to total soil respiration (R_a/R_s ratio)
R_{eco}	Ecosystem respiration
Ref	Reference site
R_h	Heterotrophic soil respiration
PAR	Photosynthetically active radiation
Pr	Prairie mixture
PRCP	Precipitation
R_s	Total soil respiration

SOC   Soil organic carbon

Sw   Switchgrass

T_s Soil temperature

u_z Vertical wind speed

VWC   Volumetric soil water content

VI   Vegetation indices, including NDVI and EVI

CHAPTER 1
DISSERTATION INTRODUCTION

1.1 OVERVIEW

1.1.1 Global carbon cycle and climatic changes

Carbon, the element constructing the chemical frame of most living things on the Earth, plays an important role in biogeochemical cycles and global climate change. Carbon's distribution, form and presence in reservoirs, the water cycle, energy flow and other cycles is modified by physical, chemical and biological processes—all of which affect climate, from the local to the global scale. Atmospheric greenhouse gases (GHGs), such as CO_2, N_2O and CH_4, can absorb radiation and trap heat when radiation penetrates the atmosphere. Atmospheric GHG concentrations can thus affect the surface energy balance, change the surface temperature and water distribution and can alter climate. The anthropogenic carbon release from fossil fuels and land use change (LUC) has been recognized as the most important cause of atmospheric CO_2 increase (Fig. 1.1, IPCC, 2013). The increase of atmospheric CO_2 concentration is believed to majorly increase total radiative forcing and induce global warming (Fig. 1.2, IPCC, 2013). The carbon fluxes between an ecosystem and atmosphere are crucial for estimating the dynamics of the global atmospheric CO_2 concentration. However, there is still much uncertainty in how ecosystem carbon budgets respond to climate. We need more research to understand the processes of carbon exchange in different ecosystem-atmosphere interfaces under different climate patterns and future climate changes, and how ecosystems and the atmosphere exchange carbon after LUC at different spatial and temporal scales.
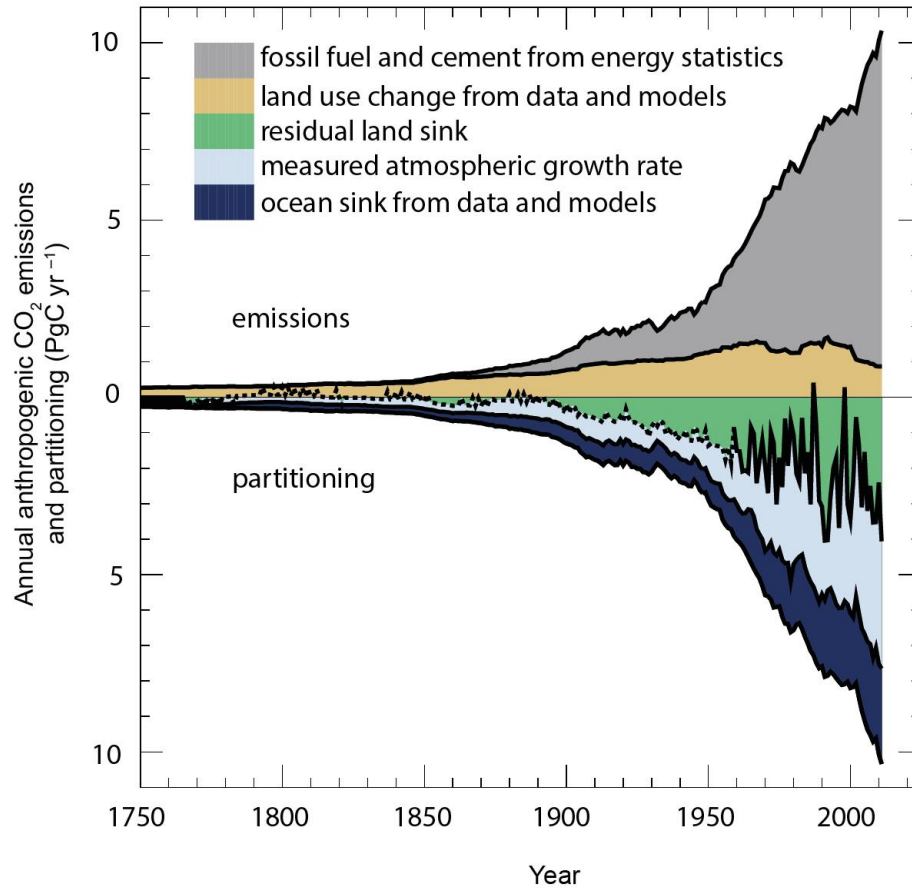
Figure 1.1. The major anthropogenic CO$_2$ emissions and the partitioning among three major carbon reservoirs. The top panel shows the dynamics of anthropogenic CO$_2$ emissions from fossil fuel combustion (gray) and land use change (khaki) after 1750. Part of the carbon sinks into land (green) or oceans (dark blue) and part remains in the atmosphere (light blue), which increases the atmospheric CO$_2$ concentration. The emission values were estimated from four models and data during 1750-1850 while the partitioning data is estimated from the combination of multiple-source atmospheric CO$_2$ concentration data, ice cores and models (source: IPCC, 2013).
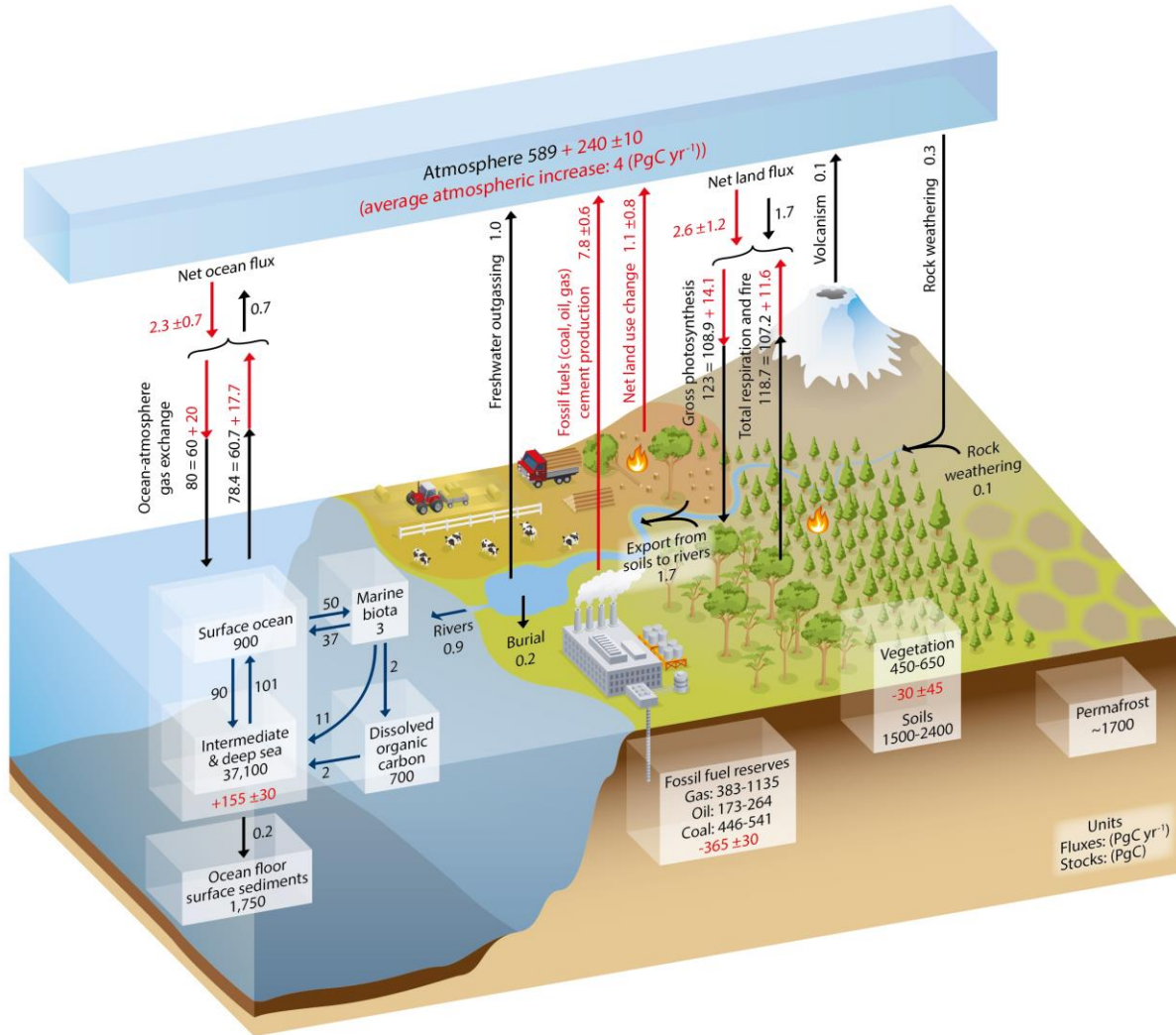
Figure 1.2. A simplified schematic of the global carbon reservoirs and annual fluxes. The units of the carbon stocks in major carbon reservoirs (PgC) and the annual fluxes between reservoirs (PgC yr^{-1}). The red arrows and numbers denote the annual anthropogenic carbon fluxes and accumulated changes over the industrial period (1750-2011) while the black arrows and numbers show annual natural fluxes and the stocks of the natural carbon reservoirs before Industrial Era (after 1750) and assumed stable. The largest two fluxes between atmosphere and other reservoirs are the land flux and the ocean flux that is stable before 1750. The annual contribution of anthropogenic carbon to the atmosphere is 7.8 and 1.1 PgC yr^{-1} by fossil fuel and cement production and land use change, respectively. Part of them were neutralized by ocean and land sink. The net annual increase of atmospheric carbon is 4 PgC yr^{-1} (source: IPCC, 2013).

1.1.2 The development of biofuel and its impacts on global carbon balance

Bioenergy crops have the potential to mitigate GHG emissions, as their net climate forcing is lower than the equivalent energy derived from fossil fuels. This reduction in the amount of GHG emissions, compared with those from fossil fuels, is denoted as "feedstock carbon uptake credit" or "fossil fuel offset credit" (Searchinger *et al.*, 2008; Gelfand *et al.*, 2013). However, there remain many uncertainties and ongoing debates on the "climate neutrality" of biofuel crops (Hansen, 1993; Roberston *et al.*, 2008; Searchinger *et al.*, 2008; Robertson *et al.*, 2011). Land use change from previously uncultivated fields, food-based farms or marginal lands into biofuel plantations, for example, can result in large CO_2 emissions during or after the conversion that increase carbon debt (Davidson and Ackerman, 1993; Guo and Gifford, 2002; Searchinger *et al.*, 2008; Kim *et al.*, 2009; Gelfand et al., 2011; Zona *et al.*, 2013) and may offset the GHG benefit of biofuels. Several studies concluded that the net GHG emissions of biofuel croplands are positive after the direct LUC (DLUC) and indirect LUC (ILUC) (Liu, 2015) are counted. However, some research has demonstrated that the management practices also play a major role. Robertson *et al.* (2000) reported the significant difference in GHG emission between till and no-till croplands and between different successional stages of forest regeneration, while Gelfand *et al.* (2011) showed that the tillage practices (68 Mg $CO_2e \cdot ha^{-1}$) tripled the carbon dioxide equivalent (CO_2e) of no-till practice (222) after land use conversion if the alterations in C stocks were counted, which changed N_2O and CH_4 fluxes and the fossil fuel offset credit. Ruan *et al.* (2013) also made evident that soil CO2 emissions from conventional tillage fields were 1.2 times those in non-tillage fields and 3.1 times those in non-conversion fields. The global warming impact (GWI) of converted soybean fields with non-tillage and conventional tillage fields were 15 and 6.37 Mg $CO_2e \cdot ha^{-1}$ higher than that at non-

converted fields. Thus, management practices directly affect soil carbon and nitrogen cycles and change the GHG emissions under different climate patterns at short-term and long-term scales.

Further understanding how the major carbon processes in biofuel agricultural ecosystems respond to climate change and variability can help us evaluate the effects of biofuel-induced LUC. More so, it is required in order to improve the estimate of the consequences of biofuel-induced LUC based on the Earth System Models (ESMs).

1.1.3 The drivers of carbon budget in biofuel cropland ecosystem after land use change

The amount of GHG emission due to LUC, also known as carbon debt, will diminish over time before reaching a new equilibrium in cropping systems (Fargione *et al.*, 2008; Mitchell *et al.*, 2012). The duration that an established biofuel crop system needs to be in production in order to "payback" the carbon debt after LUC can range from years to over a century. Some studies estimated the payback time using mathematical models that contained multiple variables such as land use history, crop type, and management practices (Gelfand *et al.*, 2011; Mitchell *et al.*, 2012). However, the corresponding mechanisms to understand the responses of GHG emissions are complex and uncertain (Robertson *et al.*, 2011; Anderson-Teixeira *et al.*, 2013), and hence we need more evidence from field studies to understand these mechanisms.

Land cover directly or indirectly affects soil erosion, water drainage and soil carbon and nutrient processes, which are important factors driving the soil carbon cycle (Montgomery, 2007; Love and Nejadhashemi, 2011). The carbon stocks prior to LUC and the carbon dynamics during and after LUC determine how the soil acts as either a carbon source or a sink after LUC (Guo and Gifford, 2002; Searchinger *et al.*, 2008). Land cover and land use type, including vegetation type and prior (land use history, LUH) and after (crop type, CROP) conversion, therefore, alter the carbon stocks and dynamics in soils and vegetation. However, LUH and CROP may alter

ecosystem carbon dynamics through different biogeochemical processes. While the processes and potential of carbon accumulation in reforestation from abandoned agricultural lands are well known (Compton *et al.*, 1998; Post and Kwon, 2000; Silver *et al.*, 2000; Paul *et al.*, 2002), the climate implications that result from converting agricultural or conservation land into biofuel croplands are not well understood. We need more studies to understand how the expansion or intensification of bioenergy cropping systems around the world impact GHG emissions.

Current and historical land use can modify soil carbon, nutrient and soil pools, as well as microbial community composition, affecting plant growth and soil microbial activities and contributing to soil biogeochemical processes. The LUH, therefore, affects the carbon fluxes among soil carbon pools and the surrounding atmosphere (Lugo and Brown, 1993; Compton *et al.*, 1998; Post and Kwon, 2000; Silver *et al.*, 2000; Paul *et al.*, 2002; Kasel and Bennett, 2007). Relatively nutrient-rich soil (e.g., a grassland in the Conservation Reserve Program, CRP) can respond very differently from nutrient-impoverished soil (e.g., fields that have been subject to long-term cultivation of crops, AGR). In the United States, the repatriation of CRP, the conversion of food-based farms (AGR) and marginal lands to biofuel crops, has been a proposed solution to the growing demand for liquid biofuel (Robertson *et al.*, 2011; Duke *et al.*, 2013). The reduction of soil carbon and nitrogen content after AGR on the Great Plains has long been reported in rangeland and prairie soil (Campbell and Souster, 1982; Tiessen *et al.*, 1982; Aguilar *et al.*, 1988; Bowman *et al.*, 1990). Comparatively, converting farmland into CRP grassland generally recovers soil carbon and nitrogen (Burke et al., 1995; Reeder et al., 1998). The understanding of the response of ecosystem carbon flux to climate patterns between CRP and AGR LUH after LUC can help the trajectory of GHG emissions associated with land conversion for biofuel production, and assist the policy making of bioenergy development.

Crop types (CROP) of a biofuel agricultural system, after LUC, may regulate the amount and timing of carbon gain/loss of the ecosystem via photosynthesis, carbon allocation strategy and soil respiration (Lugo and Brown, 1993; Raich and Tufekcioglu, 2000; Paul *et al.*, 2002; Zak *et al.*, 2003; Dias *et al.*, 2010; Barron-Gafford *et al.*, 2011; Han *et al.*, 2014). Grain-based biofuel crops and cellulosic biofuel crops are two major liquid biofuel crops that produce a significant amount of ethanol nowadays and in the near future, respectively. Grain-based corn biofuel is the major type of biofuel in the USA nowadays because corn grains contain mostly starch and can be easily converted to ethanol. However, the potential environmental impacts, such as soil erosion and nutrient runoff, of the intensive grain-based crops have been noted as a drawback of corn biofuel (Robertson *et al.*, 2011). Perennial cellulosic biofuels, such as switchgrass and mixed prairie grasses, are considered alternative biofuel feedstock because they provide better ecosystem services (Farrell *et al.*, 2006), such as reducing nitrogen leakage and fertilizer subsidies (Duke *et al.,* 2013). Perennial cellulosic biofuel crops can recover the soil organic carbon (SOC) by establishing perennial vegetation without tillage and can further mitigate the soil erosion and increase SOC stocks in roots (West and Marland, 2003). These alternatives are currently considered as target biofuel crops by the European Union (Roberston *et al.*, 2008).

1.1.4 Major carbon processes and pools of ecosystems

Many studies explored the carbon fluxes and storage in ecosystems (Chen *et al.*, 2014). The dynamics of carbon in an ecosystem are mainly determined by carbon gain (GPP) from the photosynthesis (P_N) and carbon loss from ecosystem respiration (R_{eco}) (Eq. 1-1). Carbon, energy and water participate in the reactions. The crop captures CO_2 and solar energy and transpires water to atmosphere by photosynthesis. The fixed carbon and energy are allocated to different requirements, such as basal metabolism, growth and development of stems, roots, leaves, and the

production of secondary compounds and seeds, depending on the phenology, the signal of

environmental condition they receive and their survival strategies. Some carbon is allocated to

belowground tissues or chemicals, such as coarse and fine roots, root exudates or root symbionts

by the plant itself, whereas some eventually enter soil carbon pools after senescence, such as

plant residues, litter, dead roots and root exudates. Soil microbial respiration is fueled by organic

carbon, which ultimately comes from photosynthesis.

Organisms in agricultural ecosystems, whether they are producers, consumers or

decomposers, get energy by oxidizing organic matter and releasing CO_2 when they respire. The

relative rates of photosynthesis and respiration determine the sink or source balance of carbon in

an ecosystem and, thereby, net flux of carbon dioxide from the ecosystem to the atmosphere.

This is denoted as the net ecosystem exchange (NEE) of CO_2:

$$NEE = R_{eco} - GPP \hspace{4cm} \text{Eq. 1-1}$$

where gross primary production (GPP) is the amount of carbon fixed from the atmosphere into

the ecosystem via photosynthesis (P_N). Ecosystem respiration (R_{eco}) is the sum of carbon loss

from the ecosystem/soil to the atmosphere, and NEE is the difference between R_{eco} and GPP.

Some ecologists use net ecosystem production (NEP), which is the negative value of NEE, more

often than NEE. This is because NEP determines the carbon flux from the atmosphere to the

ecosystem, which better represents the ecosystem-centric perspective. One can present the NEP

as the following equation.

$$NEP = GPP - R_{eco} \hspace{4cm} \text{Eq. 1-2}$$

The total ecosystem respiration can be partitioned into aboveground respiration (R_{above})

and belowground respiration (a.k.a. soil respiration, R_s) (Eq. 1-3).

$$R_{eco} = R_{above} + R_s \hspace{4cm} \text{Eq. 1-3}$$

Belowground respiration can also be partitioned into autotrophic and heterotrophic respiration. In my dissertation, I focus on soil respiration. The autotrophic soil respiration (i.e., by plants) is denoted as R_a, while heterotrophic soil respiration (mainly due to microorganisms) is denoted as R_h.

$$R_s = R_a + R_h \hspace{5cm} \text{Eq. 1-4}$$

Soil respiration is an important component in the global carbon cycle. First, soil stores 1500-2400 Pg C globally, which is twice as much as the atmosphere (829 ± 10 Pg C) and three times as much as terrestrial vegetation (420-630 Pg C) (Fig. 1.2, IPCC, 2013). A small change of soil carbon efflux due to widespread drivers, such as climate change and land use conversion, can alter global carbon budgets, especially the atmospheric carbon dioxide concentration. Second, soil respiration can be 60-90% of total ecosystem respiration (Goulden *et al.*, 1996). The variation of soil respiration can change the direction and the amount of carbon flux at local scales. Third, soil carbon efflux responds sensitively and quickly to the climate pattern shifts, climate-derived vegetation changes and agricultural management practices. Soil temperature, soil water and vegetation condition are major drivers of soil respiration. The temperature and rainfall patterns affect the temporal variation of soil respiration directly or indirectly via the vegetation-derived carbon subsidy.

1.1.5 The importance of grassland and cropland ecosystems

Grassland ecosystems may contain different types of grasses and forbs, with some woody plants and shrubs, and occupy 52.5 million square kilometers, or 40.5 percent of the global terrestrial area excluding Greenland and Antarctica (Suttie *et al.*, 2005). Grassland plays an important role in the global carbon cycle due to its large extent and its large carbon storage capacity. However, our understanding of grassland response to climate is still very limited due to

the highly variable vegetation types and compositions, temperature and precipitation patterns, soil properties and disturbances, and the worldwide distribution of these ecosystems. Many studies have shown that grasslands can be carbon sinks, at least during the growing season (Belelli *et al.*, 2007; Flanagan *et al.*, 2002). In contrast, some studies demonstrated that grassland ecosystems can vary between a sink or source of carbon inter-annually (Dugas *et al.*, 1998), depending on precipitation amounts and patterns. Even in the same ecosystem in the same year, the NEE may be highly variable due to the seasonal and intra-annual temperature and rainfall patterns or extreme climate events (Kim, 1992). The different responses between gross primary production (GPP) and total ecosystem respiration (R_{eco}) to the climate patterns and extremes may vary and, sometimes, shift the carbon balance from sink to source.

Agricultural ecosystems are similar to grasslands and include variable vegetation types that are distributed worldwide in different climate regimes and soils, store carbon in soil, and experience frequent disturbances that keep the ecosystem in an early successional stage. They exchange all three major GHGs with the atmosphere and are crucial for the mitigation of global warming (Robertson et al., 2000). Cropping ecosystems are intensively managed by humans. Agricultural management practices, such as crop type, the rotation of crops, cover crops, fertilization, tillage, agricultural chemical applications, harvest, and the successional stage, not only change the dominant vegetation, but also affect the physical and chemical status of soil and the soil microbial community, which impacts the biogeochemical cycles and the global warming potential (GWP) (Robertson *et al.*, 2000).

1.2 THE CONCEPTUAL FRAMEWORK

Many studies explored the carbon stocks in different carbon pools and the fluxes among the pools. The carbon fluxes are controlled by biophysical variables underlying different

10

mechanisms. The different responses of the carbon fluxes due to different mechanisms result in the seasonal and annual fluctuations of carbon dioxide NEE and the relative contributions of different carbon fluxes components (i.e., GPP:R_{eco}, R_a: R_s ratios). The conceptual framework of how the land use conversion affects carbon processes was presented in Fig. 1.3. I hypothesized that the abiotic and biotic variables (i.e., temperature, water and nutrient availability, vegetation types, leaf area index, phenology and soil microbial activities) determine the major carbon processes (i.e., photosynthesis, ecosystem respiration, autotrophic and heterotrophic soil respiration).
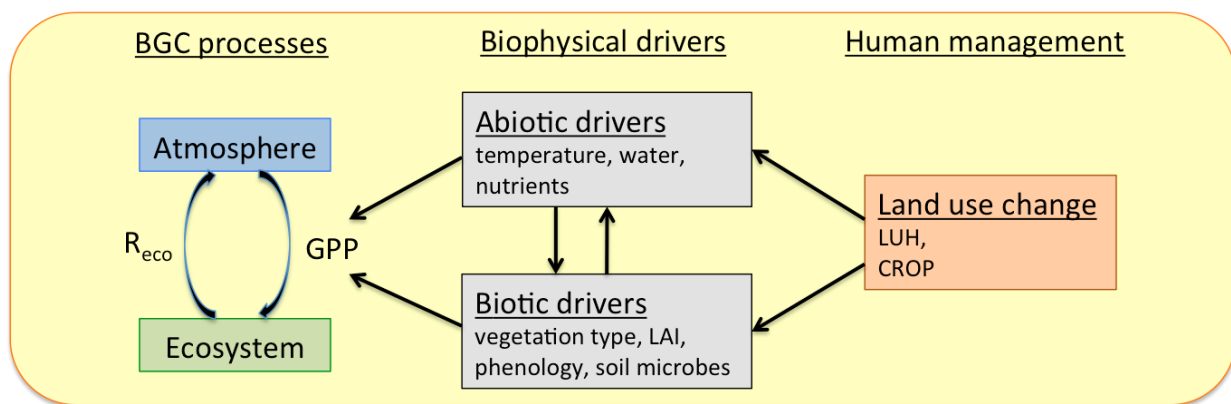
Figure 1.3. The conceptual framework of the major carbon processes between ecosystem and the atmosphere, their biophysical drivers and how human management affect them. GPP and R_{eco} determine the net ecosystem exchange (NEE) of carbon dioxide between the ecosystem and the atmosphere. Biotic and abiotic drivers affect photosynthesis and respiration, indirectly altering NEE. Human management, such as land use change, changes the crop types and soil properties and, therefore affect the biophysical variables and carbon processes. BGC: biogeochemical cycle; GPP: gross primary production; R_{eco}: ecosystem respiration; LAI: leaf area index; LUH: land use history; CROP: crop types.

More specifically, managed land use conversion from different historical land use types may affect the current crop types and soil nutrient content. Different crop types may have different length of phenology stages and carbon allocation strategies, different water tolerance abilities and, water use efficiency and, therefore, they may respond to climate differently. The

different soil carbon and nitrogen alter the available soil nitrogen to plants and soil microbes, and, thus, affect plant growth and photosynthesis and carbon emission from soil (Fig. 1.4). In this dissertation, I discuss how soil respiration responds to specific climate patterns and severe droughts across different LUH and CROP at inter-annual (Ch. 2) and intra-annual (Ch. 3) scales. I also develop Bayesian models to understand the R-T_s relationship change resulting from a severe drought (Ch. 4). In Chapter 5, I explored the different responses of GPP, R_{eco} and R_s to the climate pattern and the severe drought in a particular year.
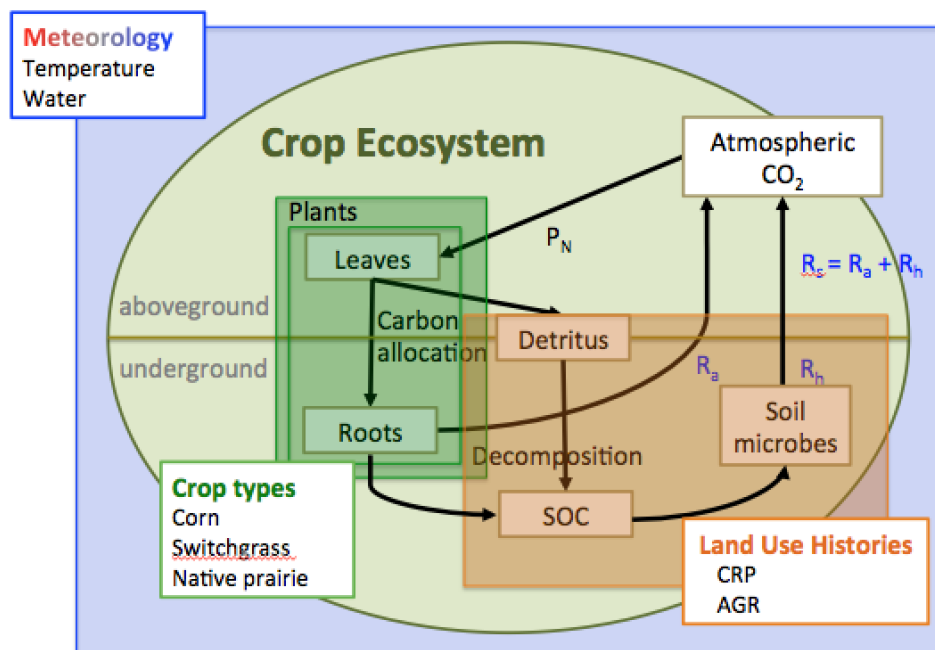
Figure 1.4. The theoretical framework on the impact of LUH and CROP on the net ecosystem exchange (NEE) of CO$_2$ and soil respiration (R$_s$). P_N: photosynthesis; R_a: autotrophic soil respiration; R_h: heterotrophic soil respiration; CRP: Conservation Reserve Program brome grassland; AGR: conventional corn-soybean rotation agricultural farm; SOC: soil organic carbon. CROP affects the biological reaction in the green square while LUH affects the soil microbiological reactions in the orange square. Meteorological factors influence all reactions.

1.3 OBJECTIVES

My dissertation aims to understand the temporal changes of net ecosystem exchange (NEE) and soil respirations (R) in an annual grain (continuous corn, C), a monoculture perennial grass (switchgrass, Sw), and a multicultural perennial grassland crop (prairie mixture, Pr), which are all managed as biofuel crops on land converted either from the Conservation Reserve Program (CRP) grassland or conventional agricultural farmland (AGR). The ecosystems with different CROP and LUH may respond differently to climate patterns within and across years in their gross primary production (GPP), ecosystem respiration (R_{eco}), and the partitioning of ecosystem respiration into total soil respiration (R_s), autotrophic respiration (R_a) and heterotrophic soil respiration (R_h). The responses of respiration to long-term climate patterns, short-term-regular climate events, and the resistance and the resilience to short-term events reveals how carbon processes in these ecosystems respond to climate after land use conversion.

1.3.1 Objectives of Study

1. How do biophysical variables affect soil respiration (R) across years after land use change:

   (A) Examine the correlation between soil respiration and biophysical variables.

   (B) Develop regression models of the effects of soil temperature, soil moisture and vegetation index on soil respiration for each study site to predict autotrophic soil respiration (R_a) and the root contribution (RC) to total soil respiration (R_a:R_s ratio).

   (C) Study the interannual changes of growing-season R_a:R_s ratio after land use changes and a severe drought in fields with different crop types (CROP) and land use histories (LUH).

2. How does seasonal variation in biophysical variables affect soil respiration (R):

(A) Quantity how the seasonal patterns of temperature and soil moisture relate to the seasonality of soil respiration (R_s and R_h)

(B) Study the shift of the relative importance of biophysical variables through the growing season.

(C) Compare the seasonality of the R_a: R_h ratio in different CROP and LUH.

3. How does the soil respiration (R) – temperature (T_s) relationship change after the severe drought?

(A) Develop an analysis method by the Bayesian approach to elucidate the relationship between soil respiration (R) and its major driver (T_s). The temperature sensitivity (β) of log R and the log R at 20 $^{\circ}$C (LR_{20}) will be estimated based on the models.

(B) Understand how the R-T_s relationship shifts after a severe spring-summer drought in different CROP and LUH combinations at the inter- and intra-annual scales.

(C) Recognize the immediate and prolonged effects of severe drought on the R-T_s relationship in different CROP and LUH.

4. How do the various carbon fluxes respond to the changes of the major drivers?

(A) Explore the predominant regulators of the major carbon fluxes.

(B) Examine how the seasonal patterns of GPP:R_{eco}, R_{above}:R_s, and R_a:R_h ratios are affected by different microclimate patterns, LUH and CROP.

(C) Study the response of important ecological processes, such as GPP, R_{eco}, R_{above}, R_s, R_a and R_h to different climatic events (e.g. spring-summer drought), and how these processes alter the NEE of CO_2.

1.3.2 Hypotheses

The estimate of carbon stocks and fluxes were complex and multifaceted, since different drivers alter carbon flow differently, underlying different mechanisms. Biophysical variables on soil respiration, ecosystem respiration and GPP vary across different biomes and climate regimes (Chen *et al.*, 2014). The following is my hypotheses.

1. How do biophysical variables affect soil respiration (R) across years after land use change:

    (A) Soil respiration exponentially correlates to soil temperature and vegetation indices, but is not significantly correlated to soil water content.

    (B) Total and heterotrophic soil respiration have different parameters to biophysical variables in different combinations of CROP and LUH fields.

    (C) Perennial crops have increasing root contributions to total soil respiration, while annual crop does not. The CRP fields have lower RC than AGR fields, but the RC values in CRP fields increase year by year.

2. How does seasonal variation in biophysical variables affect soil respiration (R):

    (A) The seasonality of soil temperature and vegetation index determines the seasonality of R_s and R_h.

    (B) Soil water content may be crucial for soil respiration during summer dry period.

    (C) The RC may be high in early spring and mid-summer due to the high growth and activities of roots while soil microbial activities respond to climate and photosynthesis-derived carbon input may be delayed and gentle. Perennial and annual crop have different RC seasonality due to different phenology among the crops.

3. How does the soil respiration (R) to temperature (T_s) relationship change with the severe drought?

(A) The probability distributions of R_s and R_h are located differently across the β-LR_{20} biplots. The Reference (Ref) field has high β and LR_{20} while corn fields have low LR_{20}. Other perennial crops have intermediate LR_{20} values.

(B) Both β and LR_{20} of R_a and R_h in perennial crops decrease in the drought year (2012) and then rebound in the following years (2013 and 2014). The prolonged effects of drought on the R-T relationship in perennial crop fields were remarked. Both β and LR_{20} of R_a and R_h in annual crops decrease in the drought year (2012). However, the prolonged effect of R_a disappears.

4. How do the various carbon fluxes respond to changing drivers?

(A) GPP correlated strongly to photosynthetically active radiation (PAR) while R_{eco} is dominated by temperature.

(B) The higher GPP:R_{eco}, R_{above}:R_s, and R_a:R_h ratios occurred in early spring and mid-summer since production was stronger than respiration, aboveground parts were quicker than belowground parts and because roots were quicker to respond than soil microbes, respectively. The different seasonality of these ratios between perennial and annual crops are due to difference in phenology among the crop types.

(C) NEE decreases in order: Ref > annual crop > perennial crops. Ref, the late succession grassland has weak carbon sequestration capability. NEE in annual crop fields are larger than those in perennial crops fields due to shorter growing seasons (GS).

(D) The impacts of severe drought on GPP are stronger than it is on R_{eco}, resulting in an increase of NEE. The increasing drought events in the future may decrease the ability to

sequester carbon in cropping ecosystems, especially for the annual crop.

(E) The R_s:R_{eco} ratio in perennial crop fields increase due to the development of dense root systems while those in annual crop fields do not.

1.4 STUDY AREA

My experimental sites are located at the Great Lakes Bioenergy Research Center scale-up fields of the Kellogg Biological Station (KBS, 42°40'N, 85°40'W), established in association with the KBS Long-Term Ecological Research (LTER) site. The sites are located in the south Michigan, USA (Fig. 1.2). with a humid continental (warm summer) climate (Dfa) (Peel *et al.*, 2007). The mean annual air temperature and mean annual precipitation at KBS are 10.1 °C and 1005 mm yr^{-1} (1981-2010), respectively (Robertson & Hamilton, 2015).
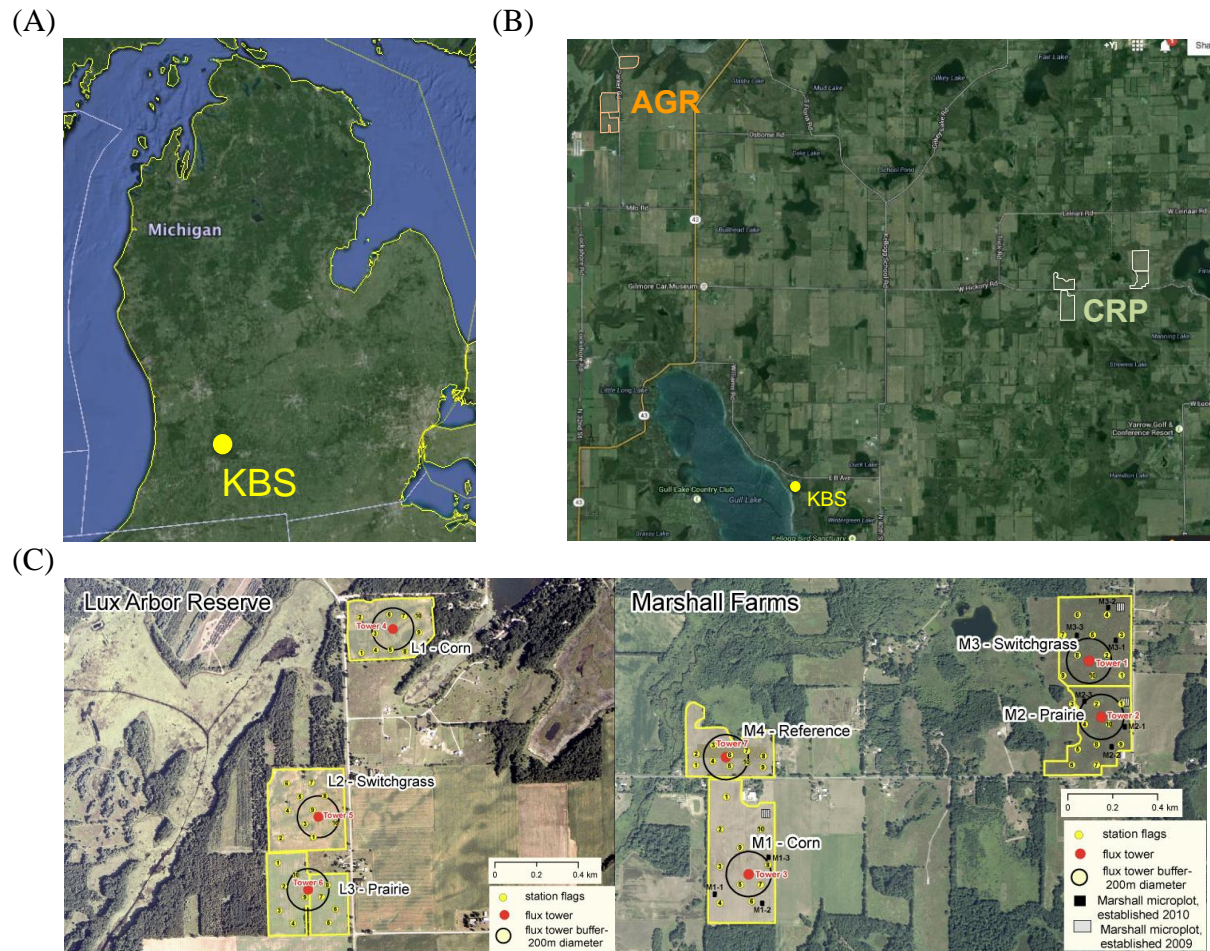
Figure 1.5. The location of research sites and experimental design. The research fields are located in two areas that have different land use histories at Kellogg Biological Station (KBS) scale-up sites in southwest Michigan (A & B). The two land use histories include CRP and AGR (C). CRP: Conservation Reserve Program brome grassland at Marshall Farms; AGR: conventional corn-soybean rotation agricultural farms at Lux Arbor Reserve. AGR converted to three crop types, switchgrass, prairie mixture and corn. CRP changed to the same crops in AGR, adding a reference site (Ref). The Ref were maintained as CRP brome grass without agricultural practices.

18

1.5 EXPERIMENTAL DESIGN AND SCHEDULE

Seven experimental plots were divided between two locations, each with its own land use history (LUH): (1) Conservation Reserve Program (CRP) grasslands at Marshall Farm; and (2) corn-soybean rotation agricultural fields (AGR) at Lux Arbor Reserve. The CRP sites have been in a monoculture of smooth brome grass (*Bromus inermis* Leyss) since 1987, while the AGR fields have been under conventional corn-soybean rotation cultivation for several decades (Fig. 1.6). The soil texture at all sites is sandy loam, except for a sandy clay loam at one field. However, soil carbon and nitrogen contents at the CRP sites were significantly higher than those at the AGR sites before the land conversions (Table 1.1).

Table 1.1. Soil texture and soil properties of the seven experiment sites before the land use conversion. In the land use history (LUH) column, CRP sites are grasslands of the Conservation Reserve Program and AGR sites are conventional corn-soybean agricultural farms. Different superscripts denote significant difference of nitrogen or carbon content using the t-test ($p<0.05$). See text and Fig. 1.6 for treatment codes (from KBS LTER datatables; https://lter.kbs.msu.edu/datatables)

Treatment	Area (ha)	LUH	Soil texture	Sand	Silt	Clay	Soil pH	Bulk density (g cm^{-3})	N	C
					(g kg^{-1} soil)				(g kg^{-1} soil)	
CRP-C	17	CRP	Sandy loam	664±29	257±24	80±8	6.0±0.1	1.58	2.0[c]	21.2[c]
CRP-Sw	13	CRP	Sandy loam	688±25	265±23	48±6	5.7±0.1	1.66	1.6[d]	18.5[c]
CRP-Pr	11	CRP	Sandy loam	697±53	245±42	58±12	6.3±0.2	1.59	1.7[d]	19.5[c]
AGR-C	11	AGR	Sandy loam	577±26	337±23	86±12	6.0±0.1	1.54	1.2[a]	12.2[a]
AGR-Sw	14	AGR	Sandy loam	651±31	271±24	79±12	6.1±0.1	1.79	1.1[a]	10.8[b]
AGR-Pr	13	AGR	Sandy clay loam	495±32	360±31	146±10	5.8±0.1	1.69	1.4[b]	13.5[a]
Ref	9	CRP	Sandy loam	583±28	342±25	75±8	6.2±0.1	1.56	1.9[c]	20.9[c]

The experiment was conducted at seven scale-up fields ranging in size from 9 to 17 hectares. Four fields are located in Marshall Farm (i.e., CRP sites) and three in Lux Arbor Reserve (i.e., AGR sites). All sites, except the reference site (Ref), were sprayed with herbicide at the end of 2008 to prepare the lands for soybean planting in 2009. The CRP and AGR sites

were then cultivated with either continuous corn (*Zea mays*, Dekalb DK-52), switchgrass (*Panicum virgatum*) or a mixture of native prairie grasses that had been dominated by Canada wild rye (*Elymus Canadensis*), little bluestem (*Schizachyrium scoparium*), Indian grass (*Sorghastrum nutans*), big bluestem (*Andropogon gerardii*) and switchgrass (*Panicum virgatum*) since 2010. One CRP grassland, dominated by brome grass, was not disturbed and retained as the historical reference site (Gelfand *et al.*, 2011; Zenone *et al.*, 2011; Deal *et al.*, 2013; Zenone *et al.*, 2013). I used an experimental code for these sites by abbreviating them as "LUH-CROP". CRP-C, CRP-Sw and CRP-Pr represent the CRP sites that were converted to corn, switchgrass and prairie mixture respectively, while AGR-C, AGR-Sw and AGR-Pr are AGR farms converted to corn, switchgrass and prairie mixture. In 2010, when the crops were established, the perennial crops (switchgrass and prairie) were accompanied by oats as nurse crop with and without fertilization, respectively (Fig. 1.6). Switchgrass fields were applied with 55 kg N ha^{-1} (28% liquid urea ammonium nitrate) on DOY 172. No other management practices were applied beyond harvesting at the end of each growing season. No-till continuous corn was seeded in mid-May with a one-time herbicide mix (Lumax, Atrazine 4L, Honcho Plus and $(NH_4)_2SO_4$). Phosphorus, potassium ($P_2O_5 + K_2O$, 168.5 kg ha^{-1} on DOY 95, 2010) and nitrogen fertilizers (112 kg N ha^{-1} on DOY 165 & 160 in AGR-C and CRP-C, respectively) were applied in 2010. Phosphorus, potassium ($P_2O_5 + K_2O$, 294 kg ha^{-1} on DOY 104, 2011) and nitrogen fertilizers (liquid nitrogen168 kg N ha^{-1} on DOY 172, 2011) were applied (Bhardwaj *et al.*, 2011; Zenone *et al.*, 2013).
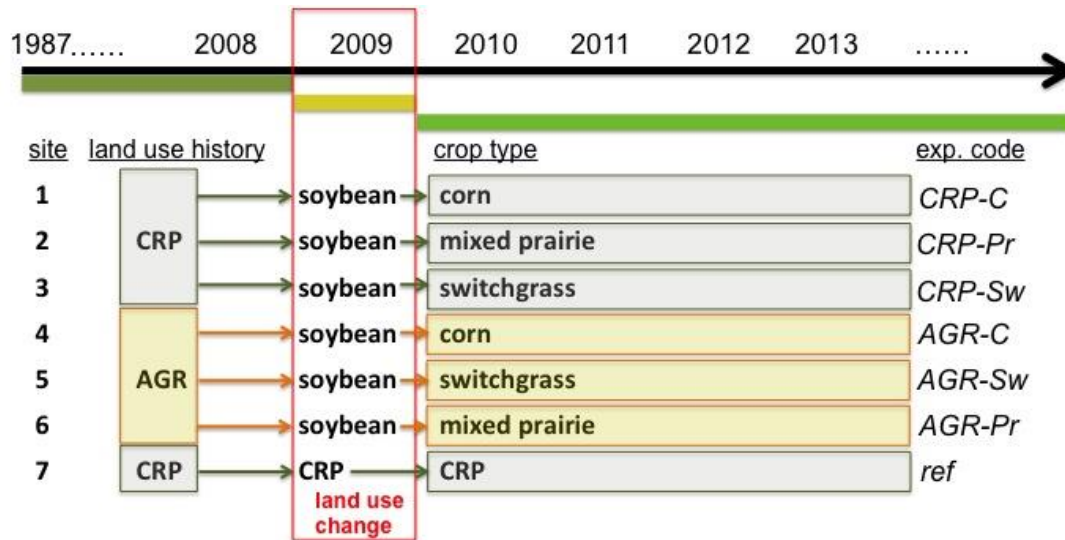
Figure 1.6. The experimental design and schedule of agricultural management. Land use before 2008 (land use history, LUH) included brome grass fields that were enrolled in the Conservation Reserve Program (CRP) for 22 years, as well as conventional corn-soybean rotation cultivations in the other fields (AGR). Research sites, except Ref, were planted in soybean in 2009 to facilitate conversion. We planted three bioenergy crops—continuous corn (C), a monoculture of switchgrass (Sw) and a polycultural prairie mixture (Pr).

LITERATURE CITED

LITERATURE CITED

Aguilar, R., Kelly, E.F., Heil, R.D., 1988. Effects of cultivation on soils in northern Great Plains rangeland. Soil Science Society of America Journal, 52, 1081-1085.

Anderson-Teixeira, K.J., Masters, M.D., Black, C.K., Zeri, M., Hussain, M.Z., Bernacchi, C.J., DeLucia, E.H., 2013. Altered belowground carbon cycling following land-use change to perennial bioenergy crops. Ecosystems, 16, 508-520.

Barron-Gafford, G.A., Scott, R.L., Jenerette, G.D., Huxman, T.E., 2011. The relative controls of temperature, soil moisture, and plant functional group on soil CO_2 efflux at diel, seasonal, and annual scales. Journal of Geophysical Research, 116, G01023.

Belelli Marchesini, L., Papale, D., Reichstein, M., Vuichard, N., Tchebakova, N., Valenini, R., 2007. Carbon balance assessment of a natural steppe of southern Siberia by multiple constaint approach. Biogeosciences, 4, 581-595.

Bowman, R.A., Reeder, J.D., Lober, R.W., 1990. Changes in soil properties in a central plains rangeland soil after 3, 20, and 60 years of cultivation. Soil Science, 150, 851-857.

Burke, I.C., Lauenroth, W.K., Coffin, D.P., 1995. Soil organic matter recovery in semiarid grasslands: Implications for the Conservation Reserve Program. Ecological Applications, 5, 793-801.

Campbell, C.A., Souster, W., 1982. Loss of organic matter and potentially mineralizable nitrogen from Saskatchewan soils due to cropping. Canadian Journal of Soil Science, 62, 651-656.

Chen, J., John, R., Sun, G., McNulty, S., Noormets, A., Xiao, J., Turner, M.G., Franklin, J.F., 2014. In: Azevedo, J.C., Perera A.H., Pinto, M.A. (Eds.). Forest Landscapes and Global Change: Challenges for Research and Management. DOI 10.1007/978-1-4939-0953-7_6, © Springer Science+Business Media New York.

Compton, J.E., Boone, R.D., Motzkin, G., Foster, D.R., 1998. Soil carbon and nitrogen in a pine-oak sand plain in central Massachusetts: Role of vegetation and land-use history. Oecologia, 116, 536-542.

Davidson, E.A., Ackerman, I.L., 1993. Changes in soil carbon inventories following cultivation of previously untilled soils. Biogeochemistry, 20, 161-193.

Deal, M.W., Xu, J., John, R., Zenone, T., Chen, J., Chu, H., Jasrotia, P., Kahmark, K., Bossenbroek, J., Mayer, C., 2013. Net primary production in three bioenergy crop systems following land conversion. Journal of Plant Ecology, 6, 1-10.

Dias, A.T.C., van Ruijven, J., Berendse, F., 2010. Plant species richness regulates soil respiration through changes in productivity. Oecologia, 163, 805-813.

Dugas, W.A., Heuer, M.L., Mayeus, H.S., 1999. Carbon dioxide fluxes over bermudagrass, native prairie, and sorghum. Agricultural and Forest Meteorology, 93, 121-139.

Duke, C.S., Pouyat, R.V., Robertson, G.P., Parton, W.J., 2013. Ecological dimensions of biofuels. Issues in Ecology, 17, 1-17.

Fargione, J., Hill, J., Tilman, D., Polasky, S., Hawthorne, P., 2008. Land clearing and the biofuel carbon debt. Science, 319, 1235-1238.

Farrell, A.E., Plevin, R.J., Turner, B.T., Jones, A.D., O'Hare, M., Kammen, D.M., 2006. Ethanol can contribute to energy and environmental goals. Science, 311, 506-508.

Flanagan, L.B., Wever, L.A., Carlson, P.J., 2002. Seasonal and interannual variation in carbon dioxide exchange and carbon balance in a northern temperate grassland. Global Change Biology, 8, 599-615.

Gelfand, I., Sahajpal, R., Zhang, X., Izaurralde, R.C., Gross, K.L., Robertson, G.P., 2013. Sustainable bioenergy production from marginal lands in the US Midwest. Nature, 493, 514-517.

Gelfand, I., Zenone, T., Jasrotia, P., Chen, J., S.K.Hamilton, Robertson, G.P., 2011. Carbon debt of conservation reserve program (CRP) grasslands converted to bioenergy production. PNAS, 108, 13864-13869.

Goulden, M.L., Munger, J.W., Fan, S.M., Daube, B.C., Wofsy, S.C., 1996. Exchange of carbon dioxide by a deciduous forest: Response to interannual climate variability. Science, 271: 1576-1578.

Guo, L.B., Gifford, R.M., 2002. Soil carbon stocks and land use change: a meta analysis. Global Change Biology, 8, 345-360.

Han, G., Xing, Q., Luo, Y., Rafique, R., Yu, J., Mikle, N., 2014. Vegetation types alter soil respiration and its temperature sensitivity at the field scale in an estuary wetland. PLoS One, 9, e91182.

Hansen, E.A., 1993. Soil carbon sequestration beneath hybrid poplar plantations in the north central Uniter States. Biomass and Bioenergy, 5, 431-436.

Houghton, R.A., House, J.I., Pongratz, J., van der Werf, G.R., DeFries, R.S., Hansen, M.C., Le Quéré, C., Ramankutty, N., 2012. Carbon emissions from land use and land-cover change. Biogeosciences, 9, 5125-5142.

IPCC, 2013: Climate Change 2013: The Physical Science Basis. Contribution of Working Group I to the Fifth Assessment Report of the Intergovernmental Panel on Climate Change. In: Stocker, T.F., D. Qin, G.-K. Plattner, M. Tignor, S.K. Allen, J. Boschung, A. Nauels, Y. Xia, V. Bex and P.M. Midgley (Eds.), Cambridge University Press, Cambridge, United Kingdom and New York, NY, USA, 1535 pp, doi: 10.1017/CBO9781107415324.

Kasel, S., Bennett, L.T., 2007. Land-use history, forest conversion, and soil organic carbon in pine plantations and native forests of south eastern Australia. Geoderma, 137, 401-413.

Kim, H., Kim, S., Dale, B.C., 2009. Biofuels, land use change and greenhouse gas emissions: some unexplored variables. Environmental Science and Technology, 43, 961-967.

Kim, J., Verma S.B., Clement, R.J., 1992. Carbon dioxide budget in a temperate grassland ecosystem. Journal of Geophysical Research, 97 (D5), 6057-6063.

Liu, J., Mooney, H., Hull, V., Davis, S.J., Gaskell, J., Hertel, T., Lubchenco, J., Seto, K.C., Gleick, P., Kremen, C., Li, S., 2015. Systems integration for global sustainability. Science, 347(6225), 1258832-8.

Love, B.J., Nejadhashemi, A.P., 2011. Water quality impact assessment of large-scale biofuel crops expansion in agricultural regions of Michigan. Biomass and Bioenergy, 35, 2200-2216.

Lugo, A.E., Brown, S., 1993. Management of tropical soils as sinks or sources of atmospheric carbon. Plant and Soil, 149, 27-41.

Mitchell, S.R., Harmon, M.E., O'Connell, K.E.B., 2012. Carbon debt and carbon sequestration parity in forest bioenergy production. Global Change Biology Bioenergy, 4, 818-827.

Montgomery, D.R., 2007. Soil erosion and agricultural sustainability. Proceedings of the National Academic of Sciences of the USA, 104, 13268-13272.

Paul, K.I., Polglase, P.J., Nyakuengama, J.G., Khanna, P.K., 2002. Change in soil carbon following afforestation. Forest Ecology and Management, 168, 241-257.

Peel, M.C., Finlayson, B.L., McMahon, T.A., 2007. Updated world map of the Kȯppen-Geiger climate classification. Hydrology and Earth System Sciences Discussions, 4, 439-473.

Post, W.M., Kwon, K.C., 2000. Soil carbon sequestration and land-use change: Processes and potential. Global Change Biology, 6, 317-328.

Raich, J.W., Tufekcioglu, A., 2000. Vegetation and soil respiration: Correlations and controls. Biogeochemistry, 48, 71-90.

Reeder, J.D., Schuman, G.E., Bowman, R.A., 1998. Soil C and N changes on conservation reserve program lands in the Central Great Plains. Soil and Tillage Research, 47, 339-349.

Robertson, G.P., Paul, R.R., Harwood, R.R., 2000. Greenhouse gases in intensive agriculture: Contributions of individual gases to the radiative forcing of the atmosphere. Science, 289: 1922–1925.

Roberston, G.P., Dale, V.H., C., D.O., Hamburg, S.P., Melillo, J.M., Wander, M.M., Parton, W.J., Adler, P.R., Barney, J.N., Cruse, R.M., Duke, C.S., Fearnside, P.M., Follett, R.F., Gibbs, H.K., Jose, G., Mladenoff, D.J., Ojima, D., Palmer, M.W., Sharpley, A., Wallace,

L., Weathers, K.C., Wiens, J.A., Wilhelm, W.W., 2008. Sustainable biofuels redux. Science, 322, 49-50.

Robertson, G.P., Hamilton, S.K., Del Grosso, S.J., Parton, W.J., 2011. The biogeochemistry of bioenergy landscapes: carbon, nitrogen, and water considerations. Ecological Applications, 21, 1055-1067.

Robertson, G.P., Hamilton, S.K., 2015. Long-term ecological research at the Kellogg Biological Station LTER site: conceptual and experimental framework. In: Hamilton, S.K., Doll, J.E., Robertson, G.P. (Eds.), The Ecology of Agricultural Landscapes. Oxford University Press, New York, pp. 1-32.

Ruan, L., Robertson, G.P., 2013. Initial nitrous oxide, carbon dioxide, and methane costs of converting conservation reserve program grassland to row crops under no-till vs. conventional tillage. Global Change Biology, 19, 2478-2489.

Searchinger, T., Heimlich, R., Houghton, R.A., Dong, F., Elobeid, A., Fabiosa, J., Tokgoz, S., Hayes, D., Yu, T.-H., 2008. Use of U.S. croplands for biofuels increases greenhouse gases through emissions from land use change. Science, 319, 1238-1240.

Silver, W.L., Ostertag, R., Lugo, A.E., 2000. The potential for carbon sequestration through reforestation of abandoned tropical agricultural and pasture lands. Restoration Ecology, 8, 394-407.

Suttie, J.M., Reynolds, S.G., Batello, C., 2005. Grasslands of the World. Food and Agriculture Organization of the United Nations. Plant production and protection series, 0259-2025; No. 34. Rome. ISBN: 9251053375.

Tiessen, H., Stewart, J.W.B., Bettany, J.R., 1982. Cultivation effects on the amounts and concentration of carbon, nitrogen, and phosphorus in grassland soils. Aaron Journal, 74, 831-835.

West, T.O., Marland, G., 2003. Net carbon flux from agriculture: Carbon emissions, carbon sequestration, crop yield, and land-use change. Biogeochemistry, 63, 73-83.

Zak, D.R., Holmes, W.E., White, D.C., Peacock, A.D., Tilman, D., 2003. Plant diversity, soil microbial communities, and ecosystem function: are there any links?. Ecology, 84, 2042-2050.

Zenone, T., Chen, J., Deal, M.W., Wilske, B., Jasrotia, P., Xu, J., Bhardwaj, A.K., Hamilton, S.K., Robertson, P.G., 2011. CO_2 fluxes of transitional bioenergy crops: effect of land conversion during the first year of cultivation. GCB Bioenergy, 3, 401-412.

Zenone, T., Gelfand, I., Chen, J., Hamilton, S.K., Robertson, G.P., 2013. From set-aside grassland to annual and perennial cellulosic biofuel crops: Effects of land use change on carbon balance. Agricultural and Forest Meteorology, 182-183, 1-12.

Zona, D., Janssens, I.A., Aubinet, M., Gioli, B., Vicca, S., Fichot, R., Ceulemans, R., 2013. Fluxes of the greenhouse gases (CO_2, CH_4 and N_2O) above a short-rotation poplar plantation after conversion from agricultural land. Agricultural and Forest Meteorology, 169, 100-110.

CHAPTER 2
INTERANNUAL VARIATIONS OF SOIL RESPIRATION AND ITS RESPONSE TO MICROCLIMATE

ABSTRACT

In this study, I discovered that soil temperature and vegetation type affect soil respiration, whereas soil moisture has weak or no effect. Soil respiration declined in 2012 as the spring-summer drought depressed plant growth and soil microbial activity. The drought lasted for just a couple of months but had an impact on soil respiration that lasted for more than one year. The root contribution to total soil respiration deceased in AGR-Sw, CRP-Pr and AGR-Pr fields, implying the drought affected autotrophic respiration more than heterotrophic respiration. The reference field, which did not experience land use change, had the highest soil respiration compared to all experimental treatments except for the CRP-Pr site in 2014, suggesting that the multicultural prairie ecosystem with high soil carbon and nitrogen content had established their extensive root systems within five years after its establishment. The annual crop (corn) had the lowest soil respiration without an obvious trend, considering the drought impact. Perennial crops (switchgrass and prairie mixture) had higher soil respiration than corn. In contrast to corn, perennial crops' total soil respiration increased over the years after land use change. Pr and CRP had higher rates of increase in R_s than Sw and AGR, respectively. The R_s and R_h in the CRP-Pr site were higher or equal to those in Ref, demonstrating that well established root systems have an association with increasing soil microbial activities. The CRP sites had higher soil respiration than the AGR sites in 2011 due to high soil carbon and nitrogen content. I did not find a clear decline in heterotrophic soil respiration, perhaps due to the legacy effect of the 2012 drought or because the experimental period was too short to detect the change. My study clarified how

autotrophic and heterotrophic soil respiration responds to the impacts of a particular year's

climate pattern and severe drought, as well as the effects caused by land use conversion (i.e.,

different land use histories and crop types at different temporal scales).

2.1 INTRODUCTION

Soil respiration (R_s) plays an important role in the global carbon cycle, as soil contains a

huge amount of carbon (Post *et al.*, 1982). Soil respiration is usually the major component of

total ecosystem respiration (Goulden *et al.*, 1996; Longdoz *et al.*, 2000) and is an important flux

to the atmosphere (Raich *et al.*, 2002; Raich & Schlesinger, 1992; Ryan & Law, 2005;

Schlesinger & Andrews, 2000). It is also sensitive to climate and susceptible to climate change,

anthropogenic management and agricultural practices. Soil respiration responses to climate- and

human-induced environmental changes are crucial components in the overall ecosystem response

to global climate change.

Many previous studies explored how major biophysical drivers affect soil respiration and

how to better model these processes. Temperature, water availability, and carbon substrate

supply from canopy photosynthesis (Arrhenius, 1889; Curiel Yuste *et al.*, 2003; Reichstein *et al.*,

2003; Lloyd & Taylor, 1994; van't Hoff, 1885) affect biogeochemical or ecological processes

from individual to ecosystem levels (Hopkins et al., 2013). These drivers can be distinguished as

either climate-driven or microclimate-driven, where microclimate is defined here as the

conditions at a particular field site (e.g., due to soils, vegetation, and management). However,

there are still many gaps in our understanding of how soil respiration responds to the changing

climate and human activity, as the net balance of soil carbon is influenced by multiple abiotic

(e.g., temperature, moisture and nutrient availability) and biotic (e.g., crop types and soil

microbial composition) factors and their interactions. The relative importance of the biophysical

drivers that regulate soil respiration vary with climate regime and biome (Hanson *et al.*, 2000).

The different components of soil respiration (i.e., R_a and R_h) may be confounding when they

have different magnitudes, timing and response durations to the drivers, and when the major

physiological and biogeochemical processes are different (Carbone *et al.*, 2011). The situation

can be even more difficult to understand when anthropogenic influences, such as land use change

and agricultural practices (e.g., due to biofuel crop production), are considered.

In this chapter, I discuss how total soil respiration (R_s) and its components (R_a and R_h)

respond to variability in climate and microclimate at interannual scale. I examined the effects of

land use histories (LUH) and crop types (CROP) on autotrophic and heterotrophic soil

respiration. I hypothesized that annual crop had lower annual soil respiration compared to

perennial crops due to the shorter growing season. I also hypothesized that conventional

agricultural fields (AGR), which have low soil carbon and nitrogen content, have lower soil

respiration than CRP fields. I clarify the correlations between soil respiration (R_s and R_h) and the

major biophysical drivers (T_a, VWC, NDVI and EVI) and establish the temperature-water-

vegetation (TWV) models for R_s and R_h based on the correlations. The adjusted R_h and R_a were

calculated and the root contribution (RC) of soil respiration was estimated for each year. I

assumed that RC would be lower in severely dry years, where water deficit depresses the growth

of plants during growing seasons and, thus, limits the activities of roots more than the soil

microbial community.

2.2 METHODS

2.2.1 Study area

My experimental sites are located at the Great Lakes Bioenergy Research Center scale-up

fields at the Kellogg Biological Station (KBS, 42°40'N, 85°40'W), established in association

with the KBS Long-Term Ecological Research (LTER) site. The sites are located in the

southwest of Michigan, USA (Fig. 1.2), with a humid continental (warm summer) climate (Dfa)

(Peel *et al.*, 2007). The mean annual air temperature and mean annual precipitation at KBS are

10.1 °C and 1005 mm yr^{-1} (1981-2010), respectively (Robertson & Hamilton, 2015).

2.2.2 Experimental design and schedule

Seven experimental plots were located at two locations, each with its own land use

histories (LUHs): (1) Conservation Reserve Program (CRP) grasslands at Marshall Farm, and (2)

corn-soybean rotation agricultural fields (AGR) at Lux Arbor Reserve. The CRP sites have been

a monoculture of smooth brome grass (*Bromus inermis* Leyss) since 1987, while the AGR fields

have been under conventional corn-soybean rotation cultivation for several decades (Fig. 1.6).

The soil texture at all sites is sandy loam, except for one field, which has sandy clay loam.

However, soil carbon and nitrogen contents at the CRP sites were significantly higher than those

at the AGR sites before land conversion (Table 1.1).

The experiment was conducted at seven scale-up fields ranging from 9-17 hectares. Four

fields are located in Marshall Farm (i.e., CRP sites) and three in Lux Arbor Reserve (i.e., AGR

sites). All sites, except the reference site (Ref), were sprayed with herbicide at the end of 2008 to

prepare the lands for soybean planting in 2009. The CRP and AGR sites were then cultivated

with either continuous corn (*Zea mays*, Dekalb DK-52), switchgrass (*Panicum virgatum*), or a

mixture of native prairie grasses dominated by Canada wild rye (*Elymus Canadensis*), little

bluestem (*Schizachyrium scoparium*), Indian grass (*Sorghastrum nutans*), big bluestem

(*Andropogon gerardii*), and switchgrass (*Panicum virgatum*) since 2010. One CRP grassland,

dominated by brome grass, was not disturbed and retained as the reference site (Gelfand *et al.*, 2011; Zenone *et al.*, 2011; Deal *et al.*, 2013; Zenone *et al.*, 2013). I used an experimental code for these sites by abbreviating them as "LUH-CROP". CRP-C, CRP-Sw and CRP-Pr represent the CRP sites that were converted to corn, switchgrass and prairie mixture respectively, while AGR-C, AGR-Sw and AGR-Pr are AGR farms converted to corn, switchgrass and prairie mixture. In 2010, when the crops were established, the perennial crops (switchgrass and prairie) were accompanied by oats as a nurse crop with and without fertilization, respectively (Fig. 1.6). No other management practices were applied beyond harvesting at the end of each growing season. No-till continuous corn was seeded in mid-May with a one-time herbicide mix (Lumax, Atrazine 4L, Honcho Plus and $(NH_4)_2SO_4$). Phosphorus, potassium and nitrogen fertilizers were applied during April and June in each year (Bhardwaj *et al.*, 2011; Zenone *et al.*, 2013).

2.2.3 The climatic and microclimatic measurements and growth season identification

Climatic factors, such as air temperature (T_a) and daily precipitation (PRCP), and microclimate, such as soil temperature and soil water content, were recorded as the independent variables. They were recorded at different spatial and temporal scales based on the requirement of research and the limitation of equipment and labor.

The daily mean T_a and daily accumulative PRCP were collected and calculated from the KBS LTER Weather station (42°24'47.1" N, 85°22'15.3" W; lter.kbs.msu.edu). The air temperature was recorded hourly by a thermometer at 3 m height. The mean daily air temperature was calculated from the hourly data. Precipitation was measured by a NOAH IV total precipitation gauge (ETi Instrument Systems Inc., Fort Collins, CO).

Soil temperature (T_s) and volumetric soil water content (VWC) were measured simultaneously with soil respiration rate measurements biweekly during late April to September

and monthly during other times. Soil temperature was measured at 10 cm depth using a *Taylor 8940N* digital thermometer (Taylor Precision Products, Las Cruces, NM, USA) while VWC was monitored from the ground surface to 10 cm depth by a *HydroSense II* with a *CS659* sensor (Campbell Scientific, Inc. (CSI), Logan, UT).

The length of the growing season is an important index for climate change and agriculture. There are several identifications that are based on climate and crop growth. Here, I used temperature-based identification, which is the most common in the North America (a.k.a. frost-free season), instead of the crop-based growing season, since soil respiration includes the soil microbe-derived carbon efflux, not only plant-derived soil carbon efflux. The onset and the end of the climatic growing season (GS) in each year was calculated based on the 9-day moving average of daily mean air temperature ($9d-T_a$) to filter short-term warm or cold events, which may not induce the start of plant growth and development in spring. The onset of the GS was identified as the first day of exceeding 0°C $9d-T_a$ in spring while the end of the GS was recognized as the latest day of exceeding 0°C $9d-T_a$ in fall. The lengths of the GS were the number of dates between the onset and the end of the GS in each year.

To compare the soil respiration rates, climate and microclimate, and the vegetation indices, I separated the data into different years based on the USGS "water year" concept using October 1st to September 30th since it is more meaningful than the calendar year in agriculture research. I identified the water year in my dissertation from the end of the previous GS until the end of this GS because the post-GS precipitation may subsidize the soil water pool and will support the consumption for plants and soil microbes in the next GS. The length of the water year may be different due to the different seasonal patterns of air temperature in fall and winter.

2.2.4 The total and heterotrophic soil respiration measurements

Four plots at each site were randomly selected to install 1 x 1 m root exclusion plots for heterotrophic soil respiration (R_h). We dug a 1 m deep trench at each edge of the square (Fig. 2.1 (B)). The trenches were lined with root-barrier sheets before refilling the soil back according to its soil profile (Fig. 2.1 (C); Tang *et al.*, 2005). The plants and roots inside the square were manually removed and/or killed by herbicide (*Monsanto Roundup®*). Two 10 cm inner diameter PVC collars were installed inside the square to accommodate flux chambers to measure R_h. Another two collars were installed surrounding the square to measure total soil respiration (R_s) (Fig. 2.1(D)). A total of 112 measurements (including R_h and R_s) were taken between 10 am to 7 pm when soil respiration is at its diel maximum.

Soil respiration was measured biweekly during the growing season and monthly during the non-growing season when snow cover was minimal to allow for measurements from October to December. The chamber-based infrared gas analyzer (IRGA) approach for soil respiration measurement was done with an LI-6400 portable photosynthesis system with a 10 cm diameter 6400-09 soil chamber or an LI-8100 with a 10 cm diameter 8100-102 soil chamber (LI-COR Biosciences, Lincoln, NE).
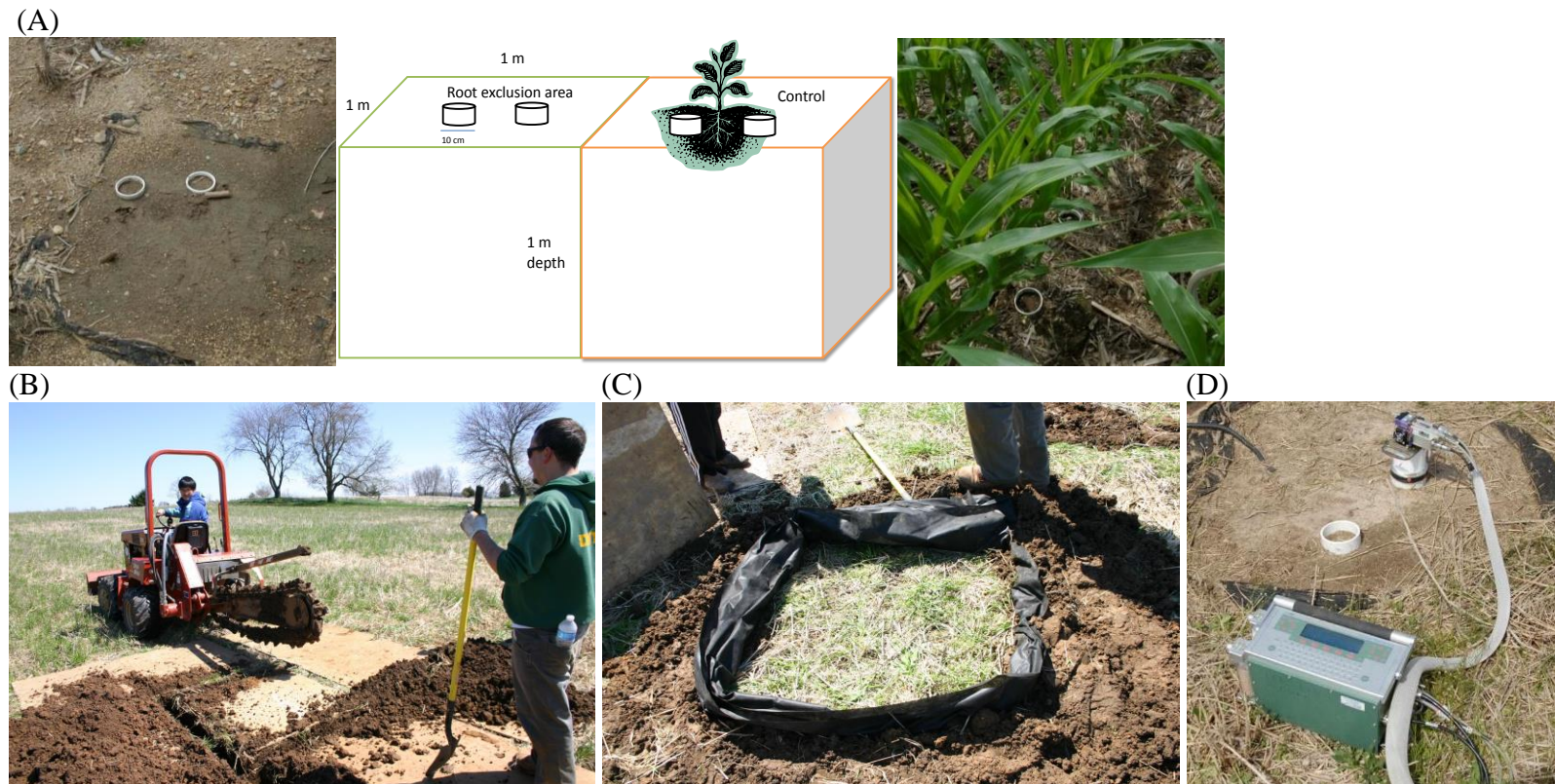
Figure. 2.1. The measurements of total (R_s) and heterotrophic soil respiration (R_h). A 1m x 1m x 1m cube was entrenched in the soil and isolated for heterotrophic soil respiration measurement. The total soil respiration plots were placed near the heterotrophic soil respiration plots (A). The four vertical sides of the cube were entrenched (B) and material-exchangeable sheets were embedded in the trenches (C) to prevent the invasion of roots. The crops were killed by *Monsanto Roundup®*. Soil respiration rate was measured by an infrared gas analysis (IRGA) of CO_2 changes in the chamber headspace (D). Two 10 cm diameter collars were installed at least one day before respiration measurement.

2.2.5 Vegetation Index data

Vegetation indices, including normalized difference vegetation index (NDVI) and enhanced vegetation index (EVI), were calculated based on satellite remote sensing using band 1 (nir), band 2 (red), and band 3 (blue) of the Moderate Resolution Imaging Spectroradiometer (MODIS). The NDVI was determined by the ratio of the difference between near-infrared reflectance and red reflectance to their sum (Tucker *et al.*, 2005), while EVI was further modified with a soil adjustment factor, L, and two atmospheric aerosol scattering coefficients—C_1 and C_2—(Huete *et al.*, 1999) and had a higher sensitivity at the "green" portion of the spectrum when vegetation was very dense. These data were developed from MODIS daily products by selecting an optimal day during every 16-day interval (i.e., low cloud cover). Missing data may appear when clouds obscured the site over an entire 16-day period. NDVI and EVI data were downloaded from the Oak Ridge National Laboratory Distributed Active Archive Center for Biogeochemical Dynamics (ORNL DAAC, http://daac.ornl.gov/MODIS/modis.shtml). I used a single pixel from each site's MODIS image at the finest spatial resolution of 250 m found mostly within each experimental site. The dates of NDVI and EVI values were paired with the nearest dates of soil respiration measurement.

2.2.6 The temperature-water-vegetation (TWV) models & R_a:R_h ratio

Multiple factor models that contain the effects of T_s, VWC, EVI and their interactions were developed and tested. The experiment treatments (seven sites: 2 LUH * 3 CROP + Ref) were set as a categorical factor and the following function was tested:

$$R = f(T_s) \cdot g(VWC) \cdot h(EVI) \cdot i(CROP, LUH) \qquad \text{Eq. 2-1}$$

where R is total (R_s) or heterotrophic (R_h) soil respiration, and f(T_s), g(VWC) and h(EVI) are the

effects of soil temperature, soil moisture and vegetation condition on R, respectively.

The functions of f(T_s), g(VWC) and h(EVI) were assumed as log-linear, quadratic, or linear based on observed relationships between R and T_s, VWC, and EVI, from previously published research, and the best correlations between R-T_s, R-VWC and R-EVI. The equations containing two-level interactions and the variables themselves were tested. The final models would include the equation with first and secondary orders in terms (Supplement 2-4). The variables and their parameters were modeled by actual data. The best models for R_s and R_h were separately selected based on Akaike Information Criterion (AIC).

The level of R_h was adjusted to the same T_s and VWC condition of R_s for calculation of the autotrophic soil respiration (R_a). The root contribution (RC) to soil respiration (R_a: R_s ratio) was calculated for all measurement dates in the growing season.

2.2.7 Data analysis

The temperature sensitivity (Q_{10}) of R was computed based on the exponential relationship between soil temperature at 10 cm depth and soil respiration at each site by year. The coefficients and Q_{10} were estimated by the function, $R = \alpha * exp^{\beta T_s}$, where $Q_{10} = exp^{10\beta}$. To compare across treatments, Q_{10} were then analyzed using a one-way analysis of variance (ANOVA) among sites for each year. The Pearson correlation coefficients were calculated between soil respiration (R_h and R_s) and their potential controlling factors (T_s, VWC, NDVI, and EVI) by site and year.

The LUH effects (i.e., AGR, CRP and Ref) on R_s and R_h were compared in different crops (i.e., C, Sw, and Pr) in each year by one-way ANOVA and Tukey's HSD test. Similar comparison of CROP effects on R_s and R_h were analyzed in different LUH in each year. The R_a: R_s ratios among years were compared by ANOVA and Tukey's HSD test as well. All statistical

analyses and graphs were conducted in *R* (R Development Core Team, 2010).

2.3 RESULTS

2.3.1 Climatic and microclimatic variables and the growing seasons

The onsets of the GS occurred each year in late March (DOY=90, 85, and 87) while the ends of the GS were in mid-November to early-December (DOY= 341, 326, and 318) in 2011, 2013, and 2014, respectively, based on the 9-day moving average air temperature (9d-T_a). The lengths of the GS were 251, 214, and 231 days in 2011, 2013, and 2014, respectively. However, 2012 had a very long GS (299 days) because of its early onset (DOY=57) and late end (DOY=356) (Fig. 2.2). Air temperature in March 2012 was extremely high (ca. 10°C higher than other years), although it fell back to normal levels in April (Table S.2.1). The maximum 9d-T_a was 26.51, 27.91, 25.84, and 22.28°C for 2011–2014, respectively. The maximum air temperature in 2014 was lower than other years. Reviewing the T_a data in more detail, 2012 had the hottest summer with a 30.67 °C mean daily T_a on July 6th. Years 2011 and 2013 also had high mean daily T_a, reaching 29.88 and 29.25 °C, respectively, while 2014 had a mean daily T_a of 24.81 °C. July T_a means in 2011 and 2012 were significantly higher than those in 2013 and 2014 (Supplement 2-1). Soil temperature showed the same patterns (Supplement 2-1) although the data were only collected biweekly during the daytime. Generally speaking, 2011 and 2012 had hotter growing seasons while 2013 and 2014 had cooler, especially in July. The year 2012 had very hot March temperatures that advanced the onset of growing season.

Annual precipitation (PRCP) ranged from 636 to 1238 mm between 1989 and 2016. Precipitation patterns seem to have shifted over those years. The precipitation was lower with smaller inter-annual variations before 1999, and was very low in 1999. Precipitation increased

and had a higher variation after 1999. During my experimental period 2011–2014, the PRCPs were 1023, 796, 1139, and 971 mm, respectively. The difference between actual PRCP and the 5-year averages were 69, -177, 119, and -33 mm in 2011 to 2014, respectively. The year 2012 had a very low PRCP while the year 2013 was very wet (Fig. 2.3). Changes in VWC were highly synchronized with precipitation. The VWCs in 2012 were very low during April and June under canopy and during April and July across bare land (Table S.2.1).
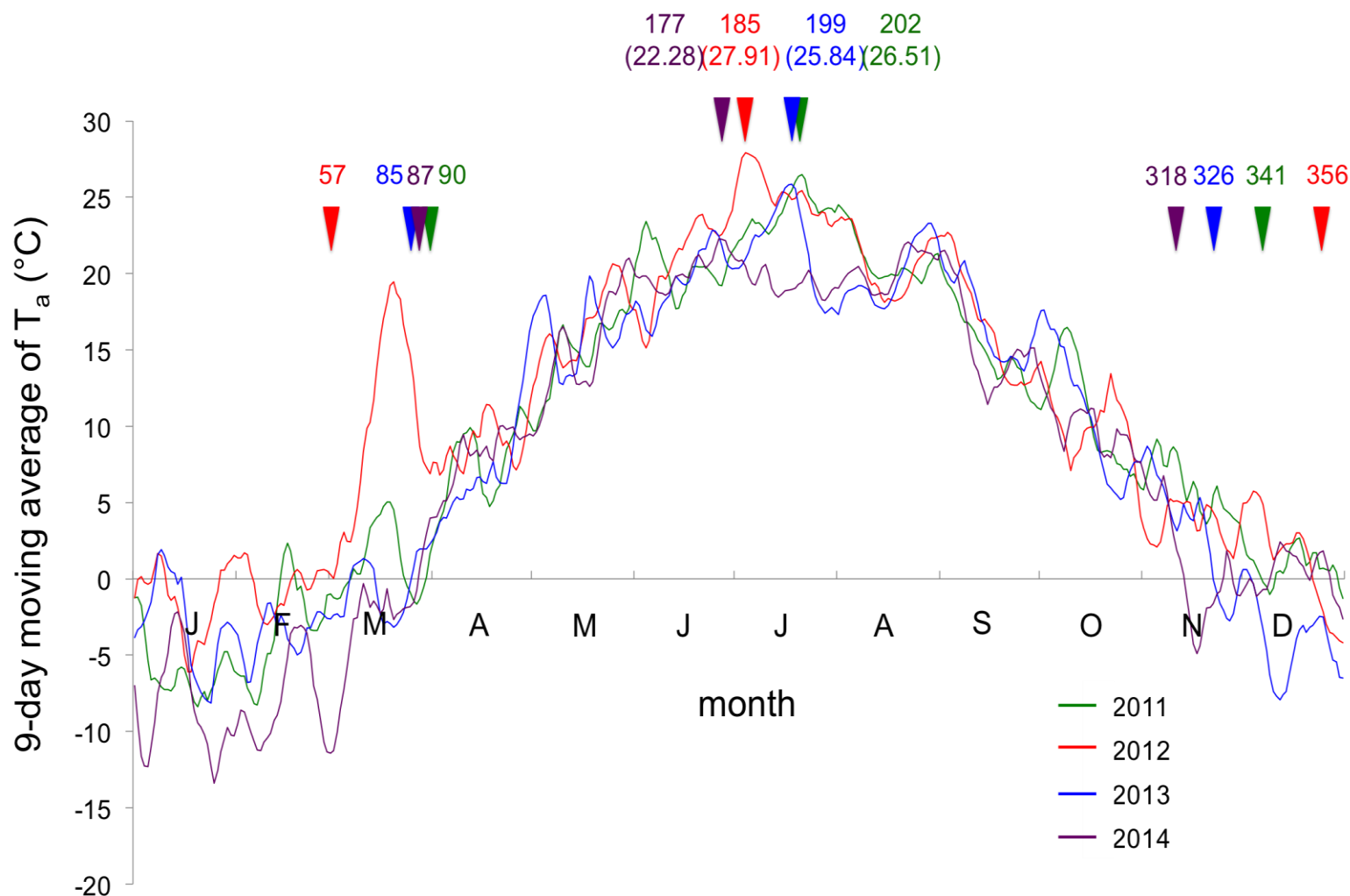
Figure 2.2. Temporal changes in nine-day moving averages of daily mean air temperature (Ta). Air temperature was measured at the KBS LTER Weather station. The green, red, blue and purple lines present daily mean Ta in 2011–2014, respectively. The Ta was calculated by an average nine-day (± 4 days) moving filter in order to more clearly display the seasonal trend. The colored arrows and the colored numbers indicate the DOY of the onset, the maximum Ta and the end of the growing season in spring, summer and fall-winter, respectively. The numbers in brackets show the maximum 9-day average of daily mean Ta (°C) in each year.
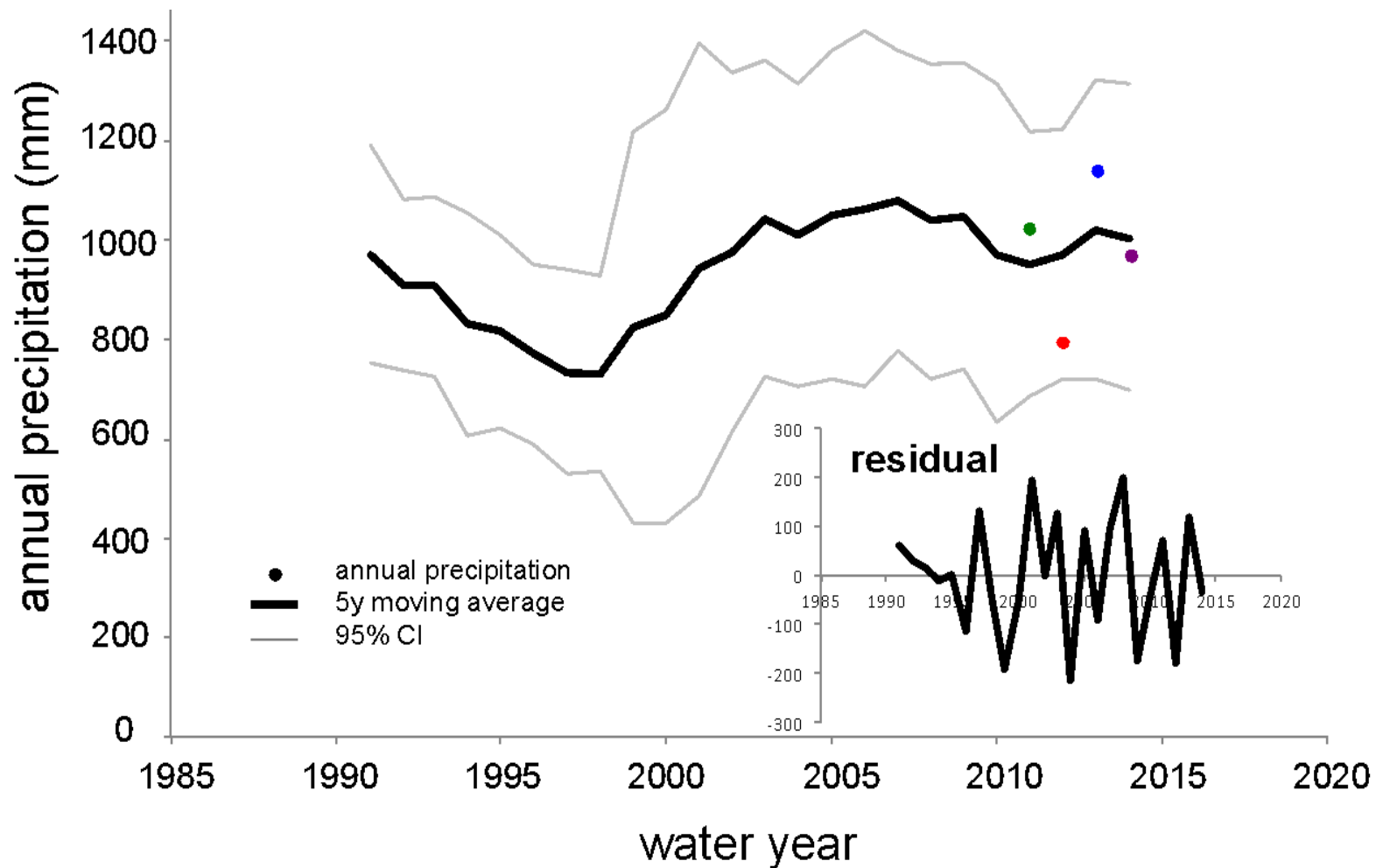
Figure 2.3. Annual precipitation by water year from 1989 to 2016. Five-year moving averages were calculated to better show the long-term trend. The 95% confidence intervals represent the variation in five-year average. The dots show the annual precipitation of each water year. Water year is defined from 1 October to 30 September from USGS. The residual is the difference between the actual annual precipitation and the five-year moving average. Green, red, blue and purple dots were the experimental years 2011, 2012, 2013 and 2014, respectively. The data were collected by the KBS LTER weather station.

2.3.2 The Vegetation Indices: NDVI and EVI

NDVI and EVI showed a hump shape, reflecting the phenology of crops. However, both NDVI and EVI dropped in June in 2012, revealing the slow growth (or even wilting) of crops due to the drought stress in that year (Fig. 2.4). The values of EVI rebounded in August, but the maximum values were lower than those in other years. The vegetation indices coincided with my field observations that crops wilted in June.
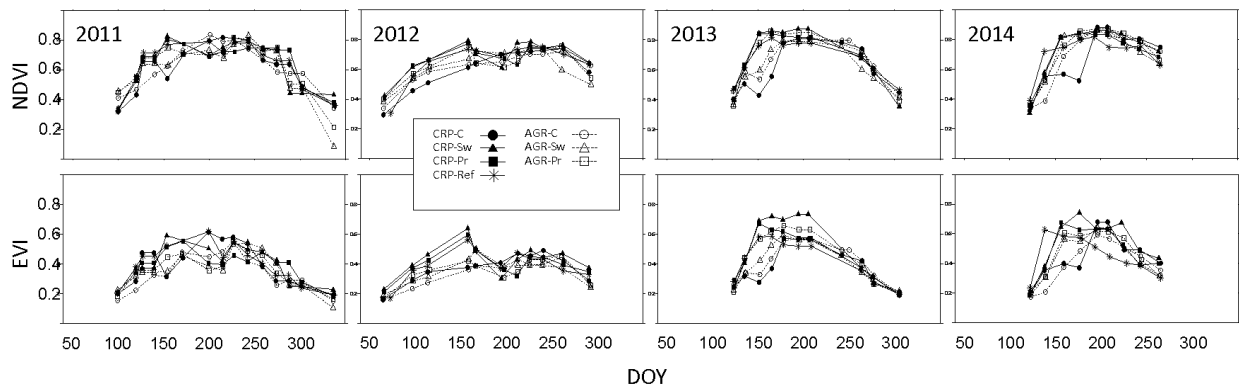
Figure 2.4. The seasonal patterns of NDVI and EVI. The NDVI and EVI values were calculated from MODIS images. Each site had one pixel. The dates of data were fit to the nearest dates of soil respiration measurements. There were dates with two missing data due to continuously cloudy days in late summer 2013.

2.3.3 CROP and LUH effects on total (R_s) and heterotrophic soil respiration (R_h)

2.3.3.1 The effects of CROP, LUH and their interactions on R_s and R_h

Both CROP and LUH had significant effects on R_s and R_h. The Ref site always had the highest means and variances of R_s and R_h in all years. In comparison to the other crop types, Ref had the highest R_s, followed sequentially by Pr, Sw and C. Also, LUH had the highest effect on Ref, followed by CRP and AGR (Supplement 2-5).

At the annual scale (2011–2014), corn had the lowest R although it was sometimes close

to Sw (R_s in 2011; R_h in 2012 and 2014). In first three years (2011–2013), R in Sw and Pr were similar and smaller than R in Ref and larger than R in corn. However, over time, the R in Pr increased and became very close to R in Ref in 2014. A similar pattern was apparent in R_s: Pr was similar to Ref, but not Sw.

The effects of CROP and LUH in 2012 were different from the other years. Both R_s and R_h in this year were lower than other years, especially for R_h. The effects of LUH and CROP were smaller since the values of Rs and Rh were very low in 2012. For CROP effects, the R_h in C-Sw-Pr and in Sw-Pr-Ref showed no significant difference while AGR-CRP showed the similar R (Supplement 2-5). The Ref field still had highest mean soil respiration but its variance was high.

2.3.3.2 The effects of CROP in different LUH

Comparing the CROP effects between the two different LUHs separately, I found that the Ref field usually had the highest R_s and R_h in all years, except CRP-Pr in 2014; Corn always had the lowest; while Sw and Pr had intermediate rates that were lower than Ref but higher than corn. The chronological comparison showed the highest soil respiration rates in 2011, which was a warm and wet year with higher than usual crop yields in the region. Both R_s and R_h were lower in 2012 when it was warm and dry and rebounded in the subsequent cooler and wetter years, 2013 and 2014. Thus, the crops had different magnitudes of response that reflected their respective LUH.

In CRP sites, both R_s and R_h were separated into two groups, annual and perennial crops, based on Tukey's HSD test. All R_h in 2012 was reduced to the similar level and the difference disappeared while the R_s in Ref was still significantly higher than R_s in Sw, Pr and C. After the dry year, R_h in Sw and Ref increased, although they did not become statistically different. The R_s

of perennial crops in 2013 and 2014 were higher than R_h. This was especially true for Pr. The R_s in Pr was higher than those in Sw in 2014 (Fig. 2.5 (A)).

In AGR sites, the relative differences of R among crops and years were similar to those in CRP sites. The Ref field always had highest R_s and R_h, followed by Pr, Sw, and C. However, the three crops usually had larger differences relative to Ref, compared to those at CRP sites. Soil respiration in Pr did not rebound strongly like those in CRP sites (Fig. 2.5 (B)).

2.3.3.3 The effects of LUH in different CROP

Comparing the two LUH (i.e., CRP vs. AGR) and Ref, AGR had the lowest soil respiration rates while Ref usually had the largest rates. The changes of R_s and R_h among years were similar to those in the description in CROP effects: they were highest in 2011, depressed in 2012 and then rebounded in 2013 and 2014. However, the speed and the magnitude of the changes of soil respiration were different between crops in fields of different LUH.

In corn fields, R_h was different between AGR and CRP in 2011, 2012 and 2014, while R_s was similar. The Ref field always had significantly higher R_s and R_h. No obvious chronological trends were found for either R_s or R_h (Fig. 2.6 (A)).

Comparing the interannual patterns in R_s and R_h between AGR- and CRP-Sw fields for only the second year after land use change (2011), CRP had a higher R_h and R_s than AGR. After 2011, however, both R_h and R_s in AGR and CRP were similar; yet, Ref always had a higher R_s than AGR. The R_s in CRP was similar to that of Ref in 2011, but reduced and then became similar to AGR and Ref in 2013 and 2014 (Fig. 2.6 (B)).

The R_h of CRP-Pr was closer to Ref and was higher than that in AGR-Pr in 2011. All R_h in three sites were not different when they were depressed in 2012, like all other crops. However, R_h and R_s in CRP-Pr increased a lot in 2013 and 2014, reaching even higher values than those in

Ref although there was no significant difference (Fig. 2.6 (C)).
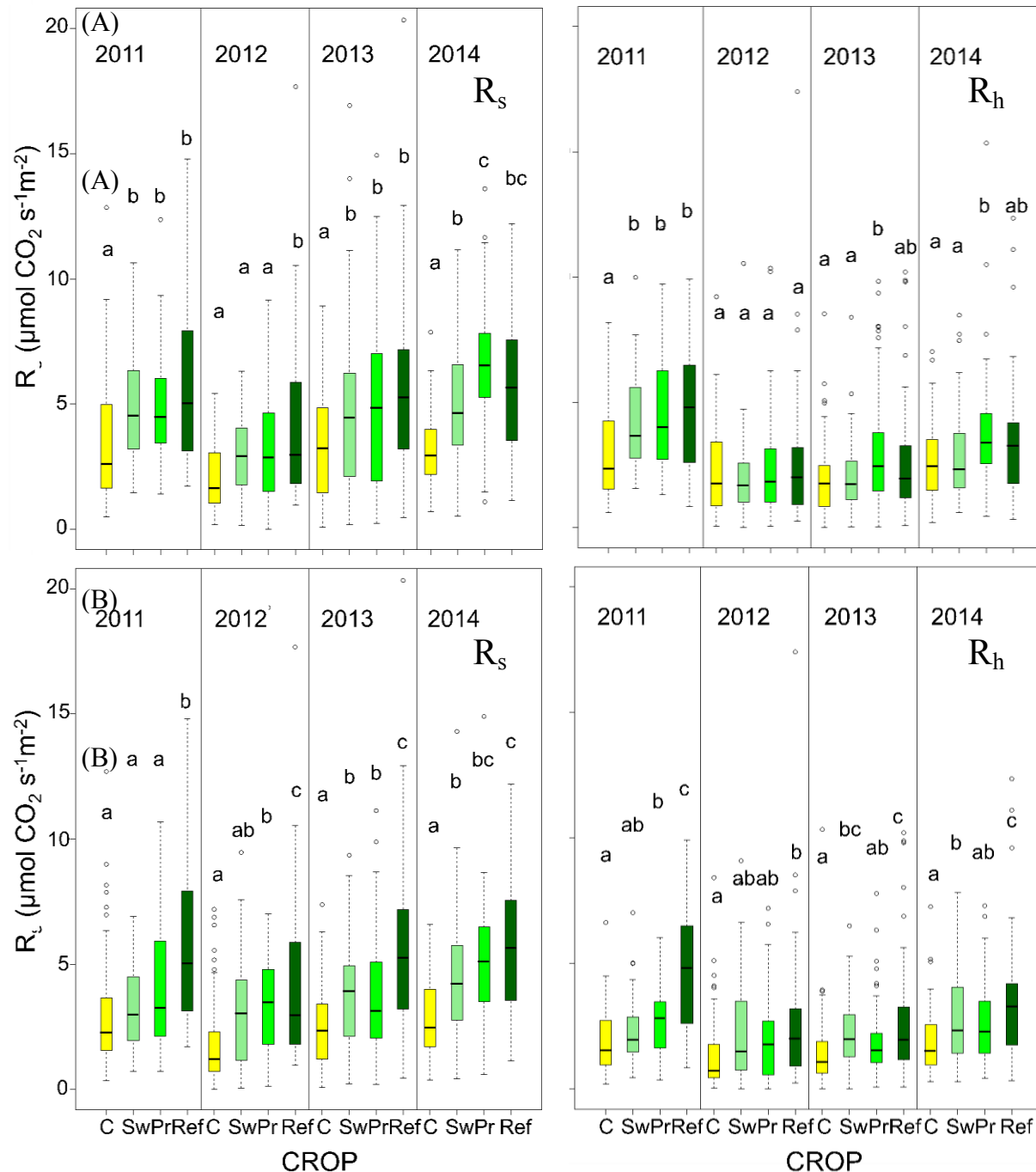
Figure 2.5. The CROP effect on total (R_s) and heterotrophic soil respiration (R_h) in fields with different LUH. CRP (A) and AGR (B) refer to the previous land use. The letters presented the statistical results from Tukey's TSD test between crops in the same LUH and in the same year. The letters display the means of R values in each treatment from small to large alphabetically.
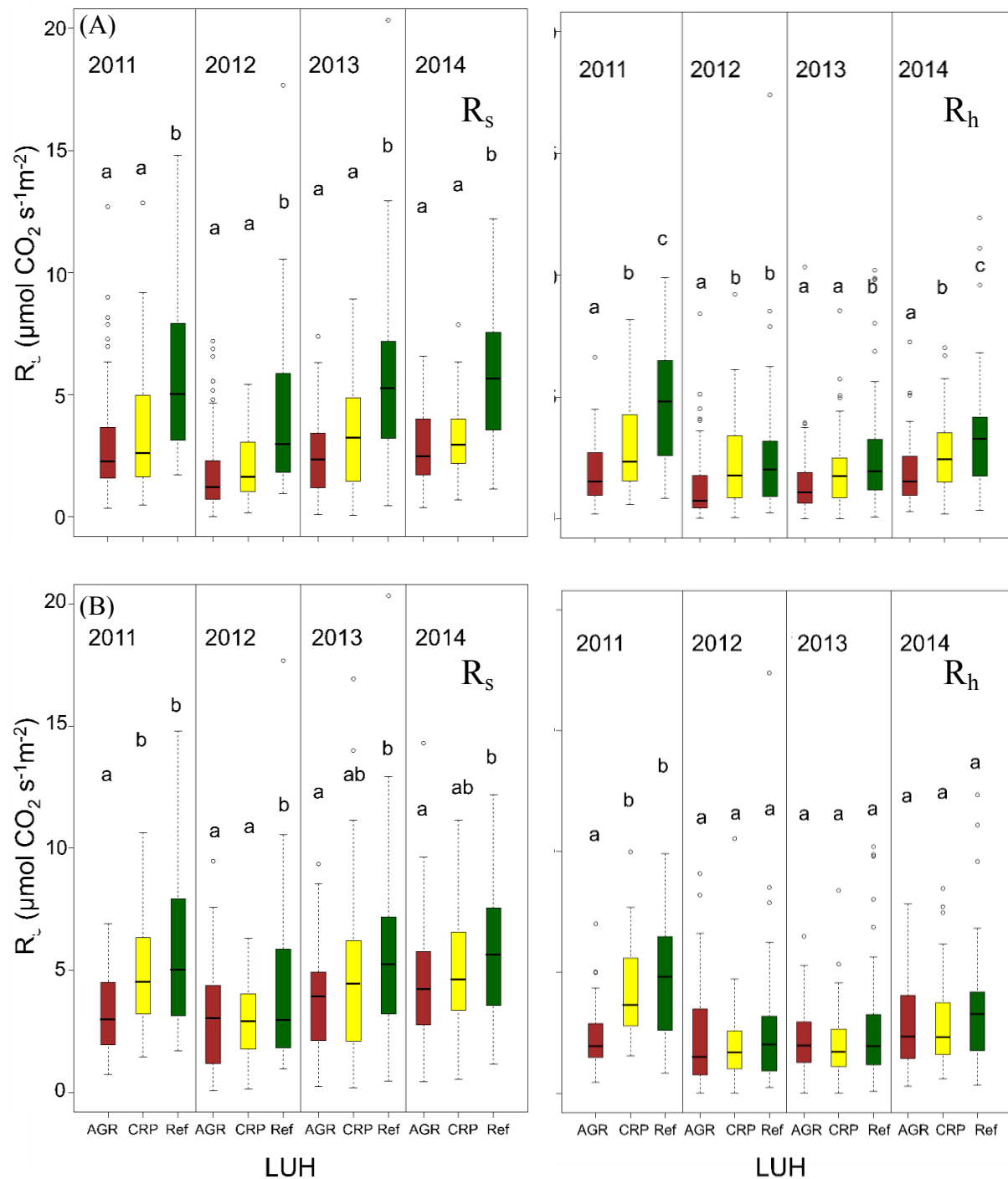
Figure 2.6. The LUH effect of total (R_s) and heterotrophic soil respiration (R_h) in different crop types. Corn (A), switchgrass (B), and prairie mixture (C) are shown with total (R_s) and heterotrophic soil respiration (R_h) in different panels. The letters presented the statistical results from Tukey's HSD test between crops in the same crop types and in the same year. The letters display the means of R values in each treatment from small to large alphabetically.

Figure 2.6. (cont'd)
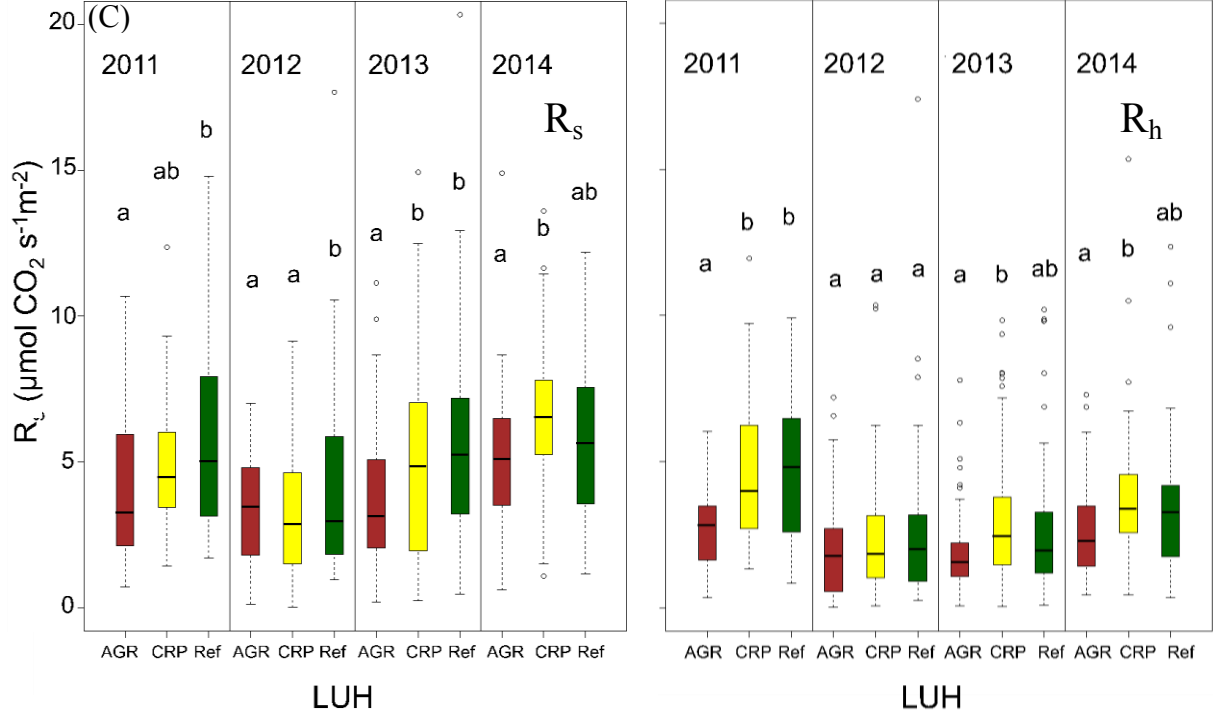
2.3.4 Soil respiration regulators

Soil respiration had different relationships with three major drivers: temperature, soil water content, and vegetation. Both R_s and R_h had similar correlations with these drivers. Soil respiration was positively, exponentially related to T_s (Tables S.2.1, 2.2 and Fig. 2.7) and positively linearly correlated to VIs (Fig. 2.9 (A) & (B)), but was weakly negative or not correlated to VWC (Fig. 2.8).

The percent variation in $\log_{10}R$ explained by T_s ranged from 47% to 90% in all data, mostly between 60% and 80%. The results revealed the strong exponential relationship between R and T_s. The regression slopes for $\log_{10}R_s$-T_s were greater than the slopes for $\log_{10}R_h$-T_s (Fig. 2.7), suggesting that the R_s had higher temperature sensitivity than R_h, although the difference was not significant because of high within-group variation (Q_{10}, Table S.2.3).

Soil VWC showed no correlation ($p > 0.05$) or a weak, negative linear correlation ($0.05 > p > 0.01$) with R_s and R_h (Table S.2.2). A quadratic relationship fit better. However, the importance of VWC to soil respiration appeared different among years. VWC was a weak driver in wet years, such as 2013 and 2014. For example, R and VWC at all sites except *AGR-Sw* were not correlated ($p > 0.05$). On the contrary, R in most sites was correlated to VWC in 2011 and 2012 when the spring and the summer were dry (Fig. 2.8; Table S.2.2).

NDVI and EVI had strong, positive linear correlations with $\log_{10}R$ (Figs. 2.9(A) & (B); Table S.2.2). The slopes of R_s-NDVI/EVI and R_h-NDVI/EVI are close, but most R_s-NDVI/EVI regressions have larger intercepts. The regression slopes in 2012 are visibly higher than those in 2011, 2013, and 2014 (Figs. 2.9(A) & (B)), suggesting that the relationship of VI on R_s was stronger in 2012 (Table S.2.2).
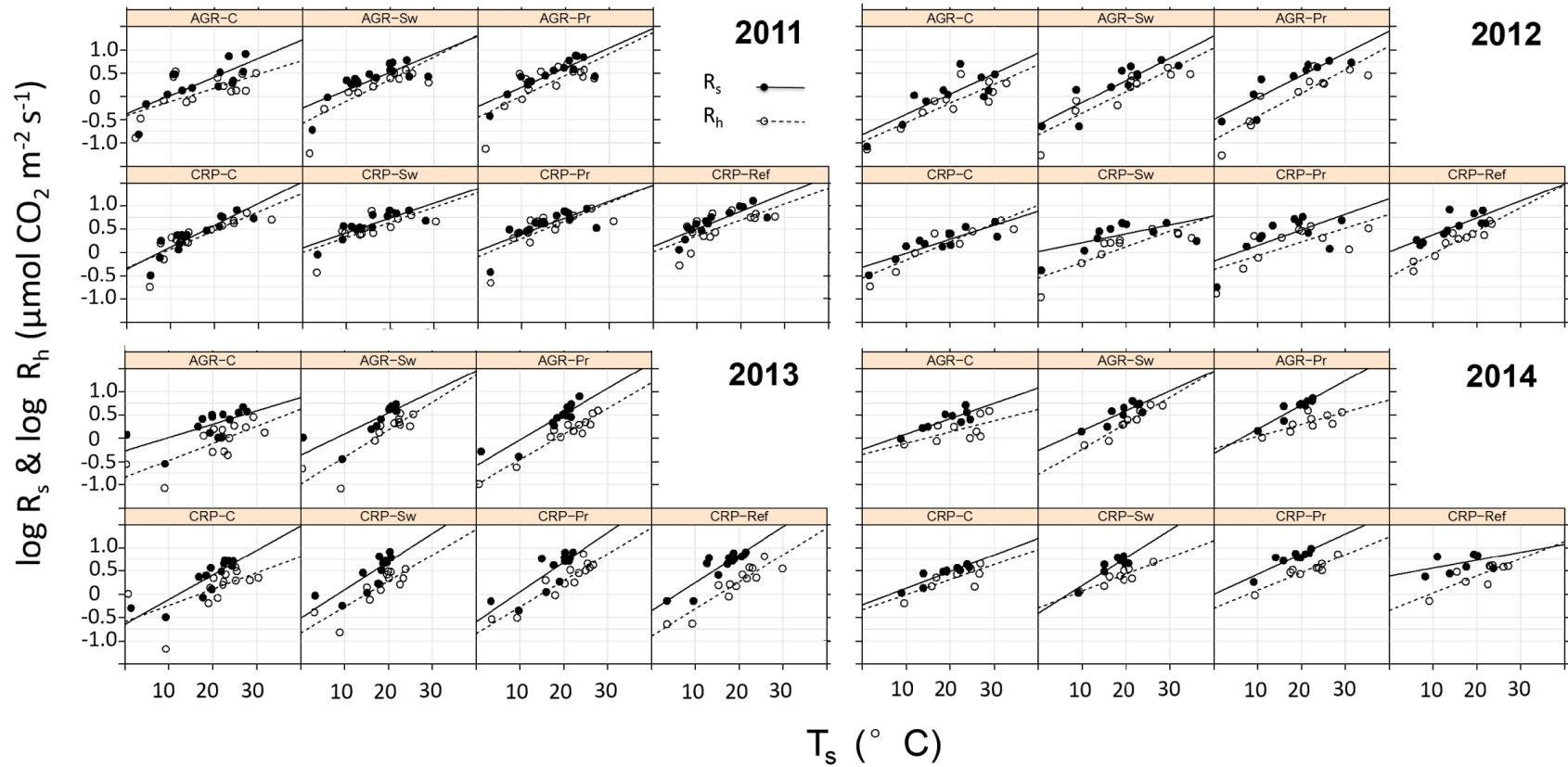
Figure 2.7. Linear regressions of soil respiration (log$_{10}$R) on soil temperature (T$_s$). The soil respiration values were the average of measurements from four plots in each field. The solid circles and solid lines were R$_s$. The empty circles and dashed lines show R$_h$.
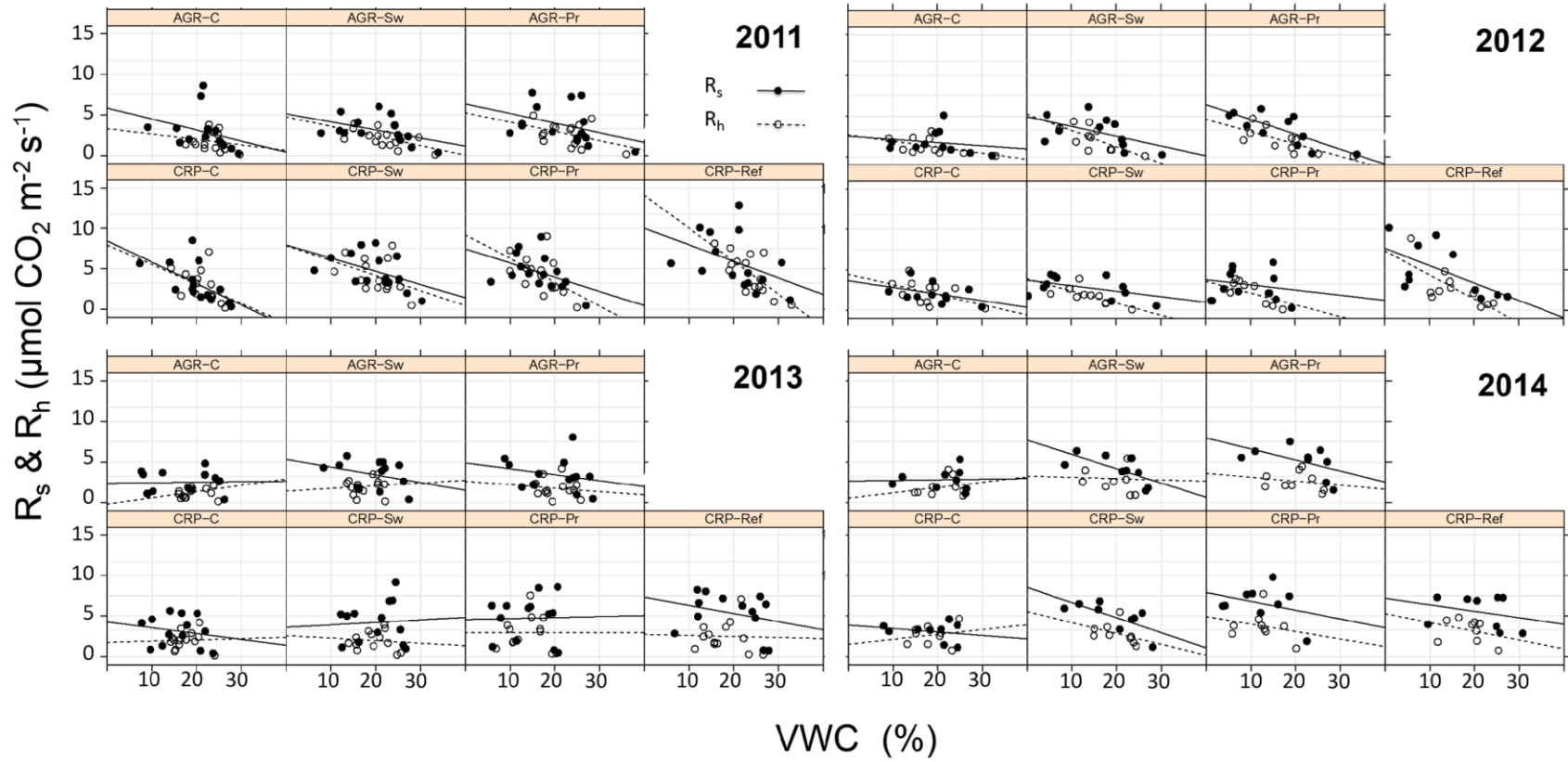
Figure 2.8. Linear regressions of soil respiration (R) on soil moisture (VWC). The solid circles show the average R_s from four plots in each research field, and the empty circles show the mean R_h. The solid lines are linear regressions for R_s-VWC while the empty circles and dashed lines are the linear regressions of R_h-VWC.

(A)
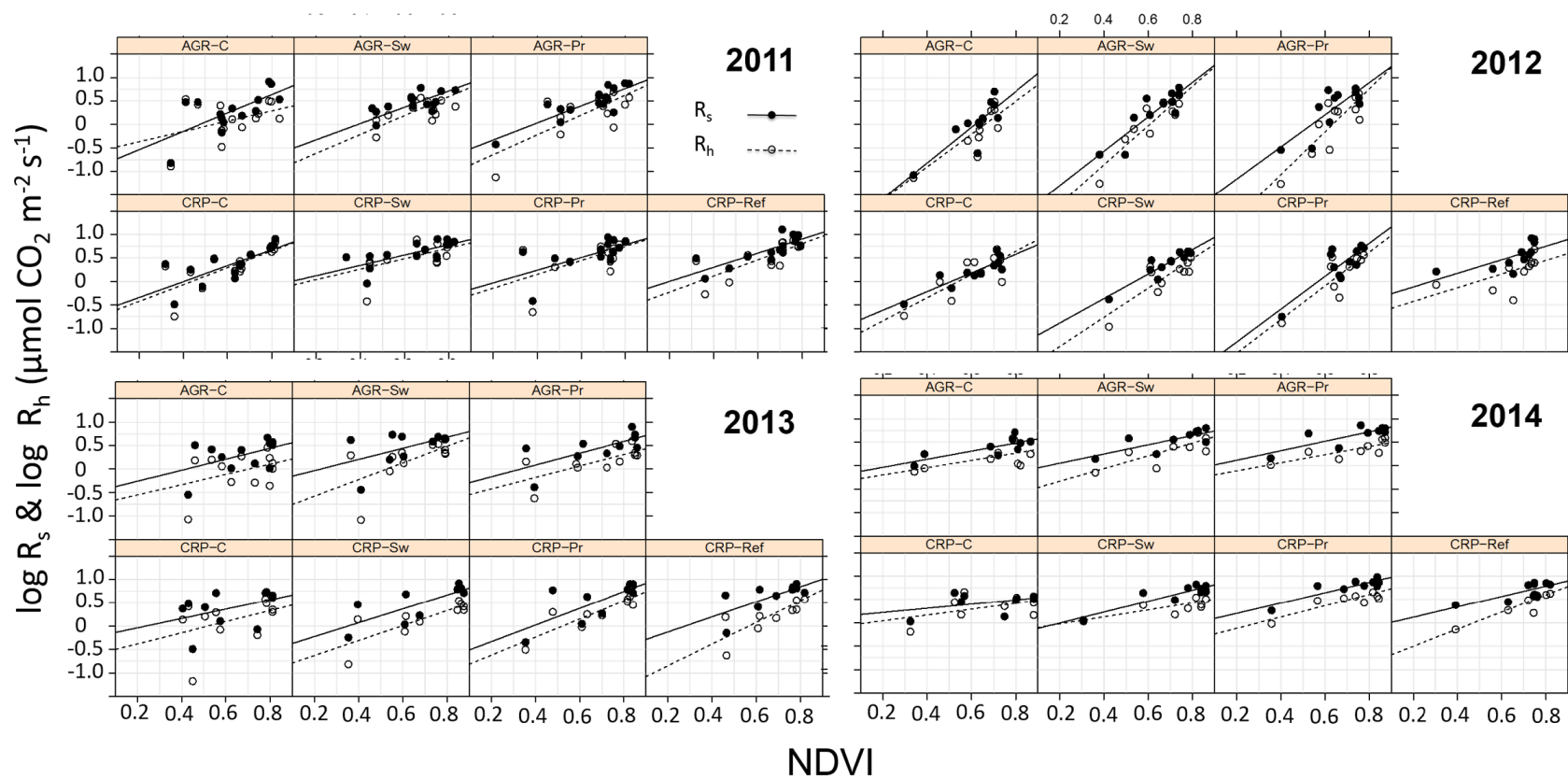
Figure 2.9. Linear regression of soil respiration ($log_{10}R$) on MODIS vegetation indices (NDVI and EVI). The soil respiration values were the average of measurements from four plots in each research site. The solid circles and solid lines were R_s. The empty circles and dash lines were R_h.

Figure 2.9. (cont'd)

(B)
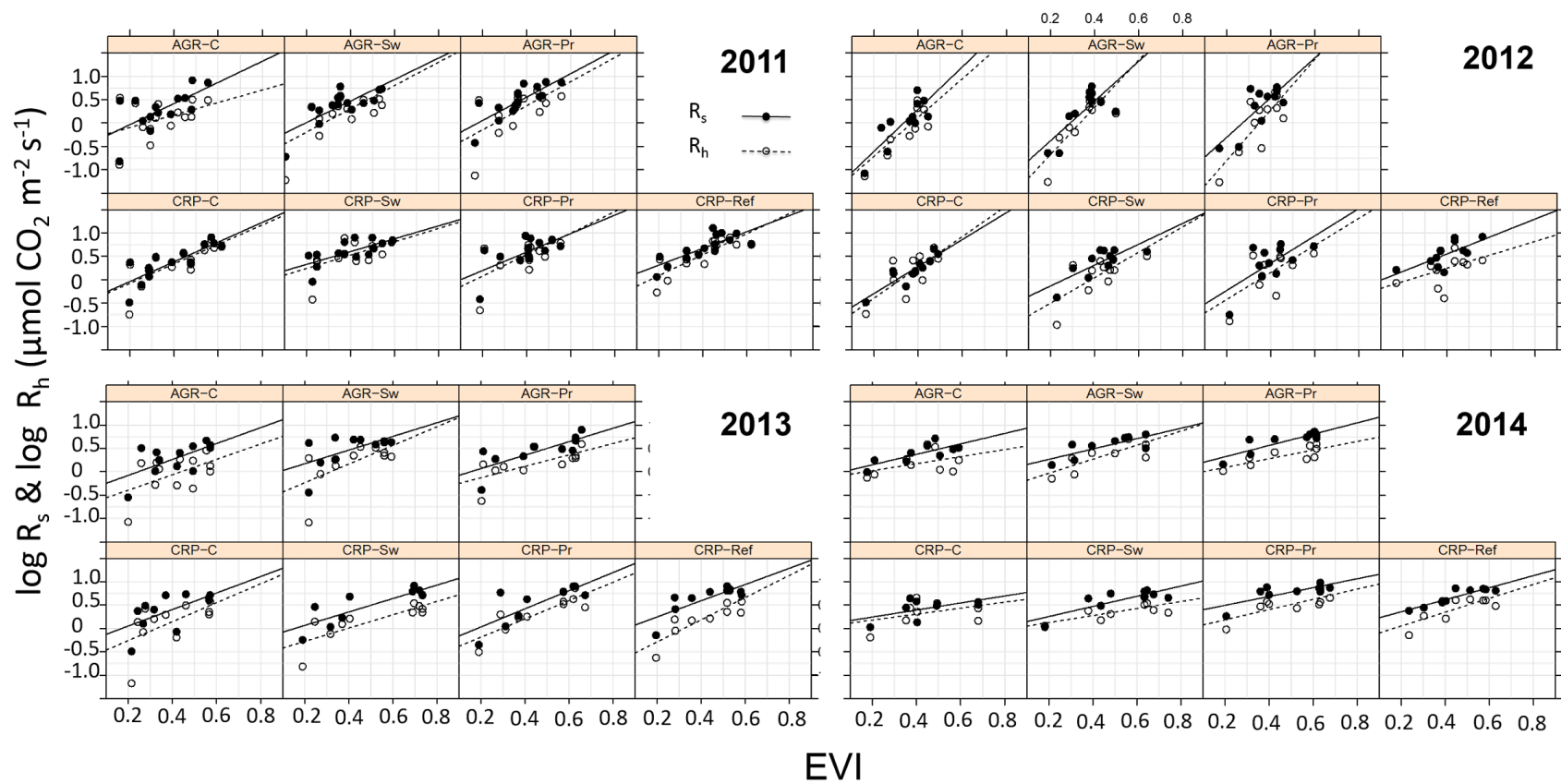
2.3.5 Temperature sensitivity (Q₁₀) of soil respiration

The Q_{10} values for soil respiration ranged from 1.20 to 1.86, although the differences are not significant due to high within-group variation. The ranges of Q_{10} were smallest in 2011 (1.31-1.57) followed by 2012 (1.20-1.60), 2014 (1.30-1.86), and 2013 (1.26-1.81 μmol CO_2 $m^{-2}s^{-1}$). The range of Q_{10} was only 0.26 in 2011 and 0.56 and 0.55 in 2013 and 2014, respectively. The smallest Q_{10} (1.20) occurred in the dry summer of 2012, and the largest Q_{10} (1.86) in the wettest year (2013) (Supplement 2-3). It is not clear whether the high variations of Q_{10} are due to the 2013 wet spring or the dry-rewet recovery in 2012-2013.

2.3.6 Temperature-Water-Vegetation (TWV) multiple variable models for soil respiration

After testing many regression models including three biophysical variables: T_s, VWC, EVI, separately and their interactions, the AIC values shows that the models that contain all three factors (i.e., T_s, VWC, and EVI) with their relationships (exponential, exponential and linear for T_s, VWC, and EVI, respectively) and some of their second-order interactions, explain R_s and R_h well. I do not include higher-order interactions between biophysical factors since it is difficult to explain the ecological meaning. The parameters of each term in the best-fit biophysical R model are listed in Supplement 2-4.

The R_s and R_h models were similar but the interactions of log_{10}VWC:EVI and T_s:CROP/LUH terms were removed from the R_s model. The adjusted R^2 are 0.62 and 0.53 for R_s and R_h, respectively. The residuals of the TWV models of $log_{10}R_s$ and $log_{10}R_h$ seem acceptable (Fig. 2.9).
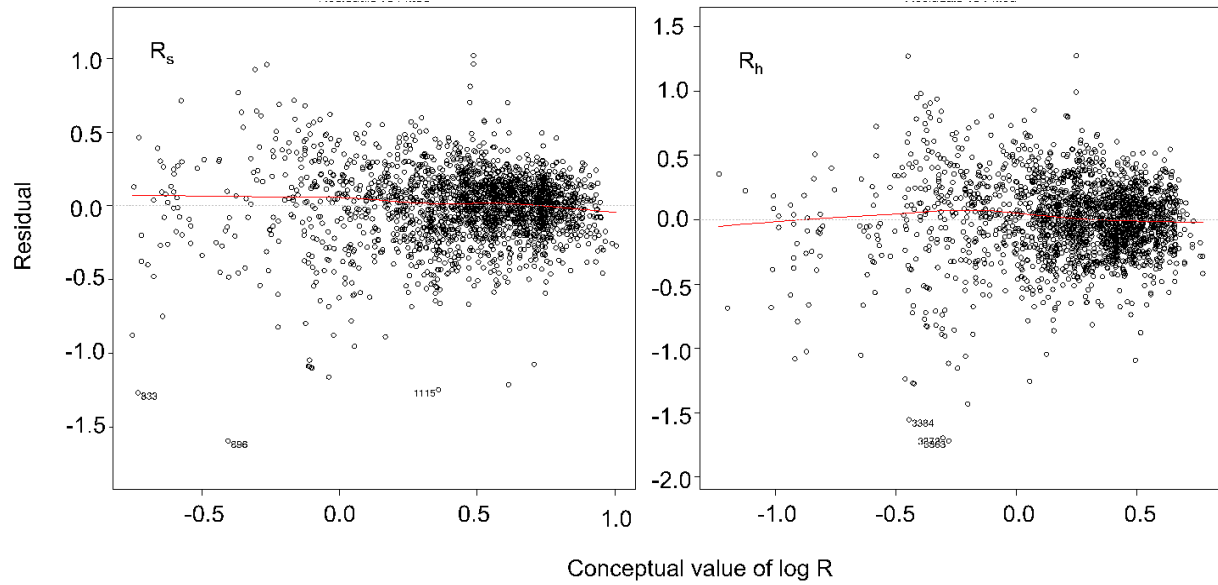
Figure 2.10. Residuals of the two-level interaction TWV models. The x-axis is the predicted value of $\log_{10}R_s$ (left) and $\log_{10}R_h$ (right) from the TWV model, while the y-axis is the residuals (i.e., difference between measured data and modeling estimates).

2.3.7 R_a:R_h ratio and the root contribution to soil respiration

The estimates of R_s and R_h were calculated based on TWV models with actual T_s, VWC and EVI values at R_s plots (canopy-covered) during the GS. The R_a was calculated as the difference between the paired measurements of R_s and R_h. The values of RC ranged from 0.31 in CRP-C field to 0.57 in CRP-Sw field. Generally speaking, CRP-C had the smallest RC values (0.31 ~ 0.33) while the Ref site always had highest RC values (0.54 ~ 0.56). The RC values in other sites were between CRP-C and Ref (Table. 2.1). RCs in CRP fields increased in the order C < Pr < Sw < Ref. In AGR fields, Sw significantly had lower RC than other three crop fields (Fig. 2.11). Between the two LUH, CRP fields usually had higher RC than AGR, except switchgrass fields. The RCs in the AGR-Pr field were the same as those in the Ref field (Figure 2.12). The RC values in most fields decreased in 2012, except for CRP-Sw (Table 2.1 & Fig. 2.13). Tukey's HSD tests showed that the R_a:R_s ratios in Ref and in AGR-Pr field were all the same over the four years. The AGR-Sw and CRP-Pr had lower RC in 2012 compared to other years while CRP-Sw had high RC in 2012 (Fig. 2.13).

Table. 2.1. The root contribution (RC) to total soil respiration. RCs (a.k.a. R_a:R_s ratios) were calculated from the estimates of TWV models. The values were mean ± 1 s.d. CROP: crop type; LUH: land use history; C: corn; Sw: switchgrass; Pr: prairie; Ref: reference; CRP: Conservation Reserve Program; AGR: corn-soybean rotation agriculture.

CROP	LUH	2011			2012			2013			2014		
C	CRP	0.32	±	0.05	0.32	±	0.04	0.31	±	0.05	0.33	±	0.06
	AGR	0.46	±	0.10	0.43	±	0.06	0.49	±	0.12	0.51	±	0.13
Sw	CRP	0.47	±	0.08	0.57	±	0.17	0.46	±	0.08	0.47	±	0.10
	AGR	0.45	±	0.14	0.35	±	0.24	0.43	±	0.14	0.44	±	0.17
Pr	CRP	0.45	±	0.06	0.29	±	0.18	0.39	±	0.12	0.41	±	0.09
	AGR	0.51	±	0.03	0.51	±	0.04	0.52	±	0.05	0.53	±	0.04
Ref		0.56	±	0.04	0.56	±	0.04	0.54	±	0.06	0.54	±	0.06
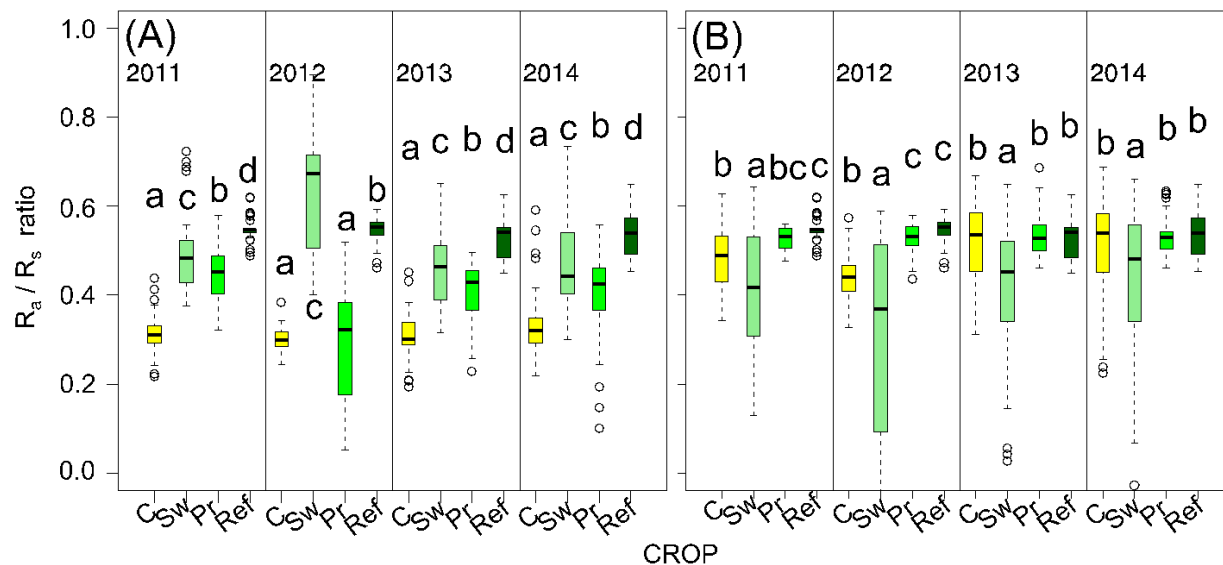
Figure 2.11. The root contribution (RC) to total soil respiration across CROP (crop types). The CROP effects on R_a/R_s ratio in CRP fields (A) and in AGR fields (B) are shown, where R_s is estimated from the TWV model and R_a is calculated as the difference between R_s and R_h. The letters indicate the results of Tukey's HSD test for different sites. The letters display the means from small to large alphabetically. CRP: Conservation Reserve Program; AGR: corn-soybean rotation agriculture; C: corn; Sw: switchgrass; Pr: prairie; Ref: reference.
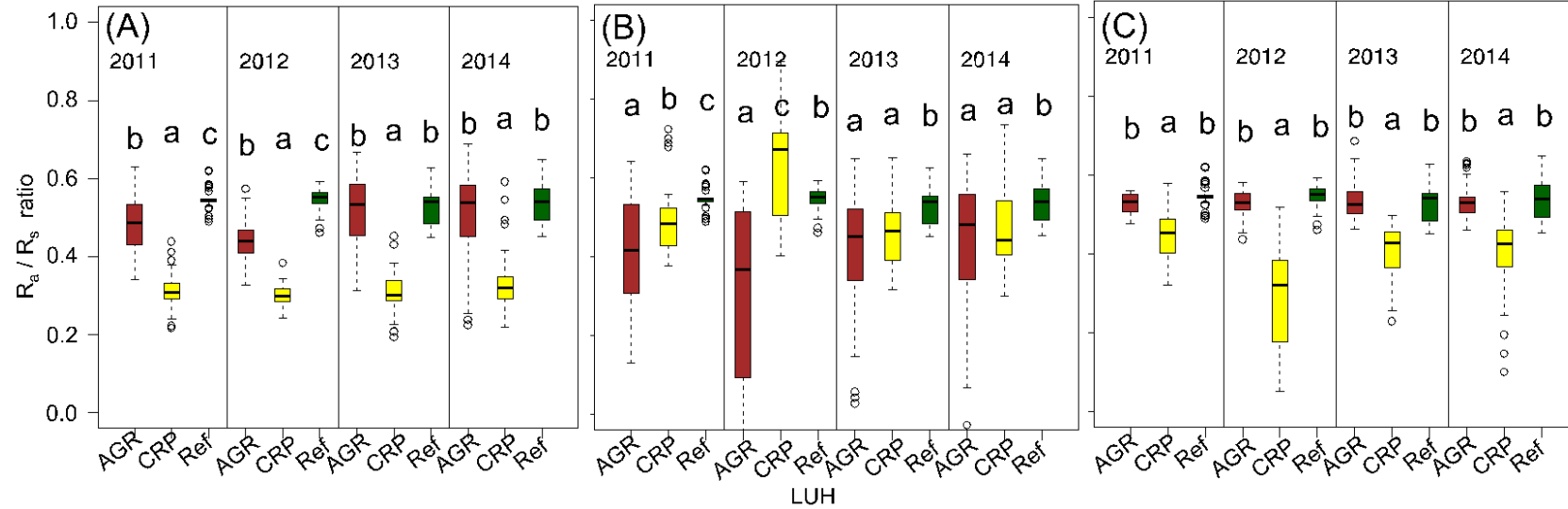
Figure 2.12. The root contribution to total soil respiration across LUH (land use histories). The LUH effects on R_a/R_s ratio in corn (A), switchgrass (B) and prairie fields (C) are shown, where R_s is estimated from the TWV model and R_a is calculated as the difference between R_s and R_h. The letters indicate the results of Tukey's HSD test for different sites. The letters display the means from small to large alphabetically. LUH: land use history; CRP: Conservation Reserve Program; AGR: corn-soybean rotation agriculture; C: corn; Sw: switchgrass; Pr: prairie; Ref: reference
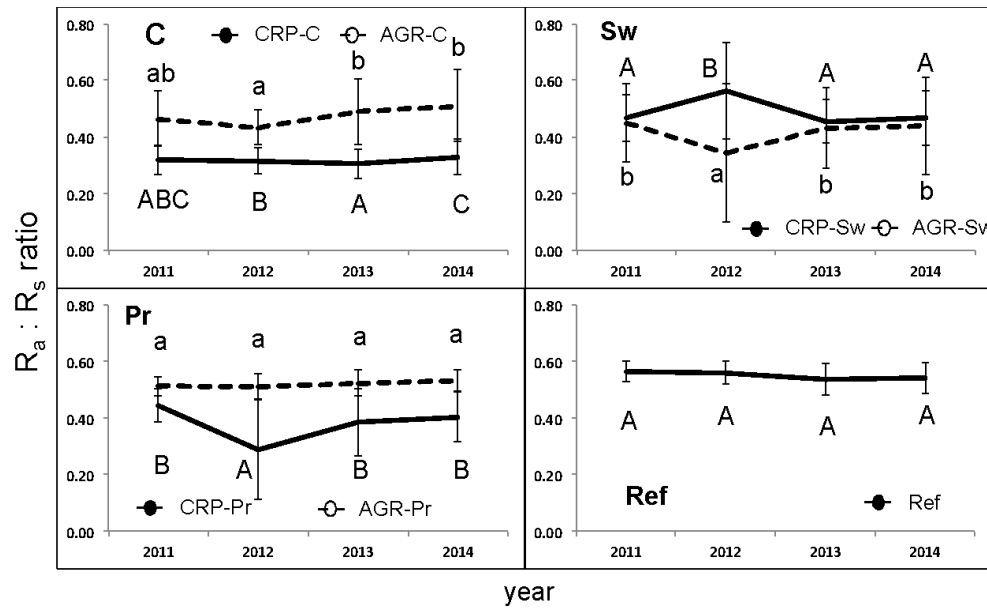
Figure 2.13. The root contribution to total soil respiration over 2011–2014. The R_s was estimated from the TWV model and R_a was calculated as the difference between R_s and R_h. The yearly variations of R_a/R_s ratios are indicated by their CROP (between panels) and LUH (within panel). Solid dots with solid lines show CRP while empty circles with dashed lines show AGR sites. The error bars were one standard deviation. The letters presented the results of Tukey's HSD test for different sites. The capitals present the statistical results of CRP and the lowercase letters represent the results of AGR fields. The letters display the means from small to large alphabetically.

2.4 DISCUSSION

2.4.1 The major biophysical drivers of soil respiration

Many recent studies show that the major biophysical drivers for soil respiration are typically temperature, soil water content, substrate supply from plants, and their interactions (Luo *et al.*, 2001; Curiel Yuste *et al.*, 2004). These drivers may affect soil respiration via different mechanisms and have different correlations to soil respiration. The relative importance of different biophysical factors may change depending on the biogeochemical processes and their feedback in different climate regimes and ecosystems within and among years. In my ecosystems, soil temperature and vegetation indices were positively and exponentially correlated

with soil respiration. Soil water content had weak or no correlation with soil carbon dioxide efflux and was more likely a limiting factor for soil respiration only when it was low (Figs. 2.7, 2.8 & 2.9).

The inter-annual and intra-annual variations and the pulses of biophysical factors affect the temporal variations of soil respiration during the growing season. Legacy effects play important roles as well. The different biophysical factors may control soil respiration by different ways and at different temporal scales. Long-term climate patterns (e.g., the temporal variations of temperature, photoperiods and light quality), short-term regular climate events (e.g., periodic flooding or drought), and short-term occasional events (e.g., heat waves, rain pulses) can alter ecosystem functions. Some of the influences of the abiotic factors explicitly change soil respiration when it is happening while others may not present effects immediately. The "carry-over effects" may alter community structure, change species richness and evenness, and affect important ecological processes within or among years (Flanagan, 2009). For example, the cumulative effect of temperature (e.g., growing degree days) affect the plant phenology and biomass production, which influence both carbon uptake and water consumption by the plants, and further alter autotrophic and heterotrophic soil respiration via the root growth and soil substrate supply and water availability. On the contrary, the soil water availability, which depends predominately on precipitation inputs and evapotranspiration outputs, can limit the activities of plant and soil microbes and affect soil respiration in the growing season when water availability is limited.

In the studied ecosystems, I hypothesized that three major forces control the soil respiration at different temporal scales and with different consequences (Fig. 2.12). I made the schematic chart for soil respiration across years based on the correlation between R and

biophysical factors and the actual values of the drivers in each year (Fig. 2.12 (A)). If I add the impacts of severe drought and assume that the sites require more than one year to recover, the values of R fit better for our data (Fig. 2.12 (B)). The effects of CROP and LUH after LUC may be different on R_a and R_h. The perennial crops may develop their extensive root systems after land use change and increase the autotrophic soil respiration while annual crop does not have such an extensive root system (Fig. 2.12 (C) CRPpere and AGRpere). Annual crops should have consistent R_a from year to year since they will die and be replanted every year (Fig. 2.12 (C) CRPann and AGRann). The CRP sites should have relatively higher root system establishment due to the more fertile soil. The year-to-year trends of R_h will be opposite to those of R_a at CRP sites since plant and soil microbes will consume soil nutrients, especially nitrogen. The changes of soil respiration may or may not be evident depending on the relative strength of different drivers and their interactions and feedback. The crop may adapt to its environment and diminish the magnitude of changes.
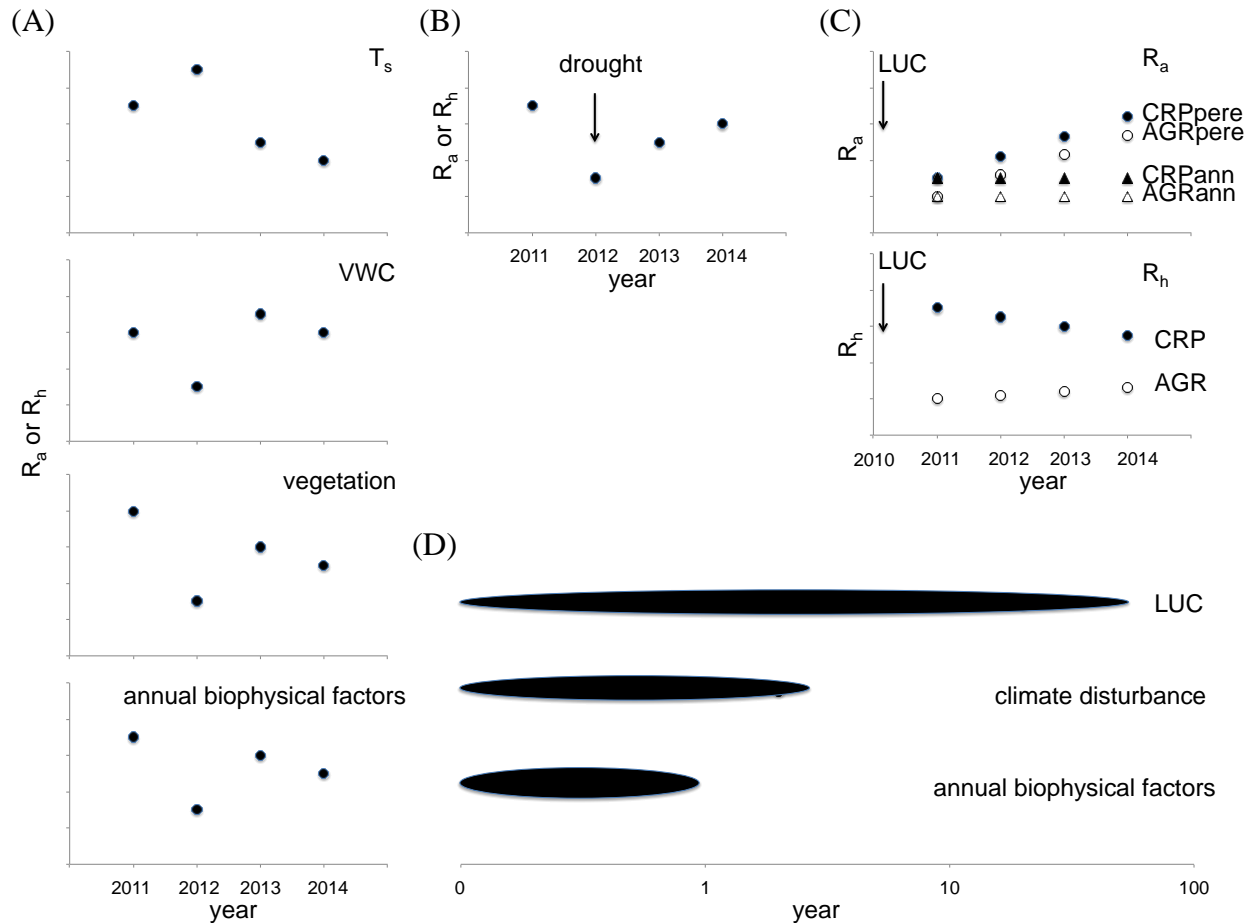
Figure 2.14. Schematic depiction of the impacts of three major forces on soil respiration at different temporal scales. (A) The interannual variation in R is driven by biophysical factors and the actual biophysical conditions in each year. The interannual variation in biophysical factors (T_s, VWC and vegetation) affect annual R. (B) The 2012 severe drought depressed soil respiration, which took more than one year to recover. (C) The R_a was affected by the establishment of root systems. Perennial crops (CRPpere & AGRpere) will have increasing R_a while the annual corn crop (CRPann & AGRann) will have consistent R_a across years after land use change. The rate of root establishment will be higher in CRP sites owing to its more fertile soil. CRP sites will have decreasing R_h chronologically that reflects the gradual depletion of soil nutrients while AGR sites will have relatively consistent R_h. The LUC occurred in 2009. (D) The temporal scales of biophysical effects on R may range from less than a year to decades in the case of LUC.

During my study period, both R_s and R_h had similar year-to-year trends, although the magnitudes were different in different CROP or LUH treatments. In 2011, soil respiration rates were highest when both temperature and precipitation were high. In 2012, the hot and spring-summer dry year, soil respiration was depressed in all sites. Soil respiration rates in 2013 and

2014 were higher than those in 2012, although it had lower summer temperatures (Figs. 2.5 & 2.6).

The combination of biophysical variables (TWV models) explained 62% and 53% of variation in R_s and R_h for all sites over all four years. The individual variables in each experimental site may explain up to 89% of the variation (i.e., the effect of T_s on R_s in AGR-Pr in 2013; Table S.2.2). However, the changes of soil respiration were confounded between responses to the biophysical variables in a particular year, the recovery after extreme climate events (i.e., severe drought), and the long-term trends after LUC. The former two were climate-induced effects while the latter one was due to human management. The Ref field is the only one that was driven by climate variability as opposed to LUH and management changes.

The R_s and R_h in Ref were highest in 2011, dropped in 2012 and then rebounded in 2013 and 2014 (Fig. 2.5). The warm temperatures with enough water in 2011 supported a good environment for plants and soil microbes, thus explaining the high soil respiration. In 2012, the hottest and longest growing season resulted in lower soil respiration. The severe spring-summer drought suppressed both plant growth and soil microbial activities, resulting in the lowest soil respiration observed over the four years. The sudden drop of NDVI and EVI in June 2012 (Fig. 3.1 (C)) confirms the drought effect on above ground plant biomass, supporting the hypothesis that the spring-summer drought affected both R_a and R_h directly or indirectly via reduced plant growth and soil carbon substrate supply. The consequences fit our hypothesis that soil water content plays a crucial role at times when water is limiting, which also tend to be the times with warmest temperatures.

Comparing the post-drought years, I found that soil respiration was higher in 2014 than in 2013, which was the reverse of the summer soil temperature levels. It means that the roots and

soil microbes had a lower metabolism in 2013 than in 2014, even though the summer temperature was higher in 2013 and when soil water was not a limitation. The drought-recovery hypothesis was a better fit (Fig. 2.12 (B)) than the biophysical hypothesis alone (Fig. 2.12 (A)). The results imply that soil respiration requires at least two years to recover from the damage of a severe spring-summer drought. The reasonable hypothesis is that the carbon-related biogeochemical processes, the community structure of plant and soil microbes, and/or their physiological traits changed during the drought and it spent longer than one year to reach a new equilibrium. However, there is a difference in the temperature sensitivity of soil respiration across the years, which had high variations. I developed a method to understand the change in the R-T relationship and find its trajectory across years, which is discussed in Chapter 4.

2.4.2 The effects of crop type (CROP) and land use history (LUH)

The six experimental sites had similar year-to-year trends to the Ref site: the highest soil respiration in 2011, lowest R in 2012, and the rebound in 2013 and 2014. However, the different crops and land use histories induced different magnitudes of impacts and different recovery speeds of R.

Comparing the inter-annual trend of R_s between the three cropping systems, the annual crop had relatively constant values from year to year while perennial crops increased chronologically. The 2014 R_s and R_h at CRP-Pr had even exceeded those in Ref, although there was no significant difference (Fig. 2.5 (A)). It implied that the extensive root system in CRP-Pr had become well-established and that the soil microbial community associated with the dense root systems had high heterotrophic respiration. In contrast to the CRP fields, the R_s and R_h in AGR-Pr fields did not quickly increase but always had similar values with AGR-Sw (Fig. 2.5 (B)). The results agree with my field observations that the AGR-Pr site changed its plant

composition and became more dominated by switchgrass after the dry year (Fig. 3.7; Abraha *et al.*, 2016). The highly similar plant compositions between AGR-Pr and AGR-Sw had similar responses to annual climate regime and to severe drought.

In 2011, most R_s and R_h rates were different between CRP and AGR. This should be the LUH effect from high carbon and nitrogen in the former CRP field soils, which stimulated the growth of plants and soil microbes. Most R_s and R_h were the same in 2012 due to the drought depression of plant and microbial activity. In 2013 and 2014, most corn and switchgrass lands had the similar R_a and R_h, but CRP-Pr had significantly higher R_a and R_h than AGR-Pr. The initial high soil carbon and nitrogen content may stimulate the establishment of root-microbe association underneath the multicultural prairie.

2.4.3 The root contribution (RC) to total soil respiration across years

Other studies have estimated that the root contribution (RC) to total soil respiration ranges 10–90% in different ecosystems, but lower RC contributions are common in non-forest ecosystems. The mean annual RC of grassland and cropping ecosystems from 14 studies was 60.4% (Hanson et al., 2000). My annual growing-season RCs ranged from 0.31 to 0.57 (Table 2.1). The CRP-C had very low means and variations of RCs (0.31 ~ 0.33, Table 2.1 & Fig. 2.13) because high soil carbon and nitrogen content supported the high soil microbial activities, adding the low root respiration of annual crop. The RC values in CRP-C are in the range of maize fields in Hanson *et al.* (2000) review (0.35 ~ 0.40 in growing season). However, RC values in AGR-C are high (0.43 ~ 0.51). This may be due to the long-term (decades) cultivation that reduced soil fertility in the AGR field, which limited soil microbial activities and thus reduced R_h. The Ref site had high RC values with small within- and between-year variations implying a highly developed root system and a very stable carbon allocation to root and soil organic carbon pool.

The resistance of RC to severe drought is high. CRP-Pr and AGR-Sw had lower RC in 2012, revealing that the impact of drought on root was stronger than that on soil microbial community. My field observation, that most plants in CRP-Pr were withered in 2012 summer, which seemingly proves this.

The dry year (2012) had lower RC with higher variation, implying that the 2012 spring-summer drought depressed R_a more than R_h and the effect lasted until the second year (2013). The responses of RC in different crop types and land use histories were different: Ref and AGR-Pr fields were stable; CRP-Pr and AGR-Sw decreased significantly; CRP-Sw increased; CRP-C and AGR-C did not change or changed slightly. In current studies, RC may change seasonally or be stimulated by climate pulses (e.g., huge precipitation or temperature fluctuation) since R_h and R_a may respond to climate differently in timing and magnitude (Carbone *et al.*, 2011; Gomez-Casanovas *et al.*, 2012). I will discuss the seasonal changes of RC and examine how the seasonality of the responses of R_a and R_h affect the annual RC in Chapter 3.

2.4.4 The responses of R_a *and* R_h *to future climate scenarios*

The trend of increasing air temperature (IPCC, 2013) and increasing extreme precipitation events (Andresen *et al.*, 2012) were expected in the Midwestern USA in the future. Grassland and cropping ecosystems are sensitive to drought events and reduce both GPP and R_{eco} in response (Hoover *et al.*, 2014; Reichstein *et al.*, 2013; Ciais *et al.*, 2005; Baldocchi, 2008). In a grassland ecosystem, R_s is the second largest carbon process and can return 50-90% of annual GPP back to the atmosphere (Bahn *et al.*, 2008). The relative strength of the reduction of GPP and R_s under drought stress may change a carbon sink to a carbon source or the amount of net CO_2 it can sequestrate from the atmosphere (Nagy *et al.*, 2007) depending on different responses of respiration and the assimilation. The two major components of soil respiration, R_a and R_h, thus

play crucial roles on the carbon dynamics of cropping and grassland ecosystems. The R_a and R_h have their own mechanisms and are controlled by different biophysical variables.

Photosynthetic carbon supply is one of the crucial variables for both R_a and R_h. The changes of photosynthetic rates and the carbon allocation strategies responding to drought, therefore, affect R_a and R_h severely. Vegetation adapts to environment conditions by modifying its ecophysiological habits. Different crop types have their own strategies and capability to adapt to different magnitudes, durations and frequencies of drought under different environmental conditions (van der Molen *et al.*, 2011). My study explains the different response of R_a and R_h in different CROP and LUH. The Ref field, the late successional grassland, always had high RC each of the four years during my study due to its highly developed root systems. The highly developed root system may connect root and soil microbial community tightly and thus the responses of Ra and Rh to severe drought were similar, resulting the constant RC even in the drought year. The RC in the AGR-Pr fields responded to the severe drought similar to Ref field. In CRP-Pr and AGR-Sw fields, RC decreased to adapt to drought and returned back to the initial values of 2011 soon after the drought year. The water stress of the 2012 drought year caused an early senescence of crops in mid-summer in the CRP-Pr. The AGR-Pr maintained the same RC in the drought year, but the composition of the C4 plant biomass increased after 2012 (Fig. 3.7; from Abraha *et al.*, 2016). The changes of the composition of vegetation and the ecosystem water use efficiency (eWUE) in CRP-Sw, AGR-Pr and AGR-Sw fields revealed how the ecophysiological adapted to severe drought. The increases of C3 vegetation composition can be expected if the occasional severe drought increases in the future. However, the mechanisms and the effect of the adaptation on the ecosystem carbon cycling and atmospheric CO_2 dynamics require more research to explore.

2.5 CONCLUSIONS

The regulatory roles of biophysical factors on soil respiration are complex. Their relationships are always non-linear, interconnected, and need to include the consideration of their threshold and relative strength of force. The dominant factor may change under different biomes and climate regimes. The adaptation of vegetation and soil microbial community increases the complexity of their responses to climate patterns and occasional climate events and human management.

In this chapter, I found that soil respiration positively and exponentially correlated to both T_s and EVI. Soil moisture had weak or no correlation to soil respiration, but instead decoupled the R-T_s or R-EVI correlations when it was low. I also explored the different responses of R_s and R_h under different LUH and CROP after land use conversion at the interannual scale. The mature grassland ecosystem had high R_a and R_h and with high resistance to drought. The CRP-Pr field, which was a multicultural prairie with carbon and nitrogen enriched soil, established a root system 5 years after land use change, despite a severe drought in the third year, and had high R_s and R_h in 2014. Corn, a annual crop, had a lower RC comparing to perennial crops, implying the high importance of heterotrophic soil respiration response to climate change.

I found evidence for the different effects of three forces on soil respiration: the particular year biophysical condition; the severe 2012 drought; and the land use conversion at different timescales. Particular year biophysical variables (annual temperature, water availability and vegetation index) support the potential values of soil respiration in each year. The severe drought in 2012 decreased both R_a and R_h in the same year but its effect prolonged to the following years. The effect of LUC was not very clear other than the CRP fields, which have high soil carbon and nitrogen content, had higher R_a and R_h than AGR fields. Perennial crops had increasing R_s and

R_h while annual did not, revealing the different capacity and ecophysiological adaptation between annual and perennial crops.

The spring-summer severe drought in 2012 depressed R_a and R_h in all fields and induced different responses of R_a:R_s ratios. The RC values in most of fields were decreased or maintained in 2012 but returned to the levels in 2011 although most R_s and R_a were still lower than those in 2011. The changes of the C3:C4 ratio of vegetation biomass and eWUE revealed the ecophysiological adaptations expressed in vegetation to severe drought. It will happen more frequently if the amplitude and frequency of extreme drought events increase in the future.

APPENDIX

Table S.2.1. Monthly climate and microclimate. The monthly air temperature (T_a) and the monthly precipitation (PRCP) were calculated from daily mean air temperature and daily precipitation measured at the KBS LTER weather station. The monthly soil temperature (T_s), and the monthly soil volumetric water content (VWC) were measured biweekly (growing season) or monthly (non-growing season) when soil respiration was measured. The values were mean ± standard deviation. The T_a, T_s, and VWC among four years were compared in a one-way analysis of variance (ANOVA). Different letters after the values denote significant ($p < 0.05$) differences among years by Tukey's HSD (honest significant difference) test. The T_s and VWC for total soil respiration (R_s) and heterotrophic soil respiration (R_h) experiments were measured and analyzed separately.

	R	year	Jan	Feb	Mar	Apr	May	Jun	Jul	Aug	Sep	Oct	Nov	Dec
T_a (°C)		2011	-6.3±3.6ac	-3.5±5.77ab	1.0±4.0a	7.6±4.3a	15.1±5.0a	20.2±3.5a	24.1±2.5a	20.8±2.4a	15.6±4.8a	10.6±4.7a	6.2±4.2a	1.0±3.1a
		2012	-1.6±4.8b	-0.4±3.04a	10.0±8.0b	8.8±3.4a	17.2±4.3a	21.0±4.3a	25.3±2.9a	20.7±3.0a	16.5±4.3a	9.8±5.0a	3.4±4.3ab	1.4±4.6a
		2013	-2.6±3.68ab	-3.9±3.88b	-0.6±3.9a	6.5±4.9a	16.7±5.3a	19.4±3.3a	21.7±3.9b	20.1±2.9a	16.7±4.6a	11.0±5.2a	2.9±5.2ab	-3.7±5.1b
		2014	-8.7±6.4c	-8.0±5.02c	-2.6±5.9a	8.1±4.4a	15.0±5.6a	20.4±2.7a	19.2±2.4c	20.3±2.1a	15.6±4.1a	9.9±3.9a	1.2±5.7b	-0.1±4.1a
PRCP (mm)		2011	19.2	75.7	66.8	146.0	142.4	47.5	186.7	96.3	82.8	89.9	109.0	62.5
		2012	68.3	52.3	78.0	109.0	30.2	22.9	45.5	70.1	58.3	143.0	12.7	52.1
		2013	178.8	107.4	29.5	170.4	118.6	107.9	82.6	117.1	19.3	106.2	73.2	66.3
		2014	73.1	60.5	52.1	67.3	80.5	148.1	102.4	74.2	67.6	98.0	75.7	33.3
T_s (°C)	R_s	2011				10.6±1.9a	15.3±3.4a	21.3±2.5ab	27.5±1.4a	22.0±2.4a	14.7±1.9a	11.8±1.0a	6.9±1.5a	3.7±1.4
		2012			2.1±2.5	10.8±3.4a		20.1±3.4a	28.3±4.4a	22.2±3.1a	15.7±3.2a	10.8±1.9b		
		2013					18.2±3.2b	22.0±2.6b	21.6±2.5b	23.2±2.2a	18.5±1.8b	17.3±2.3c	9.5±0.3b	
		2014					11.8±3.1c	21.8±2.3b	20.2±1.5c	20.4±2.1b	16.1±2.8a			
	R_h	2011				10.5±2.3a	15.0±3.2a	21.3±2.4a	29.3±2.3a	23.5±2.7a	15.3±2.5a	12.0±1.7a	7.1±2.3a	3.3±1.7
		2012			2.6±3.6	11.3±4.4a		23.2±5.3b	30.3±5.4a	22.8±4.2a	15.7±4.7a	11.1±3.3a		
		2013					21.0±3.0b	24.8±3.3c	25.1±4.0b	25.7±2.3b	19.4±2.0b	18.8±2.3b	9.2±0.3b	
		2014					13.4±3.8c	25.6±3.2c	23.3±2.8c	22.8±3.4a	17.9±2.6c			
VWC (%)	R_s	2011				23.57±5.14a	21.89±5.70a	16.49±4.91a	7.43±2.06a	18.77±5.14a	13.61±3.13a	23.11±4.20a	26.43±3.96a	31.29±5.14
		2012			28.71±5.74	20.96±4.11b		8.20±4.53b	8.84±7.24a	15.90±6.43b	11.89±6.26a	21.27±4.38a		
		2013					19.44±5.99b	22.32±4.74c	9.94±3.52a	16.57±5.24ab	12.45±3.83a	10.82±4.49b	25.88±3.99a	
		2014					24.14±5.50a	21.02±5.66c	15.18±6.80b	12.47±7.49c	23.59±6.23b			
	R_h	2011				23.22±5.33a	21.25±5.61a	16.68±5.14a	14.79±5.24a	20.68±5.05a	19.00±4.91a	22.96±4.58a	25.46±4.32a	30.19±5.11
		2012			27.12±6.26	18.59±3.87b		10.84±3.85b	10.19±5.65b	15.26±4.91b	13.04±4.17b	19.35±5.82b		
		2013					17.33±4.77b	20.05±4.42c	14.36±4.09a	18.45±4.64a	16.31±4.18a	13.99±4.70c	23.59±3.77b	
		2014					20.91±4.98a	20.74±4.43c	15.23±5.23a	15.20±5.61b	22.28±5.15c			

Table S.2.2. The Pearson's correlation between soil respiration (R or $\log_{10}R$) and its potential controls (T_s, *VWC*, *NDVI* and *EVI*).

			2011														2012								
CROP	LUH	R	$\log R \sim T_s$		$R \sim VWC$		$\log R \sim NDVI$		$\log R \sim EVI$								$\log R \sim T_s$		$R \sim VWC$		$\log R \sim NDVI$		$\log R \sim EVI$	
			r	p	r	p	r	p	r	p							r	p	r	p	r	p	r	p
C	CRP	R_s	0.83	2.22E-16	-0.42	9.46E-04	0.67	7.09E-09	0.75	9.92E-12							0.71	1.02E-14	-0.24	2.25E-02	0.73	4.44E-16	0.73	4.44E-16
		R_h	0.79	7.68E-14	-0.25	5.71E-02	0.70	8.52E-10	0.77	1.81E-12							0.80	< 2.2E-16	-0.23	2.89E-02	0.72	1.78E-15	0.66	1.74E-12
	AGR	R_s	0.68	9.64E-09	-0.29	3.37E-02	0.53	3.57E-05	0.57	4.74E-06							0.72	2.40E-14	-0.24	3.10E-02	0.72	1.02E-14	0.73	5.33E-15
		R_h	0.60	1.21E-06	0.04	7.94E-01	0.07	6.15E-01	0.14	3.25E-01							0.72	4.89E-15	-0.35	8.16E-04	0.70	3.73E-14	0.70	5.82E-14
Sw	CRP	R_s	0.73	3.16E-10	-0.37	4.35E-03	0.63	9.91E-08	0.59	7.12E-07							0.50	3.66E-06	-0.42	1.17E-04	0.81	< 2.2E-16	0.68	1.62E-11
		R_h	0.64	1.34E-07	-0.28	3.40E-02	0.52	2.27E-05	0.51	3.44E-05							0.67	1.25E-12	-0.40	1.18E-04	0.67	1.86E-12	0.56	2.17E-08
	AGR	R_s	0.64	5.81E-08	-0.28	3.03E-02	0.62	1.66E-07	0.59	9.23E-07							0.73	1.33E-15	-0.39	1.66E-04	0.75	< 2.2E-16	0.65	1.15E-11
		R_h	0.70	2.14E-09	-0.31	1.79E-02	0.48	1.16E-04	0.43	7.79E-04							0.79	< 2.2e-16	-0.58	2.27E-09	0.78	< 2.2E-16	0.71	2.18E-14
Pr	CRP	R_s	0.65	3.99E-08	-0.33	1.18E-02	0.47	2.02E-04	0.42	9.54E-04							0.58	2.38E-09	-0.20	5.98E-02	0.75	< 2.2E-16	0.60	4.46E-10
		R_h	0.69	3.71E-09	-0.43	5.79E-04	0.40	1.78E-03	0.40	1.51E-03							0.60	9.70E-10	-0.40	1.22E-04	0.74	4.44E-16	0.56	1.19E-08
	AGR	R_s	0.80	7.59E-14	-0.32	1.27E-02	0.68	3.96E-09	0.72	1.15E-10							0.80	< 2.2E-16	-0.54	7.26E-08	0.72	7.11E-15	0.71	3.40E-14
		R_h	0.66	3.27E-08	-0.31	1.59E-02	0.49	7.20E-05	0.47	1.80E-04							0.82	< 2.2E-16	-0.63	7.34E-11	0.76	< 2.2E-16	0.70	9.77E-14
Br	CRP	R_s	0.77	7.27E-12	-0.35	6.06E-03	0.63	7.13E-08	0.62	1.55E-07							0.61	2.01E-09	-0.37	6.42E-04	0.55	1.52E-07	0.56	7.53E-08
		R_h	0.65	1.06E-07	-0.57	3.11E-06	0.67	8.47E-09	0.75	8.89E-12							0.71	6.44E-15	-0.48	1.92E-06	0.44	1.49E-05	0.34	1.02E-03

			2013								2014							
CROP	LUH	R	$\log R \sim T_s$		$R \sim VWC$		$\log R \sim NDVI$		$\log R \sim EVI$		$\log R \sim T_s$		$R \sim VWC$		$\log R \sim NDVI$		$\log R \sim EVI$	
			r	p	r	p	r	p	r	p	r	p	r	p	r	p	r	p
C	CRP	R_s	0.78	< 2.2E-16	-0.09	3.36E-01	0.38	2.09E-04	0.56	8.31E-09	0.72	1.67E-12	-0.14	2.39E-01	0.33	4.31E-03	0.46	5.01E-05
		R_h	0.78	< 2.2E-16	-0.16	9.99E-02	0.35	9.45E-04	0.51	5.52E-07	0.63	3.43E-09	-0.02	8.95E-01	0.39	6.35E-04	0.33	5.27E-03
	AGR	R_s	0.66	2.24E-13	0.07	4.86E-01	0.44	7.57E-06	0.57	1.73E-09	0.70	1.01E-11	-0.01	9.56E-01	0.64	1.48E-09	0.64	2.06E-09
		R_h	0.64	2.08E-12	0.01	9.08E-01	0.33	1.12E-03	0.43	8.81E-06	0.48	1.77E-05	-0.03	8.10E-01	0.47	3.01E-05	0.35	2.75E-03
Sw	CRP	R_s	0.76	4.44E-16	0.07	5.02E-01	0.69	2.09E-12	0.74	2.89E-15	0.73	3.09E-13	-0.48	2.10E-05	0.72	1.15E-12	0.65	6.10E-10
		R_h	0.78	< 2.2E-16	-0.10	2.92E-01	0.72	3.75E-14	0.72	6.80E-14	0.54	8.68E-07	-0.08	4.81E-01	0.51	4.63E-06	0.50	9.73E-06
	AGR	R_s	0.90	< 2.2E-16	-0.18	7.02E-02	0.50	7.91E-07	0.55	2.2E-08	0.72	6.61E-13	-0.36	1.77E-03	0.60	3.19E-08	0.57	1.61E-07
		R_h	0.84	< 2.2E-16	-0.27	5.10E-03	0.54	9.07E-08	0.55	3.98E-08	0.82	< 2.2E-16	-0.35	2.90E-03	0.65	5.22E-10	0.65	7.57E-10
Pr	CRP	R_s	0.73	1.95E-14	-0.05	6.40E-01	0.69	1.43E-12	0.74	4.22E-15	0.78	4.44E-16	-0.22	5.86E-02	0.79	4.44E-16	0.67	9.31E-11
		R_h	0.80	< 2.2E-16	-0.04	6.86E-01	0.78	< 2.2Ee-16	0.78	< 2.2e-16	0.80	< 2.2E-16	-0.14	2.40E-01	0.71	1.76E-12	0.65	8.55E-10
	AGR	R_s	0.89	< 2.2E-16	-0.22	2.19E-02	0.64	2.55E-11	0.65	1.16E-11	0.79	2.22E-16	-0.28	1.73E-02	0.70	7.65E-12	0.76	1.78E-14
		R_h	0.84	< 2.2E-16	-0.05	6.25E-01	0.62	1.80E-10	0.62	1.66E-10	0.47	2.69E-05	-0.01	9.05E-01	0.56	3.28E-07	0.54	8.63E-07
Br	CRP	R_s	0.60	3.22E-09	-0.24	1.44E-02	0.60	2.37E-09	0.69	6.97E-13	0.53	1.49E-06	-0.07	5.64E-01	0.65	5.90E-10	0.64	1.37E-09
		R_h	0.71	2.03E-13	-0.05	6.31E-01	0.71	1.17E-13	0.77	< 2.2e-16	0.69	1.40E-11	0.05	6.71E-01	0.75	3.29E-14	0.66	3.15E-10

* CROP (crop type): C: corn; Sw: switchgrass; Pr: prairie mixture; Br: brome grass in reference

* LUH (land use history): CRP: Conservation Reserve Program; AGR: corn-soybean rotation conventional agriculture

* R (soil respiration): R_s: total soil respiration; R_h: heterotrophic soil respiration

* r: Pearson's correlation; *p*: *p-value*

Table S.2.3. The exponential model of total soil respiration (R_s)/heterotrophic soil respiration (R_h) and soil temperature (T_s) and the temperature sensitivity (Q_{10}) during 2011 and 2014. The soil coefficients *a* and *b* were calculated from the equation: $R = a * e^{bTs}$, temperature sensitivity of soil respiration (Q_{10}) were calculated by e^{10b}.

CROP	LUH	R	2011 a	b	Q_{10}	r^2	n	*p*	2012 a	b	Q_{10}	r^2	n	*p*
C	CRP	R_s	0.73±1.67	0.04±0.03	1.57±1.35	0.69	59	2.73E-16	0.74±1.76	0.03±0.03	1.34±1.34	0.51	88	1.03E-14
		R_h	0.75±1.72	0.04±0.03	1.46±1.34	0.63	59	7.67E-14	0.59±1.83	0.04±0.03	1.46±1.34	0.64	88	<2E-16
	AGR	R_s	0.72±2.14	0.04±0.04	1.45±1.50	0.47	55	9.64E-09	1.48±2.51	0.04±0.04	1.49±1.54	0.46	88	3.83E-13
		R_h	0.70±2.05	0.03±0.04	1.31±1.45	0.36	55	1.21E-06	0.40±2.32	0.04±0.04	1.48±1.46	0.52	88	2.28E-15
Sw	CRP	R_s	1.13±1.67	0.03±0.03	1.36±1.35	0.53	59	3.16E-10	1.04±2.01	0.02±0.03	1.20±1.40	0.25	88	3.55E-06
		R_h	1.05±1.92	0.03±0.04	1.34±1.45	0.41	59	1.34E-07	0.63±2.13	0.03±0.03	1.35±1.40	0.45	88	1.25E-12
	AGR	R_s	0.84±2.14	0.03±0.04	1.41±1.53	0.41	59	5.80E-05	0.56±2.45	0.05±0.04	1.58±1.55	0.53	88	1.45E--15
		R_h	0.63±2.24	0.04±0.04	1.51±1.56	0.47	59	3.16E-09	0.44±2.25	0.05±0.04	1.59±1.44	0.63	88	<2E-16
Pr	CRP	R_s	1.10±1.92	0.03±0.04	1.38±1.48	0.42	59	3.99E-08	0.84±2.31	0.03±0.05	1.39±1.59	0.34	88	2.38E-09
		R_h	0.97±1.97	0.04±0.04	1.42±1.47	0.47	59	3.71E-09	0.73±2.13	0.03±0.04	1.31±1.44	0.36	88	9.70E-10
	AGR	R_s	0.82±1.74	0.04±0.03	1.51±1.37	0.65	59	7.59E-14	0.62±1.98	0.05±0.03	1.59±1.42	0.65	85	<2E-16
		R_h	0.68±2.39	0.04±0.05	1.52±1.64	0.43	59	3.27E-08	0.43±2.02	0.05±0.03	1.58±1.38	0.68	85	<2E-16
Br	CRP	R_s	1.18±1.62	0.04±0.03	1.43±1.37	0.59	59	7.27E-12	1.03±2.10	0.03±0.03	1.42±1.62	0.37	88	2.01E-09
(Ref)		R_h	1.06±1.9	0.03±0.04	1.38±1.49	0.42	59	1.06E-07	0.62±2.18	0.05±0.05	1.60±1.60	0.51	88	6.43E-15

CROP	LUH	R	2013 a	b	Q_{10}	r^2	n	*p*	2014 a	b	Q_{10}	r^2	n	*p*
C	CRP	R_s	0.55±2.38	0.05±0.04	1.65±1.55	0.58	107	<2E-16	0.83±1.90	0.03±0.03	1.40±1.40	0.51	72	1.67E-12
		R_h	0.56±3.46	0.03±0.06	1.40±1.75	0.27	106	1.01E-08	0.72±2.37	0.03±0.04	1.38±1.49	0.39	72	3.43E-09
	AGR	R_s	0.79±2.39	0.03±0.04	1.30±1.52	0.29	112	1.21E-09	0.80±1.94	0.03±0.03	1.38±1.40	0.49	72	1.01E-11
		R_h	0.43±3.24	0.04±0.05	1.44±1.68	0.33	113	2.29E-11	0.71±2.72	0.02±0.04	1.27±1.55	0.23	72	1.77E-05
Sw	CRP	R_s	0.61±2.89	0.06±0.06	1.81±1.86	0.48	104	2.56E-16	0.67±2.69	0.06±0.06	1.81±1.75	0.53	72	3.09E-13
		R_h	0.44±2.45	0.06±0.05	1.74±1.62	0.57	104	<2E-16	0.88±2.26	0.03±0.04	1.31±1.53	0.29	72	8.68E-07
	AGR	R_s	0.71±2.16	0.04±0.04	1.55±1.51	0.54	104	<2E-16	0.71±2.48	0.05±0.05	162±1.60	0.52	72	6.61E-13
		R_h	0.38±2.52	0.06±0.05	1.77±1.58	0.62	105	<2E-16	0.47±2.27	0.05±0.04	1.71±1.47	0.66	72	< 2.2E-16
Pr	CRP	R_s	0.57±2.67	0.06±0.05	1.86±1.71	0.58	104	<2E-16	1.03±1.85	0.04±0.03	1.51±1.40	0.61	72	5.72E-16
		R_h	0.43±2.16	0.06±0.04	1.76±1.44	0.71	104	<2E-16	0.74±1.87	0.04±0.03	1.47±1.33	0.65	72	< 2.2E-16
	AGR	R_s	0.562.17	0.05±0.04	1.72±1.50	0.64	104	<2E-16	0.77±2.10	0.05±0.04	1.63±1.47	0.62	72	< 2.2E-16
		R_h	0.37±1.86	0.05±0.03	1.72±1.34	0.78	106	<2E-16	0.86±2.65	0.02±0.04	1.26±1.55	0.22	72	2.69E-05
Br	CRP	R_s	0.75±2.32	0.06±0.05	1.76±1.66	0.56	107	<2E-16	1.29±2.14	0.03±0.04	1.31±1.55	0.28	72	1.49E-06
(Ref)		R_h	0.47±2.20	0.05±0.04	1.67±1.47	0.65	104	<2E-16	0.71±2.32	0.04±0.04	1.45±1.48	0.48	72	1.40E-11

* CROP (crop type): C: corn; Sw: switchgrass; Pr: prairie mixture; Br: brome grass in CRP reference site.

* LUH (land use history): CRP: Conservation Reserve Program; AGR: corn-soybean rotation conventional agriculture.

* R (soil respiration): R_s: total soil respiration; R_h: heterotrophic soil respiration

Table S.2.4. The two-level interactive TWV models for R_s and R_h. The parameters of the two-level interaction multiple variable soil respiration regression models (TWE models) from soil temperature (T_s), soil water content (VWC), enhanced vegetation index (EVI) and the research sites with different land use histories and crop types. The function is:

$logR = a + b*T_s + c*logVWC + d*EVI+ e1*(AGR-Pr) + e2*(AGR-Sw) + e3*(CRP-C) + e4*(CRP-Pr) + e5*(CRP-Ref) + e6*(CRP-Sw) + f*(T_s:logVWC) + g*(Ts:EVI) + h*(logVWC:EVI) + i1*(T_s:AGR-Pr) + i2*(T_s:AGR-Sw) + i3*(T_s:CRP-C) + i4*(T_s:CRP-Pr) + i5*(T_s:CRP-Ref) + i6*(T_s:CRP-Sw) + j1*(logVWC:AGR-Pr) + j2*(logVWC:AGR-Sw) + j3*(logVWC:CRP-C) + j4*(logVWC:CRP-Pr) + j5*(logVWC:CRP-Ref) + j6*(logVWC:CRP-Sw) + k1*(EVI:AGR-Pr) + k2*(EVI:AGR-Sw) + k3*(EVI:CRP-C) + k4*(EVI:CRP-Pr) + k5*(EVI:CRP-Ref) + k6*(EVI:CRP-Sw).$

The blank cells were the terms removed from best-fit model via AIC. The R_s and R_h models were established separately. Both use actual data in 2011-2014.

	a	b	c	d	e1	e2	e3	e4	e5	e6	f	g	h	i1	i2	i3	i4	i5	i6
R_s	-2.137	0.045	0.609	4.658	0.446	0.223	0.390	0.307	0.990	0.576	0.017	-0.110	-1.154	0.012	0.013	0.005	0.014	0.007	0.013
R_h	-1.085	0.037	-0.150	1.913	0.116	0.595	0.061	0.342	0.369	-0.077	0.024	-0.095							

	j1	j2	j3	j4	j5	j6	k1	k2	k3	k4	k5	k6
R_s	-0.226	-0.106	-0.166	-0.003	-0.304	-0.193	-0.391	-0.378	-0.391	-0.425	-0.727	-0.705
R_h	-0.110	-0.569	-0.052	-0.215	-0.172	0.193	0.585	0.842	0.649	0.816	0.598	0.359

Table S.2.5. The effects of CROP and LUH on total (R_s) and heterotrophic soil respiration (R_h). (A) Effect of crop type (CROP and land use history (LUH) and their interaction on total soil respiration (R_s) and heterotrophic soil respiration (R_h). The *p-value* was calculated from the two-way analysis of variance (ANOVA) by R language for each year. (B) Pair comparisons between different CROP (C: corn, Sw: switch grass, Pr: prairie mixture and ref: brome grass in reference site) and different LUH (CRP: Conservation Reserve Program, AGR: corn-soybean rotation agriculture and Ref: reference). The *p*-value from Tukey HSD post-hoc test represented the difference of R_s (right-up corner of table) and R_h (left-down corner of table) between different crop types and between different LUHs.

(A)

		2011	2012	2013	2014
R_s	CROP	1.93e-08 ***	1.99e-13 ***	<2e-16 ***	<2e-16 ***
	LUH	3.74e-10 ***	0.00693 **	4.77e-07 ***	1.34e-05 ***
R_h	CROP	6.6e-09 ***	9.94e-10 ***	2.11e-14 ***	1.28e-06 ***
	LUH	<2e-16 ***	0.00795 **	2.48e-06 ***	5.67e-05 ***

***: *p-value* < 0.001; **: 0.001 < *p* < 0.01; *: 0.01 < *p* < 0.05; . : 0.05 < *p* < 0.1

(B)

year 2011

CROP ffect

R_h R_s	C	Sw	Pr	Ref
C		0.2111714	0.0092386***	0***
Sw	0.0383932*		0.6094264	0.0000172***
Pr	0.0000677***	0.2911074		0.0010832***
Ref	0***	0.0000297***	0.0072699***	

LUH

R_h R_s	CRP	AGR	Ref
CRP		0.0081931**	0.0000962***
AGR	0***		0***
Ref	0.0131907*	0***	

2012

CROP

R_h R_s	C	Sw	Pr	Ref
C		0.0019099**	0.0000154***	0***
Sw	0.4263716		0.8407322	0.0000026***
Pr	0.4261766	1		0.0002107***
Ref	0.0028281***	0.1072257	0.1072911	

LUH

R_h R_s	CRP	AGR	Ref
CRP		0.4526613	0.0000001***
AGR	0.7236371		0***
Ref	0.0285623*	0.0057242**	

2013

CROP

R_h R_s	C	Sw	Pr	Ref
C		0.0000006***	0***	0***
Sw	0.0286266*		0.8765797	0.0000859***
Pr	0.0000187***	0.2306837		0.0010844**
Ref	0.0000105***	0.0484249*	0.7113536	

LUH

R_h R_s	CRP	AGR	Ref
CRP		0.0000011***	0.0001504***
AGR	0.0002140***		0***
Ref	0.2538962	0.000214***	

2014

CROP

R_h R_s	C	Sw	Pr	Ref
C		0***	0***	0***
Sw	0.0566624.		0.0000812***	0.0023843**
Pr	0.0001247***	0.292746		0.9999831
Ref	0.000114***	0.1214564	0.8778098	

LUH

R_h R_s	CRP	AGR	Ref
CRP		0.0043459**	0.0141944*
AGR	0.0011549***		0.0000017***
Ref	0.421979	0.0005237***	

***: *p-value* < 0.001; **: 0.001 < *p* < 0.01; *: 0.01 < *p* < 0.05; . : 0.05 < *p* < 0.1

LITERATURE CITED

LITERATURE CITED

Abraha, M., Gelfand, I., Hamilton, S.K., Shao, C., Su, Y.J., Robertson, G.P., Chen, J., 2016. Ecosystem water-use efficiency of annual corn and perennial grasslands: contributions from land-use history and species composition. Ecosystems, 19, 1001-1012.

Andresen, J., S. Hilberg, K. Kunkel, 2012. Historical climate and climate trends in the Midwestern USA. In: U.S. National Climate Assessment Midwest Technical Input Report. J. Winkler, J. Andresen, J. Hatfield, D. Bidwell, and D. Brown, coordinators. Available from the Great Lakes Integrated Sciences and Assessments (GLISA) Center, http://glisa.msu.edu/docs/NCA/MTIT_Historical.pdf.

Bahn, M., Rodeghiero, M., Anderson-Dunn, M., Dore, S., Gi- meno, C., Drösler, M., Williams, M., Ammann, C., Berninger, F., Flechard, C., Jones, S., Balzarolo, M., Kumar, S., Newesely, C., Priwitzer, T., Raschi, A., Siegwolf, R., Susiluoto, S., Tenhunen, J., Wohlfahrt, G., Cernusca, A., 2008. Soil respiration in European grasslands in relation to climate and assimilate supply, Ecosystems, 11, 1352–1367.

Baldocchi, D., 2008. Breathing of the terrestrial biosphere: lessons learned from a global network of carbon dioxide flux measurement systems. Australian Journal of Botany, 56 (1), 1–26.

Carbone, M.S., Still, C.J., Ambrose, A.R., Dawson, T.E., Williams, A.P., Boot, C.M., Schaeffer, S.M., Schimel, J.P., 2011. Seasonal and episodic moisture controls on plant and microbial contributions to soil respiration. Oecologia, 167, 265-278.

Ciais, P., Reichstein, M., Viovy, N., Granier, A., Ogee, J., Allard, V., Aubinet, M., Buchmann, N., Bernhofer, C., Carrara, A., Chevallier, F., De Noblet, N., Friend, A.D., Friedlingstein, P., Grünwald, T., Heinesch, B., Keronen, P., Knohl, A., Krinner, G., Loustau, D., Manca, G., Matteucci, G., Miglietta, F., Ourcival, J.M., Papale, D., Pile- gaard, K., Rambal, S., Seufert, G., Soussana, J.F., Sanz, M.J., Schulze, E.D., Vesala, T., Valentini, R., 2005. Europe-wide reduction in primary productivity caused by the heat and drought in 2003. Nature, 437 (7058), 529–533.

Curiel Yuste, Y., Janssens, I.A., Carrara, A., Meiresonne, L., Ceulemans, R., 2003. Interactive effects of temperature and precipitation on soil respiration in a temperate maritime pine forest. Tree Physiology, 23, 1263-1270.

Flanagan, L.B., Johnson, B.G., 2005. Interacting effects of temperature, soil moisture and plant biomass production on ecosystem respiration in a northern temperate grassland. Agricultural and Forest Meteorology, 130, 237-253.

Goulden, M.L., Munger, J.W., Fan, S.M., Daube, B.C., Wofsy, S.C., 1996. Exchange of carbon dioxide by a deciduous forest: Response to interannual climate variability. Science, 271, 1576-1578.

Gomez-Casanovas, N., Matamala, R., Cook, D.R., Gonzalez-Meler, M.A., 2012. Net ecosystem exchange modifies the relationship between the autotrophic and heterotrophic components of soil respiration with abiotic factors in prairie grasslands. Global Change Biology, 18, 2532-2545.

Hanson, P.J., Edwards, N.T., Garten, C.T., Andrews, J.A., 2000. Separating root and soil microbial contributions to soil respiration: A review of methods and observations. Biogeochemistry, 48, 115-146.

Hoover, D., Knapp, A., Smith, M., 2014. Resistance and resilience of a grassland ecosystem to climate extremes. Ecology, 95, 2646– 2656, doi:10.1890/13-2186.1.

Hopkins, F., Gonzales-Meler, M.A., Flower, C.E., Lynch, D.J., Czimczik, C., Tang, J., Subke, J.A., 2013. Ecosystem-level controls on root-rhizosphere respiration. New Phytologist, 199, 339-351.

Huete, A., Justice, C., van Leeuwen, W., 1999. MODIS vegetation index (MOD 13) algorithm theoretical basis document, Center, N.G.S.F. (Eds.), p. 129.

IPCC, 2013: Climate Change 2013: The Physical Science Basis. Contribution of Working Group I to the Fifth Assessment Report of the Intergovernmental Panel on Climate Change [Stocker, T.F., D. Qin, G.-K. Plattner, M. Tignor, S.K. Allen, J. Boschung, A. Nauels, Y. Xia, V. Bex and P.M. Midgley (eds.)]. Cambridge University Press, Cambridge, United Kingdom and New York, NY, USA, 1535 pp, doi: 10.1017/CBO9781107415324.

Lloyd, J., Taylor, J.A., 1994. On the temperature dependence of soil respiration. Functional Ecology, 8, 315-323.

Longdoz, B., Yernaux, M., Aubinet, M., 2000. Soil CO2 efflux measurements in a mixed forest: impact of chamber distances, spatial variability and seasonal evolution. Global Change Biology, 6, 907-917.

Luo, Y., Wan, S., Hui, D., Wallace, L.L., 2001. Acclimatization of soil respiration to warming in a tall grass prairie. Nature, 413, 622-625.

Nagy, Z., Pintér, K., Czóbel, S., Balogh, J., Horváth, L., Fóti, S., Barcza, Z., Weidinger, T., Csintalan, Z., Dinh, N.Q., Grosz, B., Tuba, Z., 2007. The carbon budget of semi-arid grassland in a wet and a dry year in Hungary. Agriculture, Ecosystems & Environment, 121, 21-29.

Post, W.M., Emanuel, W.R., Zinke, P.J., Stangenberger, A.G., 1982. Soil carbon pools and world life zones. Science, 298, 156-159.

R Development Core Team, 2010. R: A language and environment for statistical computing. R Foundation for Statistical Computing, Vienna, Austria.

Raich, J.W., Schlesinger, W. H., 1992. The global carbon dioxide flux in soil respiration and its relationship to vegetation and climate. Tellus, 448, 81-99.

Raich, J.W., Tufekcioglu, A., 2000. Vegetation and soil respiration: Correlations and controls. Biogeochemistry, 48, 71-90.

Raich, J.W., Potter, C.S., Bhagawati, D.B., 2002. Interannual variability in global soil respiration, 1980-94. Global Change Biology, 8, 800-812.

Reichstein, M., Rey, A., Freibauer, A., Tenhunen, J., Valentini, R., Banza, J., Casals, P., Cheng, Y., Grünzweig, J. M., Irvine, J., Joffre, R., Law, B. E., Loustau, D., Miglietta, F., Oechel, W., Ourcival, J. M., Pereira, J. S., Peressotti, A., Ponti, F., Qi, Y., Rambal, S., Rayment, M., Romanya, J., Rossi, F., Tedeschi, V., Tirone, G., Xu, M., and Yakir, D., 2003. Modeling temporal and large-scale spatial variability of soil respiration from soil water availability, temperature and vegetation productivity indices. Global Biogeochemical Cycles, 17(4), 1104.

Reichstein, M., Bahn, M., Ciais, P., Grank, D., Mahecha, M.D., Seneviratne, S.I., Zscheischler, J., Beer, C., Buchmann, N., Frank, D.C., Papale, D., Rammig, A., Smith, P., Thonicke, K., van der Velde, M., Vicca, S., Walz, A., Wattenbach, M., 2013. Climate extremes and the carbon cycle. Nature, 500, 287-296.

Ryan, M.G., Law, B.E., 2005. Interpreting, measuring, and modeling soil respiration. Biogeochemistry, 73, 3-27.

Schlesinger, W.H. & Andrews, J.A., 2000. Soil respiration and the global carbon cycle. Biogeochemistry, 48, 7-20.

Tang, J., Misson, L., Gershenson, A., Cheng, W., Goldstein, A.H., 2005. Continuous measurements of soil respiration with and without roots in a ponderosa pine plantation in the Sierra Nevada Mountains. Agricultural and Forest Meteorology, 132, 212-227.

Tucker, C., Pinzon, J., Brown, M., Slayback, D., Pak, E., Mahoney, R., Vermote, E., El Saleous, N., 2005. An extended AVHRR 8-km NDVI dataset compatible with MODIS and SPOT vegetation NDVI data. International Journal of Remote Sensing, 26, 4485-4498.

van der Molen, M.K., Dolman, A.J., Ciais, P., Eglin, T., Gobron, N., Law, B.E., Meir, P., Peters, W., Phillips, O.L., Reich- stein, M., Chen, T., Dekker, S.C., Doubková, M., Friedl, M.A., Jung, M., van den Hurk, B.J.J.M., de Jeu, R.A.M., Kruijt, B., Ohta, T., Rebel, K.T., Plummer, S., Seneviratne, S.I., Sitch, S., Teuling, A.J., van der Werf, G.R., and Wang, G., 2011. Drought and ecosystem carbon cycling. Agricultural and Forest Meteorology, 151, 765-773.

van't Hoff, J. H., 1884. *Études de Dynamique Chimique* (Studies of Chemical Dynamics). Frederik Muller and Co., Amsterdam, the Netherlands.

CHAPTER 3
SEASONAL PATTERNS OF SOIL RESPIRATION AND ITS RESPONSE TO MICROCLIMATE

ABSTRACT

Water deficits vary in timing, duration and magnitude, and may affect plant growth and soil microbial activities differently. A short-term, normal seasonal water deficit and a long-term, occasional drought may bring very different consequences to ecosystems. For example, a mid-summer short-term (days to weeks) drought is common in humid ecosystems during the growing season, and affects the soil respiration during the dry period. In the experimental treatments studied here, soil respiration decreased when water deficit occurred, but recovered soon after once rainfall had replenished the soil water. Many cropping systems had the highest soil respiration peak in August following the drought in each year. I observed that a short-term water deficit decoupled the R-T_s relationship, which quickly recovered and possibly altered the annual soil carbon efflux depending on the timing of summer drought. In contrast to the short-term drought, the 2012 May-July long-term (months) drought, the abnormally warm March, and the consequent early onset of the growing season, depleted available soil water in June and induced the obvious decrease of vegetation indices and lowered soil respiration for the whole growing season. The result of that spring-summer 2012 drought was the extremely low R_a in the CRP-Pr, CRP-Sw and AGR-Sw fields and very low R_h in CRP-Sw. The dramatic decrease of R_a when VWC was low suggests that root respiration diminished greatly. The change of C3:C4 biomass composition and ecosystem water-use efficiency implies that the community structure and the carbon- and water-related ecological processes had altered to adapt to the drought.

I concluded that the occasional long-term spring-summer drought had very different effects on soil respiration compared to the normal short-term summer dry period. The spring-

summer drought impacted the soil respiration through the whole growing season and may have extended to the subsequent years. In the prairie and switchgrass treatments, the decreased soil respiration in subsequent years may reflect the shift of plant species composition toward greater dominance by C4 grasses, which may be better adapted to drought disturbance. However, we need more research to understand how these systems respond to climate variability.

3.1 INTRODUCTION

Soil respiration, as one of the largest fluxes of carbon between ecosystems and the atmosphere, is important for the atmospheric carbon budget and represents a major feedback mechanism that may affect future climate changes (Goulden *et al.*, 1996; Post *et al.*, 1982; Raich *et al.*, 2002; Raich & Schlesinger, 1992; Ryan & Law, 2005; Schlesinger & Andrews, 2000). The strong seasonality of soil respiration based on the intra-annual variations of soil temperature, soil moisture and plant productivity has been widely reported (Luo and Zhou, 2006; Tang and Baldocchi, 2005). However, the components of soil respiration, including autotrophic (R_a) and heterotrophic soil respiration (R_h), have different mechanisms and feedbacks in response to climate and human management. The net balance of carbon is determined by the sum of the processes of R_a and R_h and the drivers that affect them. Thus, the partitioning of soil respiration becomes essential for explaining the behavior of soil respiration and its effects on soil carbon pools.

Autotrophic respiration includes respiration from roots and rhizosphere microbes that generally respire photosynthetically produced organic carbon after a short lag time after photosynthesis. In some climate regimes and biomes, R_a may be more strongly related to daytime net ecosystem exchange (NEE) of CO_2 rather than temperature. The lags of carbon allocation from photosynthesis in leaves to root respiration was only 4-6 days (Gomez-

Casanovas *et al.*, 2012). Heterotrophic soil respiration is due to the free-living soil microbial community and is known to be controlled by soil temperature, soil moisture and daytime NEE. The major carbon source to support R_h is from photosynthesis but it may be delayed 36-42 days from photosynthesis (Gomez-Casanovas *et al.*, 2012). Climate dynamics or disturbance may impact R_a and R_h at different times intra-annually due to their distinct magnitude, the length of lags –the legacy effects.

Many studies have partitioned soil respiration into these two components to understand the relative contribution of them in different ecosystems across climate regimes with diverse results. However, studies focusing on grassland and cropping systems are very limited, especially for those with history of land use conversion. My study is important because of the increased land use conversion from grassland and other land use types to bioenergy crops in the past decade (Lark *et al.*, 2015) and the prospect for more conversion in the future. Understanding the responses of biofuel cropping systems to climate regimes and events in the Midwest US will help us evaluate the contribution of biofuel crops to net carbon balances in the US.

In Chapter 2, I explored how autotrophic (R_a) and heterotrophic soil respiration (R_h) responds to climate variability, including a severe drought at inter-annual scales. However, the timing of drought events within a growing season can alter the annual soil respiration if they depress the growth and development of plants in certain phenological stages (Curiel Yuste *et al.*, 2004; Hanson *et al.*, 2000) and can have a crucial effect on soil carbon efflux. For example, Savage and Davidson (2001) suggested that the spring and summer droughts and the advanced onset of spring had a stronger impact on annual soil respiration than those that happened during the later growing season. In this chapter, I explored the effect of that seasonality of biophysical variables have on the seasonal patterns of R_a and R_h. I hypothesized that soil temperature and the

photosynthesis-derived carbon control R_a and R_h during most of the growing season, while low soil water in dry periods diminished soil respiration—even if T_a and EVI are high. I also examined the seasonal variations of root contribution to soil respiration (RC) in each year under different climate patterns. I hypothesized that the normal climate regime drives the seasonal patterns of soil respiration within most years, while a severe drought disturbance may change ecosystem properties and the biogeochemical processes (i.e., soil respiration), as well as impact the ecosystem well after the drought ends.

3.2 METHODS

3.2.1 Study area

My experimental sites are located at the Great Lakes Bioenergy Research Center scale-up fields of the Kellogg Biological Station (KBS, 42°40'N, 85°40'W), established in association with the KBS Long-Term Ecological Research (LTER) site. The sites are located in the southwest of Michigan, USA (Fig. 1.2.). The climate is humid continental (warm summer) climate (Dfa) (Peel *et al.*, 2007). The mean annual air temperature and mean annual precipitation at KBS are 10.1 °C and 1005 mm yr^{-1} (1981-2010), respectively (Robertson & Hamilton, 2015).

3.2.2 Experimental design and schedule

Seven experimental plots were chosen at two locations, each with its own land use history (LUH): (1) Conservation Reserve Program (CRP) grasslands at Marshall Farm, and (2) corn-soybean rotation agricultural fields (AGR) at Lux Arbor Reserve. The CRP sites have been in a monoculture of smooth brome grass (*Bromus inermis* Leyss) since 1987, while the AGR fields have been under a conventional corn-soybean rotation cultivation for several decades (Fig. 1.6). The soil texture at all sites is sandy loam, except for a sandy clay loam at one field.

However, soil carbon and nitrogen contents at the CRP sites were significantly higher than those at the AGR sites before land conversion (Table 1.1).

The experiment was conducted at seven scale-up fields ranging from 9 to 17 hectares. Four fields are located in Marshall Farm (i.e., CRP sites) and three in Lux Arbor Reserve (i.e., AGR sites). All sites, except the reference site (Ref), were sprayed with herbicide at the end of 2008 to prepare the lands for soybean planting in 2009. The CRP and AGR sites have been cultivated since 2010 with either continuous corn (*Zea mays*, Dekalb DK-52), switchgrass (*Panicum virgatum*), or a mixture of native prairie grasses, which include: Canada wild rye (*Elymus Canadensis*), little bluestem (*Schizachyrium scoparium*), Indian grass (*Sorghastrum nutans*), big bluestem (*Andropogon gerardii*), and switchgrass (*Panicum virgatum*). One CRP grassland, which is dominated by brome grass, has not been disturbed, but instead retained as a reference site (Ref) (Gelfand *et al.*, 2011; Zenone *et al.*, 2011; Deal *et al.*, 2013; Zenone *et al.*, 2013). I used an experimental code for these sites by abbreviating them as "LUH-CROP". CRP-C, CRP-Sw and CRP-Pr represent the CRP sites that were converted to corn, switchgrass and prairie mixture respectively, while AGR-C, AGR-Sw and AGR-Pr are AGR farms converted to corn, switchgrass and prairie mixture, respectively. In 2010 when the crops were established, the perennial crops switchgrass and prairie were accompanied by oats as a nurse crop, with and without fertilization, respectively (Fig. 1.6). No other management practices were applied beyond harvesting at the end of each growing season. No-till continuous corn was seeded in mid-May with a one-time herbicide mix (Lumax, Atrazine 4L, Honcho Plus and $(NH_4)_2SO_4$). Phosphorus, potassium and nitrogen fertilizers were applied during April and June each year (Zenone *et al.*, 2013).

3.2.3 The climatic and microclimatic measurements and growth season identification

The climate, such as air temperature (T_a) and daily precipitation (PRCP), and microclimate, such as soil temperature and soil water content, were recorded as independent variables. They were recorded at different spatial and temporal scales based on the requirement of research and the limitation of equipment and labor.

The daily mean T_a and daily accumulative PRCP were collected and calculated from the KBS LTER Weather station (42°24'47.1" N, 85°22'15.3" W; lter.kbs.msu.edu). Air temperature was recorded hourly by a thermometer at 3 m height and mean daily air temperature was calculated from the hourly data. Precipitation was measured by a NOAH IV total precipitation gauge (ETi Instrument Systems Inc., Fort Collins, CO).

Soil temperature (T_s) and volumetric soil water content (VWC) were measured simultaneously with biweekly soil respiration rate measurements late April to September and, during other times, monthly. Soil temperature was measured at 10 cm depth using a *Taylor 8940N* digital thermometer (Taylor Precision Products, Las Cruces, NM, USA) while VWC was monitored from the ground surface to 10 cm depth by a *HydroSense II* with a *CS659* sensor (Campbell Scientific, Inc. (CSI), Logan, UT).

The length of the growing season is an important index for climate change and agriculture. There are several identifications based on climate and crop growth. Here, I use the temperature-based identification, which is the most commonly used in North America (a.k.a. frost-free season), instead of the crop-based growing season since soil respiration includes the soil microbe-derived carbon efflux—not only plant-derived soil carbon efflux. The onset and the end of the climatic growing season (GS) each year was calculated based on the nine-day moving average of daily mean air temperature ($9d\text{-}T_a$). This filters out short-term warm or cold events

that may not induce the start of plant growth and development in spring. The onset of the GS was identified as the first day exceeding 0°C 9d-T_a in spring while the end of the GS was recognized as the last day exceeding 0°C 9d-T_a in fall. The length of the GS ranges between the onset and the end of the GS in each year.

To compare soil respiration rates, climate and microclimate, and the vegetation indices, I separated the data into different years based on the USGS "water year" concept. I began my yearly analysis with October 1st and ended at September 30th, as this method is more meaningful for agriculture research. I identified the water year in my dissertation as the end of the previous GS until the end of the current GS, as post-GS precipitation may subsidize soil water pools and support the plants and soil microbes consumption in the next GS. The length of the water year may be different due to the different seasonal patterns of air temperature in fall and winter.

3.2.4 Total and heterotrophic soil respiration measurements

Four plots at each site were randomly selected to install 1x1 m root exclusion plots for measuring heterotrophic soil respiration (R_h). We dug a 1 m deep trench around the edges of each square (Fig. 2.1 (B)). The trenches were lined with root-barrier sheets before refilling the soil according to its original soil profile (Fig. 2.1 (C); Tang *et al.*, 2005). The plants and roots inside the square were manually removed and/or killed by herbicide (*Monsanto Roundup®*). Two 10 cm inner diameter PVC collars were installed inside the square to accommodate flux chambers to measure R_h. Another two collars were installed surrounding the square to measure total soil respiration (R_s) (Fig. 2.1(D)). A total of 112 measurements (including R_h and R_s) were taken between 10 am and 7 pm when soil respiration is at diel maximum.

Soil respiration was measured biweekly during the growing season and monthly during the non-growing season to allow the measurements when snow cover is minimal (from October

to December). The chamber-based infrared gas analyzer (IRGA) approach for soil respiration

measurement used an *LI-6400* portable photosynthesis system with a 10 cm diameter *6400-09*

soil chamber or an *LI-8100* with a 10 cm diameter *8100-102* soil chamber (LI-COR Biosciences,

Lincoln, NE).

3.2.5 Vegetation index data

Vegetation indices, including *normalized difference vegetation index* (NDVI) and

enhanced vegetation index (EVI), were calculated based on satellite remote sensing using band 1

(nir), band 2 (red), and band 3 (blue) of the Moderate Resolution Imaging Spectroradiometer

(MODIS). The NDVI was determined by the ratio of the difference between near-infrared

reflectance and red reflectance to their sum (Tucker *et al.*, 2005), while EVI was further

modified with soil adjustment factor L and two atmospheric aerosol scattering coefficients C_1

and C_2 (Huete *et al.*, 1999). The EVI has a higher sensitivity at the "green" portion of the

spectrum when vegetation is very dense. These data were developed from MODIS daily products

by selecting the optimal day from each 16-day interval (i.e., low cloud cover). Missing data may

appear when clouds obscured the site over an entire 16-day period. The NDVI and EVI data

were downloaded from the Oak Ridge National Laboratory Distributed Active Archive Center

for Biogeochemical Dynamics (ORNL DAAC, http://daac.ornl.gov/MODIS/modis.shtml). I used

a single pixel from the MODIS image for each site with a spatial resolution of 250 m. The dates

of NDVI and EVI values were paired with the nearest dates of soil respiration measurement.

3.2.6 The temperature-water-vegetation (TWV) models

Multiple factor models containing the effects of T_s, VWC, EVI and their interactions were developed and tested. The experiment treatments (seven sites: 2 LUH * 3 CROP + Ref) were set as a categorical factor and the following function was tested:

$$R = f(T_s) \cdot g(VWC) \cdot h(EVI) \cdot i(CROP, LUH) \qquad \text{Eq. 2-1}$$

where R is total (R_s) or heterotrophic (R_h) soil respiration, and $f(T_s)$, $g(VWC)$ and $h(EVI)$ are the effects of soil temperature, soil moisture and vegetation condition on R, respectively.

The functions of $f(T_s)$, $g(VWC)$ and $h(EVI)$ were assumed as log-linear, quadratic, or linear based on observed relationships between R and T_s, VWC, and EVI, from previously published research, and the best correlations between R-T_s, R-VWC and R-EVI. The equations containing two-level interactions and the variables themselves were tested. The final models would include the equation with first and secondary orders in terms (Supplement 2-4). The variables and their parameters were modeled by actual data. The best models for R_s and R_h were independently selected based on Akaike Information Criterion (AIC).

3.2.7 Seasonality of root contribution (RC) to total soil respiration

The R_a, R_h and R_s data were calculated based on the TWV models (Supplement 2-4) and the equation (5) in Hanson *et al.* (2000). The root contribution (RC) of total soil respiration was calculated based on the Hanson *et al.* (2000) equation (6). The RCs were plotted against DOY and compared between different treatments.

3.3 RESULTS

3.3.1 Temporal variations of biophysical factors

3.3.1.1 Climate and microclimate

As mentioned in Chapter 2, the growing season (GS), defined by the non-frost season described in Chapter 2, lasts from late-March to late November or early December in 2011, 2013 and 2014. However, it warmed up early in March 2012 and the onset of the GS advanced (Fig. 2.2).

After the onset of the growing season, the temperature gradually increased until its peak in July and then decreased until the end of the GS (Fig. 2.2). The maximum daily mean air temperatures were 29.88, 30.67 and 29.25 °C in 2011, 2012 and 2013, respectively, whereas it was only 24.39°C in 2014 (data not shown).

The length of the GS, highest temperature and hottest date differed across years. The GS in 2012 started very early (DOY=57) and finished late (DOY=356). The length of the GS in 2012 lasted almost 300 days with high degree-day (data not shown). The growing seasons in other years started from late March (DOY=57~90) and finished in mid-November to early December (DOY=318~341). Two of the years (2013 and 2014) had lower July temperatures (Fig. 2.2, Table S.2.1) and lower degree-days than in 2011 and 2012 (data not shown).

In my sites, precipitation was distributed evenly through the whole year although there were occasional very large rain events. However, VWC revealed distinct seasonal patterns in the GS. The pre-season (October-April) recharged the soil water with precipitation, which kept soil moisture high throughout winter and early spring. The VWC started to decline after the increase of temperature and crop growth, sometimes also because of the lack of rainfall. The timing,

duration and magnitude of low VWC periods varied inter-annually. For example, the major low VWC occurred during 3 June and 19 July in 2011, while in 2012 it was 6 June to 30 July in 2012. In 2013 and 2014, these were shortened and delayed and lasted only during 13-25 July and 26 July–16 August, respectively (Fig. 3.1 (B)). The most severe water deficit always happened at the end of the dry period, around late July in 2011-2013 and early August in 2014. In 2013 and 2014, large amounts of spring rainfall replenished soil water pools and delayed, shortened and weakened the water deficit (Fig. 3.1 (B), Table S.2.1). A second low VWC period happened at the end of the GS (late August to late September) when rainfall was low. However, that may not be important for the growth of plants.

When comparing the climate patterns across years, 2012 was an outlier. First, the months of February and March in 2012 had a mean T_a that was significantly higher than the other years. Historically, the March mean T_a tends to be close to or below 0°C. However, in March 2012 the mean T_a was 9.96°C while those in other years it ranged between 0.96 and -2.57°C (Table S.2.1). The nine-day moving average of daily mean air temperature (9d-T_a) revealed the early onset of warmth in the 2012 GS (Fig. 2.1). The onset of the GS based on the 9d-T_a was very early (25 February) in 2012 but later in 2011, 2013 and 2014, falling on 30, 26, and 28 March, respectively. Secondly, the low May-August precipitation in 2012 induced the low spring-summer VWC, which greatly impacted the growth of both annual and perennial crops. The cumulative precipitation from May-July was 377, 99, 309 and 331 mm from 2011 to 2014, respectively. The 2012 precipitation was less than one third of other years. Thus, the VWC in June was significantly lower than in the other years (Supplement 2-1). Third, the maximum air (T_a) and soil temperatures (T_s) were higher in 2012 than those in the other years. In contrast, the

coolest summer was in 2014 (Fig. 2.2). In addition, the variations of growing season T_s among

the research sites in 2012 were higher than other years, especial in July (Fig. 2.2 (A)).

The low rainfall in 2012 induced a severe water deficit in summer and VWC was very

low at all sites. However, the perennial crops in CRP sites (CRP-Sw, CRP-Pr and Ref)

experienced the most acute drought, as their June VWC levels dropped to near zero. Surface soil

in AGR perennial crop sites reached around 5% VWC, while the two corn sites fell to around

10% VWC (Fig. 3.1 (B)). The differences of VWC may be due to site-to-site variability or the

phenology of crops.
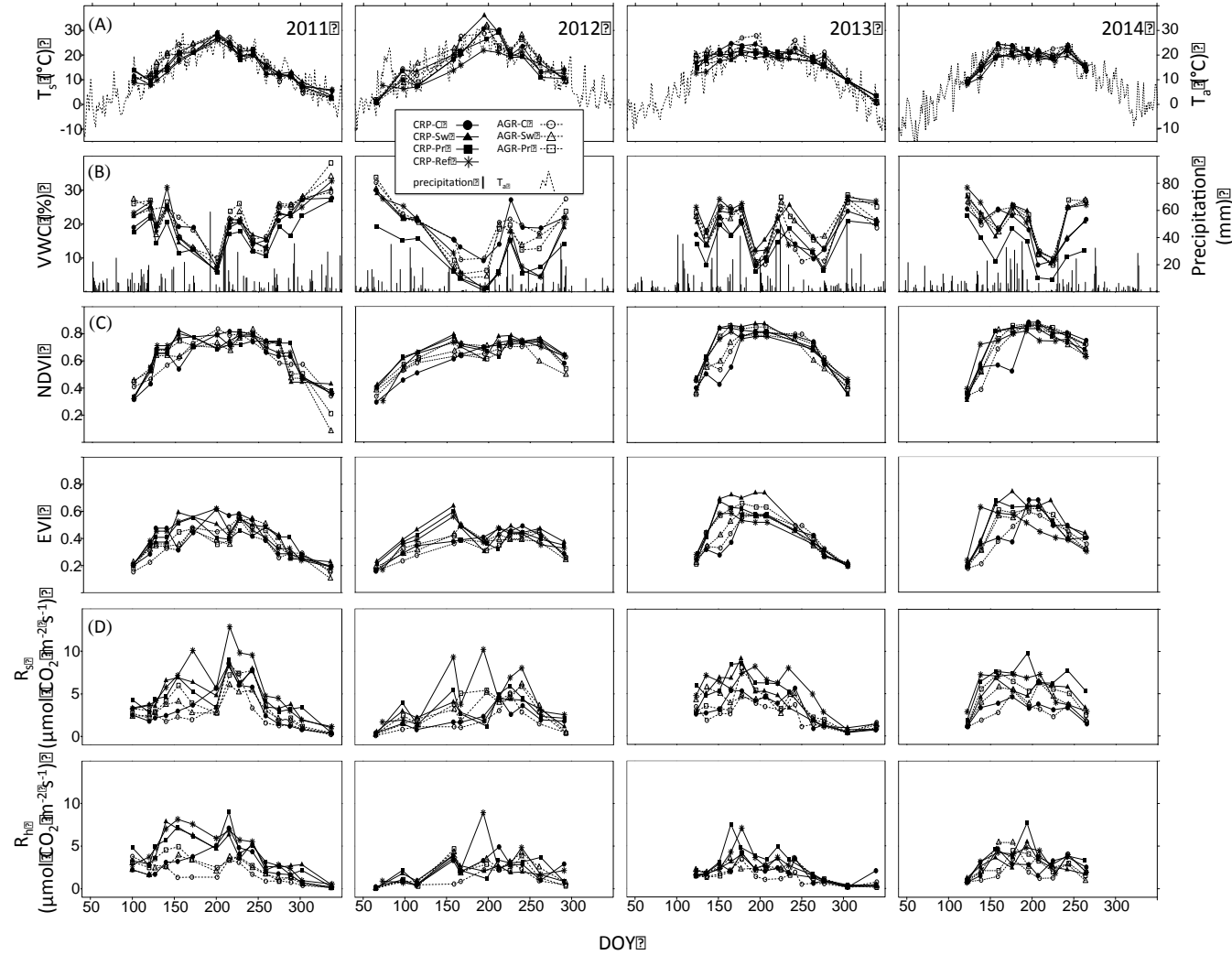
Figure 3.1. Temporal changes of soil respiration and environmental variables across sites and years. (A) Daily air temperature (T_a) and biweekly mean soil temperature (T_s) at 10 cm depth from each site; (B) daily precipitation from KBS LTER weather station and soil volumetric water content (VWC) at 0-10 cm depth; (C) normalized difference vegetation index (NDVI) and enhanced vegetation index (EVI) from MODIS; (D) biweekly total soil respiration rate (R_s); and heterotrophic soil respiration (R_h). The soil temperature and soil moisture shown in (A) and (B) were measured simultaneously with R_s measurements.

3.3.1.2 Vegetation indices

Seasonal changes in NDVI and EVI were distinctly different between the annual and perennial crops. The annual crop had only one peak, whereas the perennials had a rise-and-fall plateau June-September and longer growing seasons. At corn sites, VIs showed a small peak with weed growth before the corn was planted, and dropped after herbicide application in early May. In 2011, 2013, and 2014, corn growth began immediately after planting, reached its maximum in early July and stayed at a high biomass until late July or early August. The maximum NDVI and EVI in 2011, 2013, and 2014 occurred between mid-July and mid-August (solid and empty circles in Fig. 3.1 (C)). These results demonstrate how corn rapidly grew after seeding, and how its growth coupled with a high chlorophyll density at maturation. The VIs maintained their high values until September, decreased slightly because of the senescence and the drying of leaves before it eventually decreased sharply after the harvesting. The growth rate of corn seemed slower in 2012 compared to other years. The maximum VI delayed to late September. The average height of corn was only 1.5 m, which is around 1 m shorter than other years (data not shown). My VI data, field observations of crop conditions and eventual crop yield measurements confirm that crop growth in 2012 was lower than other years.

In contrast to annual crop, the VIs of the perennial crops during the growing season had three distinct stages: a rapid increase in the spring (March or April), stable high levels in summer (June-September) and a decrease after harvest in the fall (September-October). Perennial crops always emerge a couple of weeks after the snow melts, which is far earlier than corn is planted (128-129 DOY). However, the temporal dynamics of crop growth in 2012 were different. The plants emerged early in 2012 in response to the warmth in March. The March and April VIs were higher than that in other years, as there was a higher temperature and less limitation on water in

their beginning weeks. However, later in July the VIs dropped, accompanied by the very low

VWC. In mid- to late August, a second peak appeared since new rainfall mitigated the water

deficit. However, the second EVI peak was lower than EVI in other years. The maximum values

of NDVI and EVI in 2012 were 0.79 and 0.64, respectively, whereas those were 0.84 and 0.62 in

2011, 0.88 and 0.73 in 2013, and 0.87 and 0.74 in 2014 (triangles and squares in Fig. 3.1 (C)).

3.3.1.3 Soil respiration

Briefly speaking, both the seasonal patterns of the total (R_s) and heterotrophic soil

respiration (R_h) were hump-shaped during the GS. The R_s and R_h had similar seasonal changes,

although R_h were less than R_s during GS, especially in their peaks (Fig. 3.2). Like the VI, the

seasonal patterns of soil respiration were different between perennial grasses and annual crop.

The R in perennial crops increased in mid- to late April when T_s increased and crops germinated.

R had several peaks during June-September and then decreased in September when T_s declined

and the leaves withered up. It sharply dropped in October after harvest. The soil respiration in

corn rose slightly in April. The values of R_s and R_h were very close. The R_s obviously increased

after mid-May when the corn was cultivated. The R_s values were higher than R_h later in the GS.
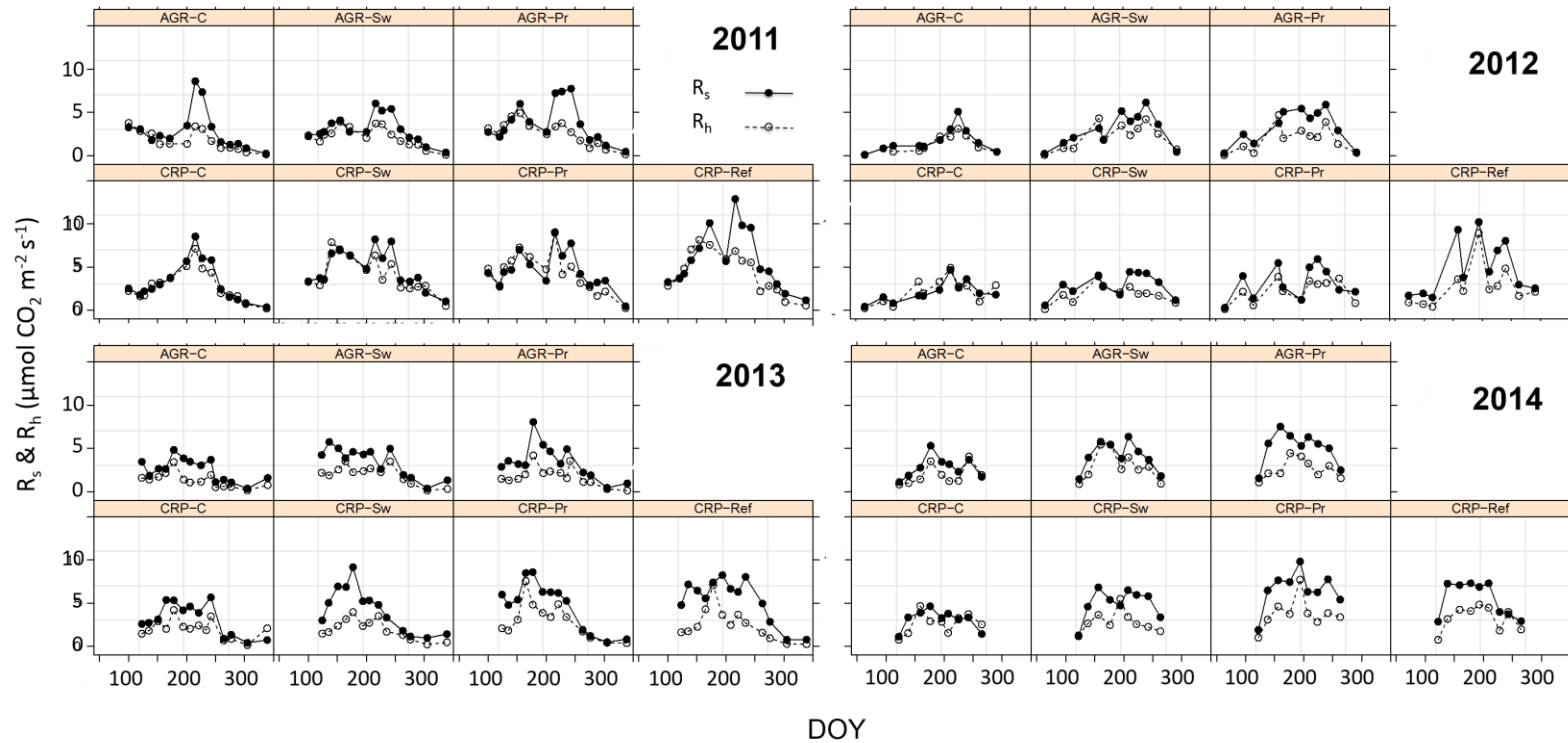
Figure 3.2. Temporal changes of total (R_s) and heterotrophic soil respiration (R_h). The soil respiration values are the averaged measurements from four plots in each research field. Soil respiration was measured biweekly during the growing season (GS) and monthly in the non-GS. The solid circles and solid lines are for R_s. The empty circles and dashed lines are for R_h.

3.3.2 The seasonality of the root contribution (RC) to total soil respiration

The mean annual RC fractional contributions to total soil respiration were 0.460, 0.427, 0.448, and 0.462 in 2011, 2012, 2013, and 2014, respectively. The RC was significantly lower in 2012 than that in other years (data not shown). The CRP-Pr and AGR-Sw had significantly decreased in 2011 across all treatments (Fig. 2.13). Seasonal variations of RC in AGR-Pr and Ref were small during the GS, while, in summer, AGR-C, CRP-C, CRP-Sw and AGR-Pr had higher RC. The AGR-Sw and CRP-Pr had low RC in the mid- to late GS (Fig. 2.3 (A)). The correlation between RC and VWC presented very low RCs when VWC close to zero in AGR-Sw and CRP-Pr in 2012. In contrast to AGR-Sw and CRP-Pr, CRP-Sw had a reverse trend with low VWC values at with high RC. Other sites did not have a distinct pattern between RC and VWC (Fig. 2.3 (B)).
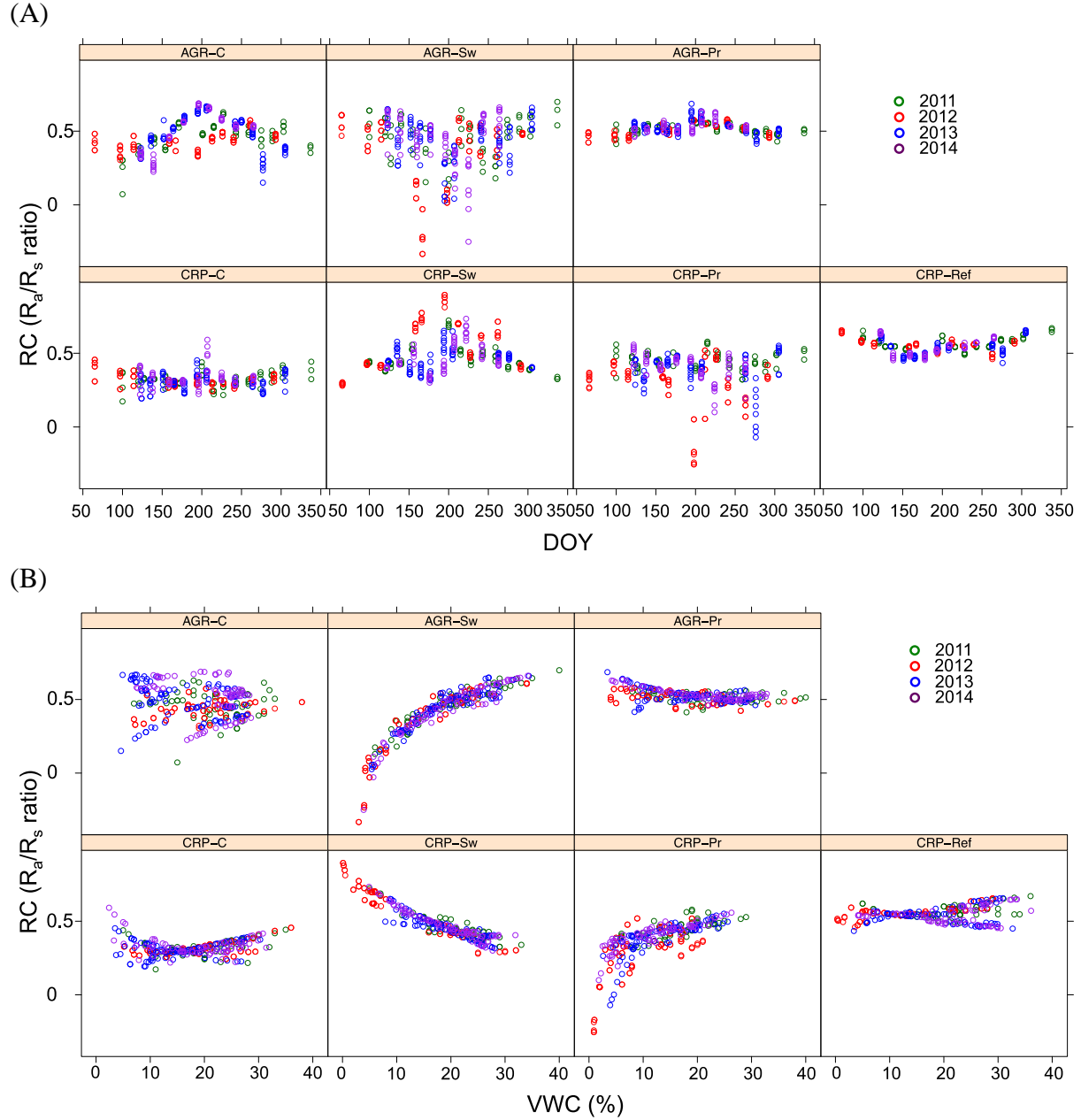
Figure 3.3. Temporal changes of the ratio of root contribution (RC) to total soil respiration and the correlation between RC and VWC. (A) The temporal variations of RC (R_a:R_s ratio) through growing seasons. The colors of circles present different years: Green, red, blue and purple represent 2011, 2012, 2013 and 2014, respectively. (B) The correlation between RC and VWC. The negative values of the ratio occurred when the model estimated R_h is larger than estimated R_s.

3.4 DISCUSSION

3.4.1 How seasonal patterns of biophysical drivers affect the seasonal patterns of soil

respiration

The major biophysical drivers affecting soil respiration are known to be temperature, soil water content, the substrate supply from plants, and their interactions (Luo *et al.*, 2001; Curiel Yuste *et al.*, 2004). However, the influences of these biophysical drivers on soil respiration may be different in different climate regimes and in different biomes due to the complex mechanisms of different components of soil respiration and their feedbacks. In arid and semi-arid ecosystems, water availability plays crucial roles in soil respiration, since it is the limiting factor (Davidson *et al.*, 2000; Luo *et al.*, 2001). The dynamics of soil moisture determines the seasonal patterns of soil respiration. In the Mediterranean climate, the soil respiration is limited by temperature in winter, while it is depressed by soil moisture in summer. The major control during the growing season often is soil moisture (Carbone *et al.*, 2011). In mesic ecosystems, temperature and radiation are always the most important drivers of seasonal soil respiration, since water supply is less of limiting (Billing *et al.*, 1998; Epron *et al.*, 2001; Borken *et al.*, 2002).

My results demonstrate that without irrigation soil respiration in these managed crop ecosystems, which often experience hot and water-deficient summers and cold winters, is mainly driven by temperature and that water deficit also plays an important role in the hottest and driest periods. My experimental treatments are in a humid continental climate and soil temperature and vegetation regulate soil respiration most of the time during the growing season. However, the soil respiration rate in mid-July, the hottest period, was low in 2011 and 2012 (Fig. 3.2 and 3.4). The wet springs in 2013 and 2014 diminished the water stress in the growing seasons but the soil respiration still decreased later in late July or August, following the seasonal decrease of soil

moisture (Figs. 3.1 and 3.5). The findings imply that the projected increases in precipitation

variation and extreme precipitation events in the Midwest US (Andresen *et al.*, 2012) may alter

ecosystem processes and carbon dynamics and seriously impact the ecosystem. The impacts of

drought on the ecosystem processes, such as photosynthesis or carbon dioxide losses from the

soil, in agricultural ecosystems can become more severe if the precipitation variability

exacerbates the summer water stress.
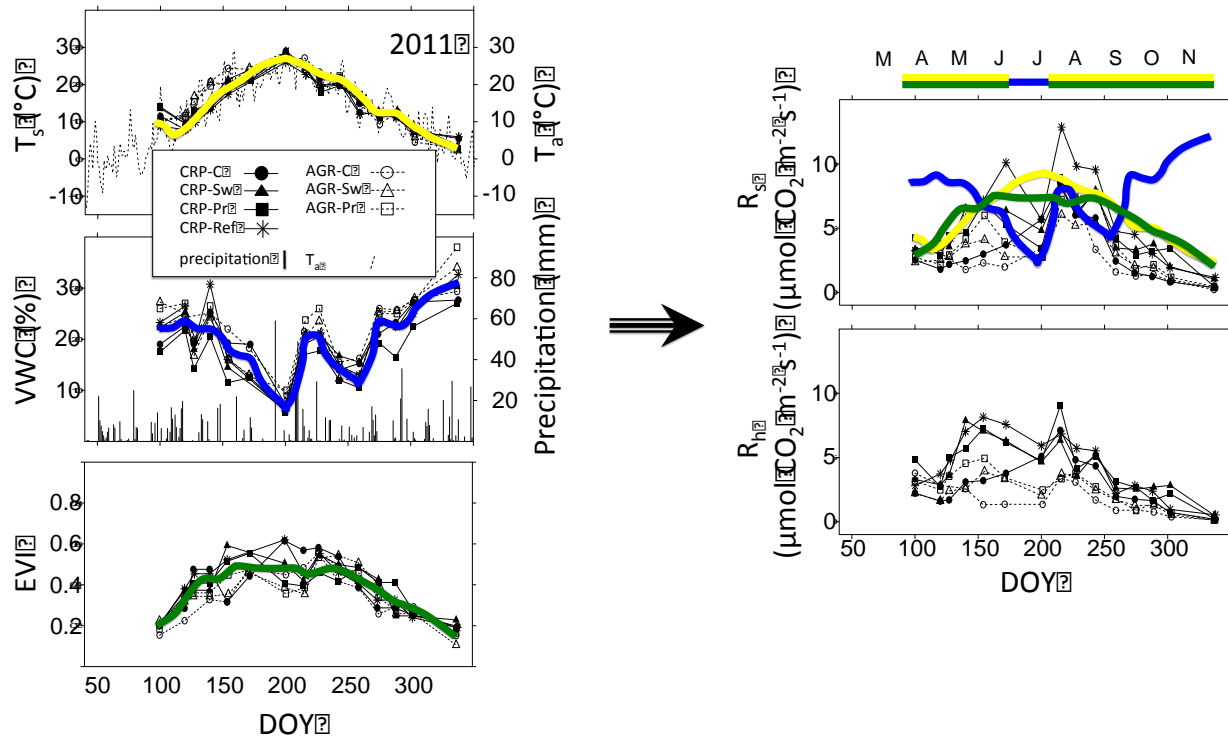
Figure 3.4. The seasonality of soil respiration and their drivers in 2011. (A) The seasonality of biophysical factors (T_s, VWC and VI) were shown by different colors. (B) The seasonality of R_s and R_h were predominantly controlled by different drivers at different times in the growing season. The color band at upper-right corner shows their period of control. DOY means the day of year.
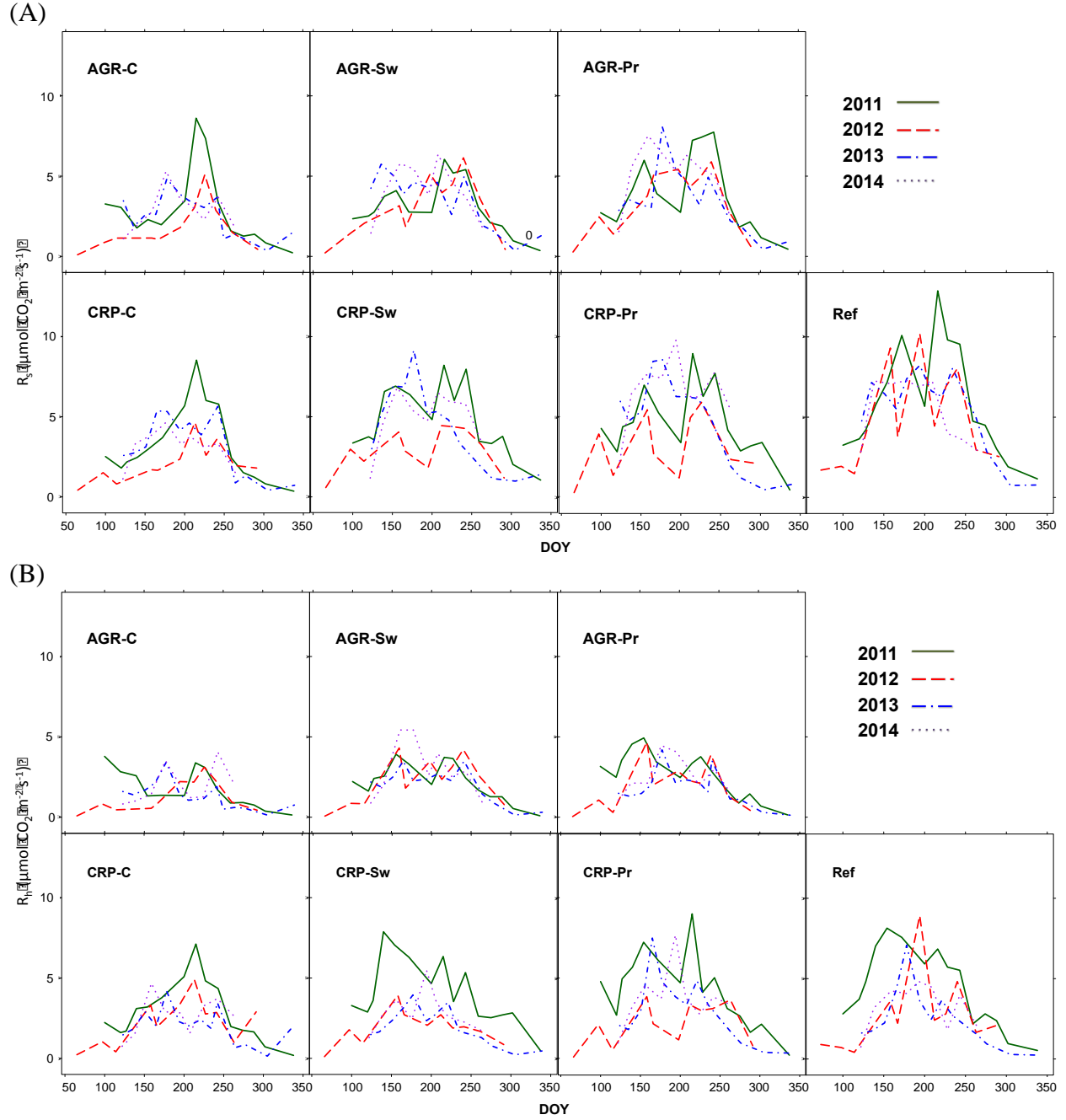
Figure 3.5. The seasonality of R_s and R_h across four years. (A) R_s and (B) R_h were plotted with DOY, which means the day of year. The measurement of R_s and R_h were biweekly during late-April and September and monthly in October to December. The colors and different types of lines display different years.

The summer decrease of R with maximum soil temperature displays the decoupling of

soil respiration and soil temperature that happened commonly in all experimental years. There

99

are two main hypotheses for the decoupled respiration-temperature relationship. The first is heat

suppression of biochemical reactions. High temperatures may break down the protoplasm system

and depress the metabolism of roots and soil microbes. The second is limitation of water deficit

to plant roots and microorganisms. High temperatures increase both transpiration and

evaporation rates with high photosynthetic and metabolic rates and high diffusion rates of water

from the surface of the ground to the atmosphere, respectively. Maximum temperature always

occurred simultaneously with minimum soil moisture in late July. The first hypothesis was not

supported by my data since the thermal threshold for the suppression of biochemical reactions is

generally higher than 35°C and, although it may vary among different plant species and soil

microbes (pp. 86-87, Luo & Zhou, 2006), soil temperatures in my data were always less than

35°C. The second hypothesis is more likely because of R-T decoupled since the July VWC fell

to below 10%. The low VWC (for weeks) in late summer depressed the metabolism of roots and

soil microbes, and thus decreased soil respiration.

3.4.2 The seasonality of R_a and R_h in the dry and hot year

The impacts of drought on ecosystems can vary depending on the magnitude, timing and

duration of the drought. My treatments experienced a severe drought in spring-summer 2012

when I found a strong ecosystem response that included the lower soil respiration, lower annual

yield, lower summer NDVI and EVI, lower plant heights and summer wilt in some research sites,

followed by the change of plant composition in 2012 and the following years in the switchgrass

and prairie fields (Abraha *et al.*, 2016). Two main events with biological feedback caused the

severe spring-summer water deficit. First, the thaw was earlier due to unusually hot March (Fig.

2.3 & Table S.2.1). The warm ground stimulated the early germination of weeds and thus

consumed soil water via high March evapotranspiration (ET) (Abraha *et al.*, 2015). Second, the

low May-August precipitation did not fully replenish the soil water pool and therefore did not satisfy the water demands of crops and soil microbes. The depletion of soil moisture in June suspended the growth and development of crops. Both NDVI and EVI values significantly decreased in June and July in all fields, and biomass did not rebound until August (Figs. 2.2 (C) & (D)).

Savage and Davidson (2001) reported similar findings in their soil respiration research in Harvard Forest "upland" (well and moderately well drained) mixed hardwood forest in Massachusetts. They argued that the late summer low soil respiration rates were due to low soil moisture and were dependent on the duration and severity of the preceding dry period and the timing of the onset of soil respiration increase in the previous spring. The preceding inter-annual variation of soil water availability may be a crucial factor affecting the soil respiration rate, although the correlation between soil respiration and soil moisture is usually not clear and confounded with other factors. The effect of soil moisture on soil respiration is more like a threshold, rather than a linear or quadratic correlation, for a well-drained habitat. The soil respiration rates were markedly suppressed when soil moisture was lower than the threshold. I will discuss more about how the community structure, ecological processes and ecosystem functions have adapted to growing-season drought (months) in the years in later chapters.

Compared to the short-term inhibition of soil respiration by water deficit in 2011, 2013 and 2014, the severe and long-term (months) drought of 2012 had great and multifaceted impacts on agricultural ecosystems, affecting plant community structure, biodiversity, and ecological processes and functions. My 2012 results revealed that there was a decreased growing-seasonal PRCP, VWC, NDVI, EVI, annual yield, R_s and R_h, although the annual ET was relatively consistent. The adaptation of ecosystems to growing-season drought may include changes in

ecosystem water use efficiency (eWUE) via shifts in plant species composition and specifically the biomass ratio of C_3/C_4 species. The changes of plant composition and ecosystem processes in response to the 2012 drought lasted into the years following (Abraha *et al.*, 2016). I will discuss how ecosystem functions respond to the common short-term drought in the late growing seasonal and the occasional long-term growing-seasonal drought in Chapter 4.

3.4.3 The seasonality of R_a and R_h in humid springs and cool summers

Post-drought years 2013 and 2014 had similar GS climate patterns, with wet springs (or wet spring-summer periods) and cool summers; although 2014 had a wetter and cooler summer than 2013 (Fig. 3.1 and Table S.2.1). The wet spring fulfilled the water demands in the early GS and supplied enough water to plants and soil microbes. The peaks of soil respiration in those two years were in the hottest month, July, during the middle of the growing season. The humid and cool summer brought high soil respiration in July, but the August and September rates were lower. Surprisingly, soil respiration did not recover to the 2011 level. In contrast to the steady decrease of R in 2012, the summer R peaks were flattened or did not occur (Fig. 3.5).

3.4.4 Seasonal variation in RC

Seasonal patterns of RC can be complex because they reflect the relative dynamics of R_a and R_h and their different responses to environmental change. The three peaks of RC can be explained separately by the phenology of plants and seasonal activity of soil microbial communities. The early-spring peak represented rapid increases of R_a due to the emergence of crops, even though raising temperature stimulates both R_a and R_h. The rise of R_h was slower than R_a and that resulted in lower RC in the mid-spring to early summer. The second peak usually happened in late July during the hottest and driest period. The lack of water depressed the soil

microbial activity more than root metabolism since roots can obtain water from deeper horizons (Carbone *et al.*, 2011). The RC decreased slightly after a couple of heavy rains in late July or early August. The responses of soil microbes to rewetting were quicker and larger than root response. The third peak occurred in November and December when the decrease of temperature limited most activities of soil microbes and roots but the relative contribution of R_a to R_s was higher than most of the growing season, except in the spring and summer peaks.

In addition to the general three-peak patterns, different treatments had their own patterns in response to drought. The Ref field had relatively consistent RC through the growing season regardless of the soil moisture, which was extremely low in summer 2012 (Fig. 3.1 (B)). The responses of R_a and R_h to low soil moisture were thus similar (Fig. 3.6 (B)). The RC in CRP-Pr and AGR-Sw had similar relationships to VWC (Fig. 3.3 (B)) due to the differential decreases of R_a and R_h when VWC decreased. The magnitude of R_a decreases was higher than those of R_h (Fig. 3.6 (A) and (B)). The R_a in these two sites dropped to near zero when soil moisture was low. I found that most of the plants in these two sites wilted during the summer 2012 drought. Combining field observations, the low R_a and the VI data, I believe that the 2012 water deficit had decreased available soil water even deep belowground. Plants were barely getting enough water to support their basic metabolism when soil water is very low. The CRP-Sw responded differently in that both R_a and R_h decreased in the 2012 drought but R_h decreased more than R_a (Fig. 3.6 (A) and (B)), resulting in increased RCs when soil moisture was low (Fig. 3.3 (B)). The two corn sites contained higher soil water compared to perennial treatments since we seeded corn in early May. The consumption of water from the corn crop in spring was not as large as that in the perennial crops. Their RC in general does not change much; but in the summer of 2012, RC in both sites were lower than in other years (Fig. 3.3 (A)).

The CRP fields may have experienced more severe drought stress than the AGR fields in 2012 because of soil differences. Three CRP-perennial cropping farms, Ref, CRP-Pr and CRP-Sw had almost zero VWC while AGR-Pr and AGR-Sw had around 6% and two corn sites had almost 10% VWC at the driest time in 2012 (Fig. 3.1 (B)). Three CRP-perennial crop sites showed a sudden drop in R_a when VWC fell below 5% (Fig. 3.6 (A)), suggesting that the root system lost its ability to respire. A dramatic drop in R_h also happened in the Ref and CRP-Sw sites. The combination of the decreases in R_a and R_h in different sites changed RCs in the summer of 2012. At the driest time, CRP-Pr and AGR-Sw had very low RC because of the extremely low R_a. Ref had a relatively stable RC since both R_a and R_h were low. The CRP-Sw had a high RC since the decrease of R_h was more than that of R_a. The R_a can be higher than R_h when VWC is low, since plants can uptake soil water from deeper soil layers. However, the 2012 drought seems to of deeply drained the soil water and both switchgrass and prairie plants had difficulty to obtaining water.

Compared to R_a at low VWC (<10%) levels across different years, the R_a in Brome grass (Ref) and prairie sites was lower in 2012-2014 than that in 2011. There are some possible reasons for the lower R_a. First, 2013 and 2014 had lower summer temperatures while 2012 had lower VI, which reflects lower biomass and photosynthetic rates. The lower temperature and lower photosynthesis-derived carbon inputs to roots reduced R_a. The second is that the 2012 drought changed the species composition of vegetation and that the changes beyond that year. Abraha *et al.* (2016) reported this dramatic decrease in the C3:C4 ratio of grasses in the CRP-Sw, AGR-Pr and AGR-Sw sites (Fig. 3.7 (A)). Switchgrass and prairie in AGR had higher ecosystem water use efficiency (eWUE) after 2012 (Fig. 3.7 (B)). The first reason seems robust while the latter one needs more evidence to improve or modify it.

(A)
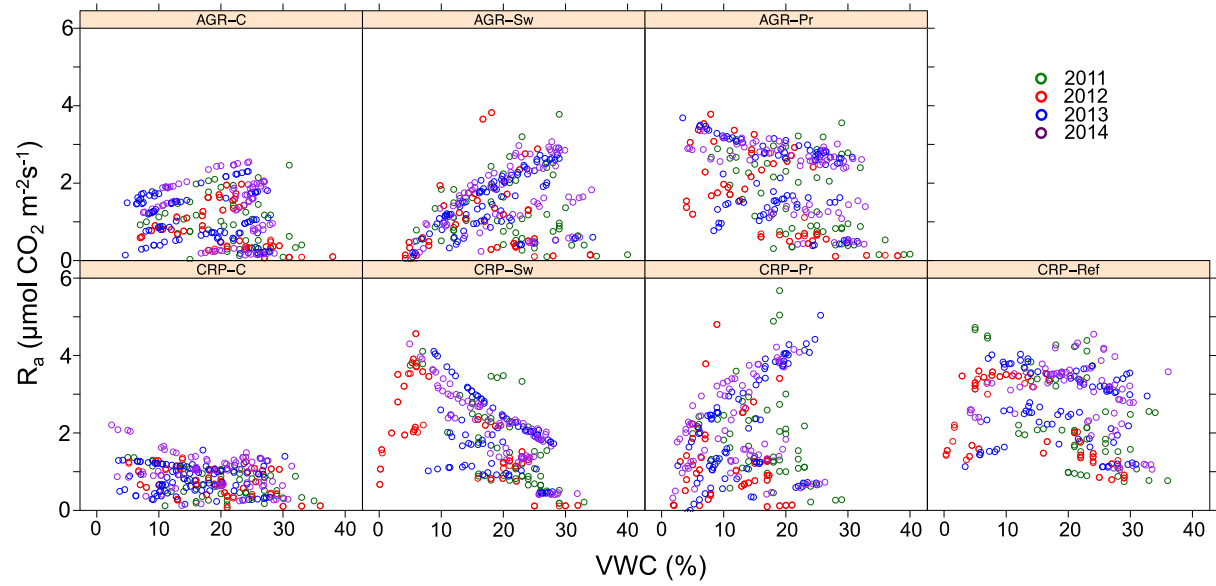
(B)
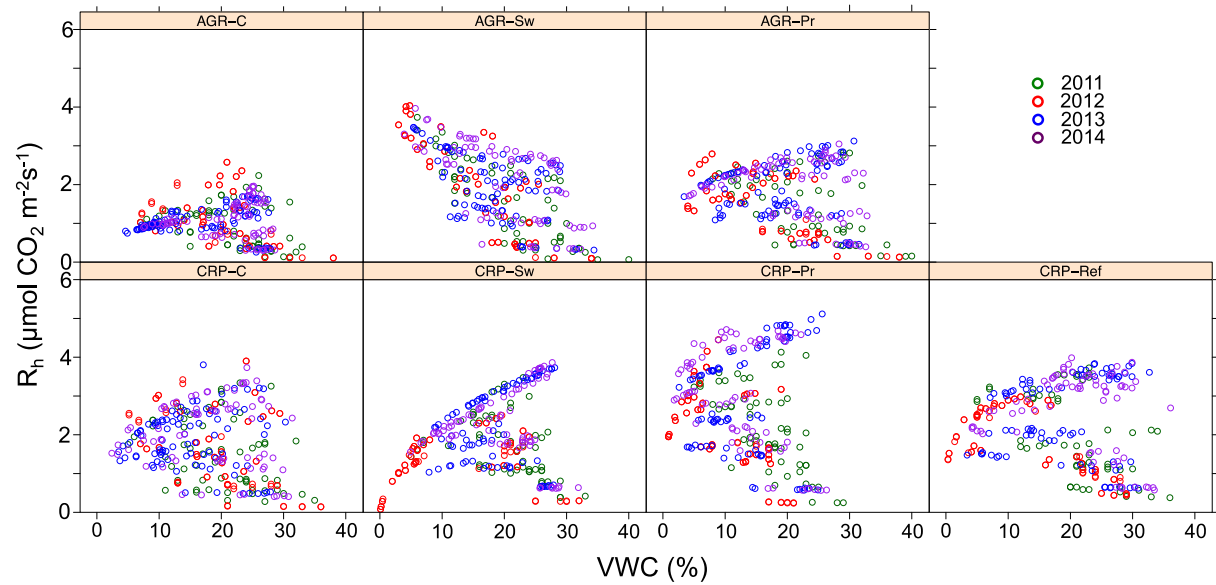
Figure 3.6. The responses of R_a and R_h to VWC. (A) R_a and (B) R_h were correlated to VWC differently in different treatments. The responses of the components of R_s changed the temporal patterns of RC during growing season. Different years are exhibited by different colors.
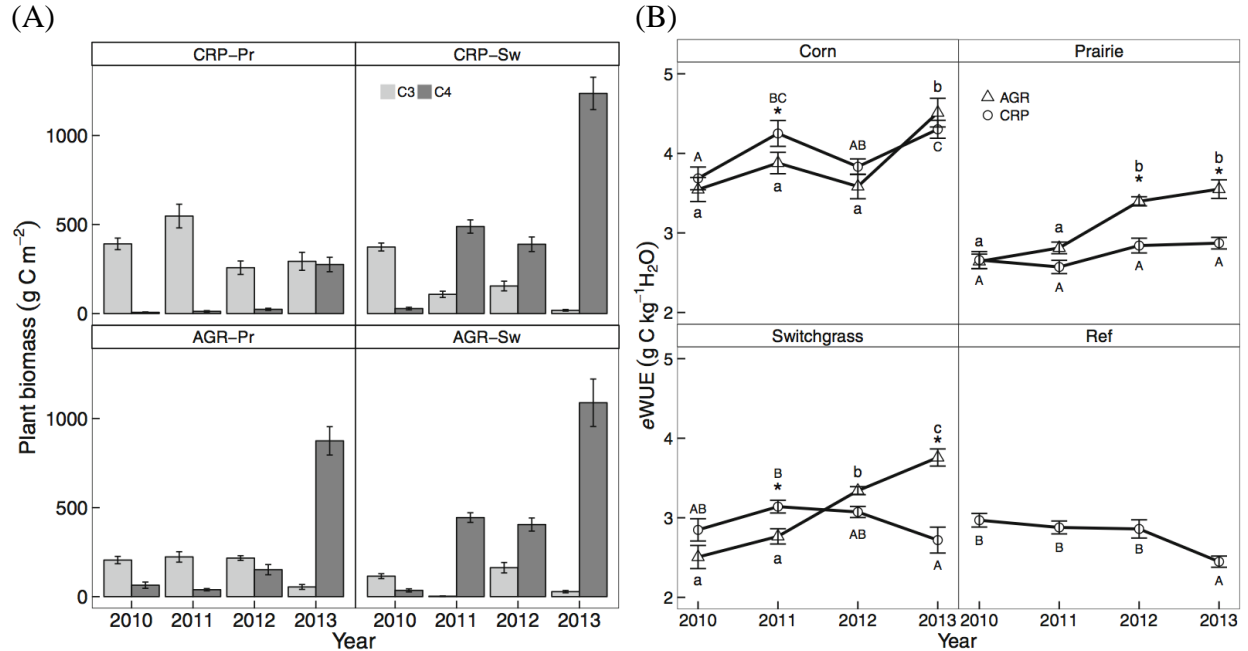
Figure 3.7. The changes of C3:C4 biomass ratio and ecosystem water-use efficiency (eWUE). (A) The changes of biomass of C3 and C4 grasses in prairie and switchgrass sites after land use change; and (B) the variation of eWUE across years in all seven sites. The eWUE was calculated by GPP/ET, where GPP is gross primary production and ET is evapotranspiration. The letters present the difference across years in the same site while the asterisks show the difference between land use histories in the same crop. Notice that the experimental period was 2010-2013 (Source: Abraha *et al.*, 2016).

3.5 CONCLUSIONS

Amplitude, duration and timing of extreme drought events leave consequences on ecosystem processes, such as R_a and R_h. At the intra-annual scale, I found that soil temperature and EVI had an exponential correlation with both R_a and R_h. However, soil water deficits limited soil respiration—even soil temperature and EVI were high. In addition, the severe drought, which had a high amplitude, long duration and occurred during spring-summer, seriously impacted R_a and R_h. The impact of the occasional severe drought altered plant composition (RC), which had responded to biophysical variables at inter- and intra-annual scales due to the different magnitudes and speeds of R_a and R_h responses to biophysical variables. Three peaks of RC occurred in early spring plant emergence, mid-summer dry and the winter low temperature

period. Different land use histories (LUH) and crop types (CROP) had different responses to the 2012 severe drought. Most perennial sites had lower RC in 2012, demonstrated that severe drought had stronger depression on R_a than on R_h. The especially low summer RCs in CRP-Pr and AGR-Sw fields and very high RCs in CRP-Sw field reflected the different responses of R_a and R_h to different levels of water deficit underneath different composition of LUH and CROP. Furthermore, the opposite responses of RC to the regular summer low soil moisture and to the occasional severe drought revealed that short-term (1-2 weeks) summer drought depressed R_h more than R_a while occasional severe drought impacted R_a more than R_h.

The depression of both R_a and R_h can be predicted if the occasional severe drought events increases in the future, especially for R_a. The decrease of root respiration ability implies that the decrease of metabolism and photosynthetic ability may increase NEE (decrease carbon sequestration ability). However, perennial crops may adapt to low water conditions and mitigate the impact of frequent severe drought by altering plant composition and increasing eWUE, while corn cannot. The benefit of perennial cellulosic biofuel crops will enlarge the difference between itself and annual crops.

LITERATURE CITED

LITERATURE CITED

Abraha, M., Chen, J., Chu, H., Zenone, T., John, R., Su, Y.J., Hamilton, S.K., Robertson, G.P., 2015. Evapotranspiration of annual and perennial biofuel crops in a variable climate. Global Change Biology Bioenergy, 7, 1344-1356.

Abraha, M., Gelfand, I., Hamilton, S.K., Shao, C., Su, Y.J., Robertson, G.P., Chen, J., 2016. Ecosystem water-use efficiency of annual corn and perennial grasslands: contributions from land-use history and species composition. Ecosystems, 19, 1001-1012.

Andresen, J., S. Hilberg, K. Kunkel, 2012. Historical climate and climate trends in the Midwestern USA. In: U.S. National Climate Assessment Midwest Technical Input Report. J. Winkler, J. Andresen, J. Hatfield, D. Bidwell, and D. Brown, coordinators. Available from the Great Lakes Integrated Sciences and Assessments (GLISA) Center, http://glisa.msu.edu/docs/NCA/MTIT_Historical.pdf.

Billings, S.A., Richter, D.D., and Yarie, J., 1998. Soil carbon dioxide fluxes and profile concentrations in two boreal forests. Canadian Journal of Forest Research, 28, 1773–1783.

Borken, W., Muhs, A., and Beese, F., 2002. Application of compost in spruce forests: Effects on soil respiration, basal respiration and microbial biomass. Forest Ecology and Management, 159, 49–58.

Carbone, M.S., Still, C.J., Ambrose, A.R., Dawson, T.E., Williams, A.P., Boot, C.M., Schaeffer, S.M., Schimel, J.P., 2011. Seasonal and episodic moisture controls on plant and microbial contributions to soil respiration. Oecologia, 167, 265-278.

Curiel Yuste, Y., Janssens, I.A., Carrara, A., Meiresonne, L., Ceulemans, R., 2003. Interactive effects of temperature and precipitation on soil respiration in a temperate maritime pine forest. Tree Physiology, 23, 1263-1270.

Curiel Yuste, J., Janssens, I. A., Carrara, A., and Ceulemans, R., 2004. Annual $Q10$ of soil res- piration reflects plant phonological patterns as well as temperature sensitivity. Global Change Biology, 10, 161–169.

Davidson, E.A., Verchot, L.V., Cattanio, J.H., Ackerman, I.L., Carvalho, J.E.M., 2000. Effects of soil water content on soil respiration in forests and cattle pastures of eastern Amazonia. Biogeochemistry, 48, 53–69.

Deal, M.W., Xu, J., John, R., Zenone, T., Chen, J., Chu, H., Jasrotia, P., Kahmark, K., Bossenbroek, J., Mayer, C., 2013. Net primary production in three bioenergy crop systems following land conversion. Journal of Plant Ecology, 6, 1-10.

Epron, D., Le Dantec, V., Dufrene, E., and Granier, A., 2001. Seasonal dynamics of soil carbon dioxide efflux and simulated rhizosphere respiration in a beech forest. Tree Physiology, 21, 145–152.

Flanagan, L.B., Johnson, B.G., 2005. Interacting effects of temperature, soil moisture and plant biomass production on ecosystem respiration in a northern temperate grassland. Agrucultural and Forest Meteorology, 130, 237-253.

Gelfand, I., Zenone, T., Jasrotia, P., Chen, J., S.K.Hamilton, Robertson, G.P., 2011. Carbon debt of conservation reserve program (CRP) grasslands converted to bioenergy production. Proceedings of the National Academy of Sciences, 108, 13864-13869.

Gomez-Casanovas, N., Matamala, R., Cook, D.R., Gonzalez-Meler, M.A., 2012. Net ecosystem exchange modifies the relationship between the autotrophic and heterotrophic components of soil respiration with abiotic factors in prairie grasslands. Global Change Biology, 18, 2532-2545.

Goulden, M.L., Munger, J.W., Fan, S.M., Daube, B.C., Wofsy, S.C., 1996. Exchange of carbon dioxide by a deciduous forest: Response to interannual climate variability. Science, 271, 1576-1578.

Hanson, P.J., Edwards, N.T., Garten, C.T., Andrews, J.A., 2000. Separating root and soil microbial contributions to soil respiration: A review of methods and observations. Biogeochemistry, 48, 115-146.

Huete, A., Justice, C., van Leeuwen, W., 1999. MODIS Vegetation Index (MOD 13) Algorithm Theoretical Basis Document, Center, N.G.S.F. (Eds.), p. 129.

Jassal, R.S., Black, T.A., Novak, M.D., Gaumont-Guay, D., Nesic, Z., 2008. Effect of soil water stress on soil respiration and its temperature sensitivity in an 18-year-old temperate Douglas-fir stand. Global Chang Biology, 14, 1305-1318.

Lark, T.J., Salmon, J.M., Gibbs, H.K., 2015. Cropland expansion outpaces agricultural and biofuel policies in the United States. Environmental Research Letters, 10, 044003.

Luo, Y., Wan, S., Hui, D., Wallace, L.L., 2001. Acclimatization of soil respiration to warming in a tall grass prairie. Nature, 413, 622-625.

Luo, Y., Zhou, X., 2006. Soil Respiration and the Environment. Elsevier.

Peel, M.C., Finlayson, B.L., McMahon, T.A., 2007. Updated world map of the Koppen-Geiger climate classification. Hydrology and Earth System Sciences Discussions 4, 439-473.Post, W.M., Emanuel, W.R., Zinke, P.J., Stangenberger, A.G., 1982. Soil carbon pools and world life zones. Science, 298, 156-159.

Post, W.M., Emanuel, W.R., Zinke, P.J., Stangenberger, A.G., 1982. Soil carbon pools and world life zones. Science, 298, 156-159.

Raich, J.W., Schlesinger, W. H., 1992. The global carbon dioxide flux in soil respiration and its relationship to vegetation and climate. Tellus, 448, 81-99.

Raich, J.W., Potter, C.S., Bhagawati, D.B., 2002. Interannual variability in global soil respiration, 1980-94. Global Change Biology, 8, 800-812.

Ryan, M.G., Law, B.E., 2005. Interpreting, measuring, and modeling soil respiration. Biogeochemistry, 73, 3-27.

Savage, K., Davidson, E., 2001. Interannual variation of soil respirationin two New England forests. Global Biogeochemical Cycles, 15, 337-350.

Schlesinger, W. H. & Andrews, J. A., 2000. Soil respiration and the global carbon cycle. Biogeochemistry, 48, 7-20.

Tang, J., and Baldocchi, D. D., 2005. Spatial-temporal variation in soil respiration in an oak-grass savanna ecosystem in California and its partitioning into autotrophic and heterotrophic components. Biogeochemistry, 73(1), 183–207.

Tucker, C., Pinzon, J., Brown, M., Slayback, D., Pak, E., Mahoney, R., Vermote, E., El Saleous, N., 2005. An extended AVHRR 8-km NDVI dataset compatible with MODIS and SPOT vegetation NDVI data. International Journal of Remote Sensing, 26, 4485-4498.

Zenone, T., Chen, J., Deal, M.W., Wilske, B., Jasrotia, P., Xu, J., Bhardwaj, A.K., Hamilton, S.K., Robertson, P.G., 2011. CO_2 fluxes of transitional bioenergy crops: effect of land conversion during the first year of cultivation. GCB Bioenergy, 3, 401-412.

Zenone, T., Gelfand, I., Chen, J., Hamilton, S.K., Robertson, G.P., 2013. From set-aside grassland to annual and perennial cellulosic biofuel crops: Effects of land use change on carbon balance. Agricultural and Forest Meteorology, 182-183, 1-12.

Zhang, Q., Lei, H.M., Yang, D.W., 2013. Seasonal variations in soil respiration, heterotrophic respiration and autotrophic respiration of a wheat and maize rotation cropland in the North China Plain. Agricultural and Forest Meteorology, 180, 34-43.

CHAPTER 4
ECOSYSTEM RESISTANCE AND RESILIENCE TO SEVERE DROUGHTS: A BAYESIAN MODELING OF SOIL RESPIRATION

ABSTRACT

The intensification of drought magnitude and frequency is predicted to occur in the future due to global climate change. The altered precipitation patterns and increasing precipitation extremes increase soil water stress and impact ecosystem structure and function with immediate and prolonged effects. How the major carbon processes of grasslands and croplands respond to the severe droughts play important roles in scientific understanding and evidence-driven policy making for biofuel development. However, at present, most drought effects on ecosystem carbon cycle studies have only focused on immediate effects based on manipulated lab or field experiments. I monitored the responses of soil respiration components of multiple crops under different land use histories for four years, which included one wet-hot year, one severe dry-hot year, and two wet-cool years. This dataset allows us to examine the resistance and recovery of one of the major carbon cycling processes, soil respiration, to a naturally occurring drought.

Bayesian models help us test the difference of the temperature sensitivity (β) and growing-season soil respiration (LR_{20}) of autotrophic (R_a) and heterotrophic soil respiration (R_h) across different crop types (CROP) and land use histories (LUH) and their responses after severe drought. My results revealed that CROP affected R_a more whereas LUH influenced R_h more. Both R_h and R_s had different β responses. Strong water stress depressed both β and LR_{20} of R_a in the drought year but stimulated β of R_h. The increased β of R_h may be due to the change in the soil microbial community structure, but more research is still required to quantify these responses. The LR_{20} of R_s rose back to the 2011 levels after a one- or two-year lag in recovery,

while those of R_h did not return back to the values of 2011 yet. The β of R_h seems to require longer recovery time or has reached a new equilibrium.

4.1 INTRODUCTION

It is predicted that future climate changes will include a greater intensity and a greater variability in extreme events in many parts of the world. Heat waves and precipitation extremes (droughts, heavy rains and floods) are projected to occur with higher frequencies and magnitudes (IPCC, 2013; Smith, 2011; Knorr *et al*., 2007) due to the amplification of the hydrological cycle (Knapp *et al.*, 2008). Rising global temperatures and the alteration of precipitation patterns have already been reported in many regions, significantly impacting various ecosystems. The intensified precipitation regimes, including larger individual precipitation events and longer intervening dry periods, on both intra- and the inter-annual scales, induce stronger soil water stress in mesic ecosystems and modify ecosystem functions by changing community structure and individual traits, seriously disturbing ecosystems (Knapp *et al.*, 2008).

Smith (2011) and Reichstein *et al*. (2013) redefined extreme climatic events (ECE) to not only consider the statistically unusual climate periods (driver) but also the changes of ecosystem functions (response) during or after the period of extreme climatic events. The new definition is not only based on statistics, but also considers the responses of an ecosystem related to important ecological processes and their drivers, and thus is better suited for ecological and environmental research.

The resilience of an ecosystem to an external disturbance has multiple definitions. Holling (1996) identified "ecological resilience" as the magnitude of the disturbance that the system can absorb before the system changes its structure and the processes that control the behavior of the system; he also defines "engineering resilience" as the speed of return to the pre-

disturbance equilibrium. These two definitions of resilience were developed from different perspectives: the former focuses on the persistence of the behavior and whether the change of ecosystem functions and the relative processes and structure exist or not, while the latter concerns the recovery speed and the time to return to the stable status (Holling, 1973). They represent two important aspects of the system's behavior after the system experiences a disturbance, reflecting the immediate and prolonged effects of the disturbance.

This chapter addresses the resilience of soil respiration in biofuel cropping systems. To mitigate the impacts of CO_2 emissions from fossil fuel combustion, the production of bioenergy has dramatically increased in the past decades. The growing bioenergy industry has stimulated worldwide land use change, converting many land use types into biofuel cropping farms or into agricultural land to address food shortage, which is caused by biofuel production. The expansion of biofuel crop production plays an important role in land use change now and in the future (Lark *et al.*, 2015). Major biofuel crops include corn and several perennial cellulosic herbaceous grasses, such as switchgrass, Miscanthus and elephant grass (Lemus & Lal, 2005; Johnson *et al.*, 2007).

Drought, as one of the most import climate-induced extremes, critically impacts the carbon cycling of grasslands and croplands (Reichstein *et al.*, 2013; Ciais *et al.*, 2005). It may bring strong soil water stress, affect the plant's growth and soil microbial activities, and ultimately impact ecosystem carbon dynamics. On the other hand, grasslands and cropping systems have high recovery plant growth potential in both managed and unmanaged ecosystems and thus, may perform better in dry years than forests (Zavalloni *et al.*, 2008; Gilgen & Buchmann 2009; Reichstein *et al.*, 2013). Most studies of drought consequences on ecosystems emphasize immediate responses. However, the protracted recovery of ecosystem functions lacks

documentation, even though it may be more important (Hoover *et al.*, 2016). In addition, most drought or drought-rewetting studies are manipulation experiments in the lab or in the field. The manipulation of water input may change some physical conditions and the radiation balance, and ultimately affect ecosystem responses.

The naturally occurring inter-annual climate variability (wet-hot, severely dry-hot, wet-cool, wet-cool, in sequence) in 2011-2014 at my experimental sites provided me with a good opportunity to examine how ecosystems respond to the severe drought in both the disturbance year and the following recovery years. In Chapter 2, I looked for differences in Q_{10} between different sites in each year but found no significant difference among sites or years because of high variability in each treatment. The Bayesian modeling approach outperforms the conventional frequentist statistical approach for testing the changes of temperature sensitivities of soil respiration among LUH and CROP, the year-to-year trend after LUC or the immediate and prolonged effects after severe drought. In this chapter, I develop a new method, based on a probabilistic Bayesian approach, to estimate how the relationships of soil respiration, including R_h and R_s, and soil temperature respond to intra-annual climate patterns, severe drought and long-term trends after LUC.

Specifically, I developed Bayesian models to test the R-T_s relationship among CROP and LUH and clarified their immediate and prolonged responses to severe drought. I hypothesized that perennial crops, which develop their dense root system after lands use change, have higher probabilities to weaken the impact of drought, have higher resistance and lower sensitivity to drought and have a high rate to recover after drought. The late successional grasslands may have high resistance and resilience of soil respiration temperature sensitivity to severe drought due to its highly developed root system while those in corn fields are weak.

4.2 METHODS

4.2.1 Study area

My experimental sites are located at the Great Lakes Bioenergy Research Center scale-up fields of the Kellogg Biological Station (KBS, 42°40'N, 85°40'W), established in association with the KBS Long-Term Ecological Research (LTER) site. The sites are located in the southwest of Michigan, USA (Fig. 1.2.). The climate is humid continental (warm summer) climate (Dfa; Peel *et al.*, 2007). The mean annual air temperature and mean annual precipitation at KBS are 10.1 °C and 1005 mm yr^{-1} (1981-2010), respectively (Robertson & Hamilton, 2015).

4.2.2 Experimental design and schedule

Seven experimental plots were located at two locations with their own land use histories (LUHs): (1) Conservation Reserve Program (CRP) grasslands at Marshall Farm, and (2) corn-soybean rotation agricultural fields (AGR) at Lux Arbor Reserve. The CRP sites have been in a monoculture of smooth brome grass (*Bromus inermis* Leyss) since 1987, while the AGR fields have been under conventional corn-soybean rotation cultivation for several decades (Fig. 1.6). The soil texture at all sites is sandy loam, except for a sandy clay loam at one field. However, soil carbon and nitrogen contents at the CRP sites were significantly higher than those at the AGR sites before land conversion (Table 1.1).

The experiment was conducted at seven scale-up fields ranging from 9 to 17 hectares. Four fields are located in Marshall Farm (i.e., CRP sites) and three in Lux Arbor Reserve (i.e., AGR sites). All sites, except the reference site (Ref), were sprayed with herbicide at the end of 2008 to prepare the lands for soybean planting in 2009. The CRP and AGR sites were then cultivated with either continuous corn (*Zea mays*, Dekalb DK-52), switchgrass (*Panicum*

virgatum), or a mixture of native prairie grasses, which have been dominated by Canada wild rye (*Elymus Canadensis*), little bluestem (*Schizachyrium scoparium*), Indian grass (*Sorghastrum nutans*), big bluestem (*Andropogon gerardii*), and switchgrass (*Panicum virgatum*) since 2010. A particular CRP grassland dominated by brome grass was not disturbed and was retained as the reference site (Gelfand *et al.*, 2011; Zenone *et al.*, 2011; Deal *et al.*, 2013; Zenone *et al.*, 2013). I used an experimental code for these sites by abbreviating them as "LUH-CROP". The CRP-C, CRP-Sw and CRP-Pr represent the CRP sites that were converted to corn, switchgrass and prairie mixture respectively, while AGR-C, AGR-Sw and AGR-Pr are AGR farms were converted to corn, switchgrass and prairie mixture. In 2010, when the crops were established, the perennial crops switchgrass and prairie were accompanied by oats as a nurse crop with and without fertilization, respectively. No other management practices were applied beyond harvesting at the end of each growing season (GS). No-till continuous corn was seeded in mid-May with a one-time herbicide mix (Lumax, Atrazine 4L, Honcho Plus and $(NH_4)_2SO_4$). Phosphorus, potassium and nitrogen fertilizers were applied during April and June in each year (Zenone *et al.*, 2013).

4.2.3 The climatic and microclimatic measurements and growth season identification

Climate, such as air temperature (T_a) and daily precipitation (PRCP), and microclimate, such as soil temperature and soil water content, were recorded as the independent variables. They were recorded at different spatial and temporal scales based on the requirement of the research and the limitation of the equipment and labor.

The daily mean T_a and daily accumulative PRCP were collected and calculated from the KBS LTER weather station (42°24'47.1" N, 85°22'15.3" W; www.lter.kbs.msu.edu). The air temperature was recorded hourly by a thermometer at 3 m height. The mean daily air

117

temperature was calculated from the hourly data. Precipitation was measured by a NOAH IV total precipitation gauge (ETi Instrument Systems Inc., Fort Collins, CO).

Soil temperature (T_s) and volumetric soil water content (VWC) were measured simultaneously with soil respiration rate measurements biweekly during late April to September and monthly during other times. Soil temperature was measured at 10 cm depth using a *Taylor 8940N* digital thermometer (Taylor Precision Products, Las Cruces, NM, USA), while VWC was monitored below the ground surface at 10 cm depth using a *HydroSense II* with a *CS659* sensor (Campbell Scientific, Inc. (CSI), Logan, UT).

The length of the GS is an important index for climate change and agriculture. Several identifications are based on climate and crop growth. I used temperature-based identification, which is the most common in North America (a.k.a. frost-free season) instead of crop-based GS since soil respiration includes the soil microbe-derived carbon efflux, not only plant-derived soil carbon efflux. The onset and end of the climatic GS each year were calculated based on a nine-day moving average of daily mean air temperature ($9d$-T_a) to filter short-term warm or cold events, which may not induce the start of plant growth and development in spring. The onset of the GS was identified as the first day exceeding 0°C $9d$-T_a in spring, while the end of the GS was recognized as the latest day exceeding 0°C $9d$-T_a in fall. The lengths of the GS were the number of dates between the onset and the end of the GS each year.

To compare the soil respiration rates, climate, microclimate and the vegetation indices, I separated the data into different years based on the USGS' "water year" concept October 1st to September 30th—as it is more meaningful than a calendar year in agricultural research. I identified the water year in my dissertation from the end of the previous GS until the end of this GS because post-GS precipitation may subsidize the soil water pool and support plant and soil

microbe consumption in the next GS. The length of the water year may be different due to the different seasonal patterns of air temperature in fall and winter.

4.2.4 The total and heterotrophic soil respiration measurements

Four plots at each site were randomly selected to install 1x1 m root exclusion plots for measuring heterotrophic soil respiration (R_h). We dug a 1 m deep trench around the edges of each square (Fig. 2.1 (B)). The trenches were lined with root-barrier sheets before the soil was refilled according to its soil profile (Fig. 2.1 (C); Tang *et al.*, 2005). The plants and roots inside the square were manually removed and/or killed by herbicide (*Monsanto Roundup®*). Two PVC collars (10 cm diameter) were installed inside the square to accommodate flux chambers to measure R_h. Another two collars were installed surrounding the square to measure total soil respiration (R_s) (Fig. 2.1(D)). A total of 112 measurements (including R_h and R_s) were taken between 10AM and 7PM when soil respiration is at its diel maximum.

Soil respiration was measured biweekly during the GS and monthly during the non-GS when snow cover is minimal to allow the measurements (October–December). The chamber-based infrared gas analyzer (IRGA) approach of soil respiration measurement was done with an *LI-6400* portable photosynthesis system with a 10 cm diameter *6400-09* soil chamber or *LI-8100* with a 10 cm diameter *8100-102* soil chamber (LI-COR Biosciences, Lincoln, NE).

4.2.5 Vegetation Index data

Vegetation indices, including *normalized difference vegetation index* (NDVI) and *enhanced vegetation index* (EVI), were calculated based on satellite remote sensing using band 1 (nir), band 2 (red), and band 3 (blue) of the Moderate Resolution Imaging Spectroradiometer (MODIS). The NDVI was determined by the ratio of the difference between near-infrared

reflectance and red reflectance to their sum (Tucker *et al.*, 2005). The EVI was further modified

with a soil adjustment factor, L, and two atmospheric aerosol scattering coefficients, C_1 and C_2

(Huete *et al.*, 1999), and has higher sensitivity at the "green" portion of the spectrum when

vegetation is very dense. These data were developed from MODIS daily products by selecting

the optimal day (i.e., low cloud cover) out of a 16-day interval. Missing data may appear when

clouds obscured the site over an entire 16-day period. NDVI and EVI data were downloaded

from the Oak Ridge National Laboratory Distributed Active Archive Center for Biogeochemical

Dynamics (ORNL DAAC, http://daac.ornl.gov/MODIS/modis.shtml). I used a single pixel from

the MODIS image that fell within each experimental site at the finest spatial resolution of 250 m.

The dates of NDVI and EVI values were paired with the nearest dates of soil respiration

measurement.

4.2.6 The concept of Bayesian modeling

In this chapter, I use a Bayesian approach to estimate the parameters of the posterior

models and analyze the changes of $\log_{10}$-transformed soil respiration temperature sensitivity (β)

and soil respiration value at 20°C (LR_{20}), both of which are used as indices to observe the

changes in the R_s-T_s and R_h-T_s relationships.

Temperature sensitivity of soil respiration (β) and $\log_{10}$ soil respiration at 20°C (LR_{20})

The Pr(C|D) was calculated with the following equation:

$$\Pr(C|D) = \Pr(C) \times \frac{\Pr(D|C)}{\Pr(D)} \qquad \text{Eq. 4-1}$$

where Pr(C|D) is the probability of event C occurring, given that event D had occurred and that

Pr(D|C) is the inverse. Here, I can consider Pr(C), the first term on the right side of the equation,

as prior knowledge from previous studies, empirical data or broad-scale data. The second term

on the right side, Pr(D|C)/Pr(D), is the likelihood that can be based on new data, specific data or

even new estimates from different mechanisms, relationships with other variables or a new

hypothesis. The posterior model on the left side of the equation is then estimated from the

combination of the prior model and the likelihood function.

For continuous data, the posterior models of Bayesian statistics were estimated from the

combination of prior information and new knowledge (likelihood). The Bayes' rule for

continuous data can be rewritten as below:

$$\Pr(C|D) = \frac{\Pr(C) \times \Pr(D|C)}{\int_0^\infty \Pr(x) \times \Pr(D|x) dx} \qquad \text{Eq. 4-2}$$

where C is the specific value for the parameter. The replacement of the denominator Pr(D) to the

integration of over all possible events, which represents the sum of the conditional probabilities

of the parameter (x).

The Bayesian model, thus, can separate into three major parts: prior model, likelihood

and posterior model. The prior model can be the estimated distribution of probabilities from

empirical data, previous knowledge or a broader scale dataset. The likelihood can be a set of new

data, a relationship from other independent variables, or the specific group of data contained in

the broad scale data. The new probability distribution was created from the prior model and

likelihood.

4.2.7 The estimations of prior models

To better develop the Bayesian model and compare R-T relationships in various CROP or

LUH and their responses to climate patterns and severe climate events, as well as the shift of R-T

relationship after LUC, I separated R_h and R_s data by year and then created Bayesian models

independently. The probabilities of the values of $\log_{10}$ soil respiration were assumed to have a

natural distribution and were fitted by the Maximum Likelihood Estimation (MLE) approach:

$$R_i \sim N(\mu, \sigma^2) \qquad \text{Eq. 4-3}$$

where μ and σ^2 were the mean and variance, respectively, to the probabilities of a particular soil respiration rate R_i.

The starting points of the suitable MLE models were determined from the means and standard variations in the raw data of soil respiration rates. The results of the well-fitted MLE models were my prior models of the Bayesian models. The MLE models were run by the "bbmle" package (https://cran.r-project.org/web/packages/bbmle/index.html) for *R* language (R Development Core Team, 2010).

4.2.8 The equations of likelihood

To elucidate the R-T relationship based on traditional exponential hypothesis and my previous analysis (Chapter 2), I assumed a linear correlation between the $\log_{10}$ soil respiration rates ($\log_{10}R$) to soil temperature (T_s). Therefore, I assumed the likelihood is as below:

$$logR = \alpha + \beta \cdot T_s + \epsilon \hspace{3cm} \text{Eq. 4-4}$$

where α, intercept of the regression line, is the value of $\log_{10}R$ at 0°C; and β, the slope of the regression line, is the raising value of $\log_{10}R$ when T_s increase by 1°C, representing temperature sensitivity of soil respiration.

In order to incorporate the different effects of CROP and LUH on R-T relationships when they respond to climate, I added "site" as a latent discrete term in the likelihood equation:

$$logR = \alpha + \beta \cdot T_s + site + \epsilon \hspace{2.5cm} \text{Eq. 4-5}$$

Both α and β were assumed to have normal distributions with small variances.

4.2.9 Calculation of estimations of posterior models

After setting up the whole model, the "R2jags" package (https://cran.r-project.org/web/packages/R2jags/index.html) for R language ran the Bayesian model using the

Markov Chain Monte Carlo (MCMC) method to estimate the posterior models for 10,000 runs with 1,000 discarded initial samples to obtain the values of α and β in each iteration. The distributions of the parameters were checked by the "mcmcplots" package (https://cran.r-project.org/web/packages/mcmcplots/index.html) to diagnose whether posteriors converged to their stationary distribution or not. Then, LR_{20}, the $\log_{10}R$ value at 20°C, was calculated based on the values of α and β:

$$LR_{20} = \alpha + 20 \cdot \beta \qquad\qquad \text{Eq. 4-6}$$

In this equation, β and LR_{20} are plotted on a bi-plot. The locations of the predictions revealed the temperature sensitivity of soil respiration and the GS soil respiration. The location of the "clouds", which are composed of the predictions of Bayesian models, on the β-LR_{20} biplot presents the R-T relationship of each field. The behaviors of clouds across years display its responses to climate. The means and standard deviations of each cloud were calculated and used to recognize the shift among years.

4.2.10 Estimation of β and LR_{20} of R_a

After simulating β and LR_{20} of R_s and R_h, I calculated the β and LR_{20} of R_a after weighing the root's contribution to soil respiration (RC). This is because both β of R_a (β_{Ra}) and β of R_h (β_{Rh}) contribute to β of R_s (β_{Rs}), according to their relative contribution, which can be presented as:

$$\beta_{R_s} = RC \cdot \beta_{R_a} + (1 - RC) \cdot \beta_{R_h} \qquad\qquad \text{Eq. 4-7}$$

where RC is the root contribution of total soil respiration (i.e., R_a:R_s ratio) for each field in each year (Supplement 4-1).

The values of β_{Ra} can be calculated by the following equation, derived from Eq. 4-7 above:

$$\beta_{R_a} = \frac{\beta_{R_s} - (1-RC) \cdot \beta_{R_h}}{RC} \qquad\qquad \text{Eq. 4-8}$$

The LR_{20} of R_a was calculated by the same methods in the equation below:

$$LR_{20_{R_a}} = \frac{LR_{20_{R_s}} - (1-RC) \cdot LR_{20_{R_h}}}{RC} \qquad\qquad \text{Eq. 4-9}$$

where LR_{20Ra} is the LR_{20} of R_a, LR_{20Rs} is the LR_{20} of R_s and LR_{20Rh} is LR_{20} of R_h.

4.3 RESULTS

4.3.1 Bayesian models for the R-T_s relationship

The prior models of R_s and R_h for each year were estimated by MLE based on the $\log_{10}$-transformed soil respiration rates that were assumed to have normal distributions. The starting points of each model simulation were the means and the standard deviations of raw soil respiration data (Table 4.1 & Fig. 4.1). The MLE models fit raw data well, although the raw data of $\log_{10}$ soil respiration were slightly left skewed. The year 2012 had the greatest variance while 2014 had the smallest variance for both R_s and R_h.

Table 4.1. The mean and standard deviation of $\log_{10}$ soil respiration by year. The values of mean and standard deviation (sd) were used as the starting point of Maximum Likelihood estimation (MLE) natural distribution. R_s is total soil respiration and R_h is heterotrophic soil respiration.

	year	mean	sd
R_s	2011	0.495	0.358
	2012	0.298	0.468
	2013	0.469	0.391
	2014	0.592	0.280
R_h	2011	0.374	0.405
	2012	0.108	0.502
	2013	0.164	0.448
	2014	0.362	0.301
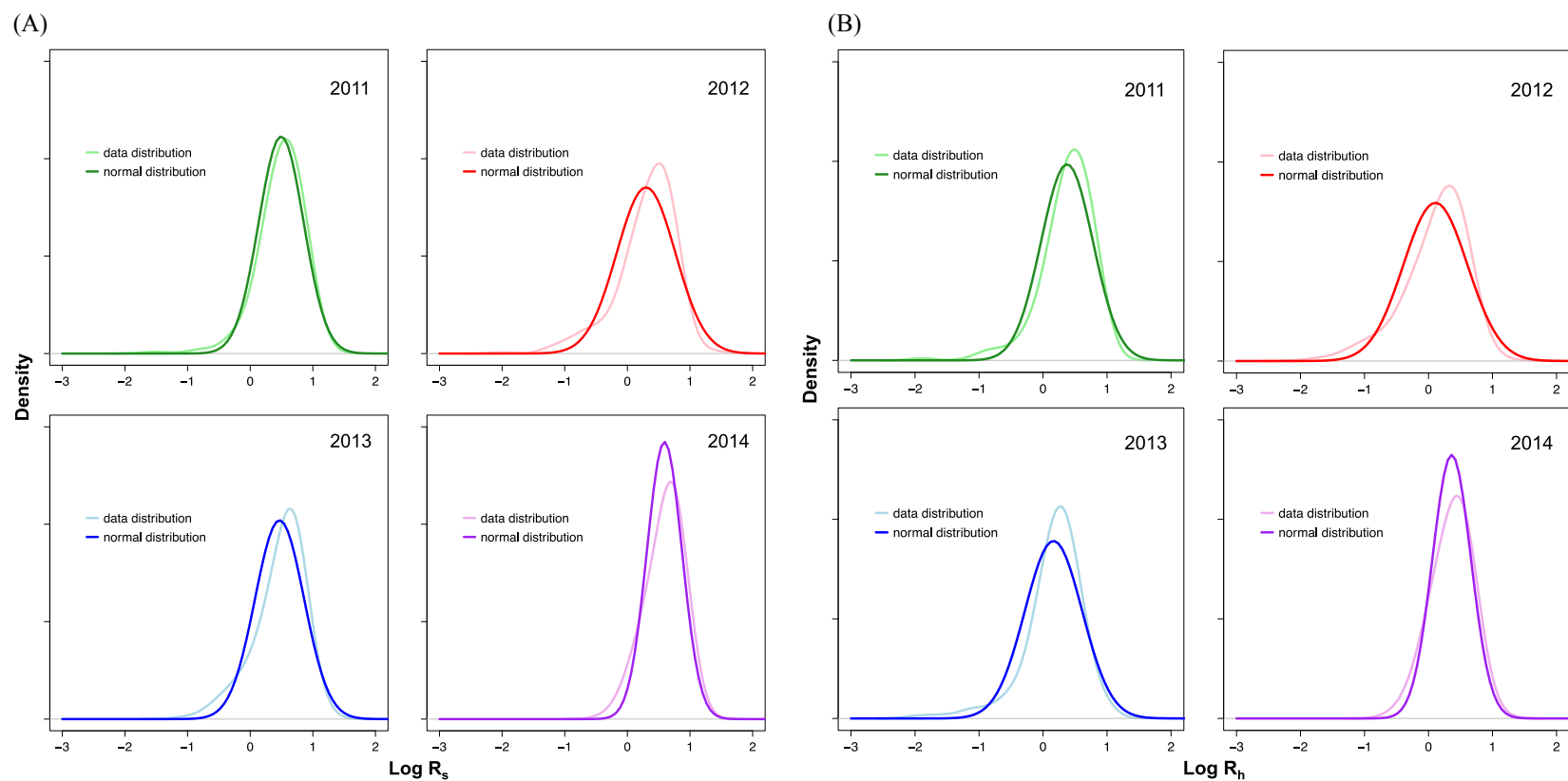
Figure 4.1. The probabilities of log$_{10}$ soil respiration in each year. For R$_s$ (A) and R$_h$ (B), the distribution of MLE models (dark colors) were based on normal distributions, with the means and standard deviations derived from the raw data. The distribution of raw data (light colors) were slightly skewed left, but most of them were well fitted. Green, red, blue and purple curves represent the distributions of log soil respiration data in 2011, 2012, 2013 and 2014, respectively.

4.3.2 The differences of β and LR$_{20}$ between CROP and LUH

CROP and LUH play important roles on the R-T relationship. I recognize the different locations of β_{Rs}-LR$_{20Rs}$ and β_{Rh}-LR$_{20Rh}$ between CROP (i.e., C, Sw, Pr and Ref) and between LUH (i.e., AGR, CRP and Ref). For total soil respiration, the Ref site had the highest LR$_{20}$ and a relatively high β in both R$_s$ and R$_h$ across all sites. In contrast, corn sites had the lowest LR$_{20}$ in both R$_s$ and R$_h$ compared to other perennial sites (switchgrass and prairie). Prairie had higher LR$_{20}$ and β than switchgrass. For the effect of LUH for R$_s$, CRP had lower β and higher LR$_{20}$ than AGR in perennial crops while AGR always had higher β in CRP fields than those in AGR fields in the annual crop (Table 4.2 & Fig. 4.2(A)). The effect of CROP and LUH on the R-T relationship for R$_h$ are similar to that for R$_s$. CRP sites had higher LR$_{20}$ than AGR sites. Ref and CRP-Pr had high LR$_{20}$, followed by CRP-Sw and then CRP-C. The LR$_{20}$ in AGR-Sw was near that of AGR-Pr and higher than that of AGR-C (Table 4.2 & Fig. 4.2(B)).
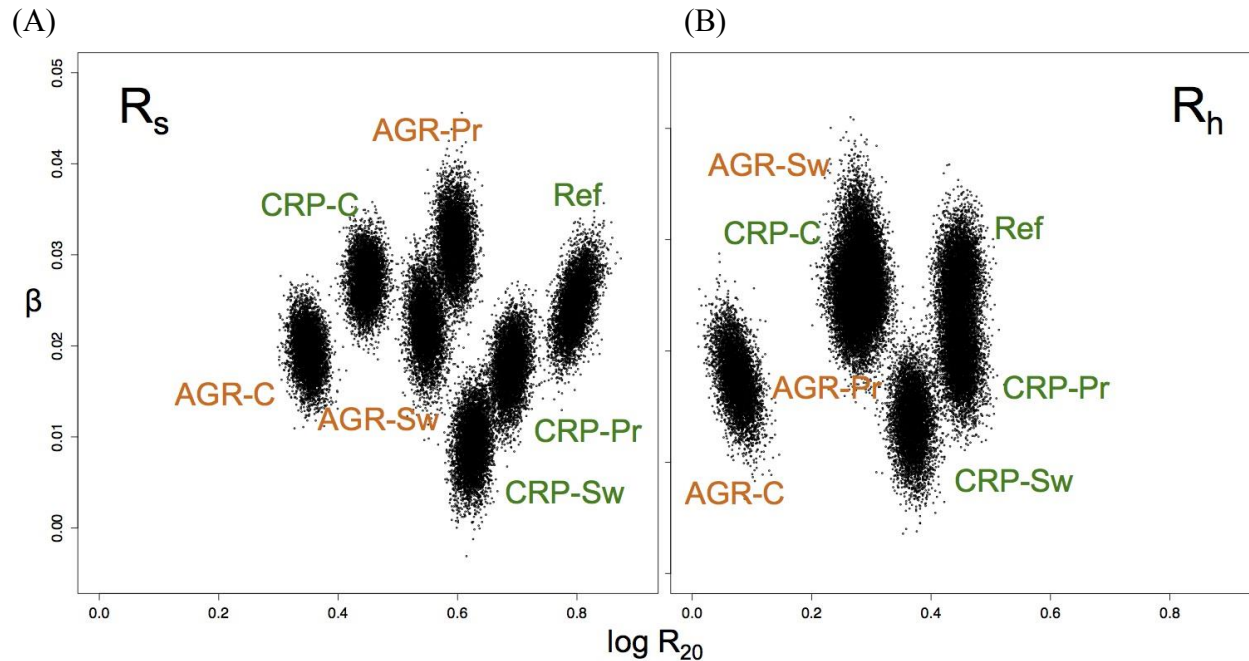
Figure 4.2. The distributions of log_{10} soil respiration temperature sensitivity (β) and log_{10} soil respiration rates at 20 °C (LR_{20}). The Bayesian models were developed based on the Bayesian approach, with data from the four growing seasons (2011-2014), which include R_s (A) and R_h (B). The predictions were simulated from Bayesian models using the Markov Chain Monte Carlo (MCMC), which is a method based on the probabilities of β and LR_{20}. Each cloud represents one site for different crop types and land use histories.

Table 4-2. The values of LR_{20} and β in the R_s-T_s and R_h-T_s relationships. The means and standard deviations were calculated from the Bayesian estimation of each site, which include data from all four growing seasons (2011-2014). CROP: crop types; LUH: former land use history; C: corn; Sw: switchgrass; Pr: prairie; Ref: reference; CRP: Conservation Reserve Program; AGR: corn=soybean rotation agriculture.

CROP	LUH	R_s		R_h	
		LR_{20}	β	LR_{20}	β
C	CRP	0.442 ± 0.051	0.027 ± 0.002	0.289 ± 0.053	0.026 ± 0.002
	AGR	0.340 ± 0.056	0.019 ± 0.003	0.081 ± 0.064	0.018 ± 0.003
Sw	CRP	0.622 ± 0.059	0.009 ± 0.003	0.374 ± 0.061	0.014 ± 0.003
	AGR	0.541 ± 0.067	0.022 ± 0.003	0.296 ± 0.073	0.029 ± 0.003
Pr	CRP	0.695 ± 0.057	0.018 ± 0.003	0.441 ± 0.054	0.019 ± 0.002
	AGR	0.591 ± 0.068	0.031 ± 0.003	0.267 ± 0.062	0.024 ± 0.003
Ref		0.804 ± 0.054	0.025 ± 0.003	0.456 ± 0.054	0.027 ± 0.003

4.3.3 The distribution of β and LR_{20} of R_a and R_h and their trajectories across years

When comparing the locations of the β-LR_{20} plots, I found that R_h had relatively smaller amounts in LR_{20} than R_s (Fig. 4.3). I calculated the β and the LR_{20} of R_a based on the weighed β and the LR_{20} of R_s and R_h (Eq. 4-7 & Eq. 4-8, Supplement 4-1). Generally speaking, R_a and R_h in the β-LR_{20} plots had very different responses to the 2012 drought (Fig. 4.4). In the drought year, all $β_{Ra}$ decreased at different levels. They then rebounded in the following years but at variable rates. The Ref site had high resistance but slow recovery. The $β_{Ra}$ decreased in 2012 and 2013 and then rose back to the 2011 level in 2014. Other sites had stronger decreases of $β_{Ra}$ in 2012, but also stronger rebounds in 2013 and 2014 from the 2011 levels. The $β_{Ra}$ in AGR-Sw, AGR-Pr and CRP-C fell back in 2014. The shifts of the LR_{20Ra} varied in 2012. Some sites increased while some sites decreased. However, all of them increased in 2013, the first year after drought. The magnitudes of increases of the LR_{20} of R_a varied. Some sites fell back in 2014 while others still increased (Fig. 4.5 (A)).

Unlike R_a, the β and the LR_{20} of R_h told very different stories. The β of R_h in all sites increased and the LR_{20} of R_h decreased in 2012, although the increasing magnitudes of β in CRP-Sw and CRP-Pr—the most dry sites (Fig. 3.1 (B))—were very small. The levels of β and LR_{20} of R_h did not change much after 2012. Some sites had slightly increasing β and LR_{20} while some β and LR_{20} rates fluctuated near the 2012 levels without returning to the 2011 levels (Fig. 4.5 (B)). It had either required more time to recover or it had reached a new dynamic equilibrium after the 2012 drought.
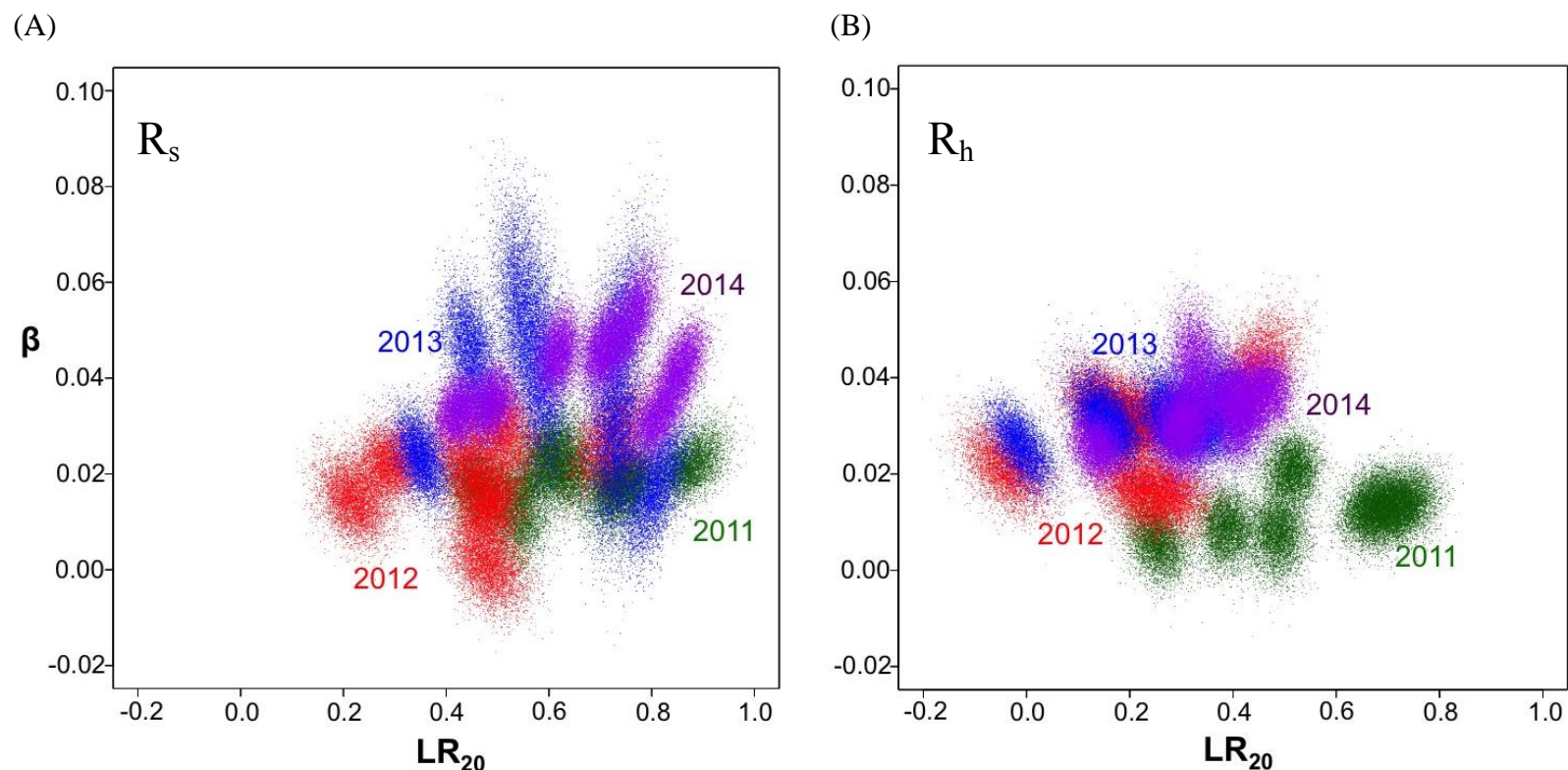
Figure 4.3. The distributions of the $\log_{10}$ soil respiration temperature sensitivities (β) and the $\log_{10}$ soil respiration rates at 20 °C (LR_{20}) across years. The clouds show β and LR_{20} of R_s (A) and R_h (B), which were predicted by Bayesian models. Each cloud contained 10,000 predictions and presented the values of β and LR_{20} for each site in each year. The locations of green, red, blue, and purple dots represent the shifts from 2011 to 2014, respectively.
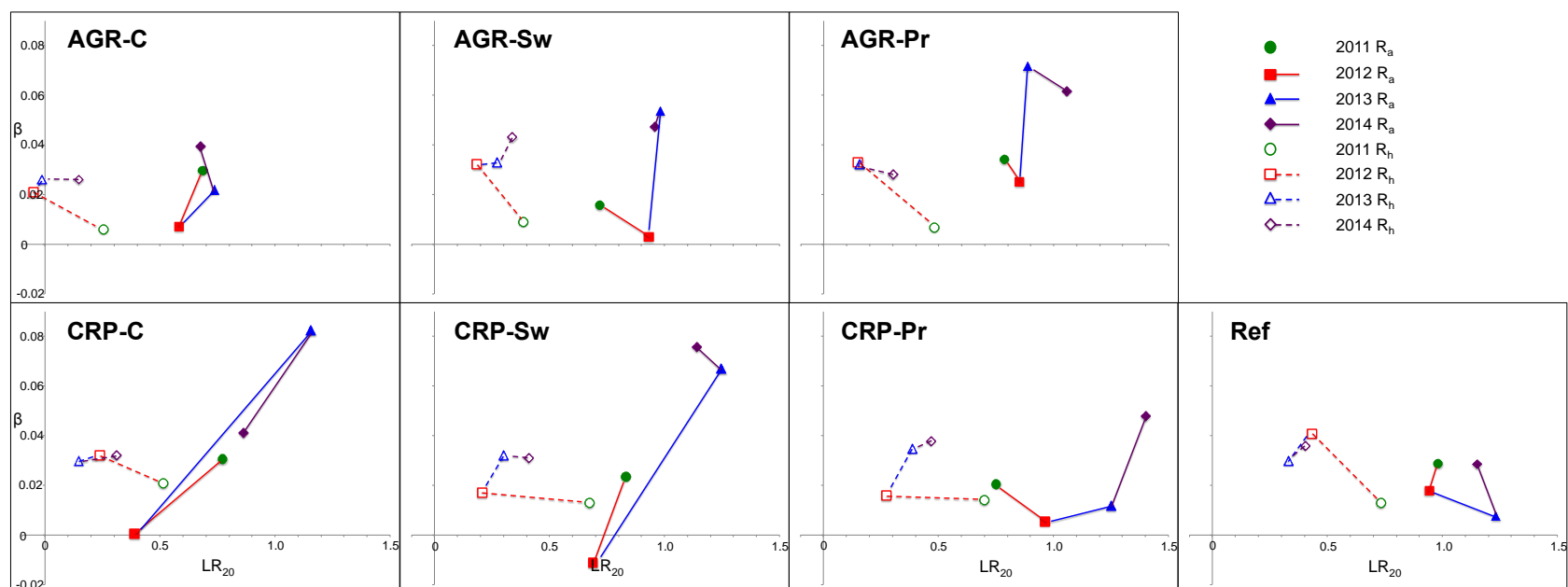
Figure 4.4. The inter-annual shifts of the log$_{10}$ soil respiration temperature sensitivities (β) and the log$_{10}$ soil respiration rates at 20 °C (LR$_{20}$) of R$_a$ and R$_h$ for each site across all years. The solid dots and lines represent β and LR$_{20}$ of R$_a$ while the empty circles and dash lines show those of R$_h$. The green, red, blue, and purple colors represent 2011–2014, respectively.

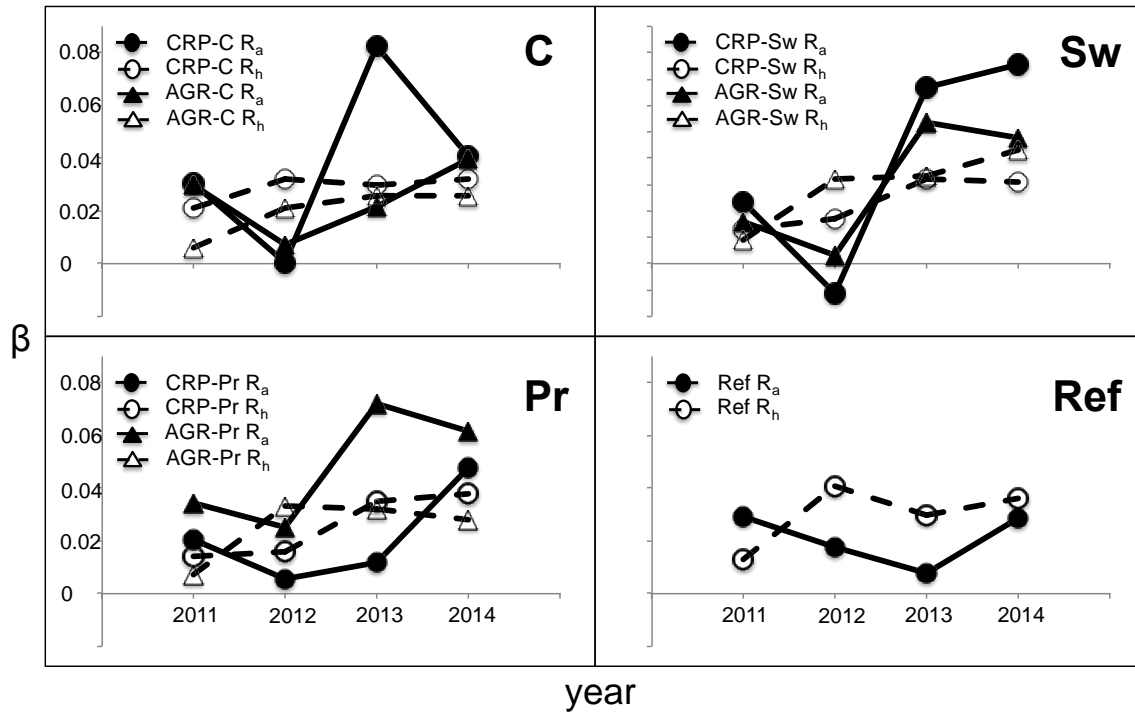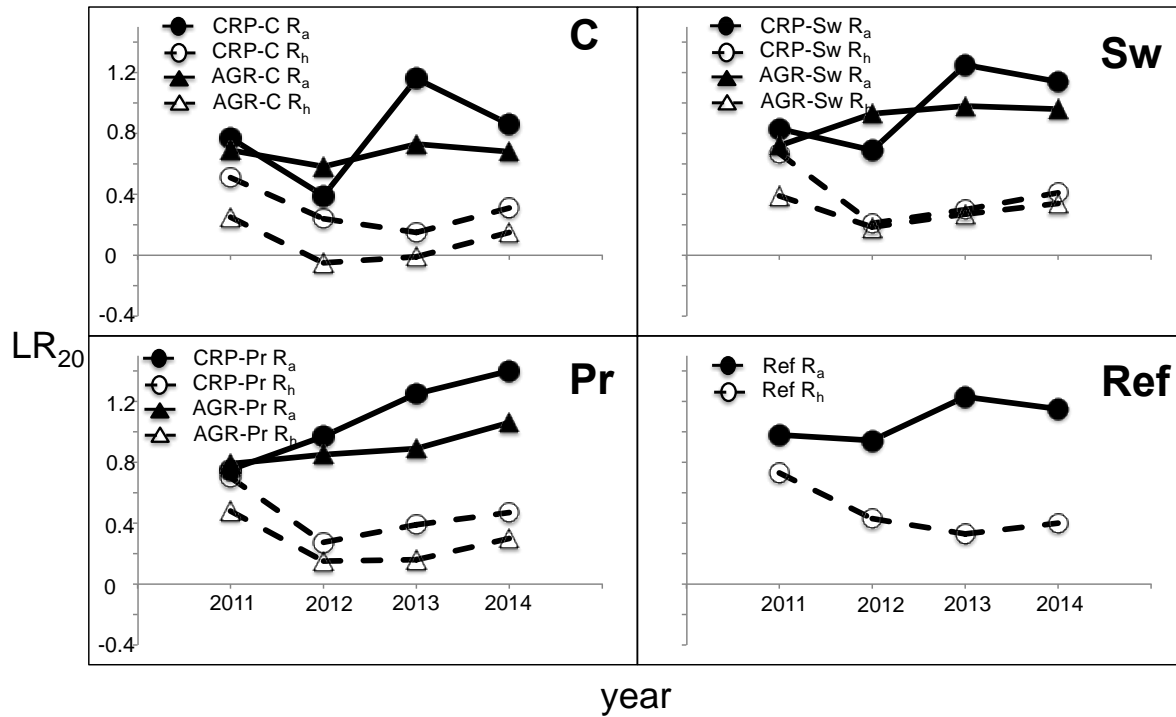**Figure 4.5. The inter-annual shifts of the log$_{10}$ soil respiration temperature sensitivities (β) and the log$_{10}$ soil respiration rates at 20 °C (LR$_{20}$) of R$_a$ and R$_h$ for different crops and land use histories across all years.** The β (A) and LR$_{20}$ (B) present different crops. The solid dots and lines display R$_a$, while the empty circles and dashed lines show R$_h$.

4.4 DISCUSSION

4.4.1 The distribution of β and LR$_{20}$ across CROP and LUH combinations

The annual soil respiration rates varied widely across treatments, as shown in Chapter 2 (Fig. 2.5). The Ref field had the highest LR$_{20}$, followed in sequence by Pr, Sw, and C (Fig. 4.2). The effect of LUH is similar. Ref had the highest LR$_{20}$, followed in sequence by CRP and AGR (Fig. 4.2). When observing the distribution of the clouds of estimates on the LR$_{20}$-β plots, it is evident that the same CROP (with different LUH) has similar R-T relationship in R$_s$ while the same LUH (with different CROP) has similar R-T relationship in R$_h$. The results support my hypothesis that CROP affects R$_a$ more because its substrate supply is mainly regulated by photosynthesis and the carbon allocation of plants. On the other hand, LUH affects R$_h$ by controlling the characteristics and processes in soil.

4.4.2 The stability of β and LR$_{20}$ in the severe spring-summer drought in the Ref field

Ref had the smallest shift in both β and LR$_{20}$ of R$_s$ across all sites inter-annually. This implies that the soil-root system in Ref was the most resistant to perturbation out of all the sites, even with the severe drought in 2012. However, for R$_h$, the LR$_{20}$ decreased and β increased enormously due to the drought (Fig. 4.4). Brome grass may have been able to take up water from deeper soil horizons and maintain its basic metabolism during the drought, whereas the soil microbial activities were impacted in the upper 10 cm soil layer. The β$_{Rh}$ in 2013 and 2014 dropped a little, but values were still higher than that in 2011. The LR$_{20Rh}$ values were very low in 2013 and 2014. The Ref field exhibited a very different R$_h$-T$_s$ relationship between 2011 and the later three years.

4.4.3 Different responses of β-LR$_{20}$ on R$_s$ and R$_h$ after severe spring-summer drought

On the inter-annual scale, the effects of a disturbance on an ecosystem may be observed as changes in the behavior of the ecosystem functions immediately (the same year) and in the recovery years (the following years) (Holling, 1973; Holling, 1996; Smith, 2011). The climate patterns I observed—wet-hot, dry-hot, wet-cool and wet-cool in the continuing four growing seasons (2011-2014)—gave me an opportunity to test the short- and long-term responses of the R-T$_s$ relationship to a severe spring-summer drought. I found that the two components, R$_a$ and R$_h$, had different responses to the drought (Figs. 4.5 (A) & (B)).

4.4.3.1 The resistance of R$_s$-T$_s$ and R$_h$-T$_s$ relationships to the drought

In the drought year, all β$_{Ra}$ decreased while β$_{Rh}$ increased regardless of the fact that LR$_{20}$ responses varied (Fig. 4.4 & Fig. 4.5). The opposite responses of R$_a$ and R$_h$ temperature sensitivities were due to their own distinctive mechanisms. Most studies have indicated that the temperature sensitivity of soil CO_2 efflux is depressed under low water moisture (Savage & Davidson, 2001; Jassal *et al.*, 2008; Harper *et al.*, 2005). My results of R$_a$ supported the conclusion of these studies.

Surprisingly, β$_{Rh}$ increased in all sites in 2012 compared to 2011 (the red dashed lines in Fig. 4.4; Fig. 4.5 (A)) when the water stress was strong. The climate pattern—early onset and a warm spring with spring-summer drought in 2012—seemed to depress all R$_h$ and increase temperature sensitivity. I noted a similar phenomenon in the R$_h$-T$_s$ relationship in Chapter 2. Most Q$_{10}$ of R$_h$ in 2012 was higher than those in 2011 (Supplement 2-3). My results of R$_h$ were opposite to most studies, which claimed that the temperature sensitivity of R$_h$ would decrease when soil moisture is low in mesic ecosystems (Suseela *et al.*, 2012; Wang *et al.*, 2014; Sampson *et al.*, 2007; Jassal *et al.*, 2008; Manzoni *et al.*, 2012; Rey *et al.*, 2002). In contrast, the driest

experimental sites (i.e., CRP-Sw and CRP-Pr) had lower magnitudes of increasing β_{Rh} in 2012 than other sites. The effects of water stress on $\log_{10} R_h$ temperature sensitivity within 2012 supported the previous studies that also claimed water deficit reduces R_h temperature sensitivity. The contrast between the intra-annual (among sites) and inter-annual (2011 vs. 2012) comparisons may be due to other causes.

Heterotrophic soil respiration results from the decomposition of soil organic matter by soil microbes. Decomposition is a biochemical reaction and is assumed to have an exponential relationship with temperature (Lloyd & Taylor, 1994; van't Hoff, 1885). The decomposition rate and its temperature sensitivity were regulated by its intrinsic kinetic properties and environmental constraints (Davidson *et al.*, 2006). The former mainly depends on the complexity of carbon compounds (i.e., labile compounds and recalcitrant compounds), the concentration of substrates, the physical protection (i.e., soil aggregates) and the chemical protection (i.e., the absorption of carbon compounds into mineral surface by chemical bonds) (Davidson *et al.*, 2006). The latter restrains intrinsic temperature sensitivity of R_h and represents the apparent temperature sensitivity (Suseela *et al.*, 2012) and may be related to surrounding temperature, water availability (Schimel *et al.*, 1994; Ise & Moorcroft, 2006), soil microbial community structure (Sheik *et al.*, 2011; Zhou *et al.*, 2014) and the affinities of the enzymes for the substrates (Davidson *et al.*, 2006). The decrease of R_h in all sites in 2012 was more possibly due to the change in the soil microbial community structure or their activities since soil physical and chemical properties are less likely to change much in the short-term in no-till fields.

In 2012, not only was there higher β_{Rh} but also lower "α", $\log_{10} R_h$ at 0 °C and LR_{20Rh} (Eq. 4-5) compared to 2011. The high β_{Rh} and low α and LR_{20Rh} means that the overall R_h in 2012 was lower than those in 2011, regardless of temperature. The impact of water stress on the

R_h-T_s relationship may result from the changes in the soil microbial community structure that shifted their intrinsic temperature sensitivity. Lipson *et al.* (2002) found that soil microbial community structure responded to the seasonal variation of climate and substrate supply and exhibited different sensitivities to temperature. It is likely that severe water stress depressed most species in the soil microbial community, but that some drought-tolerant and high temperature-sensitive species became dominant. The drought-tolerant species became dominated and thus displayed high R_h temperature sensitivity when the water stress had been mitigated. The effect of severe drought may change soil microbial community structure (Chen *et al.*, 2007) or only alter the strength of their activities without significant shifts in their community structure (Castro *et al.*, 2010). For example, Zhou *et al.* (2014) reported an increase in the fungi to bacteria ratio (F:B ratio) during drought, since fungi have hyphae, that help them to move, colonize and decompose surface litter, and a cellular wall, containing melanin and chitin that leave them unaffected by drought (Orchard & Cook, 1983; Denef *et al.*, 2001). Zhou *et al.* (2014) also found that the F:B ratio was tightly correlated with Q_{10} of R_h (r=0.617, *p*=0.014). Bradford *et al.* (2008) reported that the changes of soil microbial community composition may affect the ecosystem processes but that the mechanisms were yet to be confirmed. However, some opposite studies reported no significant changes in the F:B ratio during droughts (Castro *et al.*, 2010). More research is needed to clarify the mechanisms of the responses of soil microbial decomposers to drought.

4.4.3.2 The changes of R_s-T_s and R_h-T_s relationships in the recovery years

In 2013 and 2014, the βs were higher than those in 2011, although the Ref site and two corn sites had smaller differences compared to 2011 (Fig. 4.4). The higher differences of $β_{Rh}$ between 2014 and 2011 in Sw and Pr sites represent the shift in the soil microbial community structure. Differences of $β_{Ra}$, which is the combinations of $β_{Rs}$ and $β_{Rh}$, exhibit the well-

established root systems in perennials. The trajectories of LR_{20} in R_h and R_a were different. Most LR_{20} of R_a in 2014 had rebounded to the levels of LR20 in 2011, as some LR_{20} (such as Prairie LR_{20}) were even higher (Fig. 4.4). The well-established root system stimulated not only β but also LR_{20} in perennial cropping systems. LR_{20} of R_h in all sites in 2014 were still far less than those in 2011. The soil microbial community may be dominated by drought-tolerant, high temperature-sensitive species that result in lower decomposition rates. However, we need more studies of the soil microbial community structure and its response to changes in precipitation patterns, and how those responses affect biogeochemical cycles.

4.4.3.3 The systematic responses of the R-T relationship to the severe drought

After a two-year recovery, I observed that the spring-summer severe drought depressed both R_a and R_h in the drought year and recovered in the following years. However, different CROP and LUH had different levels of resistance and speed to recovery, implying perennial crops acclimated severe drought while annual crops did not. The high resistance of the Ref field to severe drought revealed that the climax community of perennial crops may have a well-established root-soil microbial cooperation system, which resists the severe drought well. In addition, the opposite response of R_a- and R_h-T_s relationships to drought implies there were shifts in soil microbial activities in response to the changes in soil temperature. The different location of the clouds on the β_{Rh}–LR_{20} biplots between 2011 and 2012-2014 revealed that the structure of soil microbial community might change and may shift into a new state.

4.5 CONCLUSIONS

The increasing frequencies, intensity and amplitude of climate extremes, such as heat wave, periods of heavy rains and severe drought, is already apparent and is expected in the future (IPCC, 2013; Andresen *et al.*, 2013; Schar *et al.*, 2004). Many studies explored the impacts of increasing ECEs on individual/population mortality and fitness, community structure, ecological processes and ecosystem functions (Thibault and Brown, 2008; MacGillivray *et al.*, 1995; Haddad *et al.*, 2002; Ciais *et al.*, 2005). The responses of ecosystems to these ECEs and their sensitivities varied widely due to different underlying mechanisms and thresholds in different ecosystems and climate regimes (Smith, 2011). However, the societal and ecological impacts of these increasing climatic extremes still need more research to clarify the underlying mechanisms and the consequences (Smith, 2011; Ciais *et al.*, 2005).

Considering both the immediate resistance and prolonged recovery after a severe drought underneath different crop types and land use histories helps us better understand the different responses of roots and soil microbes to severe drought, and ultimately how drought affects the behaviors of R_a and R_h. Perennial crops have the potential to acclimate to severe drought via its dense root system (and the associated microbial community) and shift in plant composition. The different plant composition at different successional stages may have different resistance and recovery abilities in response to severe drought. The annual crops have a weaker ability to buffer the impact of severe drought on soil respiration and are more vulnerable to severe drought, since they do not have a root system like the perennials. The shifts of LR_{20} and β of R_a after the severe drought, thus, were larger, especially under high soil nutrient content.

Perennial crops have a stronger ability than annual crops to buffer the perturbation of occasional severe drought. The ability of buffering increased through the succesional stages

137

when its dense root system developed. The perennial crop system, can not only reduce the input of fertilizer and reduce soil erosion and nutrient leaching, but can also reduce the drought-induced fluctuation of soil respiration. I will discuss the impacts of drought on NEE, GPP and R_{eco} and the difference responses of these major carbon fluxes facing severe drought in Chapter 5.

APPENDIX

Table S.4.1. The root contribution of soil respiration (RC) for each site in each year.
The RCs (R_a/R_s ratio) were calculated from the TWV model estimates in chapter 2. The data of R_a and R_s were grouped in pairs into each site in each year for the annual RC.

CROP	LUH	year			
		2011	2012	2013	2014
C	CRP	0.3195±0.0513	0.3171±0.0449	0.3065±0.0526	0.3310±0.0633
	AGR	0.4650±0.0983	0.4342±0.0611	0.4902±0.1159	0.5125±0.1282
Sw	CRP	0.4678±0.0826	0.5657±0.1712	0.4563±0.0772	0.4700±0.0974
	AGR	0.4512±0.1379	0.3452±0.2438	0.4331±0.1427	0.4399±0.1724
Pr	CRP	0.4477±0.0596	0.2893±0.1770	0.3864±0.1200	0.4057±0.0879
	AGR	0.5135±0.0339	0.5121±0.0430	0.5247±0.0475	0.5321±0.0376
Ref		0.5639±0.0363	0.5610±0.0410	0.5375±0.0559	0.5411±0.0559

LITERATURE CITED

LITERATURE CITED

Bradford, M.A., Davies, C.A., Frey, S.D., Maddox, T.R., Melillo, J.M., Mohan, J.E., Reynolds, J.F., Treseder, K.K., Wallenstein, M.D., 2008. Thermal adaptation of soil microbial respiration to elevated temperature. Ecology Letters, 11, 1316–1327.

Castro, H.F., Classen, A.T., Austin, E.E., Norby, R.J., Schadt, C.W., 2010. Soil microbial community responses to multiple experimental climate change drivers. Applied and Environmental Microbiology, 76(4), 999-1007.

Chen, M.-M., Zhu, Y.-G., Su, Y.-H., Chen, B.-D., Fu, B.-J., Marschner, P., 2007. Effects of soil moisture and plant interactions on the soil micorbial community structure. European Journal of Soil Biology, 43, 31-38.

Ciais, Ph., Reichstein, M., Viovy, N., Granier, A., Ggee, J., Allard, V., Aubinet, M., Buchmann, N., Bernhofer, Chr., Carrara, A., Chevallier, F., De Noblet, N., Friend, A.D., Friedlingstein, P., Grunwald, T., Heinesch, B., Keronen, P., Knohl, A., Krinner, G., Loustau, D., Manca, G., Matteucci, G., Miglietta, F., Ourcival, J.M., Papale, D., Pilegaard, K., Rambal, S., Seufert, G., Soussana, J.F., Sanz, M.J., Schelze, E.D., Vesala, T., Valentini, R., 2005. Europe-wide reduction in primary productivity caused by the heat and drought in 2003. Nature, 437, 529-533.

Davidson, E.A., Janssens, I.A., 2006. Temperature sensitivity of soil carbon decomposition and feedbacks to climate change. Nature, 440(9), 165-173.

Denef, K., Six, J., Paustian, K., Merchkx, R., 2001. Importance of macroaggregate dynamics in controlling soil carbon stabilization: short-term effects of physical disturbance induced by dry–wet cycles. Soil Biology & Biochemistry, 33, 2145–2153.

Gilgen, A.K., Buchmann, N., 2009. Response of temperate grasslands at different altitudes to simulated summer drought differed but scaled with annual precipitation. Biogeosciences, 6, 2525-2539.

Haddad, N.M., Tilman, D. & Knops, J.M.H., 2002. Long-term oscillations in grassland productivity induced by drought. Ecology Letters, 5, 110-120.

Harper, C.W., Blair, J.M., Fay, P.A., Knapp, A.K., Carlisle, J.D., 2005. Increased rainfall variability and reduced rainfall amount decreases soil CO_2 flux in a grassland ecosystem. Global Change Biology, 11, 322-334.

Holling, C.S., 1973. Resilience and stability of ecological systems. Annual Reviews, 4, 1-23.

Holling, C.S., 1996. Engineering resilience cersus ecological resilience. In: Schulze, P., (Eds.), Engineering within Ecological Constraints. National Academy Press, Wshington, D.C., pp. 31-44.

Hoover, D., Knapp, A.K., Smith, M.D., 2016. The immediate and prolonged effects of climate extremes on soil respiration in a mesic grassland. Journal of Geophysical Research: Biogeosciences, 121, 1034-1044.

IPCC, 2013: Climate Change 2013: The Physical Science Basis. Contribution of Working Group I to the Fifth Assessment Report of the Intergovernmental Panel on Climate Change [Stocker, T.F., D. Qin, G.-K. Plattner, M. Tignor, S.K. Allen, J. Boschung, A. Nauels, Y. Xia, V. Bex and P.M. Midgley (eds.)]. Cambridge University Press, Cambridge, United Kingdom and New York, NY, USA, 1535 pp, doi: 10.1017/CBO9781107415324.

Ise, T., Moorcroft, P.R., 2006. The global-scale temperature and moisture dependencies of osil organic carbon decomposition: an analysis using a mechanistic decomposition model. Biogeochemistry, 80, 217-231.

Jassal, R.S., Black, T.A., Novak, M.D., Gaumont-Guay, D., Nesic, C., 2008. Effect of soil water stress on soil respiration and its temperature sensitivitu in an 18-year-old temperate Douglas-fir stand. Global Change Biology, 14:1305-1318.

Johnson, J.M-F., Coleman, M.D., Gesch, R., Jaradat, A., Mitchell, R., Reicosky, D., Wilhelm, W.W., 2007. Biomass-bioenergy crops in the United States: a changing paradigm. The Americas Journal of Plant Science and Biotechnology, 1(1), 1-28.

Knapp, A.K., Beier, C., Briske, D.D., Classen, A.T., Luo, Y., Reichstein, M., Smith, M.D., Smith, S.D., Bell, J.E., Fay, P.A., Heisler, J.L., Leavitt, S.W., Sherry, R., Smith, B., Weng, E., 2008. Consequences of more extreme precipitation regimes for terrestrial ecosystems. BioScience, 58(9), 811-821.

Knorr, W., Gobron, N., Scholze, M., Kaminski, T., Schnur, R., Pinty, B., 2007. Impact of terrestrial biosphere carbon exchanges on the anomalous CO2 increase in 2002–2003. Geophysical Research Letters, 34, L09703.

Lark, T.J., Salmon, J.M., Gibbs, H.K., 2015. Cropland expansion outpaces agricultural and biofuel policies in the United States. Environmental Research Letters, 10, 044003.

Lemus, Q., Lal, R., 2005. Bioenergy crops and carbon sequestration. Critical Reviews in Plants Sciences, 24, 1-21.

Lipson, D.A., Schadt, C.W., Schmidt, S.K., 2012. Changes in soil microbial community and function in an Alpine dry meadow following spring snow melt. Microbial Ecology, 43: 307-314.

Lloyd, J., Taylor, J.A., 1994. On the temperature dependence of soil respiration. Functional Ecology, 8, 315-323.

MacGillivray, C.W., Grime, J.P. & The Integrated Screening Programme (ISP) Team, 1995. Testing predictions of the resistance and resilience of vegetation subjected to extreme events. Functional Ecology, 9, 640-649.

Manzoni, S., Schimel, J.P., Porporato, A., 2012. Responses of soil microbial communities to water stress: results from a meta-analysis. Ecology, 93, 930-938.

McCarthy, M.A., 2013. Bayesian methods for ecology. Cambridge University Press.

Orchard, V.A., Cook, F.J., 1983. Relationship between soil respiration and soil moisture. Soil Biology and Biochemistry, 15, 447-453.

R Development Core Team, 2010. R: A language and environment for statistical computing. R Foundation for Statistical Computing, Vienna, Austria.

Reichstein, M., Bahn, M., Ciais, P., Grank, D., Mahecha, M.D., Seneviratne, S.I., Zscheischler, J., Beer, C., Buchmann, N., Frank, D.C., Papale, D., Rammig, A., Smith, P., Thonicke, K., van der Velde, M., Vicca, S., Walz, A., Wattenbach, M., 2013. Climate extremes and the carbon cycle. Nature, 500, 287-296.

Rey, A., Pagoraro, E., Tedeschi, V., De parri I., 2002. Annual variation in soil respiration and its components in a coppice oak forest in central Italy. Global Change Biology, 8: 851-866.

Sampson, D.A., Janassens, I.A., Curil Yuste, J., Ceulemans, R., 2007, Basal rates of soil respiration are correlated with photosymthesis in a mixed temperate forest. Global Change Biology, 13, 2008-2017.

Savage, K.E., Davidson, E.A., 2001. Interannual variation of soil respiration in two New English forests. Global Biogeochemical Cycles, 15(2), 337-350.

Schar, C., Vidale, P.L., Luthi, D., Frei, C., Haberli, C., Liniger, M.A. & Appenzeller, C., 2004. The role of increasing temperature variability in European summer heatwaves. Nature, 427, 332–336.

Sheik, C.S., Beasley, W.H., Elshahed, M.S., Zhou, X., Luo, Y., Krumholz, L.R., 2011. Effect of warming and drought on grasslad microbial communities. The International Society for Microbial Ecology Journal, 5,1692-1700.

Shimel, D.S., Braswell, B.H., Holland, E.A., McKeown, R., Ojima, D.S., Parton, W.J., Townsend, A.R., 1994. Climatic, edaphic, and biotic controls over storage and turnover of carbon in soils. Global Biogeochemical Cycles, 8(3), 279-293.

Smith, M.D., 2011. An ecological perspective on extreme climatic events: a synthetic definition and framework to guide future research. Journal of Ecology, 99, 656-663.

Suseela, V., Conant, R.T., Wallenstein, M.D., Dukes, J.S., 2012. Effects of soil moisture on the temperature sensitivity of heterotrophic respiration vary seasonally in an old-field climate change experiment. Global Change Biology, 18, 336-348.

Thibault, K.M., Brown, J.H., 2008. Impact of an extreme climatic event on community assembly. Proceedings of the National Academy of Science USA, 105, 3410-3415.

van't Hoff, J. H., 1884. *Études de dynamique chimique* (Studies of chemical dynamics). Frederik Muller and Co., Amsterdam, the Netherlands.

Wang, Y., Hao, Y., Cui, X.Y., Zhao, H., Xu, C., Zhou, X., Xu, Z., 2014. Responses of soil respiration and its components to drought stress. Journal of Soils Sediments, 14, 99-109.

Zavalloni, C., Gielen, B., Lemmens, C.M.H.M., De Boeck, H.J., Blasi, S., Van den Bergh, S., Nijs, I., Ceulemans, R., 2008. Does a warmer climate with frequent mild water shortages protect grassland communities against a prolonged drought? Plant Soil, 308, 119-130.

Zhou, W., Hui, D., Shen, W., 2014. Effects of soil moisture on the temperautre sensitivity of soil heterotrophic respiration: A laboratory incubation study. PLoS One, 9(3), e92531.

CHAPTER 5
THE RESPONSE OF NET ECOSYSTEM EXCHANGE (NEE) OF CARBON DIOXIDE AND ITS PARTITIONING TO THE BIOPHYSICAL VARIABLES

ABSTRACT

The dynamics of carbon dioxide net ecosystem exchange (NEE), which is determined by gross primary production (GPP) and ecosystem respiration (R_{eco}), decides the direction and amount of carbon flux between ecosystems and the atmosphere. The sum of regional carbon fluxes contributes to global atmospheric CO_2 balances and decides the rate of atmospheric CO_2 increase. Managed ecosystems, including grasslands and croplands, can be managed to sequester carbon dioxide in soil carbon pools. The understanding of the seasonality of GPP and R_{eco} and how they respond to climate events and human activities is critical to mitigate global climate change.

Major carbon processes, GPP and R_{eco}, have different dominant drivers and these drivers have different seasonal patterns. The asynchronous seasonality of GPP and R_{eco} determine the carbon fluxes between the ecosystem and the atmosphere; however, crop type and soil nutrient content also play important roles. My results revealed that the different phenology of annual and perennial crops can affect carbon sequestration capacity according to the differences in the length of the growing season. Moreover, the different phenology between annual and perennial crops may affect crop tolerance to different seasonal patterns of climate events. The early onset of the growing season in perennial crop ecosystems heightens the risk of severe the spring and summer drought. In contrast, the delay of a regular summer water deficit may dramatically increase carbon sequestration ability. Changing land use from undisturbed conservation lands to corn may release a huge amount of carbon via ecosystem respiration, while the perennial crops would be better able to maintain the carbon.

146

5.1 INTRODUCTION

Regional net ecosystem exchange (NEE) of carbon dioxide, defined by the difference between gross primary production (GPP) and ecosystem respiration (R_{eco}), determines global carbon cycling. However, the rules of biotic and abiotic reactions on NEE have complicated and uncertain interactions and feedbacks across different climate regions and different biomes. The understanding of how biophysical variables and their interactions influence GPP and R_{eco} is crucial to estimating the contribution that biofuel cropping ecosystems have on future climate GHG mitigation in different climate scenarios.

Eddy-covariance and chamber-based approaches have been widely used in the monitoring ecosystem CO_2 exchange across different regions with different climate regimes and ecosystems. However, compared to the large number of NEE studies on forests, croplands have received far less attention even though they may have important contributions to regional carbon budgets, especially in mid-latitude areas (Soegaard *et al.*, 2003). This kind of managed ecosystem has large variation on its functions, such as carbon sequestration, since agricultural practices (i.e., fertilization, plantation, harvest, irrigation and tillage) determine important ecosystem structure and biogeochemical processes, such as soil nitrogen content, the type of crops, the land cover and the water management, which in turn determine the carbon, nitrogen, water and energy cycles of croplands (Schimel *et al.*, 2000). Research on managed grasslands and croplands can contribute to how we understand the responses of carbon fluxes and how to determine when an ecosystem converts between a carbon source and sink.

NEE of CO_2 in an ecosystem depends on the interplay of gross primary production (GPP) and ecosystem respiration (R_{eco}). The GPP, determined by photosynthetic rate, is mainly controlled by photosynthetically active radiation (PAR) when temperature and water are

147

adequate. Light intensity and patterns determine GPP and alter daytime NEE in most ecosystems. Ecosystem respiration rates are exponentially correlated to temperature and regulate nighttime NEE. Temporal variations in two physical variables, PAR and temperature, alter the variation of GPP and R_{eco} and the NEE (Falge *et al.*, 2002; Gilmanov *et al.*, 2007; Zhang *et al.*, 2015; Chen *et al.*, 2015). Asynchrony of light and temperature seasonal variations, combined with the plant's phenology and the activity fluctuation of soil microbial activity, determine the annual NEE of grasslands and croplands.

In this chapter, I will focus on how the seasonal variations of GPP and R_{eco} affect the annual NEE and the seasonality of NEE across different crop types and land use histories, especially after the impact of severe drought. I hypothesized that annual and perennial crops have different seasonal patterns and different annual NEE due to their different phenology and the length of growing season. I also expected that annual and perennial crops have different magnitudes of NEE increases in the growing season's drought period and different recovery speeds after severe drought, due to different water use efficiencies and drought-adaptation ability. I will also discuss the R_s:R_{eco} ratio in different crop types after land use change. I assumed that the R_s:R_{eco} ratio in perennial croplands would increase from 2011 to 2014 due to root systems development. The R_s:R_{eco} ratio in Ref and corn fields will not change significantly since Ref fields have had a well-established root system and corn does not have a perennial root system.

5.2 METHODS

5.2.1 Study site

My experimental sites are located in the Great Lakes Bioenergy Research Center scale-up fields of the Kellogg Biological Station (KBS, 42°40'N, 85°40'W), and are established in association with KBS Long-Term Ecological Research (LTER). The sites are located in south Michigan, USA (Fig. 1.5). The climate is humid continental (warm summer) climate (Dfa) (Peel *et al.*, 2007). The mean annual air temperature and mean annual precipitation at KBS are 10.1 °C and 1005 mm yr^{-1} (1981-2010), respectively (Robertson & Hamilton, 2015).

5.2.2 Experimental design and schedule

Seven experimental plots were located at two locations with their own land use histories (LUHs): (1) Conservation Reserve Program (CRP) grasslands at Marshall Farm, and (2) corn-soybean rotation agricultural fields (AGR) at Lux Arbor Reserve. The CRP sites had been in a monoculture of smooth brome grass (*Bromus inermis* Leyss) since 1987, while the AGR fields had been under conventional corn-soybean rotation cultivation for several decades (Fig. 1.6). The soil texture at all sites is sandy loam, except for a sandy clay loam at one field. However, soil carbon and nitrogen contents at the CRP sites were significantly higher than those at the AGR sites before the land conversions (Table 1.1).

The experiment was conducted at seven scale-up fields ranging in size from 9 to 17 hectares. Four fields are located in Marshall Farm (i.e., CRP sites) and three in Lux Arbor Reserve (i.e., AGR sites). All sites, except the reference site (Ref), were sprayed with herbicide at the end of 2008 to prepare the lands for soybean planting in 2009. The CRP and AGR sites were then cultivated with either continuous corn (*Zea mays*, Dekalb DK-52), switchgrass

(*Panicum virgatum*), or a mixture of native prairie grasses that was dominated by Canada wild rye (*Elymus Canadensis*), little bluestem (*Schizachyrium scoparium*), Indian grass (*Sorghastrum nutans*), big bluestem (*Andropogon gerardii*), and switchgrass (*Panicum virgatum*) since 2010. One CRP grassland, dominated by brome grass, was not disturbed and retained as the historical reference site (Gelfand *et al.*, 2011; Zenone *et al.*, 2011; Deal *et al.*, 2013; Zenone *et al.*, 2013). I used an experimental code for these sites by abbreviating them as "LUH-CROP". CRP-C, CRP-Sw and CRP-Pr represent the CRP sites that were converted to corn, switchgrass and prairie mixture respectively, while AGR-C, AGR-Sw and AGR-Pr are AGR farms converted to corn, switchgrass and prairie mixture. In 2010, when the crops were established, the perennial crops (switchgrass and prairie) were accompanied by oats as nurse crop with and without fertilization, respectively (Fig. 1.6). Switchgrass fields were applied 55 kg N ha^{-1} (28% liquid urea ammonium nitrate) on DOY 172. No other management practices were applied beyond harvesting at the end of each growing season. No-till continuous corn was seeded in mid-May with a one-time herbicide mix (Lumax, Atrazine 4L, Honcho Plus and $(NH_4)_2SO_4$). Phosphorus, potassium ($P_2O_5 + K_2O$, 168.5 kg ha^{-1} on DOY 95, 2010) and nitrogen fertilizers (112 kg N ha^{-1} on DOY 165 & 160 in AGR-C and CRP-C, respectively) were applied in 2010. Phosphorus, potassium ($P_2O_5 + K_2O$, 294 kg ha^{-1} on DOY 104, 2011) and nitrogen fertilizers (liquid nitrogen168 kg N ha^{-1} on DOY 172, 2011) were applied (Zenone *et al.*, 2013).

5.2.3 The calculations of NEE, GPP and R_{eco} by eddy-covariance approach

5.2.3.1 The measurements of eddy-covariance and microclimatic data

      One open-path eddy-covariance (EC) system was established in each site (Figs. 1.5 & 5.1) at the end of 2008 before land use change (2009) to measure the carbon, water and energy

fluxes. Carbon dioxide, water vapor concentration and three-dimensional wind speed were recorded for the calculation of net ecosystem CO_2 exchange and water vapor between the ecosystems and the atmosphere. The CO_2 and water vapor concentrations were measured by a LI-7500 open-path infrared gas absorption analyzer (IRGA, LI-COR Biosciences, Lincoln, NE). The three-dimensional wind speed was measured by a CSAT3 anemometer (Campbell Scientific Inc. (CSI), Logan, UT). Inbound (top-down) and the outbound (bottom-up) short- and long-wave radiation were measured by a CNR1 radiometer (Kipp & Zonen, Delft, The Netherlands), while the photosynthetically active radiation (PAR) was measured by a LI-190SB (LI-COR Biosciences). Air temperature (T_a) and relative humidity (RH) were recorded by a HMP45C (CSI). Most of the above instruments were mounted at about 1.5 m above the canopy surface. Soil temperature (T_s at 2, 5, and 10 cm depths belowground) and soil water content (0-30 cm depth VWC) were measured by CS107 temperature probes (CSI) and a CS616 Time Domain Reflectometer (TDR) probe (CSI), respectively. Three HFT3 flux plates (CSI) were placed randomly 2 cm below the soil surface to measure soil heat flux. A Campbell CR5000 datalogger (CSI) was used to collect the eddy-covariance (10 Hz) and microclimatic (30 min) data (Fig. 5.1).

Figure 5.1. Eddy-covariance tower with instruments for carbon, water and energy cycle monitoring. The eddy-covariance (EC) tower was established in late 2008 to measure high frequency CO_2 and water vapor concentration and 3D wind velocity (u). It also records incoming and reflecting long- and short-wave radiation, photosynthetically active radiation (PAR), air temperature (T_a), relative humidity (RH), soil temperature (T_s), soil water moisture (VWC) and soil heat storage. Most aboveground instruments were mounted 1.5 m above the canopy surface.

5.2.3.2 Data processing and gap-filling

The eddy-covariance data were processed by the EdiRe software (University of Edinburgh, UK). Out-of-range data (i.e., spikes greater than four standard deviations), which may have been generated by bad weather or instrument failure, as well as time lags between CO_2 and water vapor concentrations and the vertical wind speed were removed (McMillen, 1988). The CO_2 and H_2O fluxes were adjusted for frequency response and air density fluctuations (Webb *et al.*, 1980), including the warming of the IRGA (Burba *et al.*, 2008). Coordinate rotation was applied to the wind components using planar fit rotation (Wilezak *et al.*, 2001). The high frequency data were processed in 30-minute blocks averages without detrending (Moncrieff

et al., 2004). The missing or poor quality data were replaced based on the standardized

FLUXNET gap-filling approach (Reichstein *et al.*, 2005, http://www.bgc-

jena.mpg.de/~MDIwork/eddyproc/). More details of the data processing can be found in Abraha

et al. (2015).

5.2.3.3 Estimation of NEE, GPP and R_{eco}

The net ecosystem exchange (NEE) of CO_2, defined by the net CO_2 exchange between an

ecosystem and the atmosphere, is the difference between gross primary production (GPP) and

ecosystem respiration (R_{eco}) (Eq. 5-1; Chapin *et al.*, 2006):

$$NEE = R_{eco} - GPP \hspace{4cm} \text{Eq. 5-1}$$

where GPP and R_{eco} are the absolute amounts of carbon captured and lost from the ecosystem to

the atmosphere. The values of nighttime NEE were recognized as R_{eco} since there is no

photosynthesis at night. An exponential model based on the correlation between R_{eco} and air

temperature was developed, and daytime R_{eco} was adjusted by the $R_{eco} - T_a$ model. The GPP then

calculated the difference between daytime NEE and the adjusted daytime R_{eco} (R_{eco} ').

$$GPP = R_{eco}' - NEE \hspace{4cm} \text{Eq. 5-2}$$

Thirty-minute GPP, R_{eco} and NEE were recorded and the daily GPP, R_{eco} and NEE were

calculated for later analysis.

5.2.4 Estimation of R_s', R_a' and R_h'

5.2.4.1 The TWV model and its variables

The adjusted 30-minute R_s (R_s') were estimated by the TWV model developed in Chapter

2 (Eq. 2-2 & Supplement 2-4). The 30-minute soil temperature (T_s) data were measured at each

plot (four plots in each site) by a HOBO datalogger (Onset Computer Co., Bourne, MA) with

two thermal couples. Thirty-minute soil water content (VWC) data were recorded at 0-30 cm

depth by a TDR at each site's eddy-covariance tower. Enhanced Vegetation Index (EVI) data

from the MODIS satellite were downloaded from the Oak Ridge National Laboratory Distributed

Active Archive Center for Biogeochemical Dynamics (ORNL DAAC,

http://daac.ornl.gov/MODIS/modis.shtml; details can be found in the methods section of Chapter

2).

5.2.4.2 Data processing and gap filling

Out-of-range data of T_s, which was mainly generated by failed thermocouples, HOBO

dataloggers or power outages, includes extremely high or low values, abnormal jumpy data (>5°C

changes between two measurements) and high magnitudes of fluctuation. The out-of-range data

were recognized and removed manually. The whole data set in a measured period (weeks to

months) may be removed if most of data of that sensor was abnormal. The gap-filling of data

followed different methods depending on its length. The short-term (hours) gaps were replaced

based on the normal data before and after the gap with the following equation:

$$T_{s_i} = T_{s_{i-1}} + \frac{T_{s_{n+1}} - T_{s_0}}{n+1}$$ Eq. 5-3

where T_{s_i} was the ith cell of the gap and n was the number of the gap cells. The T_{s_0} was the last

normal datum before the gap, while $T_{s_{n+1}}$ was the first normal datum after the gap. The i were

calculated from 1 to n.

The long-term (days) gaps were filled based on the fluctuation trend at the nearest sensor,

either within the same site or between sites. The calculation followed the equation 5-3:

$$T_{s_{a_i}} = T_{s_{a_{i-1}}} + (T_{s_{b_i}} - T_{s_{b_{i-1}}})$$ Eq. 5-4

where $T_{s_{a_i}}$ was the ith cell of the gap and $T_{s_{a_{i-1}}}$ was the $(i\text{-}1)^{th}$ cell in the thermal couple *"a"*, which contained the data gap. The $T_{s_{b_i}}$ and $T_{s_{b_{i-1}}}$ were the ith cell and the $(i\text{-}1)^{th}$ cell that synchronized to $T_{s_{a_i}}$ and $T_{s_{a_{i-1}}}$, respectively, in the nearest thermal couple *"b"*. Equation 5-4 can mimic the diurnal temperature fluctuations at local scale.

The post-processing of VWC was similar to T_s. The missing data due to the failure of the CR5000 datalogger were filled depending on the length of gaps. The VWC data were filled based on Eq. 5-3 and Eq. 5-4.

The quality of EVI data was good, although there were some one-cell gaps due to continuous 16-day cloudy periods. The gaps were filled by the average of the EVI values immediately before and after the gap.

The 30-minute R_s' values were estimated based on the TWV model and the 30-minute T_s, VWC and EVI data. The daily average R_s' were calculated for later statistical analysis and chart drawing.

5.2.4.3 The components of ecosystem respiration and their calculation

Ecosystem respiration can be partitioned into aboveground (R_{above}) and belowground (soil respiration; R_s):

$$R_{eco} = R_{above} + R_s \qquad\qquad \text{Eq. 5-5}$$

The aboveground and belowground contributions to the ecosystem respiration depend on the carbon allocation of plants, the phenology and its different responses and time lags to changes in environmental conditions.

The 30-minute R_s' data were thereafter combined with NEE, GPP and R_{eco} data. The aboveground respiration (R_{above}) was calculated by the difference of R_{eco} and R_s.

$$R_{above} = R_{eco} - R_s'$$ Eq. 5-6

The chronological variations of daily mean NEE, GPP, R_{eco}, R_{above} and R_s were plotted to observed inter- and intra-annual fluctuations, response to climate patterns and their resistance and recovery after a severe drought. There are still some long-term missing data of R_s' since the late start of the first year (21 May 2011) and early stop of the second year summer (20 August 2012) measurements of T_s. The mid-growing season (21 May to 20 August) data were selected to calculate the R_{eco}:GPP ratio, R_s':GPP and R_s':R_{eco} ratio since only this period had data with all components of the carbon cycle in all years. The ratios across years were compared by one-way ANOVA and the Tukey's HSD test.

5.3 RESULTS

5.3.1 The seasonal variations of NEE, GPP, R_{eco} and R_s'

The variations of the components of carbon cycle, including NEE, GPP, R_{eco}, R_{above} and R_s', were presented in Fig. 5.2. The seasonality of NEE, which is the difference between GPP and R_{eco}, was affected by GPP, R_{eco} and the interplay between the two. They always showed hump-shaped curves that increased in spring with the growth of plants and decreased with the senescence or harvest of the plants. However, annual and perennial crops had different lengths of photosynthetic active periods and influenced the seasonal patterns of NEE.

The NEE in corn fields started to decrease in mid-June, around two weeks after the corn was planted. Theoretically, the decreases of NEE were determined by the variations of R_{eco} and GPP. The onset of the R_{eco} active period was in April depending on the temperature. The date of GPP increase started after the emergence of corn in late May to early June. The values of NEE were positive (carbon source) before mid-June when R_{eco} > GPP. The NEE then became negative

and decreased sharply due to the dramatic increase of GPP in late June, whereas the increase of R_{eco} was less over the same period. The NEE attained its minimum (negative value, carbon sink) in mid-July before the soil water deficit became a limiting factor (Figs. 5.2 (A) & (B); Fig. 3.1 (B)) in 2011, 2013 and 2014. The decrease of the NEE values was slower in 2012 due to the poor growth of corn in July (low NDVI & EVI, Fig. 3.1 (C)). Regardless of year, a remarkable decrease in the absolute NEE value and low VWC occurred in phase, although it occurred at different times in different years. The regular concaves of absolute NEE values were due to the decreases of both GPP and R_{eco} due to water deficit. For example, the concave happened in late June in 2011, 2012 and 2013 and in mid-August in 2014 (Figs. 5.2 & 3.1 (B)). The water deficit-derived low values of NEE, GPP and R_{eco} in the middle of the growing season (GS) separated the hump-shaped seasonal curves into two periods: early GS and late GS. The seasonality of R_s' highly coincided with GPP and R_{eco} but generally had smaller amplitude.

Corn usually had smaller minimum NEE with large maximum GPP comparing to other crops (Table 5.1), especially the CRP-C field. The minimum GPP in CRP-C was 91.86 g CO_2 m^{-2} d^{-1} occurring in 2014. It had a shorter growing season (Fig. 5.2) with higher peaks of GPP in the late GS.

Like the seasonality of R_s described in Chapter 3, perennial and annual crops had different onset dates of active NEE, GPP and R_{eco}. In perennial croplands, the onsets of GPP and R_{eco} active periods, depending on the date of spring warming, were in phase but different amount of increase. The date when the ecosystem converted from a carbon source (positive NEE) to a sink (negative NEE) were several weeks after the onsets of GPP and R_{eco} active periods, ranging from late March (2012) to late May (2014) when the amount of GPP was higher than R_{eco}. Perennial crops and annual crops have different seasonal patterns of NEE due to their different

157

phenology and length of growing season. In spring (April – May), perennial crop's NEE is small while GPP is higher than R_{eco} (Figs. 5.2 (C)-(G)). The NEE in corn fields was high since we planted corn in late May, thus April-May NEE was high (Figs. 5.2 (A)-(B)). The June-July NEE in corn fields was lower than that in perennial croplands, since there was a rapid corn growth after it emerged. The high GPP in corn ecosystems maintained itself until the late summer water deficit, which occurred in late July in 2011-2013 and mid-August in 2014. In sum, perennial crops have lower NEE early on (April-July) with a longer GS overall, while annual crops have lower NEE mid-GS (June-July).

Table 5.1. The minimum NEE, maximum GPP and maximum R_{eco} among sites across years. The unit is g CO_2 m^{-2}d^{-1}. Negative NEE means carbon flow from the atmosphere to the ecosystem (the ecosystem was carbon sink).

CROP	LUH	2011			2012		
		Min NEE	Max GPP	Max R_{eco}	Min NEE	Max GPP	Max R_{eco}
C	CRP	-44.89	83.28	58.2	-29.55	59.92	39.28
	AGR	-38.01	67.23	32.81	-24.16	54.14	33.25
Sw	CRP	-22.24	47.57	33.8	-22.87	48.48	34.44
	AGR	-25.16	48.06	37.18	-25.33	54.73	35.13
Pr	CRP	-19.92	48.27	31.27	-19.56	45.28	33.8
	AGR	-12.59	38.53	27.77	-41.09	70.03	40.87
Ref	CRP	-32.86	61.2	56.08	-25.5	57.45	40.93
CROP	LUH	2013			2014		
		Min NEE	Max GPP	Max R_{eco}	Min NEE	Max GPP	Max R_{eco}
C	CRP	-46.6	83.42	56.24	-57.21	91.86	46.48
	AGR	-45.82	83.06	51.61	-62.49	75.87	32.82
Sw	CRP	-37.45	73.75	37.06	-46.81	77.62	40.08
	AGR	-42.72	69.05	42.15	-35.25	62.36	33.93
Pr	CRP	-24.38	53.78	38.97	-34.97	65.96	37.07
	AGR	-41.09	70.03	40.87	-43.65	69.55	33
Ref	CRP	-30.21	59.22	41.55	-23.79	45.24	37.42
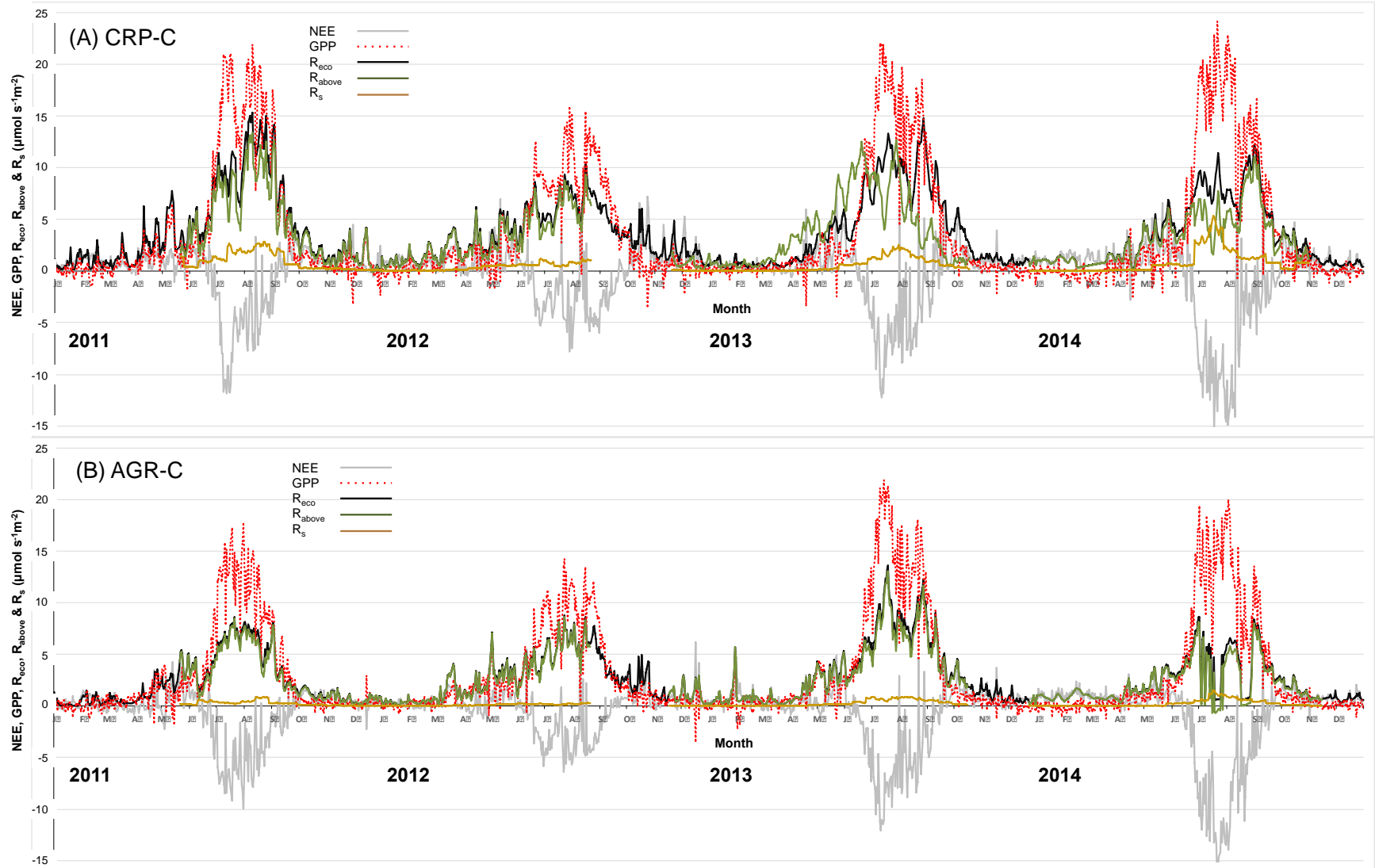
Figure 5.2. The seasonal and interannual variations of daily NEE, GPP, R_{eco}, R_{above} and R_s among sites during 2011-2014. Grey lines indicate net ecosystem exchange (NEE) of CO_2. The negative NEE means a carbon sinks. Red dotted lines show gross primary production (GPP) while black solid lines display ecosystem respiration (R_{eco}). Green and brown lines present the aboveground (R_{above}) and belowground (R_s) respiration. (A) CRP-C; (B) AGR-C; (C) CRP-Sw; (D) AGR-Sw; (E) CRP-Pr; (F) AGR-Pr; and (G) Ref.
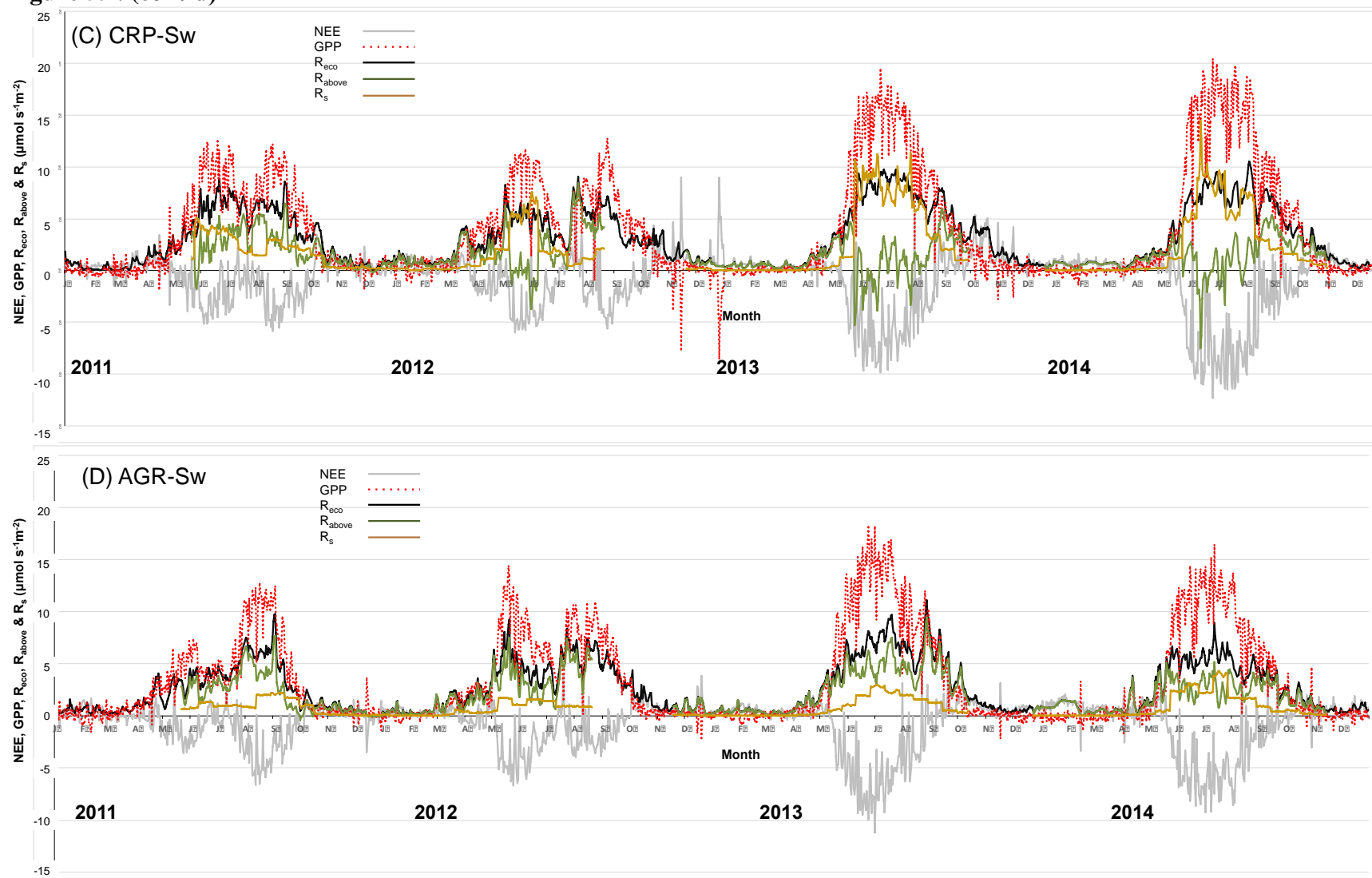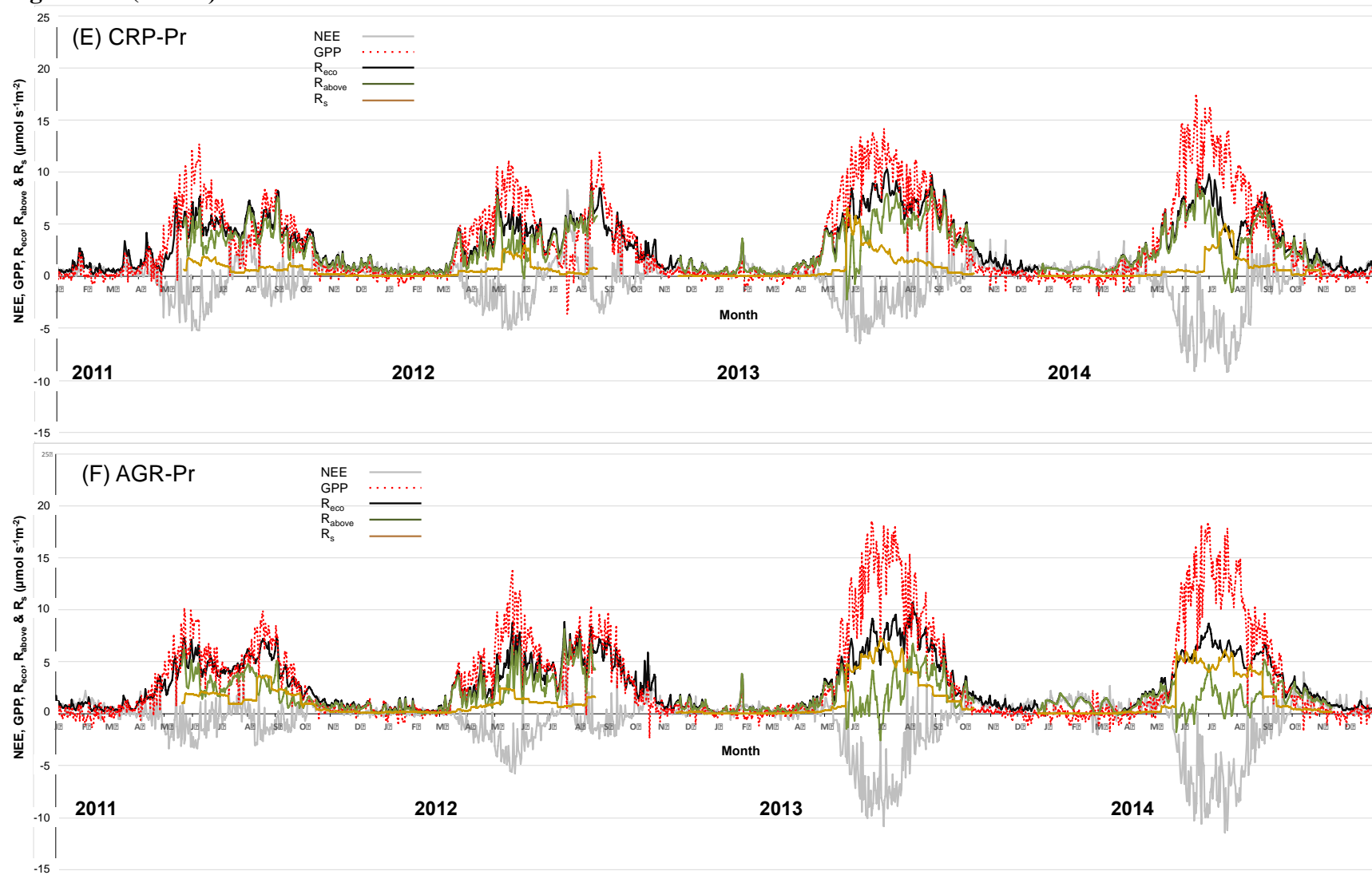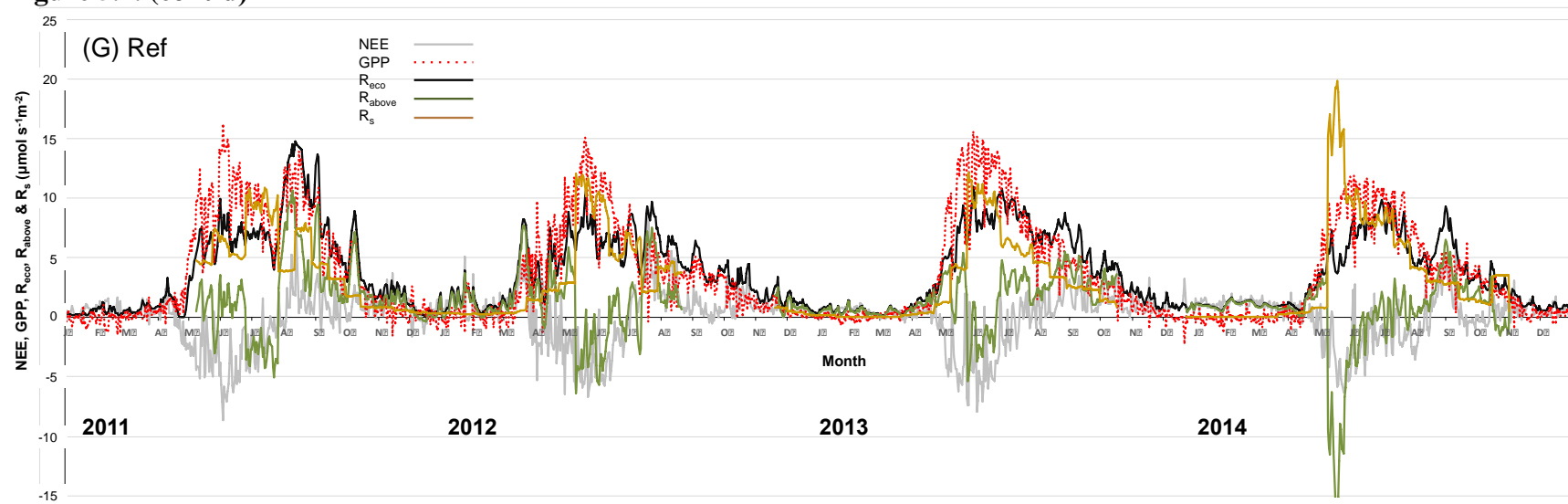
Figure 5.2. (cont'd)

Figure 5.2. (cont'd)

Figure 5.2. (cont'd)

5.3.2 The mid-growing season NEE, GPP, R_{eco}, R_{above} and R_s among CROP and LUH

Generally, perennial croplands had lower NEE (higher carbon sequestration rates) due to higher GPP with lower R_{eco} (Figs. 5.3 (A)-(C)). The NEE increased in the order Sw ~ Pr < C < Ref except during the drought year (2012) when GPP and R_{eco} both showed no differences between annual and perennial crops. Compared NEE across years, the Ref site had low NEE since it had a high GPP in 2011. The value of NEE, on the contrary, became the highest among all sites 2012 – 2014 due to its low GPP. In the experimental perennial crops (Sw and Pr), the CRP-Pr had highest NEE and the lowest GPP out of any other perennial crops in 2012 and 2013. Its R_{eco} did not show any significant difference from other perennial crops. The CRP-Sw had a higher GPP and R_{eco} among perennial crops in non-drought years. Corn always had higher temporal variations of NEE, GPP and R_{eco} than any other crops in my analytical period (21 May – 20 August).

5.3.3 The mid-growing season R_{eco}:GPP, R_s:GPP and R_s:R_{eco} ratios among CROP and LUH

There is no significant difference in the R_{eco}:GPP ratio among sites due to high temporal variation in the mid-GS. The within site variation was larger than the between-site variation (Fig. 5.3 (A)). The within-site temporal variation of R_{eco}:GPP ratios can be very large or very small when GPP becomes small or large, but R_{eco} has different responses or time lags.

Unlike R_{eco}:GPP ratio, R_s:R_{eco} and R_s:GPP ratios have very different values between the undisturbed Ref site and other sites. Ref always had high values of R_s:R_{eco} and R_s:GPP ratios, following CRP-Sw , AGR-Pr and others in order (Figs. 5.4 (B) & (C); Table 5.2). Annual crops always had lowest R_s:R_{eco} and R_s:GPP ratios among all crops regardless of year.
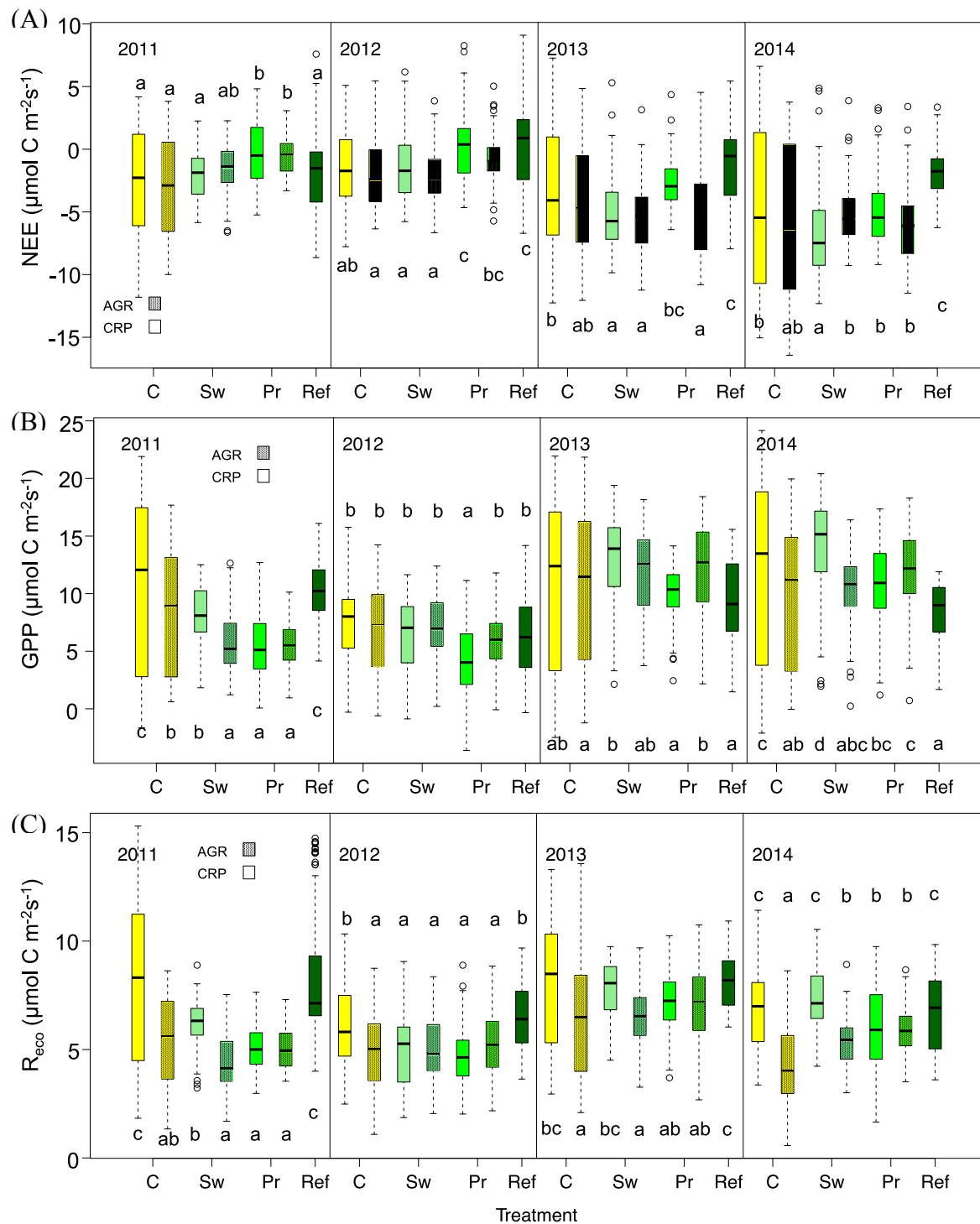
Figure 5.3. The mid-growing season (21 May-20 August) average NEE, GPP, R$_{eco}$, R$_{above}$ and R$_s$ for each of the four years. The boxplots show the quartiles, median values and outliers. The letters indicate the results of Tukey's HSD test for different sites. The letters display the means from small to large alphabetically. Different colors show different CROP (yellow: C; light green: Sw; bright green: Pr; forest green: Ref) while the dashed and transparent column shows different LUH (non-textured: CRP; dotted: AGR). The mid-growing season is identified as 21 May – 20 August due to the limitation of available data.

Figure 5.3. (cont'd)

(D)
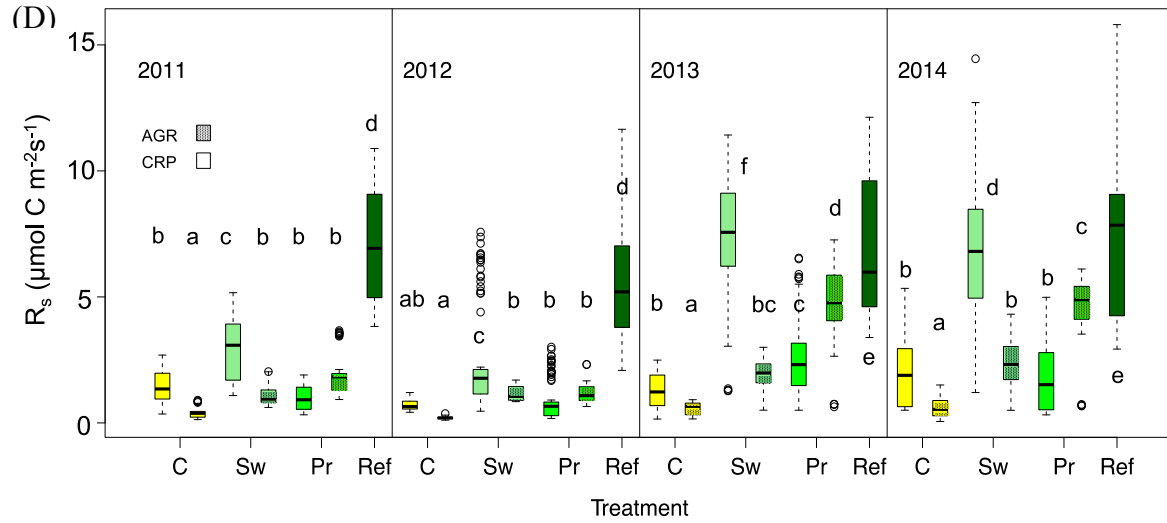
5.3.4 The shift of mid-growing season R_{eco}:GPP and R_s:R_{eco} ratios across years

Most sites did not have substantial changes in the R_{eco}:GPP ratio across years because the within-GS temporal variations of the R_{eco}:GPP ratio were larger than between-GS variations. Only two sites had statistically significant shifts during the experimental period. The CRP-Sw showed a decrease 2012–2013 while CRP-Pr decreased 2011–2014. The decreases in the R_{eco}:GPP ratio to less than one means the system converted from a carbon source to a carbon sink mid-GS. The R_{eco}:GPP ratio in the Ref site in 2012 exceeded one, which means it was a carbon source in the drought year (Fig. 5.5 (A)).
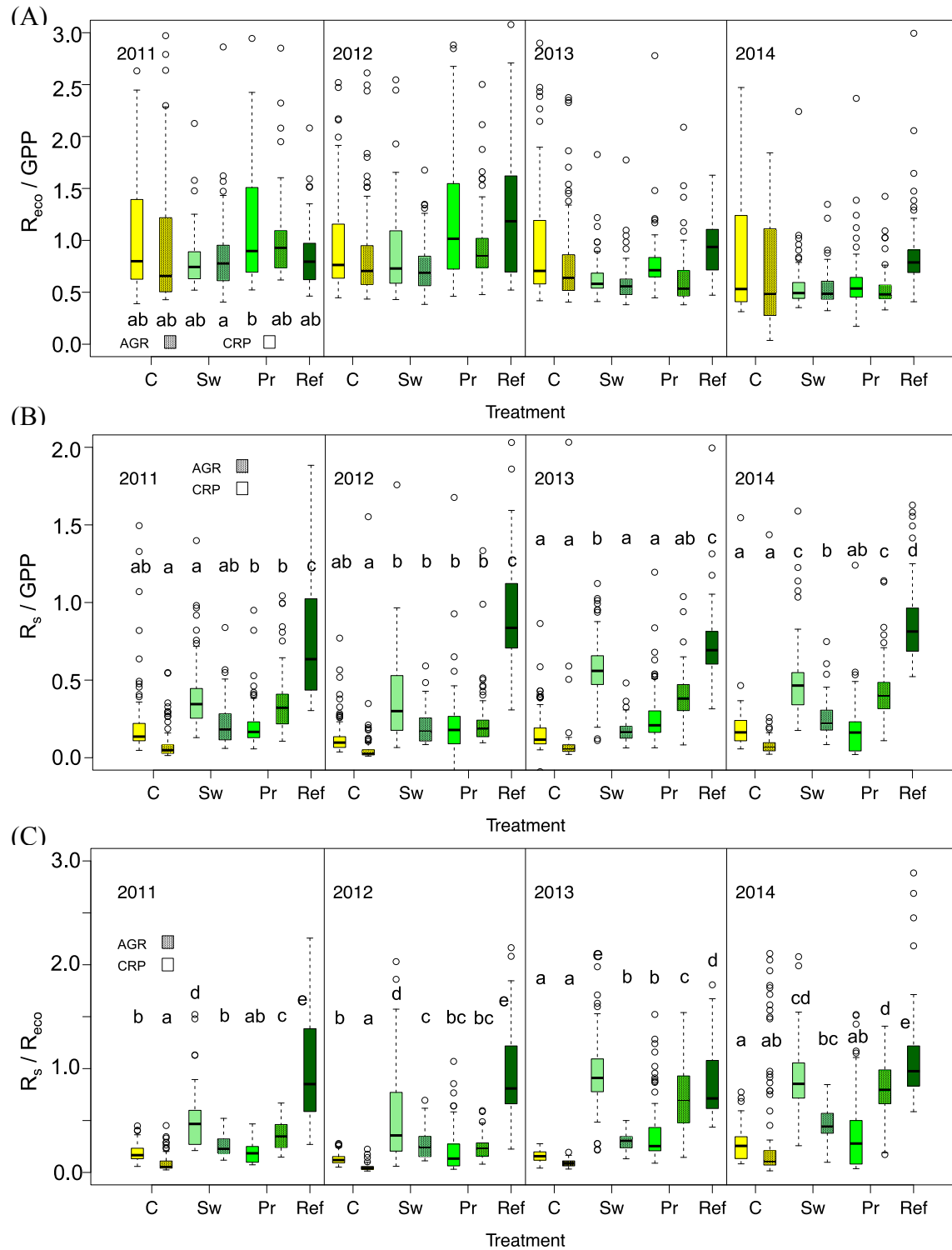
Figure 5.4. The R$_{eco}$:GPP, R$_s$:GPP and R$_s$:R$_{eco}$ ratios among CROP and LUH over four years. The boxplots show the quartiles, middle values and outliers. The letters indicate the results of Tukey's HSD test for different sites. The letters display the means from small to large alphabetically. Different colors show different CROP while different: yellow: corn; light green: Sw; bright green: Pr & dark green: Ref. Textured column show AGR LUH. The panels without letters indicate there is no significant difference among treatments ((A) 2012-2014).

Table 5.2. The R$_{eco}$:GPP, R$_s$:GPP and R$_s$:R$_{eco}$ ratios among CROP and LUH over four years. CROP: current crop type; LUH: land use history; C: corn; Sw: switchgrass; Pr: prairie; Ref: reference; CRP: Conservation Reserve Program; AGR: corn: soybean conventional rotation agriculture; R: ecosystem respiration; GPP: gross primary production; R: soil respiration. The data presents mean ± 1 S.D.

CROP	LUH	R$_{eco}$:GPP										
		2011			2012			2013			2014		
C	CRP	1.180	±	1.181	0.851	±	1.973	-3.090	±	40.181	0.797	±	2.006
	AGR	0.972	±	0.875	0.963	±	2.175	1.377	±	4.935	-0.081	±	9.657
Sw	CRP	0.801	±	0.247	0.897	±	1.089	0.668	±	0.357	0.610	±	0.467
	AGR	0.837	±	0.348	0.900	±	1.435	0.581	±	0.188	0.719	±	1.737
Pr	CRP	1.870	±	5.993	1.305	±	2.395	0.767	±	0.275	0.613	±	0.432
	AGR	1.030	±	0.498	0.605	±	4.237	0.620	±	0.259	0.587	±	0.569
Ref		0.847	±	0.282	1.142	±	3.230	0.962	±	0.468	0.851	±	0.342

CROP	LUH	R$_s$:GPP										
		2011			2012			2013			2014		
C	CRP	0.243	±	0.378	0.098	±	0.380	-0.037	±	1.933	0.140	±	0.398
	AGR	0.085	±	0.103	0.059	±	0.171	0.093	±	0.220	0.071	±	0.227
Sw	CRP	0.382	±	0.209	0.406	±	0.589	0.621	±	0.378	0.510	±	0.309
	AGR	0.213	±	0.129	0.233	±	0.423	0.170	±	0.067	0.324	±	0.721
Pr	CRP	0.321	±	1.137	0.199	±	0.240	0.265	±	0.174	0.179	±	0.174
	AGR	0.354	±	0.184	0.096	±	1.262	0.419	±	0.232	0.465	±	0.502
Ref		0.762	±	0.397	1.026	±	1.289	0.746	±	0.325	0.881	±	0.321

CROP	LUH	R$_s$:R$_{eco}$										
		2011			2012			2013			2014		
C	CRP	0.191	±	0.085	0.130	±	0.052	0.159	±	0.053	0.270	±	0.160
	AGR	0.089	±	0.080	0.049	±	0.033	0.088	±	0.033	0.350	±	0.542
Sw	CRP	0.491	±	0.249	0.524	±	0.429	0.947	±	0.429	0.894	±	0.307
	AGR	0.250	±	0.095	0.270	±	0.134	0.294	±	0.080	0.470	±	0.152
Pr	CRP	0.198	±	0.110	0.209	±	0.205	0.377	±	0.283	0.368	±	0.377
	AGR	0.354	±	0.129	0.237	±	0.102	0.717	±	0.291	0.800	±	0.231
Ref		0.956	±	0.473	0.911	±	0.456	0.835	±	0.316	1.127	±	0.555

The R$_s$:R$_{eco}$ ratios had stronger inter-GS trends across years. Over the longer-term period (four years), the trends of R$_s$:R$_{eco}$ ratios were increasing, except in Ref. The R$_s$:R$_{eco}$ ratios in four perennial sites (CRP-Sw, CRP-Pr, AGR-Sw and AGR-Pr) significantly increased. The CRP-Sw had the largest amplitude of increase, rising from 0.49 to 0.89, whereas AGR-Pr increased from 0.35 to 0.80. The ratios in annual crops increased slightly while Ref did not have a significant increase. The drought year had a small or no change in R$_s$:R$_{eco}$ ratios (Fig. 5.5 & Table 5.1).
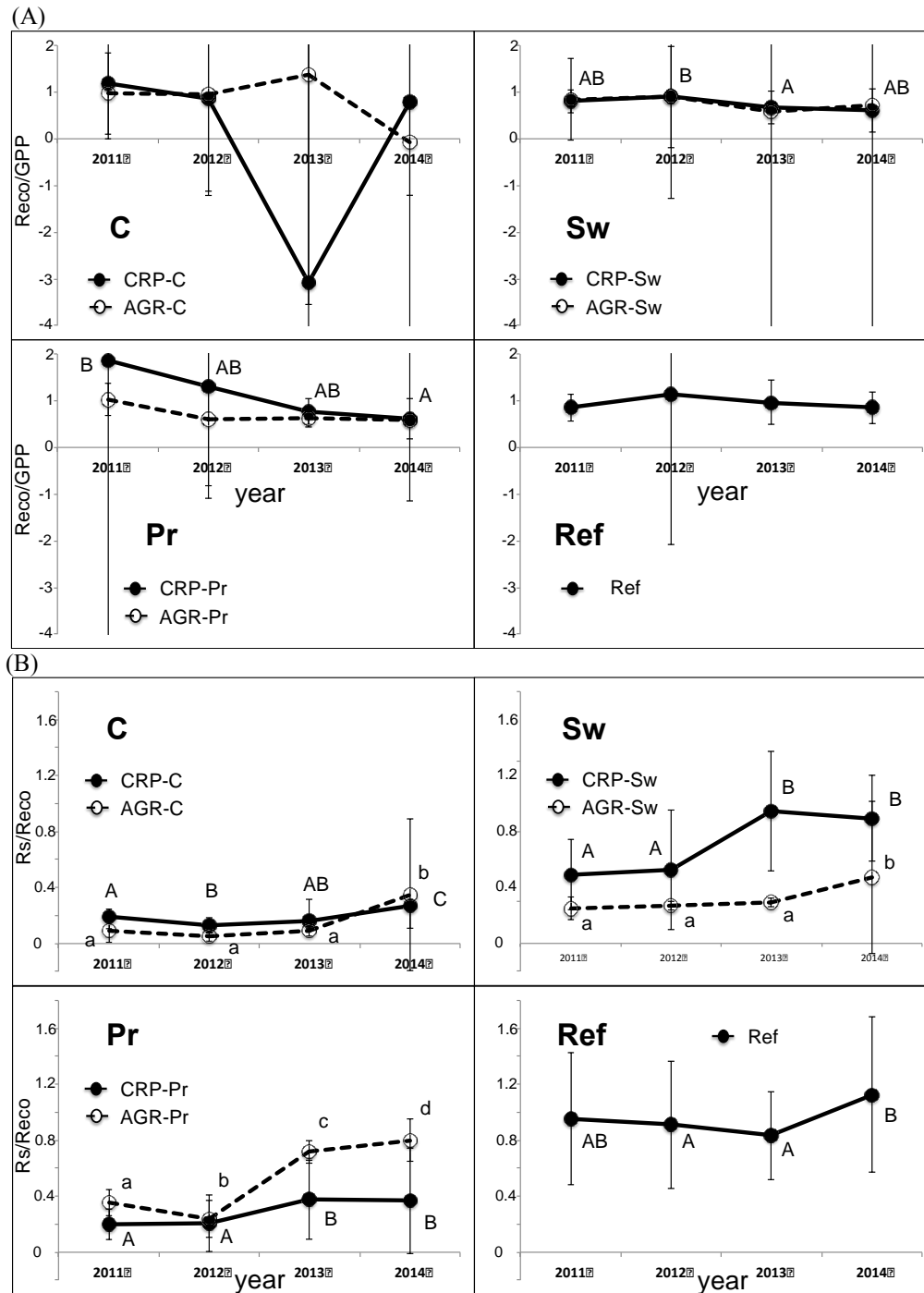
Figure 5.5. The mid-growing season R_eco:NPP and R_s:R_eco ratios across years in different sites. The yearly variations of R_{eco}:GPP (A) and R_s:R_{eco} ratios (B) are indicated by their CROP (between panels) and LUH (within panel). Solid dots show CRP while empty circles show AGR sites. The letters present the results of Tukey's HSD test for different sites, where upper-case letters present the statistical results of CRP and the lowercase letters represent the results of AGR sites. The letters display the means from small to large alphabetically. The curves without letters mean there is no significant difference between all years. The R_{eco}:NPP ratio (A) does not show the high or low standard deviations completely since the range is too large.

168

5.3.5 *The shift in annual NEE, GPP, R_{eco} and R_s among CROP and LUH across years*

In all treatments, NEE increased in the drought year (2012) and then decreased in the following years (2013 and 2014). In the drought year, the increases in NEE are more likely due to the decrease of GPP than the increase of R_{eco}. The NEE decreased in most fields in 2013 and 2014. However, GPP and R_{eco} contributed differently to the NEE decrease in two years—2013 and 2014. In 2013, the decrease of NEE was due to the different magnitude of increase on GPP and R_{eco}, although both of them had remarkable increases. The decrease of NEE in 2014 was likely due to the coincident decrease of R_{eco}, while the change of GPP varied (Figs. 5.6 (B) & (C)).

Comparing the change of NEE across years, each field had its own distinct trajectories due to different GPP and R_{eco} responses to climate. The Ref always had the highest annual NEE. It was positive in 2012, 2013 and 2014, meaning it was a carbon source. At other sites, most NEE was negative, implying most biofuel cropping fields were carbon sinks (Fig. 5.6 (A)). The CRP-C, the annual crop with high soil carbon and nitrogen content, had the highest R_{eco} out of any other perennial crop or AGR-C fields (close to Ref site, Fig. 5.6 (C)), resulting in its high NEE. The CRP sites generally had a higher GPP and R_{eco} than AGR sites. The mid-GS R_s had a similar yearly trend to GPP. Annual GPP explained 74% of mid-GS R_s and 38% of annual R_{eco} (Fig. 5.7).

The AGR sites always had a smaller NEE than CRP sites under the same crop type. The higher soil carbon and nitrogen content may increase R_{eco} in CRP fields although GPP in CRP fields was generally higher than those in AGR fields. The CRP-Pr field had a remarkably low NEE with high GPP and Rs (Figs. 5.6 (A), (B) & (D)), implying that its well-established root

system may have helped the growth of plants and stimulated a higher photosynthetic rate and

higher root metabolism.
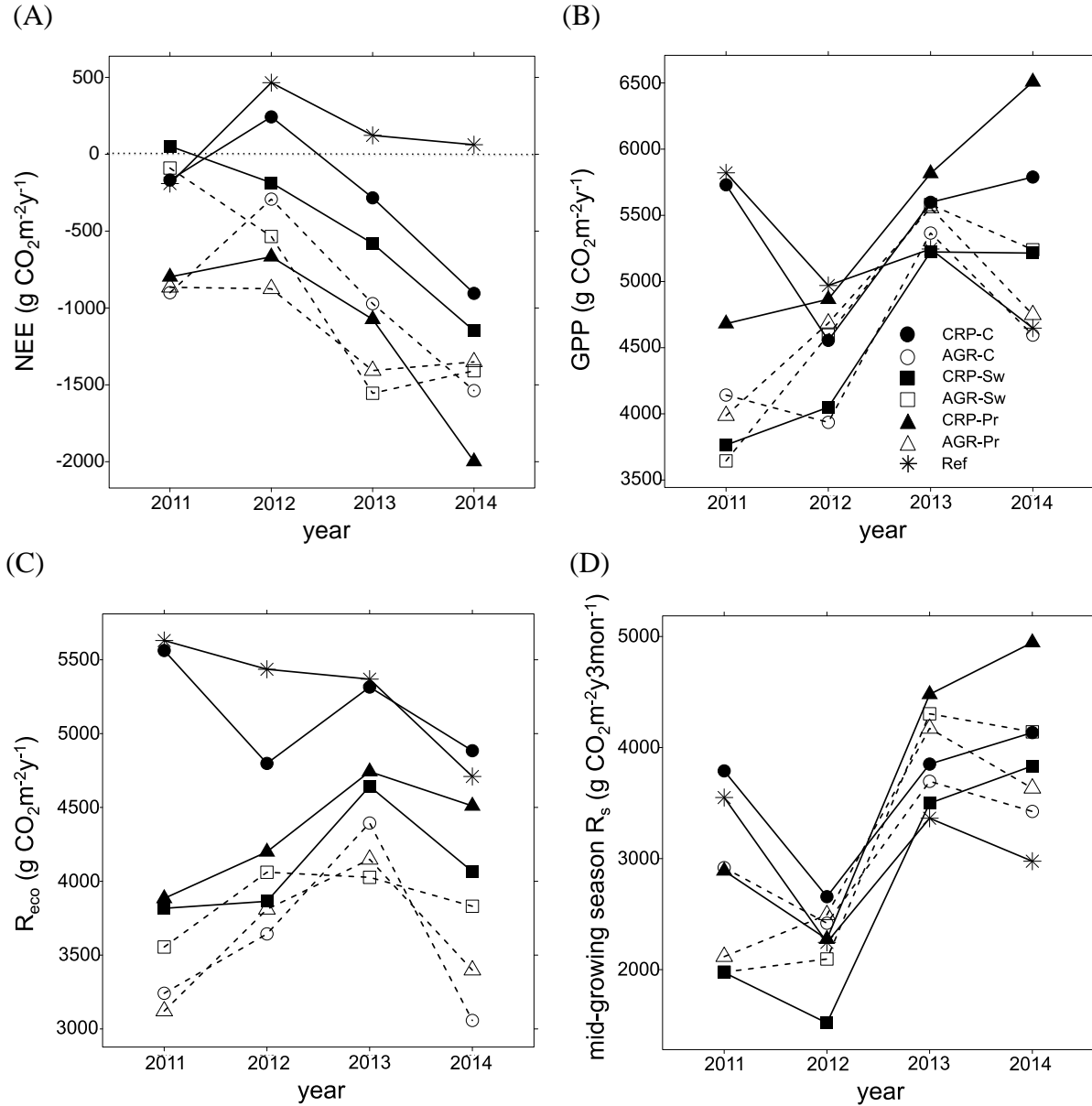
Figure 5.6. The cumulative annual NEE, GPP, R$_{eco}$ and mid-growing season R$_s$ across years in different sites. The net annual NEE (A), GPP (B), R$_{eco}$ (C) and mid-GS R$_s$ (D) in all sites were presented in different panels. The stellate figures presented Ref sites while circles, squares and triangles shows corn, switchgrass and prairie, respectively. The solid figures with solid lines display CRP sites and the empty figures with dash lines show AGR sites. The mid-growing season is identified as May 21 - August 20 due to the limitation of available data.
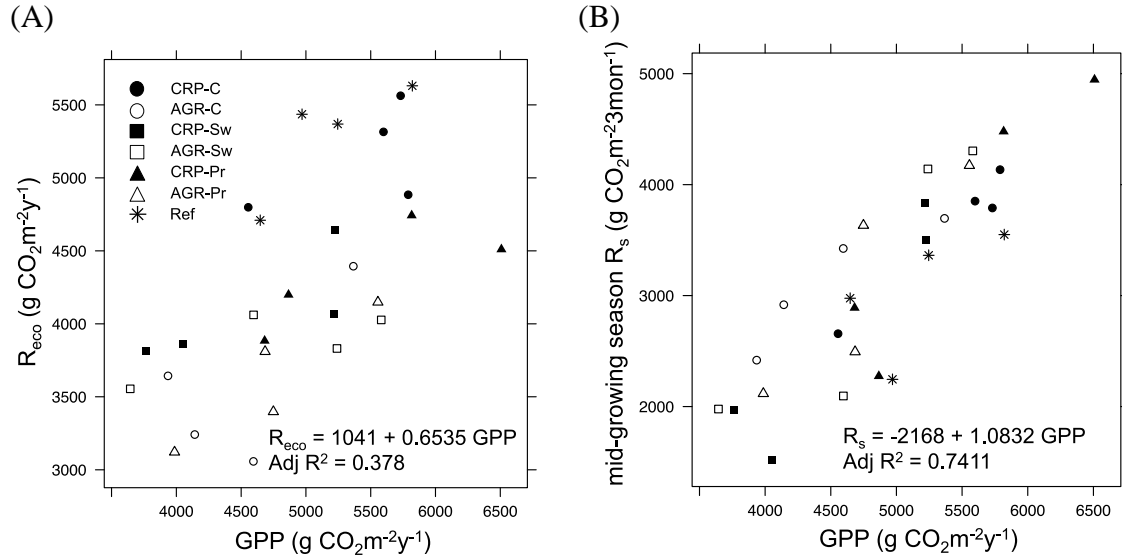
Figure 5.7. The linear regression models of R_{eco} and mid-growing season R_s to annual GPP.
The correlation between mid-GS R_s and annual GPP (A) and between R_{eco} and annual NEE (B).
The GPP (B), (C) and (D) in all sites were presented in different panels. The stellar figures
present Ref sites while circles, squares and triangles shows corn, switchgrass and prairie,
respectively. The solid symbols display CRP sites and the empty symbols show AGR sites. The
mid-growing season is identified as May 21 - August 20.

5.4 DISCUSSION

5.4.1 The seasonality of NEE, GPP & R$_{eco}$ between annual and perennial crops

The seasonality of NEE can be mostly explained by the different phenology between corn and other perennial crops. We always planted corn in May, resulting in a short GS due to late onset. The low GPP before June determined the positive spring NEE in corn fields (carbon source) during this period. Perennial crops, in contrast, germinated when the soil temperature rose in spring, generally in April. The two-month difference of carbon assimilation explained the different seasonality of NEE and GPP between annual and perennial crops, which also reflected annual NEE. Corn sites had a weaker carbon sequestration capacity than switchgrass and restored prairie, with a lower annual GPP (Figs. 5.6 (A) & (B)) at an annual scale. However it had a very strong peak of NEE in July and August (Fig. 5.2) and its minimum daily NEE was always lower than that in perennial crops (Table. 5.1).

Falge *et al.* (2002) analyzed FLUXNET data from 35 different sites across diverse biomes, climate regimes and latitudes. They inferred that the future climate warming in temperate and high latitude areas would alter the terrestrial ecosystem carbon balance by increasing the net primary production (NPP) by changing the difference between GPP and autotrophic respiration and the length of growing season. The latter will have a stronger impact on the ecosystem carbon budget than the former. In My experimental farms, the length of GS is important for the annual carbon budget, however, the climate benefits from annual and perennial cropping ecosystems can be very different resulting from different mechanisms. On one hand, the increasing temperature would lengthen the growing season of perennial crops, but would have little effect on corn in the croplands. The climate warming would enhance the difference in GS length between corn and perennial crops and would enlarge the difference in their annual

173

carbon sequestration capacities. On the other hand, the advanced onset of a GS may increase the risk of a summer water crisis in perennial crop fields, since the high spring evapotranspiration may consume most of the soil water. The impacts that future climate will have on NEE on annual or perennial crop ecosystems are "context-dependent".

The timing of unusual climate events or the seasonality of temperature and precipitation may also play different roles on the annual NEE in crop ecosystems. For example, low summer temperature may increase the value of NEE in an annual crop more than in a perennial crop, since corn has higher GPP in a short summer period while perennial grasses have a relatively gentle variation and a longer active period of GPP. In contrast, the spring drought may impact perennial more than annual crops since early emergence, which is characteristic of perennial, may drain soil water and induce a high risk of water deficit in the summer.

In sum, the integration of temperature and water availability interplay, the timing of climate events and their gradients should be considered when we estimate effects of the future climate scenarios on different ecosystems.

5.4.2 The mid-growing season R_{eco}:GPP and R_s:R_{eco} ratios

The seasonality of NEE is comprised of the seasonality of respiration assimilatory fluxes and processes (Falge *et al.*, 2002). Carbon assimilation and respiration have distinct drivers. Daytime NEE was more controlled by photosynthetically active radiation (PAR) while nighttime NEE and ecosystem respiration were dominated by temperature (Gilmanov *et al.*, 2007; Zhang *et al.*, 2015; Chen *et al.*, 2015). The time lags between the response of GPP to PAR and the responses of R_{eco} to temperature may increase the R_{eco}:GPP ratio dramatically. The high temporal variation of the R_{eco}:GPP ratio reveals time lags in my systems. Only the R_{eco}:GPP ratio in CRP-Pr between 2011 and 2014 and in CRP-Sw between 2012 and 2013 had significant

differences. CRP-Pr seems to have a long-term decrease in the R_{eco}:GPP ratio from 2 in 2011 to less than 1 in 2014, while CRP-Sw obviously decreased in the R_{eco}:GPP ratio between 2012 and 2013 (Fig. 5.5 (A)). Both of them were due to the significant increase of GPP after 2012. There are several possible reasons for the dramatic increase of GPP after 2012. First is the shorter and delayed summer water deficit. The summer water deficit occurred mid- to late July in 2011 and 2012 (Fig. 3.1 (B)), which depressed all components of NEE, including GPP, R_{eco} and R_s (Fig. 5.2). This is because the low availability of water limited biological activities and reduced the photosynthetic carbon source indirectly. The weak and delayed water deficit mitigated the limitation of photosynthesis and brought high GPP and R_{eco}. The amplitude of increase in GPP was greater than R_{eco}, resulting in lower NEE. Second, the decrease of the R_{eco}:GPP ratio in all Sw and Pr sites coincided with the increase of C_4:C_3 biomass after the severe drought in 2012 (Fig. 3.7, Abraha *et al.*, 2016). The increased dominance of C_4 grasses may explain the higher photosynthetic rates in 2013 and 2014.

5.4.3 The interannual trend of mid-GS R_s:R_{eco} ratios

One of the most important differences between annual and perennial crops is the development of their root systems. Perennial crops develop dense root systems to increase their water and nutrient uptake ability and store carbon belowground. The establishment of the root system requires more than one year and may strongly affect soil respiration. The contribution of belowground respiration may increase year by year due to the development of root systems in perennial crop ecosystems. My results across different crops proved this hypothesis and revealed that the development of root systems increase the R_s contribution to R_{eco} after land use change. The Ref field had a high R_s:R_{eco} ratio across treatments, while corn fields had a low R_s:R_{eco} ratio. Perennial crops Pr and Sw had remarkable increasing trends from 2011 to 2014 (Fig. 5.5 (B)).

The $R_s:R_{eco}$ ratios in CRP-Sw and AGR-Pr sites increased and arrived at similar levels to the Ref site, implying that they had established their root systems five years after land use change.

5.4.4 The limitation of the TWV model

For the estimation of soil respiration, I assumed that total soil respiration (R_s) is a function of soil temperature (T_s), soil moisture (VWC) and the Enhanced Vegetation Index (EVI) (i.e., TWV model in Chapter 2; Eq. 2-2 & Supplement 2-4). There are some uncertainties that may affect the estimates of R_s.

First, I combined the four-year data set to develop the parameters of the equation. However, we experienced a severe drought (2012) and two cool summers (2013 and 2014). The effects of climate regimes in a certain year and the immediate and lagged responses to severe drought may be complex and hard to recognize because the model ignored the differences in parameters between years. For example, my TWV model may have underestimated R_s in the disturbed year (2012) and overestimate the R_s in the recovery years (2013 & 2014). It would be better to add a "year" term in the equation to correct the problem.

Second, the extrapolation of soil respiration from the growing season to the whole year may introduce uncertainties. The soil respiration data were collected biweekly during the growing season. However, the soil respiration may show different patterns in different seasons. The cross-seasonal estimation brought uncertainty. Based on my model, the winter R_h was always higher than R_s since R_h had a smaller sensitivity to temperature change (Supplement 2-4). It would have been better to monitor soil respiration in winter to address this problem.

Third, the EVI data were collected from MODIS and had low spatial (250 by 250m) and temporal resolution (16 day). My experimental site fits into only one grid cell of the image and had no replication of the EVI value. The 16-day temporal resolution is adequate to follow the

dynamics of vegetation, but that is too long of a time period for soil respiration estimation. The seasonal curves of R_s were stepped. Higher spatial and temporal resolution of vegetation index or leaf area index may improve the TWV model. The *in situ* measurement of LAI may reduce the uncertainty of EVI.

5.5 CONCLUSIONS

Most studies on ecosystem carbon fluxes response to climate focused on interannual scale and ignored the seasonality of climate variables. My research reveals that the impacts of climate change on NEE of CO_2 are context-dependent and require emphasize at the intra-annual level. The different phenology between annual corn and perennial grasses affect the seasonality of GPP and R_{eco}. The timing of specific climate events, such as common summer drought, the occasional spring severe drought or cool summer may impact annual and perennial crops differently, whereas the annual mean temperature and precipitation are similar.

Severe drought increases NEE by decreasing both GPP and R_{eco}. The responses of GPP and R_{eco} in the following years were different, although both GPP and R_{eco} rebounded remarkably. Huge amounts of dead organic carbon entered the soil due to the 2012 drought and stimulated the growth of plants. This resulted in high GPP and R_{eco} in 2013. R_{eco} dropped dramatically in 2014 while GPP in CRP fields maintained a high level. The different responses of GPP and R_{eco} two years after the severe drought supported the high ability of carbon sequestration in CRP fields, especially in the CRP-Pr field. The combination of high soil nutrients and perennial crops stimulated a quick development of a root system with a strong carbon sequestration ability.

The net increase of NEE in the drought year for annual crop fields was higher than perennial crops, implying that there is a low resistance in corn—even though the NEE decreased

in the following year. In contrast, perennial crops increased their tolerance to drought by developing root systems that can absorb deeper water sources and store carbon and nutrients for further use. Soils in perennial and annual crops have different strategies to tolerant severe drought.

LITERATURE CITED

LITERATURE CITED

Abraha, M., Chen, J., Chu, H., Zenone, T., John, R., Su, Y.J., Hamilton, S.K., Robertson, G.P., 2015. Evapotranspiration of annual and perennial biofuel crops in a variable climate. Global Change Biology Bioenergy, 7, 1344-1356.

Abraha, M., Gelfand, I., Hamilton, S.K., Shao, C., Su, Y.J., Robertson, G.P., Chen, J., 2016. Ecosystem water-use efficiency of annual corn and perennial grasslands: contributions from land-use history and species composition. Ecosystems, 19, 1001-1012.

Burba, G.G., McDermitt, D.K., Grelle, A., Anderson, D.J., Xu, L.K., 2008. Addressing the influence of instrument surface heat exchange on the measurements of CO_2 flux from open-path gas analyzers. Global Change Biology, 14, 1854–1876.

Chapin, F.S., Woodwell, G.M., Randerson, J.T., Rastetter, E.B., Lovett, G.M., Baldocchi, D.D., Clark, D.A., Harmon, M.E., Schimel, D.S., Valentini, R., Wirth, C., Aber, J.D., Cole, J.J., Goulden, M.L., Harden, J.W., Heimann, M., Howarth, R.W., Matson, P.A., McGuire, A.D., Melillo, J.M., Mooney, H.A., Neff, J.C., Houghton, R.A., Pace, M.L., Ryan, M.G., Running, S.W., Sala, O.E., Schlesinger, W.H., Schulze, E.-D., 2006. Reconciling carbon-cycle concepts, terminology, and methods. Ecosystems, 9, 1041-1050.

Chen, C., Li, D., Gao, Z., Tang, J., Guo, X., Wang, L., Wan, B., 2015. Seasonal and interannual variations of carbon exchange over a rice-wheat rotation system on the north China Plain. Advances in Atmospheric Sciences, 32, 1365-1380.

Deal, M.W., Xu, J., John, R., Zenone, T., Chen, J., Chu, H., Jasrotia, P., Kahmark, K., Bossenbroek, J., Mayer, C., 2013. Net primary production in three bioenergy crop systems following land conversion. Journal of Plant Ecology, 6, 1-10.

Falge, E., Baldocchi, D., Tenhunen, J., Aubinet, M., Bakwin, P., Berbigier, P., Bernhofer, C., Burba, G., Clement, R., Davis, K.J., Elbers, J.A., Goldstein, A.H., Grelle, A., Granier, A., Guðmundsson, J., Hollinger, D., Kowalski, A.S., Katul, G., Law, B.E., Malhi, Y., Meyers, T., Monson, R.K., Munger, J.W., Oechel, W., U, K.T.P., Pilegaard, K., Rannik, Ü., Rebmann, C., Suyker, A., Valentini, R., Wilson, K., Wofsy, S., 2002. Seasonality of ecosystem respiration and gross primary production as derived from FLUXNET measurements. Agricultural and Forest Meteorology, 113, 53-74.

Gelfand, I., Zenone, T., Jasrotia, P., Chen, J., S.K.Hamilton, Robertson, G.P., 2011. Carbon debt of conservation reserve program (CRP) grasslands converted to bioenergy production. Proceedings of the National Academy of Sciences, 108, 13864-13869.

Gilmanov, T.G., Soussana, J.F., Aires, L., Allard, V., Ammann, C., Balzarolo, M., Barcza, Z., Bernhofer, C., Campbell, C.L., Cernusca, A., Cescatti, A., Clifton-Brown, J., Dirks, B.O.M., Dore, S., Eugster, W., Fuhrer, J., Gimeno, C., Gruenwald, T., Haszpra, L., Hensen, A., Ibrom, A., Jacobs, A.F.G., Jones, M.B., Lanigan, G., Laurila, T., Lohila, A., Manca, G., Marcolla, B., Nagy, Z., Pilegaard, K., Pinter, K., Pio, C., Raschi, A., Rogiers, N., Sanz, M.J., Stefani, P., Sutton, M., Tuba, Z., Valentini, R., Williams, M.L., Wohlfahrt, G., 2007. Partitioning European grassland net ecosystem CO_2 exchange into gross primary productivity and ecosystem respiration using light response function analysis. Agricultural, Ecosystems and Environment, 121, 93-120.

McMillen, R.T., 1988. An eddy correlation technique with extended applicability to non-simple terrain. Boundary-Layer Meteorology, 43, 231–245.

Moncrieff, J., Clement, R., Finnigan, J.J., Meyers, T., 2004. Averaging, detrending, and filtering of eddy covariance time series. In: Handbook of Micrometeorology: A Guide for Surface Flux Measurement and Analysis, Lee X, Massman W, Law B (Eds). Kluwer Acadamic: Dordrecht, Netherlands, 7–32.

Peel, M.C., Finlayson, B.L., McMahon, T.A., 2007. Updated world map of the Koppen-Geiger climate classification. Hydrology and Earth System Sciences Discussions 4, 439-473.Post, W.M., Emanuel, W.R., Zinke, P.J., Stangenberger, A.G., 1982. Soil carbon pools and world life zones. Science, 298, 156-159.

Reichstein, M., Falge, E., Baldocchi, D., Papale, D., Aubinet, M., Berbigier, P., Bernhofer, C., Buchmann, N., Gilmanov, T., Granier, A., Grunwald, T., Havrankova, K., Ilvesniemi, H., Janous, D., Knohl, A., Laurila, T., Lohila, A., Loustau, D., Matteucci, G., Meyers, T., Miglietta, F., Ourcival, J.M., Pumpanen, J., Rambal, S., Rotenberg, E., Sanz, M., Tenhunen, J., Seufert, G., Vaccari, F., Vesala, T., Yakir, D., Valentini, R., 2005. On the separation of net ecosystem exchange into assimilation and ecosystem respiration: review and improved algorithm. Global Change Biology, 11, 1424–1439.

Robertson, G.P., Hamilton, S.K., 2015. Long-term ecological research at the Kellogg Biological Station LTER site: conceptual and experimental framework. In: Hamilton, S.K., Doll, J.E., Robertson, G.P. (Eds.), The Ecology of Agricultural Landscapes. Oxford University Press, New York, pp. 1-32.

Schimel, D., Melillo, J., Tian, H., McGuire, A.D., Kicklighter, D., Kittel, T., Rosenbloom, N., Running, S., Thornton, P., Ojima, D., Parton, W., Kelly, R., Sykes, M., Neilson, R., Rizzo, B., 2000. Contribution of increasing CO_2 and climate to carbon storage by ecosystems in the United States. Science, 287(5460), 2004-2006.

Soegaard, H., Jensen, N.O., Boegh, E., Hasager, C.B., Schelde, K., Thomsen, A., 2003. Carbon dioxide exchange over agricultural landscape using eddy correlation and footprint modeling. Agricultural and Forest Meteorology, 114, 153-173.

Webb, E.K., Pearman, G.I., Leuning, R., 1980. Correction of flux measurements for density effects due to heat and water vapor transfer. Quarterly Journal of the Royal Meteorological Society, 106, 85–106.

Wilczak, J.M., Oncley, S.P., Stage, S.A., 2001. Sonic anemometer tilt correction algorithms. Boundary-Layer Meteorology, 99, 127–150.

Zenone, T., Chen, J., Deal, M.W., Wilske, B., Jasrotia, P., Xu, J., Bhardwaj, A.K., Hamilton, S.K., Robertson, P.G., 2011. CO_2 fluxes of transitional bioenergy crops: effect of land conversion during the first year of cultivation. GCB Bioenergy, 3, 401-412.

Zenone, T., Gelfand, I., Chen, J., Hamilton, S.K., Robertson, G.P., 2013. From set-aside grassland to annual and perennial cellulosic biofuel crops: Effects of land use change on carbon balance. Agricultural and Forest Meteorology, 182-183, 1-12.

Zhang, L., Sun, R., Xu, Z., Qiao, C., Jiang, Q., 2015. Diurnal and seasonal variations in carbon dioxide exchange in ecosystems in the Zhanfye oasis area, northwest China. PLoS ONE, 10(3), e0120660.

CHAPTER 6
CONCLUSIONS AND IMPLEMENTATIONS

Global climate change, which mainly results from the past centuries' anthropogenic greenhouse gas emissions, alters Earth's energy, hydrological and carbon cycles. This impacts both natural and human systems. To address the critical challenges on human well-being and the ecosystem health and to achieve the purposes of Millennium Development Goals (MDGs; United Nations, 2015) and the Convention on Biological Diversity (CBD; United Nations, 1992), the jointly research were incorporated (Sachs *et al.*, 2009) to mitigate the impacts of climate change on human well-being, biodiversity loss and ecosystem service degradation. The integration and the convergence of ecological and socio-economic sustainability has quickly become the largest challenge in contemporary sustainability science. The human-natural nexus system has dramatically developed to address climate change-derived problems from different perspectives, such as the coupled human and nature system (CHANS; Liu *et al.*, 2007a, b; McConnell *et al.*, 2011; Chen & Liu, 2014; Chen *et al.*, 2015), water-energy-food nexus (NEF Nexus; FAO, 2014) and ecosystem stewardship (Chapin *et al.*, 2010). However, these frameworks are still in their initial stages, and they require fundamental knowledge to fill the gaps between how subsystems mechanisms and their respond to climate scenarios.
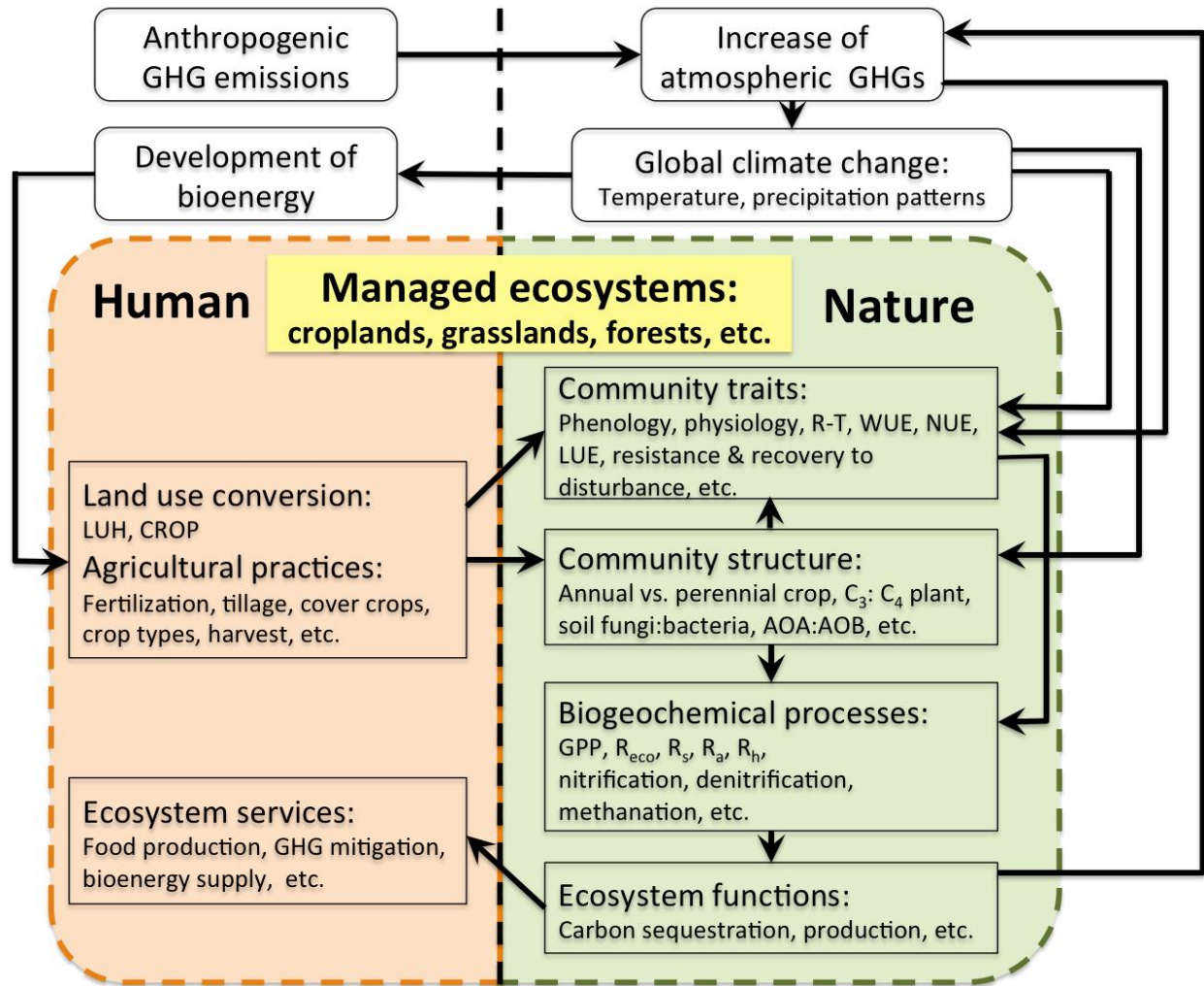
Figure 6.1. The framework of coupled human and nature systems (CHANS) on the impacts that bioenergy development has on managed ecosystems. Bioenergy-induced land use change and agricultural practices may change the community structure of vegetation, affect their traits, modify biogeochemical processes, and ultimately alter ecosystem functions, such as carbon sequestration ability. The changing climate, such as temperature and precipitation patterns, may affect biogeochemical processes via community traits with or without altering community structure. The framework focuses on the impact that bioenergy has on agricultural ecosystem developments at local scale—disincluding economic and telecoupling effects. LUH: land use history; CROP: crop type; GHG: greenhouse gas; R-T: respiration-temperature correlation; WUE: water use efficiency; NUE: nutrient use efficiency; LUE: light use efficiency; AOA: ammonia-oxidizing archaea; AOB: ammonia-oxidizing bacteria; GPP: gross primary production; R_{eco}: ecosystem respiration; R_s: total soil respiration; Ra: autotrophic soil respiration; and R_h: heterotrophic soil respiration.

The purpose of biofuel development is to reduce total carbon dioxide emission per unit of fuel used. However, direct and indirect land use conversion and agricultural practices in the biofuel croplands may affect the benefits that bioenergy has on climate. Development of bioenergy and bioenergy-derived land use change have been the most hotly disputed topics in the past decade (Liu *et al.*, 2015), leaving many gaps in current knowledge. I developed a nexus framework of bioenergy, including coupled human and nature systems (Fig. 6.1). My study mainly focused on the responses of the nature system under some settings of land use conversion and agricultural practices. I explored the response of community traits, community structure, major carbon processes and ecosystem carbon sequestration underneath different crop types and land use histories. This framework does not include socio-economic and telecoupling effects, but can be expended in the future if required.

My dissertation emphasized the relative contributions that the components of carbon dioxide processes have on net ecosystem CO_2 flux and how they respond to climate patterns in different lands use histories (before land use conversion) and crop types (after land use conversion) at inter- (Chapter 2) and intra-annual (Chapter 3) scales—especially in regards to immediate and prolonged effects on a drought during the growing-season. I also developed Bayesian models to explore the soil respiration's temperature correlations and its shift after severe drought (Chapter 4). Chapter 5 discussed the different responses that gross primary production (GPP) and ecosystem respiration (R_{eco}) have in regards to NEE and its amount as well as the seasonality of net ecosystem CO_2 exchange (NEE) caused by the asynchrony of GPP and R_{eco}.

In Chapter 2 and Chapter 3, I found that both soil temperature and vegetation index were positively correlated with total and heterotrophic soil respiration. The temperature and

photosynthetic-derived carbon via carbon allocation determines the intrinsic potential of soil respiration. Soil water content has weak or no correlation with soil respiration. However, it plays crucial roles during summer drought periods and limits soil respiration.

In my studied ecosystems, different effects and magnitudes of three different natural and anthropogenic forces on soil respiration were recognized at different temporal scales. First, the seasonal patterns of temperature and water availability in a specific year affected the annual soil respiration. Not only did temperature and precipitation affect vegetation growth —and therein total and heterotrophic soil respiration—but also the timing of the microclimate. The spring and summer drought had stronger impacts on annual soil respiration than those occurring in fall since the spring-summer drought degraded the vegetation growth and photosynthesis, which ultimately impacted total and heterotrophic soil respiration. Second, the severe drought in 2012 not only depressed soil respiration within the same year, but also affected one or more following years by changing vegetation composition in perennial crop fields and ecosystem water use efficiencies (eWUE; Abraha *et al.*, 2016). The effect of severe drought was strong and lasted more than one year by changing the vegetation community structure. Third, the long-term trend of autotrophic soil respiration (T_s) was remarkable in CRP-Pr and AGR-Pr field in the 5th year (2014) following land use conversion due to well-established root systems.

Generally speaking, annual and perennial crops had different strategies to adapt to severe drought. Corn has late onset and a shorter growing season to alleviate summer water stress on vegetation and soil microbes. It also has a higher eWUE (4.1 g C m^{-2}/mm H_2O in CRP-C & 3.8 in AGR-C) than perennial crops (2.5-3.3 in prairie and switch grass croplands) (Abraha *et al.*, 2016). In contrast, perennial crops had highly developed dense root systems helping them absorb deep water storages. The mature perennial ecosystem at the Ref site had the highest resistance

and soil respiration recovery after a severe drought, even though it had the lowest eWUE (2.3; Abraha *et al.*, 2016). Perennial crops also increased eWUE to acclimate to severe drought by increasing its C_4 plant composition. The different strategies between annual and perennial crops to cope with drought determined their resistance to increasing risks caused by extreme temperatures and drought events. Under different climate scenarios and different combinations of temperature and precipitation gradients, annual and perennial crops may exhibit different benefits. The increase of temperature may improve photosynthesis rates, elongate the growing season and stimulate the carbon sequestration abilities of perennial crops, but may also increase the risk of summer a water crisis. Also, the presence of heavy rain in late July may convert a cropland from a carbon source to a carbon sink in a hot year. Vegetation composition, which reflects the cross-year acclimation to the temperature-precipitation regimes, and the succession of perennial grasslands/croplands also determine the resistance and resilience of soil respiration to future climate regimes.

After understanding the soil respiration between different crop types and how they respond to three different forces, I studied the correlation between soil respiration and its major driver, soil temperature (R-T correlation), in different LUH and CROP and how it responds to severe drought using Bayesian models. I found that the LR_{20}, which denotes the growing season mean soil respiration, ranks from high to low in the following ecosystem types: Ref > prairie > switchgrass > corn. This order coincides with root density, where: late succession perennial crop (Ref) > early succession perennial crop (Pr and Sw) > annual crop (C). Soil respiration in Ref had the highest soil respiration temperature sensitivity (β) resistance and recovery and LR_{20} on R_a. The well established LR_{20} and β of Ra remained even in severe drought conditions. All β of R_a decreased while those of R_h increased in Pr, Sw and C fields. The decrease of β_{Ra} coincided

with most previous studies that found severe drought depresses soil respiration and its temperature sensitivity by inhibiting cellular biochemical reaction when water is not available. The increase of β_{Rh} was surprising. The possible reason is the change of soil microbial community structure, which caused the high β with low R when severe drought was experienced. After a two-year recovery from the 2012 drought, the R-T relationship of R_a and R_h seemed have different trajectories. The R_a was likely returning to equilibrium while R_h moved toward a new equilibrium with higher β and lower LR_{20}. Both the immediate and prolonged reactions of the R-T relationship implied that the soil microbial community exhibited higher "plasticity" in adapting severe drought while vegetation roots were likely to return to pre-drought condition. When comparing the locations of different LUH-CROP treatments on the β-LR_{20} biplots between 2014 and 2011, the Euclidean distances of annual crop and the Ref fields were very small. This implies no long-term trends in the R-T relationship in annual crops and in late successional grass ecosystems. Other perennial crop fields had larger Euclidean distances that revealed long-term trends toward higher growing season R_a with higher temperature sensitivities due to the development of dense root systems.

The combination of Chapters 2-4 tells an interesting story on how late successional grassland ecosystems have well-established root systems and high resistance and recovery to drought disturbances—even with high respiration and low eWUE. Early successional grasslands have slightly a lower stability (higher magnitude of fluctuation after disturbance and longer duration to recover) than Ref fields. However, the development of root systems, the shift of vegetation composition and the possible change in soil microbial community structures may help an ecosystem better adapt to severe drought in the future.

GPP and R_{eco} have different driving forces. The asynchrony of the drivers and the time lags for carbon reallocation result in the seasonality of NEE. Differences in phenology between annual and perennial crops determine NEE, GPP and R_{eco} seasonality. Corn has a late growing seasonal onset with low NEE in the mid-summer while perennial grasses have early onset and a longer growing season. However, early onset of the GS may increase the risk of the summer water deficit, since high spring evapotranspiration may drain soil water in the early growing season. The climate regimes and the timing of extreme events may stimulate or dampen the carbon sequestration ability based on the different ecosystem characteristics. For example, spring drought may depress perennial grasslands while cool summers may increase the NEE in annual crop ecosystems by dramatically reducing GPP. Perennial grasses have lower eWUE and higher soil respiration. Both increase their risk in the face of extreme drought. However, well-established root systems may tap into deep-water storages and strengthen drought resistance and recovery. The carbon and nutrients stored in roots may also support future use.

LITERATURE CITED

LITERATURE CITED

Abraha, M., Gelfand, I., Hamilton, S.K., Shao, C., Su, Y.J., Robertson, G.P., Chen, J., 2016. Ecosystem water-use efficiency of annual corn and perennial grasslands: contributions from land-use history and species composition. Ecosystems, 19, 1001-1012.

Chapin III, F.S., Carpenter, S.R., Kofinas, G.P., Folke, C., Abel, N., Clark, W.C., Olsson, P., Smith, D.M.S., Walker, B., Young, O.R., Berkes, F., Biggs, R., Grove, J.M., Naylor, R.L., Pinkerton, E., Stefen, W., Swanson, F.J., 2010. Ecosystem stewardship: sustainability strategies for a rapidly changing planet. Trends in Ecology and Evolution, 25(4), 241-249.

Chen, J., Liu, Y., 2014. Coupled natural and human systems: a landscape ecology perspective. Landscape Ecology, 29, 1641-1644.

Chen, J., John, R., Zhang, Y., Shao, C., Brown, D.G., Batkhishig, O., Amarjargal, A., Ouyang, Z., Dong, G., Wang, D., Qi, J., 2015. Divergences of two coupled human and natural systems on the Mongolian Plateau. BioScience, 65(6), 559-570.

Liu, J., Mooney, H., Hull, V., Davis, S.J., Gaskell, J., Hertel, T., Lubchenco, J., Seto, K.C., Gleick, P., Kremen, C., Li, S., 2015. Systems integration for global systainability. Science, 347, 1258832.

McConnell, W.J., Millington, J.D.A., Reo, N.J., Alberti, M., Asbjornsen, H., Baker, L.A., Brozovic, N., Drinkwater, L.E., Drzyzga, S.A., Fragoso, J., Holland, D.S., Jantz, C.A., Kohler, T.A., Maschner, H.D.G., Monticino, M, Podesta, Jr., G., Pontius, R.G., Redman, C.L., Sailor, D., Urquhart, G., Liu, J., 2011. Research on coupled human and natural systems (CHANS): approach, challenges, and strategies. The Bulletin of the Ecological Society of America, 92, 218–228.

FAO, 2014. The Water-Energy-Food Nexus: A New Approach in Support of Food Security and Sustainable Agriculture. Food and Agriculture Organization of the United Nations, Rome.

Liu, J., Dietz, T., Carpenter, S.R., Folke, C., Alberti, M., Redman, C.L., Schneider, S.H., Ostrom, E., Pell, A.N., Lubchenco, J., Taylor, W.W., Ouyang, Z., Deadman, P., Kratz, T., Provencher, W., 2007a. Coupled human and natural systems. Ambio, 36(8), 639-649.

Liu, J., Dietz, T., Carpenter, S.R., Alberti, M., Folke, C., Moran, E., Pell, A.N., Deadman, P., Kratz, T., Lubchenco, J., Ostrom, E., Ouyang, Z., Provencher, W., Redman, C.L., Schneider, S.H., Taylor, W.W., 2007b. Complexity of coupled human and natural systems. Science, 317, 1513-1516.

Sachs, J.D., Baillie, J.E.M., Sutherland, W.L., Armsworth, P.R., Ash, N., Beddington, J., Blackburn, T.M., Collen, B., Gardiner, B., Gaston, K.J., Godgray, H.C.J., Green, R.E., Harvey, P.H., House, B., Knapp, S., Kumpel, N.F., Machonald, D.W., Mace, G.M., Mallet, J., Matthews, A., May, R.M., Petchey, O., Purvis, A., Roe, D., Safi, K., Turner, K., Walpole, M., Watson, R., Jones, K.E., 2009. Biodiversity conservation and the Millennium Development Goals. Science, 325, 1502-1503.

United Nations, 2014. The Millennium Development Goals Report 2015. United Nations, New York.